COMSAT
Technical Review

Acknowledgments

TDMA network control facility*

G. D. HODGE, R. J. COLBY, C. KULLMAN, AND B. H. MILLER

(Manuscript received November 15, 1985)

Abstract

The critical role of the INTELSAT Operations Center TDMA Facility (IOCTF) in ensuring the proper functioning of the time-division multiple-access (TDMA) network requires a highly responsive, real-time communications facility. This paper describes the overall monitoring and control requirements of a centralized system and focuses on the provision of a distributed networking facility to permit real-time communications between the TDMA reference and monitoring station sites and the IOCTF. The IOCTF is required to support throughput of message traffic up to a rate of four messages per second. Simulation of throughput performance was demonstrated during IOCTF system development, and the results of those tests are summarized.

Introduction

The INTELSAT Operations Center TDMA Facility (IOCTF) was developed and installed by COMSAT Laboratories to monitor and control the operation of the INTELSAT time-division multiple-access (TDMA) networks. The IOCTF serves as a focal point at which the performance of each network can be observed and recorded. It initiates synchronous burst time plan (BTP) changes and TDMA system startup with the consent of the master primary station

---

operator, assumes control of any TDMA reference and monitoring station (TRMS) site to initiate routine and diagnostic measurements, instructs any TRMS site to collect and transmit event history files for operator review, distributes BTPs to each of the traffic terminals through the engineering service circuit (ESC) network in an automatic mode (or in the backup mode through direct-distance dialing), and provides off-line computer support for operation and maintenance of the TDMA system through a background processor (BGP).

The three major components of the INTELSAT TDMA digital speech interpolation (DSI) system are traffic terminals, consisting of common TDMA terminal equipment (CTTE) coupled with DSI/digital noninterpolation (DNI) units; TRMSs, consisting of reference terminal equipment (RTE) and TDMA system monitor (TSM) equipment; and the IOCTF. Figure 1 is a block diagram of the system elements.

The traffic terminal connects revenue-producing traffic and voice orderwires (VOWs) to the TDMA frame in strict accordance with the BTP and control data from the RTE. The RTE establishes TDMA frame timing, coordinates and synchronizes BTP changes, measures satellite range, provides other terminals with TDMA acquisition and synchronization control, monitors service channels for alarms, establishes ESC call routing via VOW/teletype (TTY) channels, provides IOC gateway ESC facilities and TDMA/DSI system maintenance support, and transmits system operational status to the IOCTF via the TRMS packet data link. The TSM receives and measures the signal parameters of all bursts specified in the TSM BTP, performs signal parameter limit checks for normalcy, and provides measurement display and alarms both locally and remotely at the IOC via the TRMS data link. The TSM also provides a local and IOC-controlled diagnostic mode for more detailed signal analysis.

IOCTF description

Broadly stated, the role of the IOCTF is to control, coordinate, and maintain the TDMA/DSI system components listed above, with particular emphasis on the coordination and synchronization of BTP changes. The objectives of the IOCTF are to achieve maximum availability in performing these functions and to provide a maximum level of service for the TDMA/DSI communications system.

The IOCTF can operate with up to six TDMA satellite networks and is coupled to each reference station in the network via voice-grade packet-switched data links. For each network, a network packet recirculator/ concentrator (NPRC) is provided which forms an interface between each satellite network and the IOCTF. In addition, each reference station serves as a gateway terminal for the TDMA voice and TTY ESC system connected to the IOCTF via leased voice circuits.
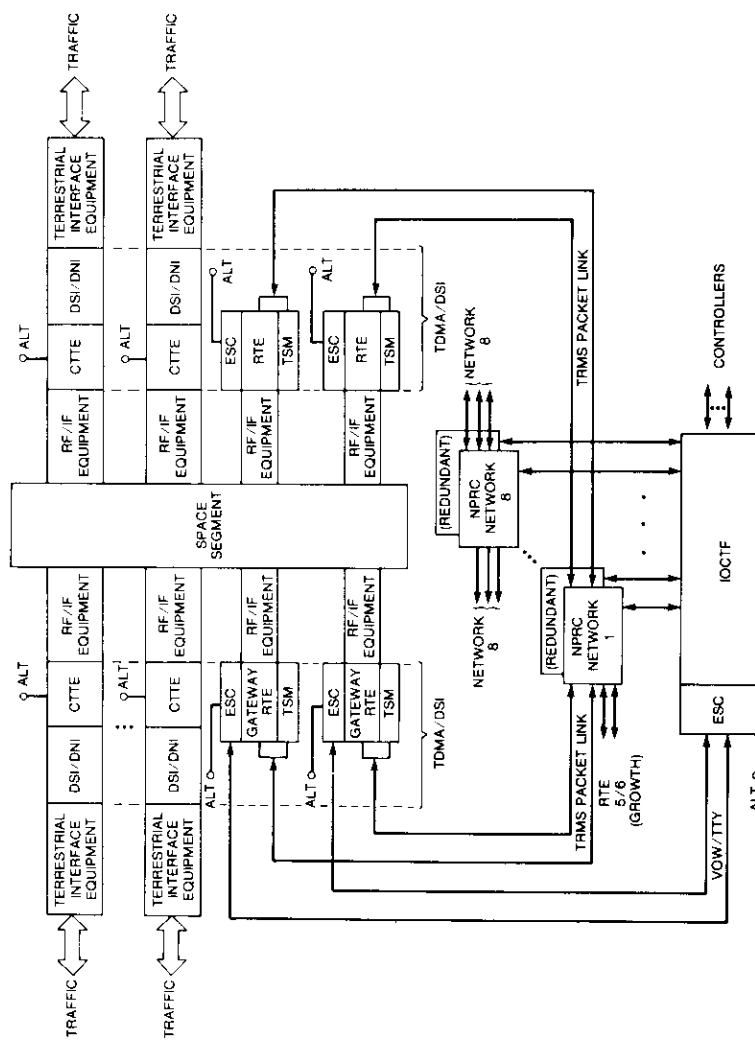
Figure 1. Block Diagram of INTELSAT TDMA/DSI System Elements
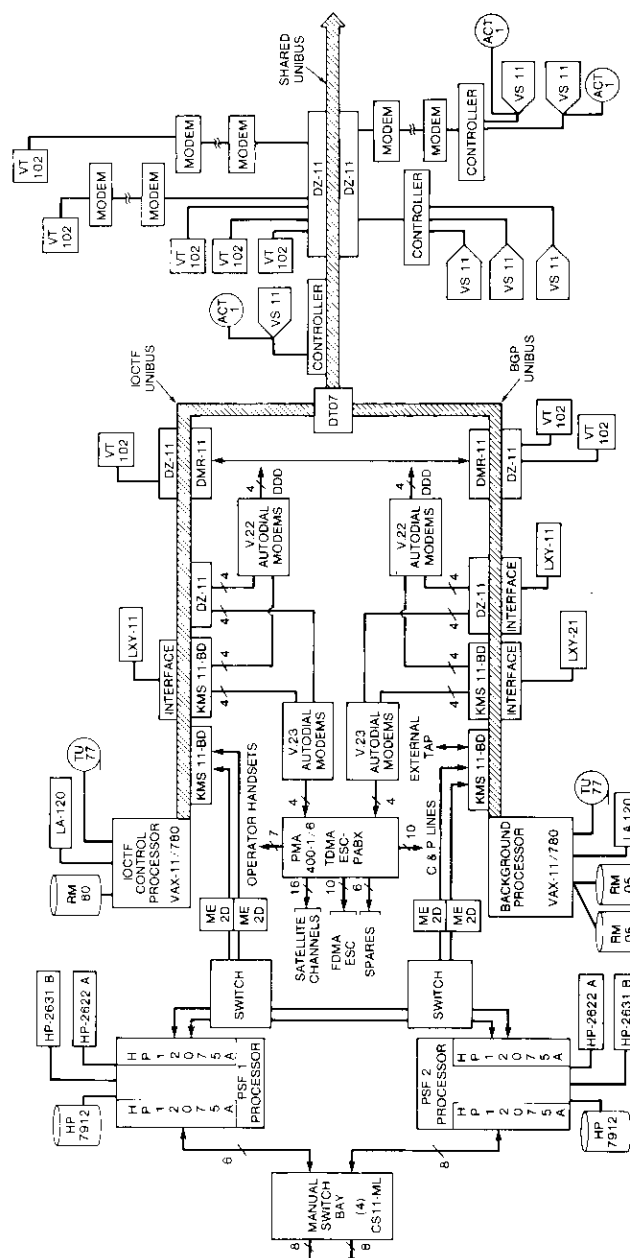
Figure 2. IOCTF Hardware Configuration

Figure 2 is a block diagram of the IOCTF equipment. Two processors are used, one on-line and one in background mode. All communications functions associated with the TRMS packet network are performed by a pair of redundant packet store and formatters (PSFs) based on Hewlett-Packard (HP) A900 computers and chosen to be compatible with similar computers used at the TRMS sites, thus allowing the use of vendor-supplied networking software between sites. Each PSF processor can communicate with a maximum of six NPRCs (one per network) at one time. The PSF performs the necessary conversion between the data format on the interface and the format used in the internal IOC architecture. To ensure minimal interruption of service, each TRMS is connected to two NPRCs, only one of which is normally active at any given time. A manual switch bay connects a network's pair of NPRCs with a PSF processor and its backup.

The IOCTF control processor, based on the VAX 11/780 computer, handles functions related to operator control and data storage and display. This processor provides the computer resources to service up to eight IOCTF local and two remote operator stations, and two remote engineering stations. It also accepts data from the operation and engineering stations and passes the data to the PSF for transmission to the reference stations. In addition, it drives a local printer and plotter which can take full-color snapshots of an operator station's graphic display. Each display is normally associated with one network.

The operator stations consist of a video terminal (VT) and graphics display unit (GDU) which generate and reproduce the displays available to the RTE operators. This allows IOCTF operators to monitor and control the status of the RTEs and the associated TDMA networks. The transfer of displays and alphanumeric data from the RTEs to the IOCTF via the data lines enables IOCTF operators to view the network performance from the perspective of any or all RTEs, thus enabling the operators to assist in the maintenance support for RTEs and traffic terminals. This remote control includes the coordination of synchronous time plan changes and system startup following an outage. In both cases, commands and responses are exchanged over the data lines. In addition, the IOCTF uses the ESC and VOW/TTY circuit to verbally control all significant terminal activities which can affect TDMA system operation.

The IOCTF employs the BGP to store, distribute, and verify the critical BTP information which configures the operation of each network reference and traffic terminal. The BTP also provides system archival storage facilities and off-line processor support. In the event of IOCTF control processor failure, the BGP fulfills this function, suspending its normal operations.

Functional requirements

As with frequency-division multiple-access (FDMA) satellite communications, TDMA is critically dependent upon full coordination of the independent actions of every system participant. The IOCTF plays a key role in accomplishing this coordination. First and most importantly, the IOCTF prepares and distributes BTP data via the ESC to each participant facility to establish traffic and VOW/TTY interconnectivities and apportion transponder utilization. Second, the IOCTF regularly distributes satellite orbit prediction parameters to all RTEs via the TRMS packet data link to ensure reliable and interference-free TDMA acquisition by all terminals. As a manually selected option at the master primary reference terminal (MPRT), the IOCTF may start the system via the TRMS data link INITIATE STARTUP packet. In a like manner, the IOCTF provides BTP change commands either verbally to the MPRT via VOW, or optionally via the TRMS data link using the START PLAN CHANGE and CANCEL COUNTDOWN packets. Finally, via the ESC VOW/TTY facility, IOCTF controllers provide voice coordination as needed for all required interterminal activities.

In the INTELSAT TDMA/DSI system design, many maintenance activities are performed by the TRMS and traffic terminal operators. The IOCTF manages and oversees these activities to ensure their effectiveness and efficiency, providing interterminal discipline as needed for cooperative troubleshooting, and intervening directly when problems approach the network level or exceed TRMS capabilities. In this case, the IOCTF may manage the TSM in the diagnostic mode and direct specific troubleshooting activities.

Figure 3 provides a macroscopic view of the IOCTF, identifying eight categories of external interface. These interfaces must be effective and reliable for the IOCTF to perform its role.

Data display requirements

Effective control such as that exercised by the IOCTF requires extensive monitoring of TDMA/DSI system status and automatic indication of failure conditions. The IOCTF monitors system status via the TRMS packet data links to each network. Figure 4 shows the hierarchical arrangement of 12 required display monitors, along with their associated data link packets. To provide these displays, the IOCTF must generate composite displays based on independent TRMS inputs and duplicate selected video display unit images from any TRMS. Furthermore, the IOCTF must provide the capability for adding future displays.

TRMS data packets are generated by every reference station in each of the INTELSAT TDMA networks. Some of the TRMS packets are routinely sent to
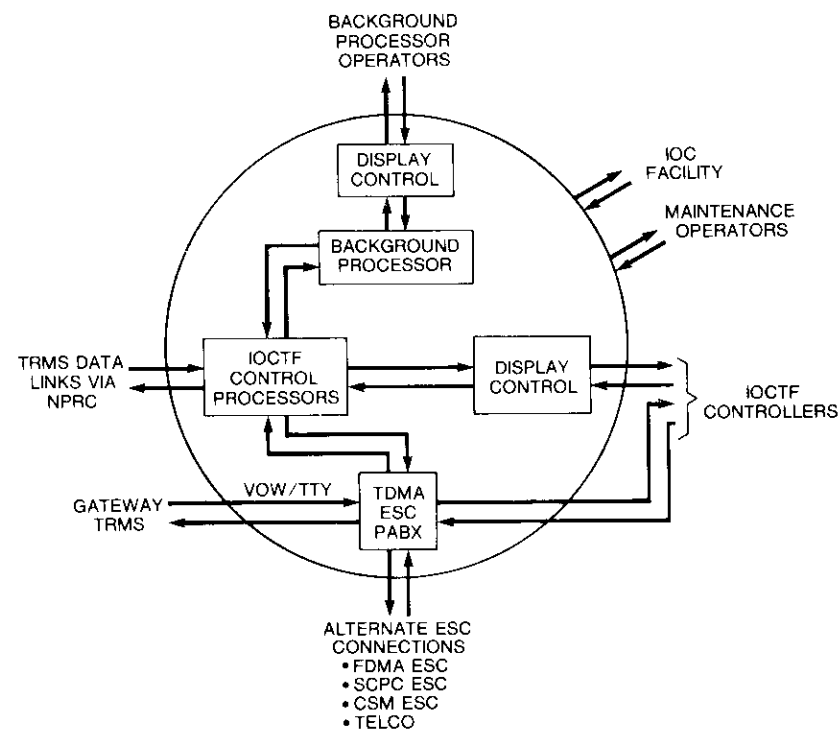
Figure 3. *IOCTF External Interfaces*

the IOCTF, others are sent only upon request of the IOCTF. The TRMS packets include network station information, event histories, orbit prediction data, RTE routine data, and TSM status and measurement data.

Selected TRMS data packets constitute the TRMS data base and are stored in files in the BGP at the IOCTF for each network. One file per TSM stores the measurement data, and a network file holds all other TRMS data requested by the IOCTF/BGP operator. Certain packets are large, and separate files are generated for each stored packet.

The TRMS data base for each of the six networks consists of one RTE data file containing the following message types:

* Ready To Initiate Countdown
* BTP Change Enable
* BTP Change Failed
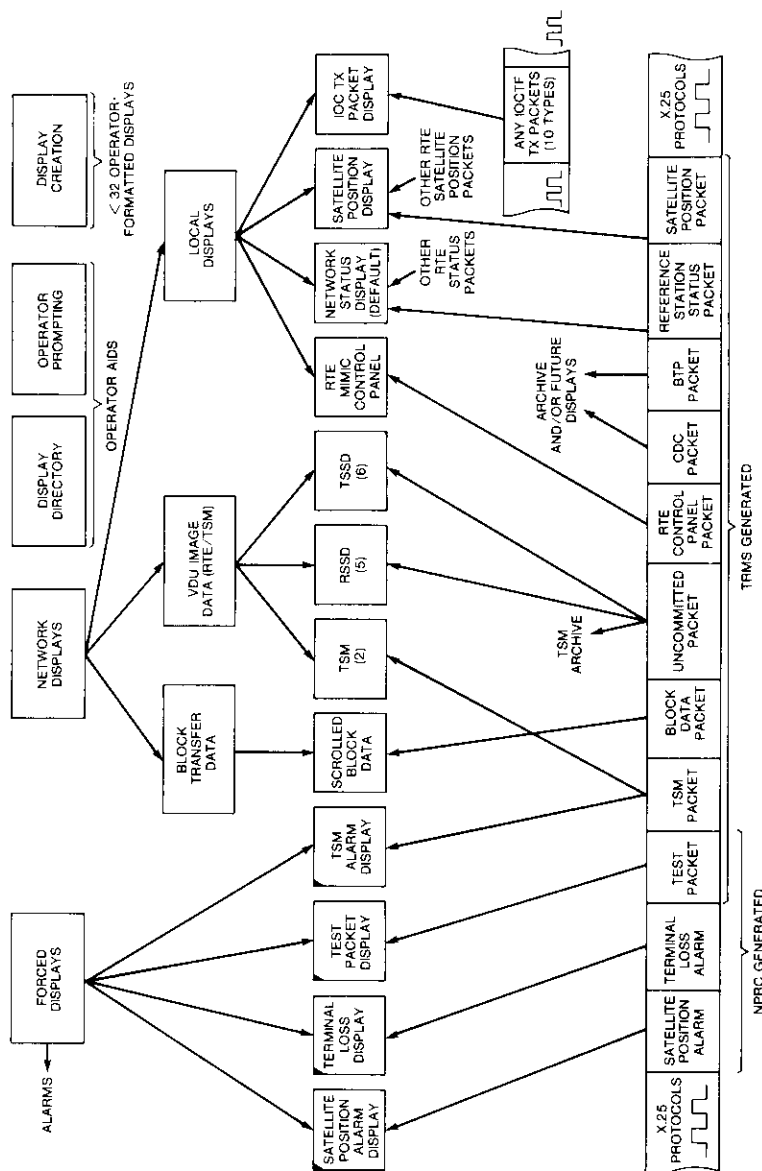
Figure 4. *IOCTF Display: Hierarchy and TRMS Packet Data Associations*

* RTE Startup Enabled
* RTE Startup Failed
* RTE Routine Data
* Control and Delay Channel (CDC)/BTP Data
* CDC Data Only
* RTE Satellite Position Alarm
* TSM Status Data.

All messages will be stored as received in an indexed, sequential file that uses the time of transmission as the primary key.

Four TSM data files contain TSM Measurement Data and the TSM 24-Hour Log. These two message types are stored in several 128-byte data blocks in an indexed, sequential file which uses the internal time in the data blocks as the primary key.

A miscellaneous data file for each completed transaction contains the following (a total of N files):

* RTE Block Transfer
* Reference Station Status Display (RSSD) Event History
* TDMA System Status Display (TSSD) Selected Traffic Event History
* RTE 24-Hour Log
* Signal Processing Equipment (SPE) Control 24-Hour Log
* TSM Block Transfer

These messages will be stored for display, one message per record, in simple sequential files. The messages are stored within each master file in chronological order. It is anticipated that the TRMS data base will be used at INTELSAT for all statistical and trend analysis applications for the TDMA/DSI system.

IOCTF network communications

Real-time control functions require effective and rapid communication of data and voice with the TRMS and traffic terminals. Figure 3 depicts the two major communications facilities used by the IOCTF to meet these requirements: the TRMS packet data link and the ESC facility.

The TRMS packet data link provides the IOCTF with the fundamental means to monitor system performance and execute control. The link connects the IOCTF to each TRMS by using dedicated transmission facilities at full duplex. Also, NPRCs broadcast certain status and satellite ranging data derived from each RTE to all other RTEs operating in a given network, thus ensuring coordinated RTE operation.

The IOCTF uses the ESC facility primarily for voice and telegraph communications, but also to efficiently distribute and verify condensed time plan (CTP) data to all system participants. The ESC facility interconnects the IOCTF with all TRMS and traffic terminals for voice, data, and TTY transactions. To ensure availability of this critical link, transmission facilities from several communications systems are utilized: TDMA ESC, FDMA ESC, single-channel-per-carrier (SCPC) ESC, communications system monitor (CSM) ESC, and ultimately, the public telephone network.

Network architecture

Specifying a total system architecture for the TRMS packet network necessitated integrating the networking products of Hewlett-Packard and Digital Equipment Corporation. Three major requirements had to be satisfied:

    a. an international communications standard (X.25) for specifying the various corresponding levels between network nodes,

    b. commercially available communications software to minimize development costs, and

    c. communication of every node in a given TDMA network with every other node in the same network, as well as communication of the IOCTF with each node in different TDMA networks.

Hence, it was necessary to specify not only the network architecture between central processing units (CPUs) within the IOCTF, but also certain levels of network architecture between the IOCTF and TRMS and between CPUs within the TRMS (see Figure 5).

The network layer for X.25, known as the packet level, provides routing and virtual circuit management. In the TRMS packet network, all CPUs are connected by permanent virtual circuits to eliminate having to establish a new virtual circuit for each communications transaction.

The DS1000-IV networking software supplied by Hewlett-Packard, based on a layered architecture, provides all the underlying layers up to the applications layer. At the physical and data link layers, the HP uses RS-232C and high-level data link control (HDLC), respectively. Any inconsistencies between the HP level-3 definition and the X.25 packet level are handled by HP-customized software. Hewlett-Packard also provides X.25 software and firmware to enable an HP-1000 to act as either data terminal equipment (DTE) or data communications equipment (DCE) in a private X.25 network. The customer assumes responsibility for providing the layers above level 3.

The DS1000-IV differs from X.25 in that flow control is handled at a higher layer than the packet level. Therefore, when DS1000-IV is used in normal operation mode with X.25, the flow control function is essentially duplicated.
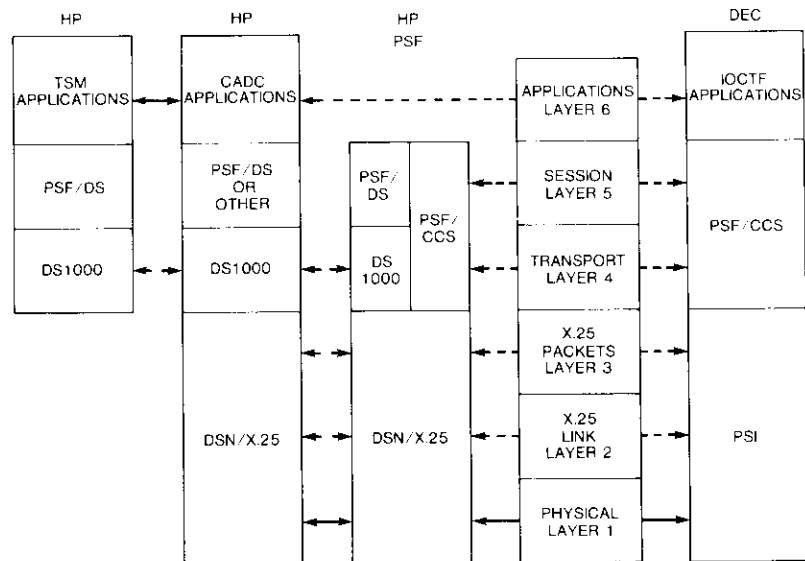
Figure 5. *Communications Software Protocol Layers*

There is no provision in the HP-supplied customized interface to delegate selected DS1000-IV functions to the X.25 layers.

Three HP-A600 minicomputers are located at each TRMS site. Two are redundant command and display console (CADC) processors, and the third is dedicated to TSM data collection and control. Each CADC communicates with other TRMS sites in the same TDMA network, as well as with the PSF processor at the IOCTF. Within this subnetwork, applications-level messages are transmitted using DS1000-IV. To each node within the subnetwork, the NPRC appears as a combination of two DCEs and a data switching exchange (DSE). Permanent virtual circuits between each of the five nodes in the subnetwork enable the messages to flow between the various TRMS sites and the IOCTF.

Within the IOCTF, the PSF processor communicates with the external TRMS networks (and internally with the IOCTF control processor) using COMSAT's communications control software (CCS), which combines the functions of transport layer and session layer software and resides on top of the three X.25 levels provided by the HP-A900 PSF processor and by the VAX-11/780 IOCTF control processor. The CCS provides point-to-point message integrity between the two different vendor CPUs and supports the message priority scheme required in the TRMS packet network.

Figure 5 shows the levels of protocol implemented for each of the processors in the TRMS packet network. Transport and session layer protocols within the PSF are provided by two major software components: the PSF/CCS and the PSF DS1000 driver software (PSF/DS). The PSF/CCS is responsible for communications in both directions across the VAX/HP X.25 interface. The PSF/DS is responsible for communications in both directions across the HP/NPRC interface. Reliable data transfer is ensured by a well-defined interface between the PSF/CCS and the PSF/DS.

Communications control software

The CCS, constructed from a collection of primary and secondary processes, is configured so that each node (host) has at least one primary and one secondary process. A CCS primary transmits messages and processes responses from the receiving secondary. A CCS secondary receives messages and initiates responses to the transmitting primary. A primary must be paired with a secondary on the opposite end of a network link because a secondary cannot transmit. As shown in Figure 6, a secondary must send its responses back to its primary via another primary/secondary pair configured in the opposite direction.

The primary, which is usually transmitting both messages and responses, uses the responses to determine how well the link is performing and to direct remedial action when problems arise. By design, the response protocol allows a response to be lost without affecting the delivery of the message, so the primary need not be supplied with feedback to ensure that a response has not been lost.

Two other programs are necessary to complete the CCS: a network generator and a priority updater. The network generator initially configures the network, assigns all channels, constructs routing tables, and stores all external applications program names. The priority updater allows a privileged operator to change the priorities of message types for a particular channel.

CCS primary

The CCS primary is a data transmitter responsible for message buffering, message priority management, flow control, response (feedback) processing, routing, and message retransmission. Its software components include a send interface (one for each transmitting applications program), queue (one per node), dequeue (one per outgoing physical link), and secondary response processor (one per node). Figure 7 shows the flow of data within the CCS primary.
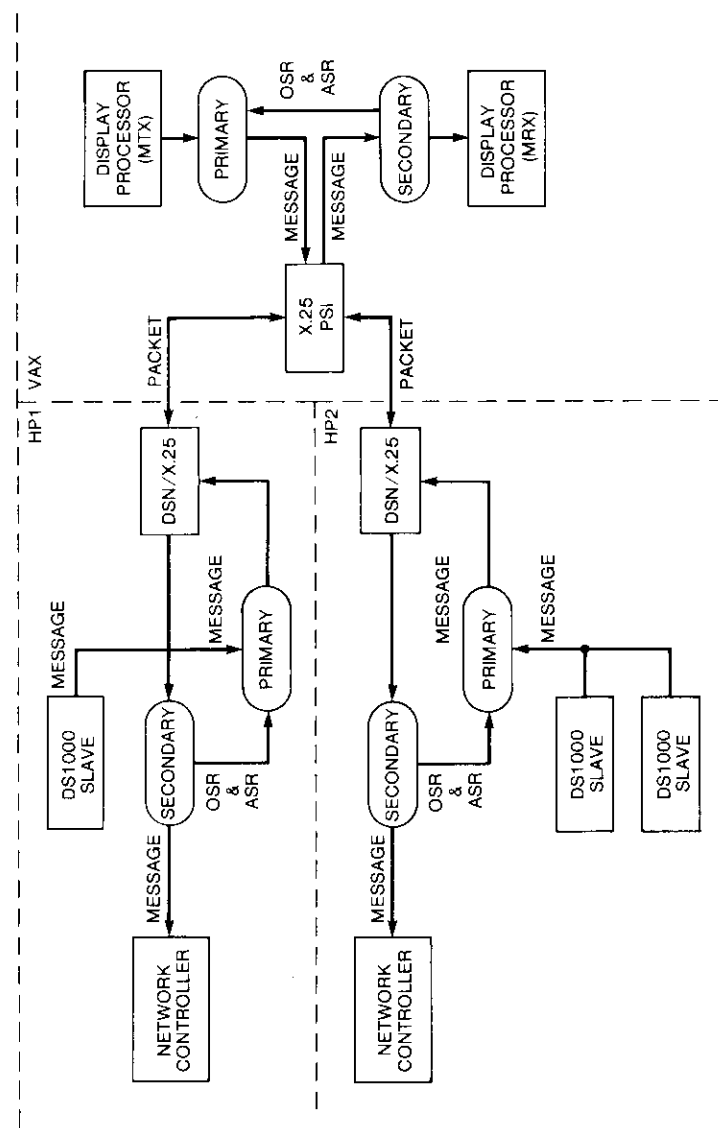
Figure 6. CCS Data Flow Diagram
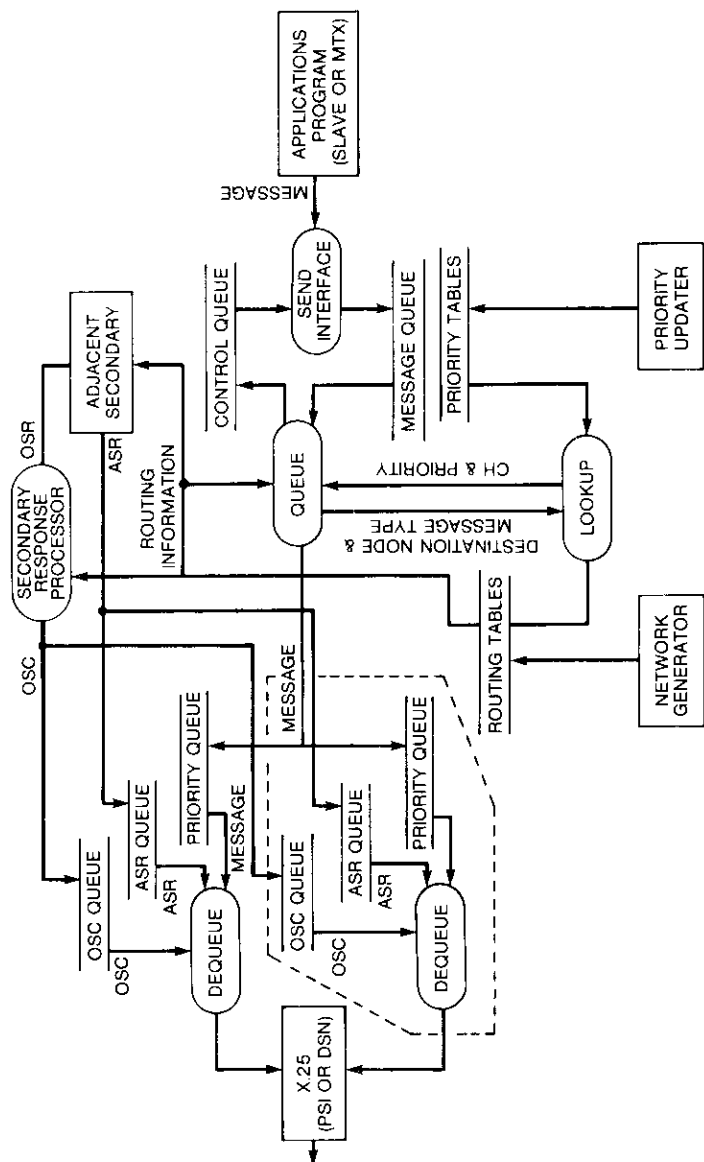
Figure 7. Primary Data Flow Diagram

The CCS send interface is linked into each transmitting applications program, allowing the program to make a simple subroutine call to obtain network access, while handling the details of communicating with the remainder of the PSF subsystem. Each message passed to the send interface by the applications program is held for input into the queue process, which causes the queue process to be scheduled by the operating system. The queue process determines if the CCS is capable of accepting the message into the PSF subsystem and notifies the send interface of the decision. When this notification is received, the send interface returns to the calling applications program and an appropriate return code is generated. If the queue process does not accept the message, then the application program may immediately retire the message or attempt transmission of a different message.

The queue process uses a lookup table to find the correct channel number and priority for the message, and routes the message to the correct dequeue process if there is more than one outgoing physical link. The dequeue process performs the following functions:

- provides the X.25 level-3 interface with messages to transmit,
- processes CCS opposite secondary commands (OSCs),
- transmits CCS opposite secondary responses (OSRs),
- transmits CCS adjacent secondary responses (ASRs),
- transmits applications program messages in priority order,
- suspends itself if it has nothing to do,
- wakes up immediately when new work is queued, and
- defers transmission of messages on flow-controlled channels.

There is one dequeue process for each outbound physical link connected to a given node.

The secondary response processor takes a given secondary response and determines the appropriate action for the primary. If an action is necessary, the secondary response processor issues a command to the appropriate dequeue process and updates the channel state accordingly.

The secondary response processor has access to the current state of any channel and is therefore capable of initiating remedial action in the event of a failure. As part of the above responsibilities, the secondary response processor implements the primary's communications protocol with the opposite secondary and handles message buffer release processing upon receipt of an acknowledge or reset.

CCS secondary

The CCS secondary receives messages, creates a response for every message received, and routes messages to the appropriate destination program. It must

be capable of buffering one window of messages for each channel supported by the node. These statically allocated buffers are referred to as window buffers. The CCS secondary consists of a receive interface (one for each receiving applications program), router (not needed if there is only one receiving applications program), secondary control (one per node), and responder (one per node). Figure 8 shows the flow of data within the CCS secondary.
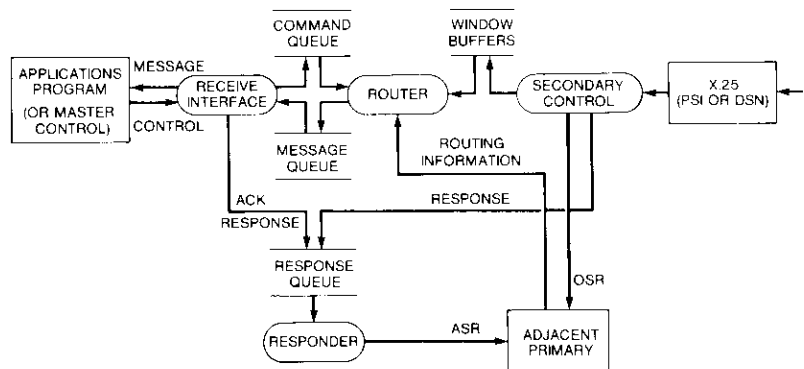
Figure 8. *Secondary Data Flow Diagram*

The CCS receive interface is linked into each receiving applications program, allowing the program to make a simple subroutine call to access the network, while handling the details of communicating with the remainder of the PSF subsystem. The receiving applications program calls the receive interface and supplies an empty buffer for the message. The receive interface issues a command to the router, which takes appropriate action. The receiving applications program may inform the router that it is busy, causing the router to begin flow control procedures for the affected channel. The router will usually deposit the next message destined for the applications program into the receive interface message queue, thereby causing the applications program to be rescheduled. The receive interface will read the message in the queue and deposit it into the applications program buffer, responding with an appropriate return code.

Several optional calls are available to the applications program. It may wait for a message to arrive, or poll for a message arrival on a particular channel or any ready channel. Individual channels may be busied or readied independently. The router retrieves messages from the window buffers on a demand basis, as directed by the applications program receive interface. The router queues requests for message data when necessary and delivers messages

to the applications program receive interface when a queued request can be satisfied. The applications program may request to be suspended until a message is received.

When a message is delivered to the receive interface, it is kept in the window buffer until the receive interface indicates that the message was received successfully. The responder releases the window buffer when the router directs it to do so. All CCS communications with a receive interface are accomplished through the router. The router passes receive interface status information to the responder, which can then forward the status information to the opposite primary.

The secondary control process is the X.25 receive interface, which is always waiting for a receive input/output operation to be completed. As messages are received, the secondary control process deposits them in an empty window buffer. If a message is received out of sequence or some other error is detected, the secondary control process issues a secondary response to the responder process, which determines what remedial action should be taken.

The responder provides feedback to the opposite primary's secondary response processor in the form of secondary responses, centralizing all secondary responses and determining what action to take. All channels are handled independently. The responder sends its responses to the adjacent primary for forwarding to the opposite secondary. Every message received by the secondary requires some response. The responder is responsible for correctly implementing the secondary's portion of the communications protocol.

Applications program interface

The CCS provides a standard interface to applications programs. An applications program is attached to the CCS through subroutines provided at the time the program is linked. The linking loader attaches a separate subroutine for each CCS primitive. The subroutines are externally declared in the applications program, and the external references are resolved by the linker when the CCS subroutine library is loaded.

The subroutine library is copied into each applications program. These subroutines perform initial error checking of the call's parameter string and attempt to communicate with the other CCS processes. All applications program communications to and from the CCS are handled by the primitive subroutine library. The interface subroutines format the request and forward it to the other CCS processes. The CCS then formats and forwards a response to the applications program's library-supplied interface subroutine. This approach allows the CCS interface to appear to the applications program as

several external subroutine calls, relieving the applications program from having to consider interprocess communications details.

Flow control procedures invoked by the CCS limit the number of messages buffered by the CCS at any given time, thus limiting the CCS buffering requirements to an acceptable level for each channel in service. Whenever messages cannot be removed from the CCS as fast as they are entered, flow control will eventually be enacted. Four conditions can cause flow control procedures to be invoked. First, a channel may be rendered busy by the destination applications program. Second, for a significant period of time the destination applications program may not receive messages on a specific channel as frequently as the source applications program sends messages. Third, the channel may be down due to a physical link outage. And finally, the network may be unable to keep up with the message input frequency of all the channels combined, causing messages to enter the CCS faster than they can be removed. This will force the CCS to reduce the message input frequency by applying flow control procedures. The *link down* condition is simply a special case of network overloading.

Network condition handling

Notification of certain conditions existing within the network will be forwarded to higher level protocol layers. It is assumed that the level-5 CCS will be notified when a link traversed by the permanent virtual circuit (PVC) of interest is down. This is determined first by link-level software, and passed to higher levels whenever a communications request is made. The CCS notification will also occur when a buffer for a requested transmission is unavailable. The layer-5 software may later attempt retransmission.

Notification of these conditions may be returned whenever the level-5 software requests that a transmission be initiated. In this case, the level-5 software will notify the calling applications program when the next CCS call is made. The level-5 software may elect to accept the applications program's transmission buffer, even though the above conditions exist. However, if the condition persists, the CCS will be forced to flow-control the sending applications program.

The primary and opposite secondary are constantly handshaking, except when the primary has no messages to send. When the primary has nothing to send, the channel will fall idle (*i.e.*, no command/response handshaking is required). Test messages may be sent periodically by the applications layer to ensure that the network is operational, but no attempt will be made at level 5 to make that determination. Nor are fault isolation procedures implemented within the level-5 CCS.

A dialogue between the primary and opposite secondary is continuously in progress when the primary has a message to send. In effect, the secondary cannot completely silence the opposite primary through the use of flow control procedures if the primary has a message to send. When flow control procedures are invoked by the secondary, the primary will continue to poll the secondary to ensure that the link is still established. This polling will continue at a specified frequency that is not overhead intensive until the secondary releases the flow control mechanism.

If polling were not implemented during a flow control condition, the link, node, and PVC could all be operational, but the opposite secondary might no longer exist. This condition must be detected at the primary as soon as possible so that system resources can be released and the transmitting applications program notified. In some cases, a malfunction may be detected at lower protocol layers, which in turn causes the higher layers to be informed.

IOCTF simulated throughput tests

The IOCTF is required to support message traffic at a rate of 4 messages per second (msg/s). Most messages are directed from the TRMS sites to the IOCTF. Simulation of throughput demonstrated the requirements for messages received by the IOCTF. Table 1 gives the messages that constitute a normal operational scenario for the IOCTF when all six networks are active and when input traffic volume equals 4 msg/s.

TABLE 1. NORMAL OPERATIONAL TRAFFIC MODES FOR THE IOCTF

MESSAGE TYPE	NUMBER OF MESSAGES	LENGTH (bytes)	PERIOD (s)	NUMBER OF SITES
RTE Routine	42	488	16	24
TSM Measurement	141	522	16	24
CDC Only	52	102	2	1
CDC/BTP	51	170	2	1

Description of the test bed

The IOCTF network simulator (INS) program can simulate message traffic from TRMS sites for up to eight networks with six TRMS sites per network. The INS program creates separate processes to generate the periodic messages. The RTE message generator process sends the RTE routines messages for all active RTE sites. Similarly, the TSM message generator process sends the TSM measurement messages for all active TSM sites. A separate process is needed for each TRMS site in order to send the CDC only or the CDC/BTP message. The message period can be changed to simulate any desired rate. Since INS

counts the messages sent during a test, the actual average message rate can be calculated.

The INS program resides in the BGP VAX processor and communicates with the IOCTF applications programs in the IOC VAX via the simulation PSF (PSF-2). The master and slave programs that reside in the actual TRMS sites and communicate with the IOCTF during actual IOCTF operation reside in the simulation (PSF-2) and the on-line (PSF-1) computers. The CCS provides the communications interface between the VAX and PSF HP processors. Messages generated by a sender program (the DP program in the IOC VAX or the INS program in the BGP VAX) are transmitted to CCS. The INS messages go from the BGP VAX to PSF-2 to PSF-1 to the IOC VAX; IOC messages take the reverse path. During testing with INS, most of the traffic is generated by INS in the BGP VAX and received by DP in the IOC VAX.

In one approach (method 1), messages coming from INS are collected by the BGP subsystem and stored in the BGP data base. The INS program is run for some set period at some desired message rate, and the BGP (received) message count is compared with the INS (transmitted) message count to establish that no messages were lost in transit. This procedure also gives the average throughput during the test by dividing the message count by time. In addition, the test tool SENDSTAT gives the instantaneous message output rate for INS. Therefore, once message transfer reliability is established, the SENDSTAT program can determine system throughput.

The SOURCE test program provides a second method (method 2) for determining throughput for the communications part of the IOCTF, which includes running the CCS in the VAX computers and in the PSF computers. The SOURCE program, running in the BGP VAX, generates messages of a selected length (e.g., 500 bytes) and sends these messages at a specified frequency. The messages are transferred to the IOC VAX by the CCS through the PSF processors, where a SINK process receives the messages.

Method 1, using INS, gives the throughput for a combined INS and IOCTF. The INS program transmits the messages for all TRMS sites in a single burst during each message period, resulting in a very high instantaneous message rate during the bursts. Method 2 gives a better indication of the throughput with real, rather than simulated, traffic because SOURCE transmits messages at an even rate which is closer to the random message arrival pattern expected from the TRMSs. Method 2 can also determine message throughput as a function of message length. Method 1 was used during formal testing, while method 2 was used during CCS development and when modifications were made to the communications system.

Acceptance testing was performed to determine the IOCTF throughput and to stress the IOCTF. In this test, INS is initially set up with SENDSTAT providing

the starting rate for sending the messages shown in Table 1, and the message volume is gradually increased. The SENDSTAT program indicates when the message traffic volume begins to load CCS. This is the point at which INS begins to receive flow control response from CCS. The IOCTF is further stressed by increasing the message volume to verify that IOCTF software will not crash at abnormally high traffic loads, although IOCTF performance and response time will degrade. The IOCTF should recover when the traffic volume returns to the normal level.

Initial test results

Method 1 gave a throughput of 3.2 msg/s, and method 2 gave a throughput of about 3.7 msg/s. The higher throughput value for the second method was expected because of the simpler transmitter and receiver programs involved, but both rates were considerably smaller than the required value of 4.

A detailed examination of these results revealed that INS was flow-controlled by the CCS at message rates above 3.2 msg/s, preventing the rest of the IOCTF from being stressed above this message rate. The INS program creates a process to generate and send each periodic message. For example, the RTE message generator process creates and sends messages for 24 sites (or all active RTE sites) to the IOCTF in a very short time as a burst. This gives a very high instantaneous message rate which causes a flow control response by CCS even at low average message rates. When INS receives a flow control response, it waits for a short time and then retransmits the message. Examination of INS source code showed that INS was waiting for 1 s before retransmission to enable the CCS to clear its backlog before the next transmission attempt. The longer wait gives a high probability for a successful transmission following a flow control response, but also limits the throughput to 3.2 msg/s because INS spends most of the time waiting under CCS flow control, thereby preventing achievement of the required message transmission rate.

The actual throughput was slightly higher than 3.2, and dropped by a small amount after INS was flow-controlled for the first time because INS waits between retransmissions, and the flow control situation activates additional logic in both INS and CCS. In addition, the INS message generator processes go into the MWAIT state when the transmitter process is being flow-controlled by CCS. The changing of state from normal to MWAIT and back to normal requires additional overhead.

Examination of the PSF processor revealed that some messages were retransmitted several times because a separate master process was used in PSF-2 for each RTE and TSM simulated by INS. These processes contend for available resources and are also frequently swapped in and out of memory, thus creating some incorrect time-out situations that result in multiple message

transmissions. In a real TDMA network, each TRMS site is serviced by a separate HP processor, whereas the simulation environment has only simulation processor and cannot easily simulate the entire network. It was later determined that DS1000 software errors (subsequently corrected) also caused the time-out conditions.

Throughput with simulated system variables

Several bottlenecks in the test setup resulted in a reduced throughput. The simulation system was modified as follows to eliminate these bottlenecks and improve throughput:

    a. The INS wait time was reduced from 1 s to 0.1 s. This meant that INS would waste much less time during flow-control situations and consequently would attempt to send more messages. However, this also meant that INS might get multiple flow controls for a single message before successful transmission because CCS might be unable to clear its backlog in the shorter 0.1-s wait time.

    b. The INS internal message buffer was enlarged so that INS could store more messages when CCS was busy. This reduced the MWAIT time for the message generator processes, but was expected to provide only a small improvement in throughput.

    c. The CCS routing tables in the BGP VAX were changed to assign a single channel for each network to serve six RTEs and six TSMs in the network. With one master serving two networks, only three masters fixed in memory were created in the simulation PSF. This eliminated the costly swapping in the previous design. The logic for the simulation masters was changed slightly to support the new traffic requirements. For example, when a message cannot be sent, the master attempts to send a message from another TRMS to maximize the output.

When tests were run with these modifications, throughput values of 3.6 and 4 were obtained with methods 1 and 2, respectively. The lower throughput with INS is a direct consequence of the message bursts INS sends to CCS. With the current setup, INS sends a burst of eight messages (four RTEs and four TSMs per network) on each channel. The CCS currently has a window size of 7, which means that it must flow-control the INS during every routine data period. The PSF-2 master handles two channels and 16 messages during a single burst, but there is less resource contention because there are fewer masters, and the new simulation masters are more efficient for transmitting a large number of messages.

Throughput can be further improved at this stage by modifying INS so that it will not send message bursts, but will send single messages at shorter,

regular intervals. Such a message pattern is closer to the anticipated random message pattern in a real TDMA network where the TRMS sites send messages independently of all other sites. In this test, a single RTE and TSM from each network was put on active status. The message frequency was then increased by a factor of 6 to compensate for the reduction in the number of TRMS sites. This means that INS sent only two messages per channel during a single transmission, but with a higher frequency, giving the same average message rate. The CCS can handle this load without flow control because INS is not sending a large number of messages in bursts. The INS output can be further increased by activating only one network per master (a PSF-2 master handles two channels and two networks during simulation) and by increasing the frequency as required to keep the message rate at the previous value.

A final modification would consist of using only RTE or TSM data at a further doubling of the frequency. The INS message output is increased in this case because INS has to support only one periodic message generator instead of two. When throughput tests were run with the new RTE and TSM configurations, methods 1 and 2 showed nearly identical throughput results.

Throughput with DS1000 parameter changes

The RTE and TSM messages and CDC/BTP messages exceed 128 bytes, which was the previous packet size used in the simulation PSF. Consequently, each message was transmitted from the BGP VAX to the simulation PSF in two or more packets, causing the simulation masters in PSF-2 to wait for the complete message to arrive before they could signal a successful reception condition to the message-originating program. The waiting period can be significantly reduced if the entire message can be transmitted in a single DS1000 packet. Increasing window size from 2 to 7 would allow more messages to be buffered in PSF-2 at level 2. Again, these changes only refer to the simulation system and did not require any modification to PSF-1 or IOCTF.

Tests run using these modifications to the DS1000 parameters gave throughput values of 4.2 or more for both methods. In addition, the throughput for method 1 (with INS) was obtained with the normal configuration of 24 TRMS sites and with INS sending RTE/TSM data at the normal 16-s rate. The CCS in the BGP VAX (and PSF-2) can forward INS messages as soon as they are handed to CCS, so there are no backlogs in CCS and the CCS windows (message buffers) remain unfilled even when INS is sending data in bursts.

Summary and conclusions

Table 2 summarizes the IOCTF throughput results obtained in this study. As described above, method 1 uses INS to generate message traffic from the

TRMSs, and method 2 uses the SOURCE and SINK programs to exercise only the communications part of the IOCTF system. The throughput requirement is 4 msg/s. Initial throughput measurements were made with two master programs assigned in the simulation PSF to handle each TRMS site. Because system throughput was significantly smaller than required, two major modifications were made to the simulation part of the IOCTF. First, a single master process was assigned to handle all TRMS sites associated with two networks. Second, DS1000 window size and packet size parameters were changed. After this second change, IOCTF met and exceeded the throughput requirement. It should be emphasized that the measured message throughput was for the combined system (consisting of the IOCTF part and the simulator part) and represents the throughput limit for the simulator part.

TABLE 2. IOCTF THROUGHPUT RESULTS

METHOD	MEASUREMENT APPROACH	TWO MASTERS PER TRMS	ONE MASTER FOR TWO NETWORKS	DS1000 WINDOW SIZE AND PACKET SIZE PSF-2
1	With INS	3.2	3.6	4.2
2	With SOURCE and SINK	3.7	4.0	4.2

In a TDMA system, the need to collect, store, and display information from numerous network nodes in a timely manner and with a high degree of reliability is paramount. These goals have been achieved in the INTELSAT IOCTF, and the throughput performance of a real-time network control facility will have a significant impact on the long-term reliability and availability of the TDMA network.

This study has revealed that the IOC VAX shows only 40-percent CPU utilization, even at a message rate above 4 msg/s. The IOC network monitor process also shows that the incoming CCS channels are practically empty, which means that the IOCTF message receiver process is reading incoming messages as soon as they arrive from the CCS and can support a much higher throughput. Finally, the TSM measurement period may be increased from 16 to 64 s, reducing the expected operational message rate to below the 4 msg/s value. If the TSM data frequency is thus reduced, the IOCTF will have even more reserve capacity to handle peak traffic loads and to support six fully configured TRMS networks.

References

[1] B. A. Pontano *et al.*, "The INTELSAT TDMA Control and Monitor System," Satellite Communications Conference, Ottawa, Canada, June 14–17, 1983, *Proc.*, pp. 12.8.1–12.8.4

[2] J. F. Phiel and C. R. Thorne, "INTELSAT TDMA System Monitor," Sixth International Conference on Digital Satellite Communications, Phoenix, Arizona, September 19–23, 1983, *Proc.*, pp. IV–14—IV–21.

[3] C. A. King, "Burst Time Plan Development in the INTELSAT System," Satellite Communications Conference, Ottawa, Canada, June 14–17, 1983, *Proc.*, pp. 24.8.1–24.8.3

[4] G. D. Hodge *et al.*, "INTELSAT Operations Center TDMA Facility," *International Journal of Satellite Communications*, Vol. 3, Nos. 1 and 2, January–June 1985, pp. 71–76.

Gene D. Hodge received a B.S.E.E. from the Illinois Institute of Technology, a B.S. in Mathematics from the University of Texas at El Paso, and an M.S.E.E. from George Washington University. As Executive Director of the System Development Division at COMSAT Laboratories, he is responsible for technical direction and project management control over the design and implementation of complex computer-based systems developed under external contracts or in support of COMSAT lines of business. Recently, he managed COMSAT's involvement in the INTELSAT Operations Center TDMA Facility and the INTELSAT TDMA System Monitor development programs, which are related to the deployment of INTELSAT's worldwide TDMA system facilities.
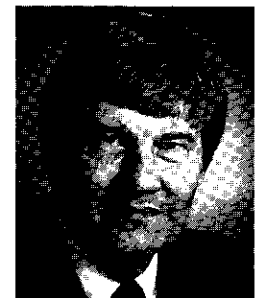
Roger J. Colby has been a Member of the Technical Staff of INTELSAT's Communication Engineering Department since 1980. He has been responsible for major sections of the INTELSAT TDMA/DSI traffic terminal, reference terminal, and IOC specifications. Dr. Colby holds an Honors Degree in Electrical Engineering from Lanchester Polytechnic, England; his Ph.D. studies were concerned primarily with hybrid digital modulations. He then worked for the British Post Office, Satellite Systems Division, where he was an Executive Engineer at the laboratories at Goonhilly Earth Station. He was responsible for a team researching digital communications for satellites and participated extensively in CEPT and ESA studies concerning the TDMA aspects of the European OTS and ECS satellites. In 1978, Dr. Colby was an INTELSAT nominee from the United Kingdom, assigned to the Communications Processing Laboratory at COMSAT. In this capacity, he was involved with the INTELSAT TDMA field trial and became Team Leader of COMSAT's support for the revised INTELSAT TDMA/DSI specifications.

Conny L. Kullman, a Senior Engineer with INTELSAT's Technical Programs and Projects Division, received an M.S.E.E. degree from Chalmers University of Technology, Gothenburg, Sweden. He has had overall responsibility for the TDMA network software, amounting to 800,000 lines of code residing in more than 45 different computer designs replicated worldwide. Currently, he is also responsible for the integration and testing of the INTELSAT VI TT&C system. Prior to joining INTELSAT, Mr. Kullman was a Senior System Design Engineer at SAAB Space AB, specializing in real-time, fault-tolerant, on-board computer systems.
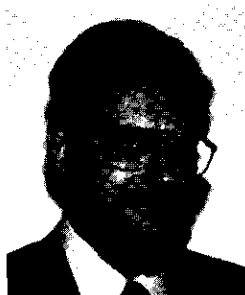
Barrick H. Miller received a B.E.E. from the Georgia Institute of Technology in 1979. He is currently Manager of Computer Engineering for the StarCom product line at COMSAT Corporation, where he is responsible for systems integration of computer hardware and software in VSAT data networking products and service offerings.
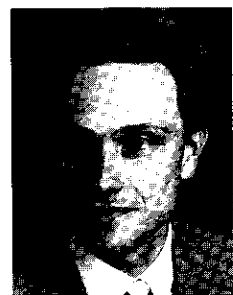
The INTELSAT TDMA system monitor*

J. S. BARNETT, C. R. THORNE, H. L. PARKER, AND A. BERNTZEN

(Manuscript received July 12, 1985)

Abstract

This paper discusses the operational features of the measurements performed in the INTELSAT time-division multiple-access (TDMA) system monitor, which is used to assist in the operation of the TDMA digital speech interpolation network. The four routine measurements discussed are relative burst power, carrier center frequency, burst position error, and pseudo bit error rate. Three additional measurements can be made: transponder operating point, transmit e.i.r.p., and carrier-to-noise ratio. Normally, the TDMA system monitor cyclically checks each traffic and reference burst in up to four transponders to retrieve records of system performance and to indicate out-of-tolerance conditions at the reference station and the INTELSAT operations center. When required, the monitor may be taken under more direct control for measurement of selected bursts in troubleshooting. System design, software architecture, and hardware implementation measurements are described and system performance is assessed.

Introduction

The INTELSAT TDMA system consists of four independent networks, each controlled and monitored by four TDMA reference and monitor stations

---

* This paper is based on work performed at COMSAT Laboratories under the sponsorship of the International Telecommunications Satellite Organization (INTELSAT). Views expressed are not necessarily those of INTELSAT.

(TRMSs) [1]–[3]. This paper describes the role and features of the TDMA system monitor (TSM) resident in each TRMS.

The TSM shown in Figure 1 is not required to perform simultaneous measurements on the four transponders. Because simultaneous monitoring of all down-links would require higher central processing speed in normal operation, hardware requirements are reduced by hopping among the down-links. Depending on the burst time plan, a complete cycle of measurements on all four transponders requires less than 4 minutes, including calibration time.

Each TSM performs the following measurements on all bursts received from the reference station from any transponder: relative burst power, burst position error, quadrature phase-shift keying (QPSK) carrier frequency, pseudo bit error rate (PBER), satellite transponder operating point, and carrier-to-noise ratio. Additionally, the TSM measures the e.i.r.p. of the reference burst (RB) from the colocated reference terminal equipment (RTE).
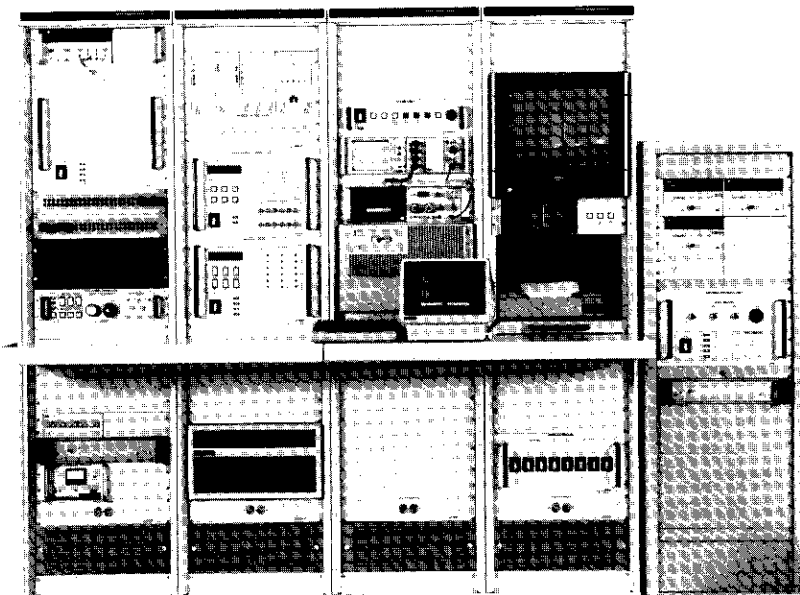
Figure 1. *The TSM System*

The TSM equipment derives the following important items from the INTELSAT TDMA frame structure [3]:

> *a. Start of Frame (SOF).* The epoch which defines the start of each 2-ms frame, divided into 120,832 symbol periods for the TDMA frame.
> *b. Carrier-and-Timing Recovery Period.* A sequence of 128 alternate 1's and 0's which is used for measurement of noise and transponder operating point.
> *c. Unique Word (UW).* The last bit of the UW relative to the SOF, which defines burst position.
> *d. UW Identification.* The UW identifies the type of burst once each 16 frames, with UW1, RB1; UW2, RB2; and UW3, the traffic burst.

Each TSM meets an availability requirement of 0.99 with a mean time to restore (MTTR) of 5 hours when there is no redundant equipment at each site. The 87 hours of TSM nonavailability per year is inconsequential for the monitoring function.

Table 1 summarizes measurement performance requirements for the INTELSAT TSM. Typically, these measurements require the accurate determination of a set of parameters for computer processing to statistically combine burst samples and the application of various calibration transformations. TSM testing in-plant and on-site has demonstrated compliance with Table 1 requirements.

The TSM system

Figure 2 shows the basic TSM architecture, its integration into the reference station, and its interface with the RTE. The TSM system is designed to avoid interruptions or harmful interference to the RTE or the TDMA/digital speech interpolation (DSI) equipment resulting from system operation or failure. The TSM can operate in five distinct modes: initialization, routine measurement, diagnostic measurement, calibration, and maintenance. In the routine measurement mode, four basic measurements are performed (relative burst power, burst position error, carrier center frequency, and PBER). Three additional measurements can be made under the diagnostic mode: transponder operating point, transmit e.i.r.p., and carrier-to-noise ratio.

The four principal subsystems of the TSM are the TSM processor, the TSM measurement subsystem, the TDMA controller, and the antenna interface. The TSM processor subsystem receives, measures, and controls INTELSAT Operations Center (IOC) data. The TSM measurement subsystem processes the TDMA IF signal under control of the TSM processor. The TDMA controller

TABLE 1. TSM MEASUREMENTS

MEASURED QUANTITY	MODE APPLICABILITY	ACCURACY	MEASUREMENT CONSTRAINTS	PROGRAMMABLE LIMIT CHECK RANGE
Relative Burst Power	Routine and diagnostic	±0.3 dB (repeatability ±0.15 dB)	Signal dynamic range of +3 dB to −7 dB	0 ± 3 dB
Recovered Carrier Frequency	Routine and diagnostic			
• Reference Burst		±3 kHz	—	0 ± 100 kHz
• Traffic Burst		±0.2 kHz	Burst length ≥ 2000 symbols	0 ± 100 kHz
Burst Position Error	Routine and diagnostic	±2 symbols	—	0 ± 32 symbols
Pseudo Bit Error Rate	Routine and diagnostic			
• Reference Burst		±21% to 95% confidence interval	True BER range of 10^{-2} to 10^{-4}. Symbols observed $\geq 1.4 \times 10^5$	Fixed: PBER $\geq 1 \times 10^{-3}$
• Traffic Burst		±21% to 95% confidence interval	True BER range of 10^{-2} to 10^{-5}. Symbols observed $\geq 1.0 \times 10^6$	Fixed: PBER $\geq 1 \times 10^{-3}$
Transponder Operating Point	Diagnostic	±1.0 dB	—	None
Transmit e.i.r.p.	Diagnostic	±0.5 dB	—	None
Carrier-to-Noise Ratio	Diagnostic	±0.5 dB	—	None
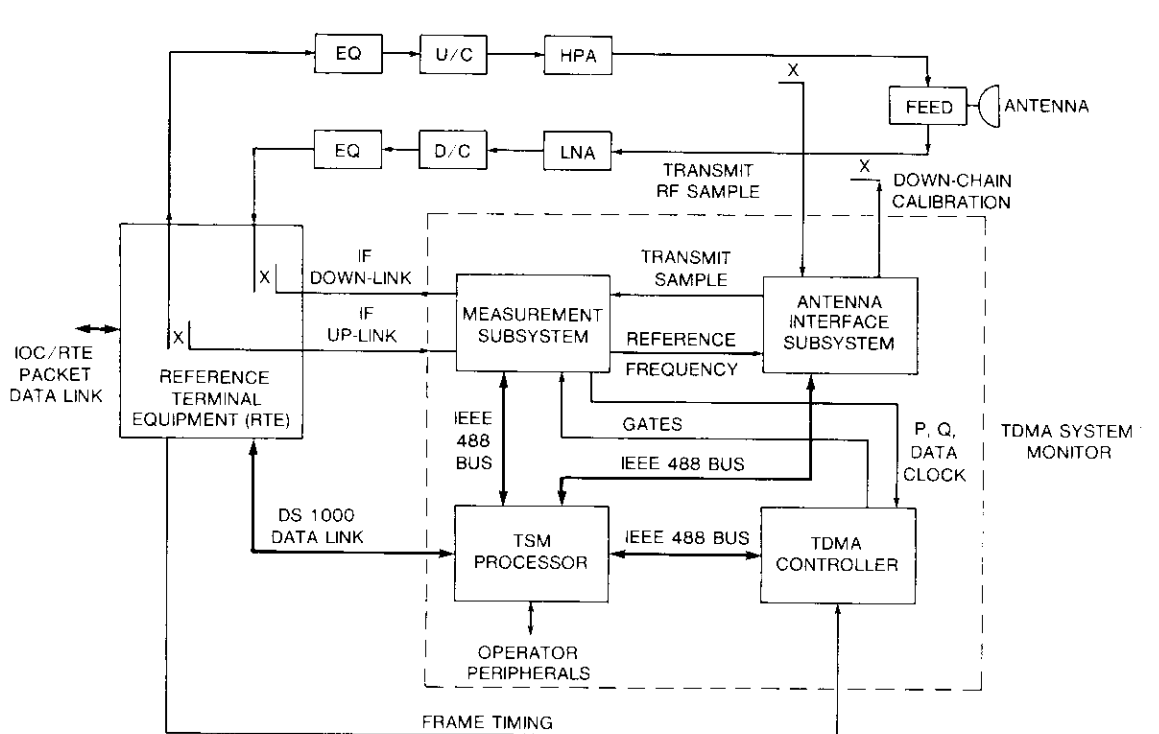
Figure 2. *TSM System Configuration*

subsystem synchronizes the TSM to the TDMA frame. The antenna interface subsystem provides remotely controlled injection of a pilot signal into the low-noise amplifier (LNA). The function and specifications of these four TSM subsystems are described in Appendix A. Appendix B discusses the TSM software architecture.

Relative burst power measurement

Figure 3 shows the burst power measurement system. Each 120-Mbit/s burst occupies an entire 80-MHz transponder which operates at an input backoff of 2 to 3 dB.
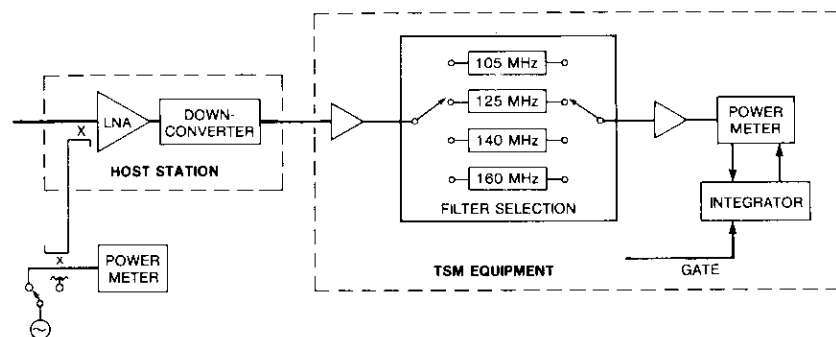
Figure 3. *Simplified Gain and Power Measurement Block Diagram*

Normally, the TSM cyclically checks each traffic and reference burst in up to four transponders to measure system performance and to indicate out-of-tolerance conditions at the reference station and the IOC. When required, the TSMs may be taken under more direct control for measurement of selected bursts in troubleshooting.

Measurement technique

Burst power can be measured by two techniques. The first, which uses the RF system monitor [4], [5], involves an analog power meter gated at the occurrence of the burst. A conversion factor is needed to account for the ratio of the measurement gate width to the frame length. In the INTELSAT system, this factor amounts to about 33 dB for the RB.

The other technique uses a peak-reading power meter with a built-in narrow sample gate. Problems arising from data scatter due to the nature of the QPSK spectrum and the random fluctuations of the noise level are eased by using an integrator after the preamplifier and ahead of the sampling circuit. The

integrator is designed to sample the selected burst power parameter by utilizing a measurement gate from the measurement control unit. The selected burst is sampled for 64 consecutive frames and then the power meter is triggered to read the integrator output.

Reference burst power

The TSM measures individual burst power and compares and displays the results in decibels relative to a reference power level of one of the previously measured RBs.

Determination of RB power referred to the LNA input requires several measurements to remove system noise from the carrier and to ensure that changes in gain within the earth station equipment and the TSM are not reflected in the displayed RB power. These measurements are QPSK carrier-plus-system-noise power, system noise power during the QPSK burst, and down-chain gain from the LNA input to the IF power meter.

Proper calibration constants must be introduced to account for coupler losses for calibrating oscillator-to-LNA input, TSM input-to-output losses relative to the 105-MHz filter path, and the noise bandwidth of each filter.

The RB power (carrier plus noise) is measured through the 140-MHz filter, with a bandwidth of about 85 MHz. The noise measurement is made during the carrier and timing recovery period through a filter centered at 160 MHz. Figure 4 shows that only two spectral lines exist; however, it is important to note that during this time the satellite transponder noise, near saturation, is suppressed. Finally, in order to make the correction from carrier-plus-noise to carrier level, the noise bandwidths of these two filters must be known, as well as the difference in gain of the two filter paths.
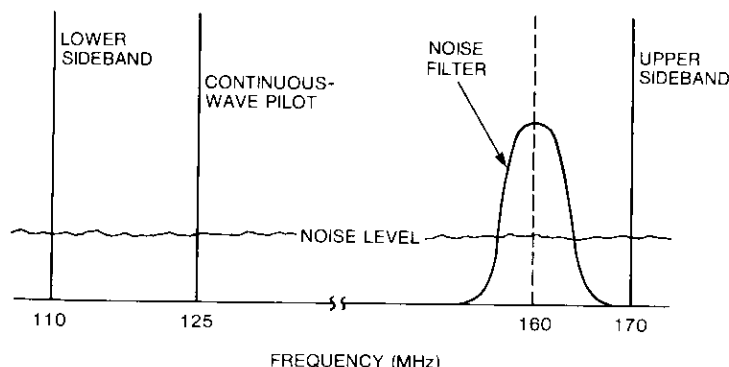
Figure 4. *IF Spectrum During Carrier and Bit Timing Recovery*

To refer the measured IF power to the LNA input, the gain between the LNA input and the TSM IF power meter is measured by inserting a pilot signal at the LNA and ascertaining its level at the TSM. The accuracy of the gain measurement depends on the calibration of the two power meters and the coupler loss. The pilot signal power is measured at RF before the injection coupler and at the TSM IF output. A noise power reading is also taken to enable correction of the pilot-plus-noise reading at IF with reference to a pilot signal IF level measured during the frame idle time period when no bursts are present.

Received relative burst power is the measured power of any burst compared to the power of the selected RB. The burst power level at the LNA input is measured in the same manner as described for RB power measurement. After this measurement and the corrections to refer measured burst power to the LNA input, relative power is calculated by subtracting the RB measured power.

The TSM can also measure the transmit burst power of the colocated reference station. The TSM down-converts the transmit signal to the 140-MHz IF and adds a signal at 105 MHz to calibrate the gain of the measurement path from the high-power amplifier (HPA) to the TSM IF power meter. The measurements are essentially identical to those made on received signals, except that the carrier-to-noise ratio is assumed to be high enough that carrier-plus-noise correction is not required.

Carrier center frequency measurement

Carrier center frequency measurement is another of the four measurements performed on either RBs or traffic bursts in the routine measurement mode or the diagnostic mode.

Measurement technique

As the reference burst is much shorter than the traffic burst, a longer measurement time is required to achieve identical accuracy. Considering the different lengths of the two kinds of bursts, the accuracy for the RB is about an order of magnitude less than that for a traffic burst.

A reciprocal frequency counter with an external gating capability was chosen for several reasons. First, external gating allows control of the starting time of measurement and the exact duration over which a measurement is to be formed. Second, external gating allows positioning, as needed, of the measurement window within the RF burst to avoid transients at the beginning and end of the RF pulse. Third, with external gating, burst frequency measurements can be averaged over several frames, thus improving the

worst-case rms resolution by $\sqrt{N}$ over that of a single pulse measurement, where N is the number of averaged samples. And finally, the reciprocal counting technique, which operates on a synchronized gating, helps reduce measurement uncertainty.

Figure 5 shows the measurement sequence of a typical reciprocal counter for a single-shot frequency, which is initiated at $T = 0$ when reset. The event register begins accumulating counts at time T_{es} where the input signal crosses the threshold. The opening of the events register causes the time register to begin accumulating time counts with the leading edge of the next clock pulse of the internal, high-speed, 500-MHz clock (T_{cs}). At the end of the selected main gate time, T_{gc}, the events register is disarmed and closed when the input signal reaches threshold (T_{ee}). This in turn disarms the time register and allows it to close with the next clock pulse (T_{ce}). Using the data contained in the time and event registers, the frequency can be expressed as
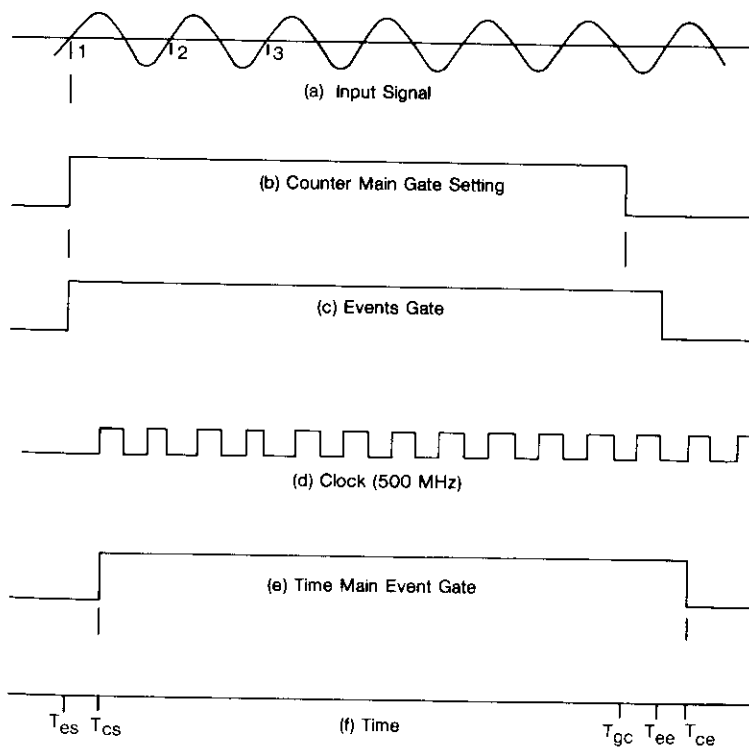
Figure 5. *TSM Counter Measurement Timing*

the number of events in a measurement window divided by the window width.

As shown in Figure 5, the measurement accuracy of the clock pulse is within ±2 ns. The best achievable single-shot frequency measurement accuracy of a 140-MHz carrier is ±279 kHz for the RB and ±9.333 kHz for the traffic burst, for which the measurement gate periods are 1 μs and 30 μs, respectively.

The reciprocal counter incorporates frequency averaging capability under externally gated conditions. Averaging is accomplished when the measurement gate width is smaller than the counter main gate width. In this case, the counter will collect N measurements, where N times the measurement gate width is equal to or greater than the counter main gate width.

The number of samples needed for achieving the required accuracy is over 2,400 for a measurement frequency at 140 MHz. At a frame rate of 2 ms, the total measurement time would then be 4.8 s for the burst frequency measurement, which is too long. Performing burst frequency measurements at a carrier frequency of 2 MHz rather than at 140 MHz results in improved measurement accuracy and speed. This frequency translation is accomplished by down-converting the 140-MHz signal using a very high-frequency local oscillator locked to the frequency standard.

The number of one-way threshold crossings of the input signal in a measurement window are counted. As shown in Figure 5, the measurement window will stretch as needed to always include integral multiples of the input signal. The window duration is determined by counting the number of clock pulses of the 500-MHz internal clock, which is locked to the frequency standard. As the accuracy of this measurement is 2 ns (one clock pulse), it is clear that if the number of events can be reduced significantly for a given window width, the accuracy will improve considerably. There is no truncation error in measuring the events.

Burst frequency measurement

From the host station equipment, the TSM receives a down-converted IF signal which may drift slightly in frequency. Since the TSM should measure only external TDMA burst frequency offsets, an injected pilot signal at the LNA, locked to a rubidium standard, is used to measure the offset of the host station down-converter.

Burst carrier center frequency measurement is made with reference to the frequency of the phase-locked oscillator in the demodulator. The 140-MHz phase-locked oscillator signal is down-converted to 2 MHz before being counted. After the frequency is measured, the raw data value is corrected

for the frequency offset contributed by the host station down-converter and for calibration constants of the gated measurements counter.

Counter calibration, using a 2-MHz signal derived from the rubidium standard, is performed at three different gate widths for the RB, the down-converter frequency offset, and the traffic burst.

Burst position error measurement

The position error of a burst, defined as the difference in time (symbol periods) between its expected arrival in the burst time plan and its actual arrival, is another of the four routine measurements performed. Arrival times are counted from the start-of-receive-frame (SORF) signal to the last symbol of the UW of the measured burst. The SORF itself is obtained by applying a fixed offset to the instant of the last symbol of the UW of either of the two RBs (primary) received from the designated timing and reference transponder (TRT).

Since the TSM employs transponder hopping to minimize measurement hardware and complexity, it periodically accesses the transponder from which SOF timing is derived from the TRT. Valid burst position error measurements can only be performed using frame timing from the TRT, since other transponders in the synchronized community reflect multisymbol variations in frame timing which arise from differences in RF, IF, and digital processing paths. To overcome this source of measurement error, the TDMA controller uses frame sync pulses of the colocated RTE because this timing is continuously generated from the TRT.

As shown in Figure 6, a differential time delay exists between the IF path to the TDMA controller and the derived frame sync path through the RTE. While the problem is shown for the down-link IF, in practice the up-link IF problem is more severe since the TSM input signal is sampled after the HPA, where greater differential delays are encountered.

The TDMA controller automatically compensates for a time shift by synthesizing the correct frame sync in the following manner. The microprocessor-stored program employs a control algorithm which first establishes internal frame sync using RTE pulses without phase correction. This is followed by a programmed search on either side of the frame sync for the RB, using a stepped aperture to gate UW detections. Upon RB detection, a dwell cycle is programmed to carefully measure position error within the aperture, which provides an accurate determination of the magnitude of the shift in symbols. Using the measured shift and a determination of whether RTE frame sync leads or lags behind the internal TSM frame, the program computes the absolute position (in symbols) of the RTE frame sync relative
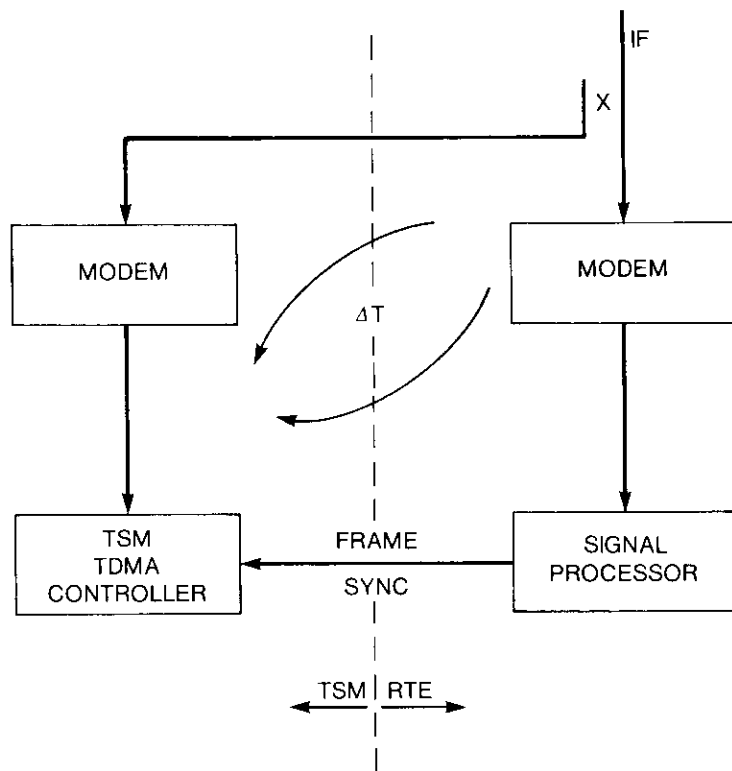
Figure 6. *RTE/TSM Differential Delay Paths*

to the TSM internal frame. The controller utilizes the phase-variable, synchronous counter circuit to synthesize the frame synchronization using the RTE sync pulse. The measured RTE sync pulse position is down-loaded to the frame counter load input (count IN). Thereafter, each time an RTE sync pulse is received, the symbol counter is preset to the computed value. The local symbol clock then drives the counter upward until the maximum count comparator detects the last symbol value (120,831), whereupon the symbol counter is reset to zero and a corrected frame sync is generated.

The synchronization process allows TSM to maintain continuous and accurate frame synchronization relative to TRT without the additional IF and demodulator hardware necessary for synchronization from TRT RBS. The penalty is ±1 symbol of additional burst position measurement uncertainty due to the relocking of RTE sync pulses with the local TSM clock.

After establishing frame synchronization using RTE SORF pulses, the TSM measures burst position error by counting the number of symbols from the

leading edge of a predictive aperture to the occurrence of UW detection. The measurement is processed and displayed in + or − symbols up to the maximum of 32 symbols permitted by the UW detector aperture. Including a time delay calibration accuracy of ±1 symbol, burst position error measurement is accurate to within ±2 symbols.

In the routine measurement mode, burst position measurements are performed for 256 consecutive frames, and peak and average position errors are computed and displayed. In the diagnostic measurement mode, the peak and average values of the burst position error are measured over 16 consecutive frames.

Pseudo bit error rate measurement

The final of the four routine measurements, PBER measurement, provides a means of estimating the quality of the QPSK/TDMA links in a relatively short measurement time without interrupting operation or having knowledge of the transmitted bit sequence. QPSK modems employ two sets of decision thresholds to distinguish between the four possible signal states. The PBER monitor is implemented by including an additional set of decision thresholds which create four pseudo error regions, as shown by the vector diagram in Figure 7. The probability of a pseudo error, P_p, is the probability that the signal vector will fall into the pseudo error regions at the sampling time. The true probability of bit error, P_e, is the probability that the signal vector, as a result of channel impairment, will cross a decision threshold at the sampling time.

Snyder and Hersey [6] have previously shown that log P_p and log P_e are linearly related over a wide range of channel conditions. Thus, pseudo errors
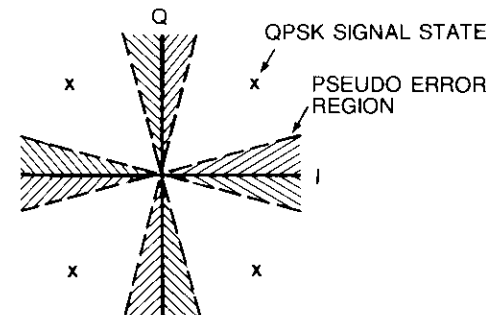
Figure 7. *Pseudo Error Regions for PBER Measurement*

can be used to estimate BER. Basically, a pseudo error is sensed by comparing the analog P and Q outputs of the demodulator to the tangents of the angles defining the pseudo error regions. The pseudo error counter is gated ON after burst UW detection and gated OFF after 4,000 symbols for typical traffic bursts or 60 symbols for RBs.

In the routine mode, pseudo error counts are accumulated over a fixed number of frames (approximately 250 frames for traffic bursts, 2,300 frames for RBs). This enables the observation of 1×10^6 symbols for traffic bursts and approximately 1.4×10^5 symbols for RBs.

The TSM processor determines BER from a stored calibration of pseudo error rate vs BER. The calibration at PBER vs BER is obtained by using a BER test set on a looped test mode. The operator establishes an accurately known E_b/N_o ratio at the QPSK demodulator input and measures the BER; then at each ratio the TSM measures the pseudo error rate. The data for BER vs PBER are stored in the TSM processor.

The accuracy of the measurement has been specified to be ± 21 percent, with a confidence interval of 95 percent. Because the errors are random, the error rate cannot be uniquely determined in a finite measurement interval. Therefore, an error rate measurement is always an estimate of the actual error rate. The accuracy requirement recognizes the limited number of symbol periods. Consequently, statistical variations in an error rate measurement of limited duration are bounded by the confidence interval expressed as a percentage. In other words, 95 percent of the processed measurements will be within ± 21 percent of the actual BER.

The use of pseudo error regions, which are functions of angle, makes the pseudo error counts insensitive to amplitude fluctuations; however, a small deviation due to demodulator phase errors is introduced and additional calibration errors are encountered. In the routine mode, the PBER monitor is expected to meet specifications for traffic bursts having actual BERs of 1 in 10^2 to 1 in 10^5. RBs, which provide only 60 observed symbols per frame, are accurately measured over actual BER ranges of 1 in 10^2 to 1 in 10^4.

Performance results

The TSM was qualified during in-plant testing to assess its performance against the specification requirements. In all cases, performance was within the limits required. Table 2 depicts the typical TSM performance under laboratory conditions where the input parameters can be closely controlled. Field experience has demonstrated that the repeatability of the results remains unchanged.

TABLE 2. TSM PERFORMANCE

RELATIVE POWER MEASUREMENT

ACTUAL RELATIVE POWER (dB)	MEASURED RELATIVE POWER (dB)	STANDARD DEVIATION (dB)
3.0	3.10	0.14
0.0	0.10	0.13
−2.0	−2.01	0.10
−4.0	−4.10	0.09
−6.9	−6.95	0.13

BURST FREQUENCY MEASUREMENT

RELATIVE POWER (dB)	FREQUENCY OFFSETS (Hz)	MEASURED ERROR RELATIVE TO OFFSETS (Hz)	STANDARD DEVIATION (Hz)
3.0	−58,300	−2	42
0.0	0	−24	51
−2.0	0	16	56
−4.0	0	−57	51
−6.9	58,300	−8	58

PSEUDO BIT ERROR RATE MEASUREMENT

RELATIVE POWER (dB)	E_b/N_o (dB)	PBER	STANDARD DEVIATION
3.0	18.1	2.6×10^{-7}	5.9×10^{-8}
0.0	15.1	1.6×10^{-6}	2.6×10^{-7}
−2.0	13.1	6.0×10^{-6}	6.6×10^{-7}
−4.0	11.1	3.4×10^{-5}	2.6×10^{-6}
−6.9	9.2	6.0×10^{-4}	1.9×10^{-5}

Conclusions

The design of the INTELSAT TDMA TSM involved innovative solutions to meet specified measurement accuracy and timing requirements. A monitoring system which routinely causes no network interference was built, and achievement of the required accuracy was demonstrated in the laboratory under controlled conditions. Initial experience in the field under operational conditions has confirmed the stability and reliability of the measurement system. The TSM has proven to be an effective tool in the operation of the INTELSAT TDMA network.

Acknowledgments

References

[1] B. Pontano *et al.*, "A Description of the INTELSAT TDMA/DSI System," Fifth International Conference on Digital Satellite Communications, Genoa, Italy, March 1981, *Proc.*, pp. 327–334.

[2] B. Pontano *et al.*, "The INTELSAT TDMA/DSI System," *IEEE Transactions on Selected Areas in Communications*, Vol. SAC-1, No. 1, January 1983, pp. 165–173.

[3] B. A. Pontano, S. J. Campanella, and J. L. Dicks, "The INTELSAT TDMA/DSI System," *COMSAT Technical Review*, Vol. 15, No. 2B, Fall 1985, pp. 369–398.

[4] D. J. Schaefer, "Techniques for TDMA System Monitoring," *COMSAT Technical Review*, Vol. 9, No. 2A, Fall 1979, pp. 387–412.

[5] J. R. Potukuchi, F. T. Assal, and R. C. Mott, "A Computer-Controlled Communications Satellite Monitoring System for Time Division Multiple Access," *COMSAT Technical Review*, Vol. 14, No. 2, Fall 1984, pp. 391–430.

[6] J. S. Snyder and W. J. Hersey, "Pseudo-Bit-Error-Rate Measurement for 120-Mbit/s TDMA," *COMSAT Technical Review*, Vol. 14, No. 2, Fall 1984, pp. 285–311.

Appendix A. The four TSM subsystems

The TSM consists of four subsystems: the processor, measurement devices, TDMA controller, and antenna interface. These four subsystems can operate in five distinct modes:

- *Initialization:* sets the hardware and software to prescribed conditions.
- *Routine measurement:* measures all parameters on each burst in the time plan.
- *Diagnostic measurement:* measures selected parameters on selected bursts.
- *Calibration:* provides computer-aided system calibration.
- *Maintenance:* provides computer-aided troubleshooting diagnostics.

Processor subsystem

The TSM processor subsystem illustrated in Figure A-1 receives raw measurement data, performs calculations, and controls the display of processed measurements and status data to the IOC by a packet data network via the RTE. This subsystem consists of a computer, disk, operator's console, system console, color video display, and printer. The TSM software is described in detail in Appendix B.
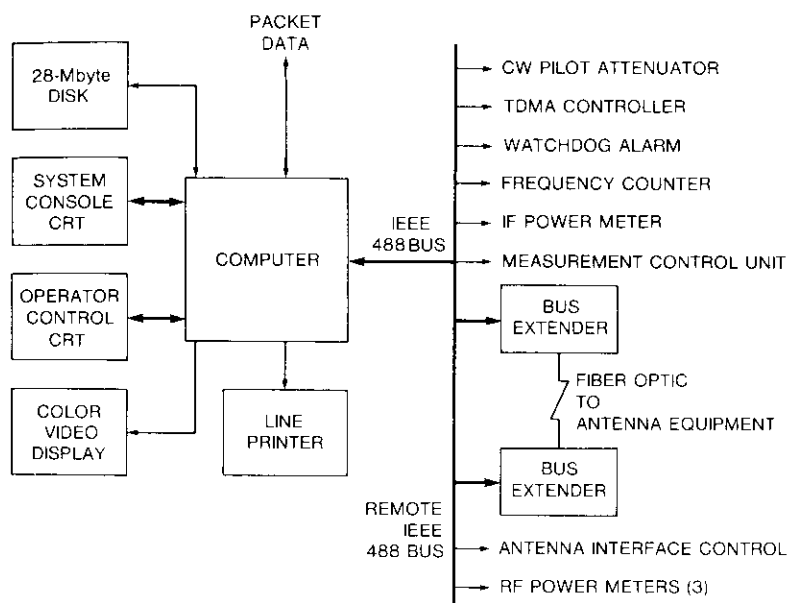
Figure A-1. *TSM Processor Subsystem Block Diagram*

Measurement subsystem

The TSM measurement subsystem diagrammed in Figure A-2 consists of the IF measurement unit (IFMU), the measurement control unit (MCU), and several instruments which process the TDMA IF signal and perform power, frequency, and pseudo bit error measurements under the control of the TSM processor.

The IFMU provides IF signal routing, filtering, frequency conversion, and envelope detection, as well as a low-level, 125-MHz pilot signal which can be added to the transmitted RB from the reference terminal for use in measuring the transponder operating point.

The MCU controls the IFMU switches and provides measurement gates that are properly timed to compensate for delays through the IFMU. The principal measurement gates and their functions are described in Table A-1.
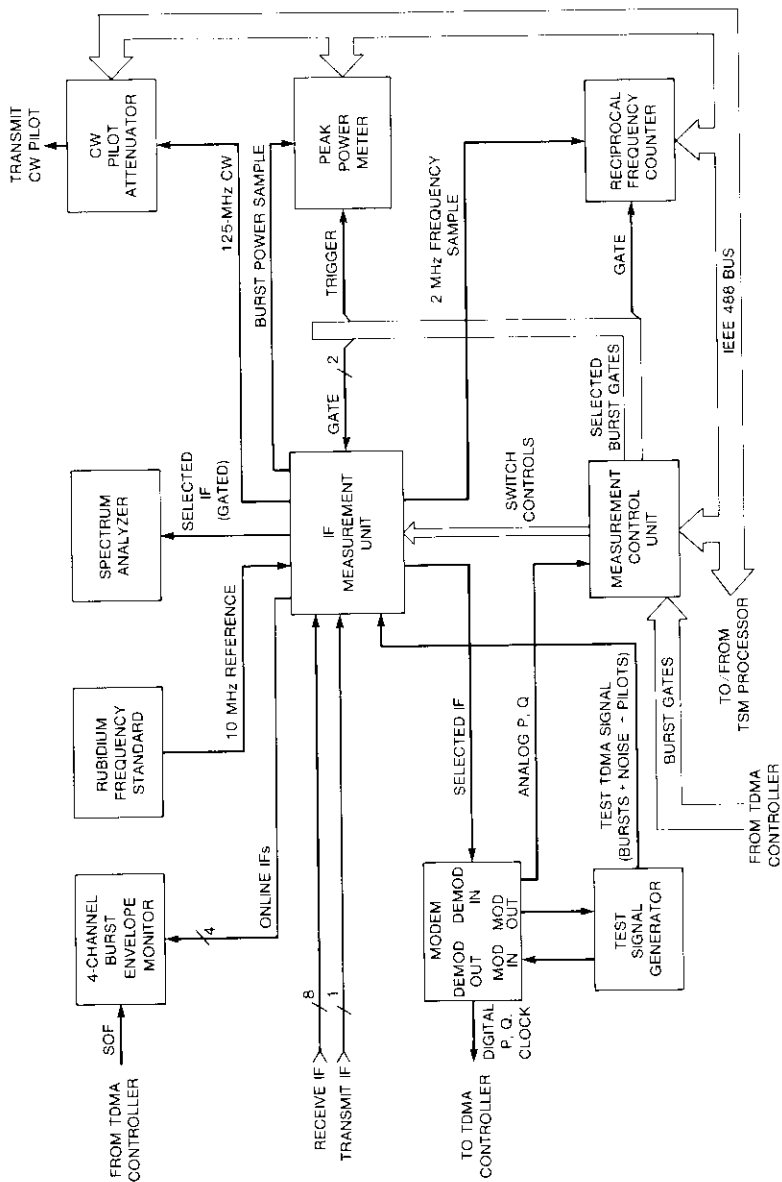
Figure A-2. *TSM Measurement Subsystem Block Diagram*

TABLE A-1. MEASUREMENT GATE FUNCTION

GATE NAME	FUNCTION	POSITION IN BURST OR FRAME
Full Burst Gate	Power measurements of noise and pilot signals in the absence of bursts.	During idle time in frame.
Carrier and Timing Recovery Gate	Power measurements of noise and pilot during bursts.	Centered in the 128-symbol carrier and timing recovery period of the burst.
UW-Initiated Gate	Frequency and BER measurements.	Starts at the UW.
Programmable Burst Gate	Burst power measurements.	Starts at the UW.

The MCU also receives analog P and Q signals from the burst demodulator and estimates the BER after processing these signals in the PBER circuitry. The demodulation section of the burst modem provides digital P, Q, and clock signals to the TDMA controller for frame synchronization and burst detection purposes. The modulation section receives test P, Q, and clock signals from the test signal generator to initiate a test TDMA frame at IF.

The test signal generator provides a TDMA spectrum for TSM off-line calibration and diagnostic troubleshooting. The test signal generator output consists of a test frame at baseband formed by RB1, RB2, and a traffic burst. The test signal generator adds test pilot signals at 105 MHz and at 125 MHz, plus broadband noise to the IF signal from the modulator. The modulated signal is routed to the demodulator during testing and troubleshooting.

The following instruments are included in the measurement subsystem:

- *Reciprocal frequency counter:* measures burst frequency.
- *Peak power meter:* measures burst, noise, and pilot signals.
- *Rubidium frequency standard:* provides a stable reference signal for the locking of internal oscillators.
- *IF spectrum analyzer:* displays the spectrum of a selected transponder output.
- *Four-channel oscilloscope:* displays detected bursts from four transponders.

TDMA controller

The TDMA controller synchronizes the TSM to the TDMA frame using RTE and SOF signals, generates the measurement gates, and measures the burst position error. Figure A-3 is a simplified block diagram of the TDMA controller. An 8085-based microprocessor provides an IEEE 488 interface for command reception and data transmission with the TSM processor. A firmware program controls internal processes via an input/output data bus which is available to all functional elements.
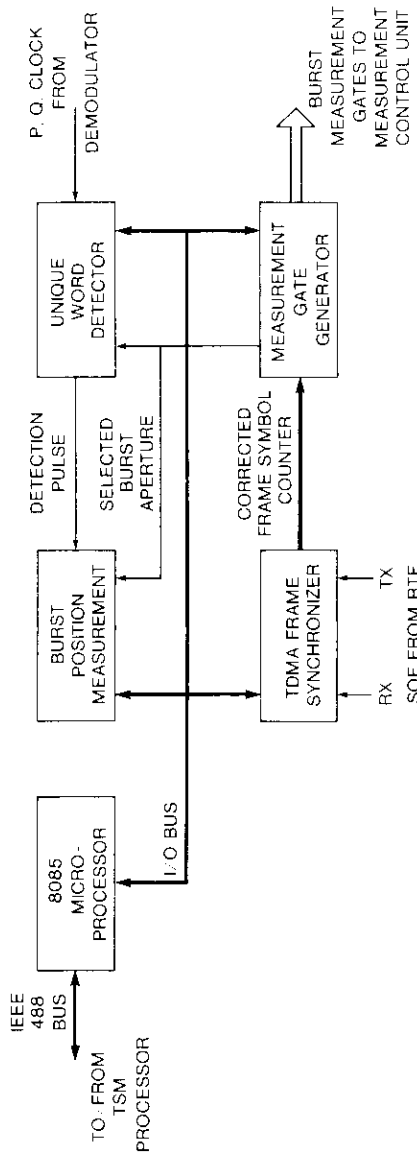
Figure A-3. TDMA Controller Functional Block Diagram

FRAME SYNCHRONIZATION

The TDMA frame synchronizer accepts transmit and receive SOF synchronization pulses from the colocated RTE. Differential delay correction is provided between the colocated RTE SOF and the TSM-generated SOF. The output of the frame synchronizer is a cyclic, modulo 120,832 digital counter sequence with each output value interpreted as a corresponding symbol position within the frame. The measurement gate generator uses frame symbol count values to digitally generate measurement gates and burst apertures at specified positions within the frame. The UW detector correlates 24 symbol sequences to detect the presence of UWs.

BURST MEASUREMENT GATE GENERATION

After establishing frame synchronization, the TDMA controller generates the burst measurement gates. Each type of gate is generated by identical start and stop symbol count comparators that continuously examine the frame symbol counter. The TDMA controller microprocessor computes start and stop symbol counts for each measurement gate based on the burst position from the burst time plan. These start and stop values are loaded into latches feeding one side of the comparators. As the comparators are actuated by start symbol count, the gates are initiated. The stop symbol count terminates the gate.

Antenna interface subsystem

The antenna interface subsystem (AIS) shown in Figure A-4 indicates that all switches and power meters are controlled and operated remotely from the TSM. The AIS provides the following measurement capabilities:

a. pilot signal injection to calibrate host station down-chain gain and down-converter frequency offset,

b. transmit power measurement of the RB and continuous wave pilot signal, and

c. calibration of transmit monitor path gain between the host station HPA and the TSM measurement subsystem.

The AIS injects either a 3,710- or 3,790-MHz pilot signal into the LNA input at a level 30 dB below the nominal TDMA traffic signals, which, after down-converting, results in a pilot signal of 105 MHz for measurement at IF. A gain measurement from the transmit sample output to the TSM IF is made by a similar method. The TSM injects either a 5,935- or a 6,015-MHz signal, which is down-converted to 105 MHz by the AIS.
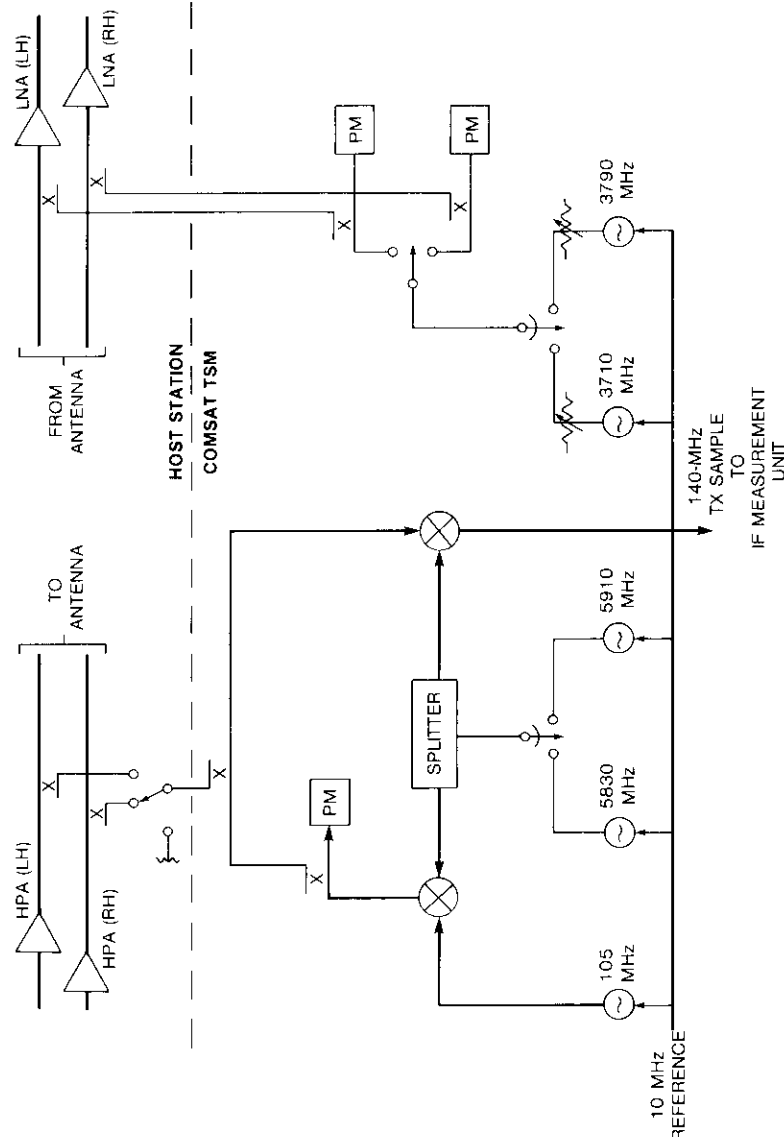
Figure A-4. *Antenna Interface Subsystem Block Diagram*

Appendix B. TSM software architecture

The TSM software allows automatic and continuous measurement of INTELSAT TDMA network performance to be made by local or remote operator control at the INTELSAT Operations Center TDMA Facility (IOCTF). The software architecture, illustrated in Figure B-1, consists of six subsystems and four data bases. In Figure B-1, each subsystem (circled) consists of several programs which perform a part of the total task of controlling the TSM. These programs interact with each other and with external units (the hardware, indicated by rectangles) to control the acquisition and processing of raw data. The data bases (specified between parallel lines) contain the information which defines the monitored TDMA network and produces the data.

The largest of the six subsystems incorporates a measurement control program, three device-handling programs, and several data base load programs to perform the measurements that make up the principal function of the TSM. The operator interface is the next most complex subsystem of the six, providing a tree-driven menu for the selection of operational commands. The display processing subsystem controls the printer and the video screen, exhibiting either real-time or retrieved stored data. The IOCTF interface subsystem provides a two-way communications link to the INTELSAT operations center via the control and display console of the RTE. The data storage and retrieval subsystem provides two-way access to the four major data bases: 24-hour measurement data, event log, burst time plan, and initialization parameters. The last of the six subsystems, status and event monitoring, provides two-way access to the event log data base, a history of recent commands, and status changes in the TSM or in the measurement burst parameters.
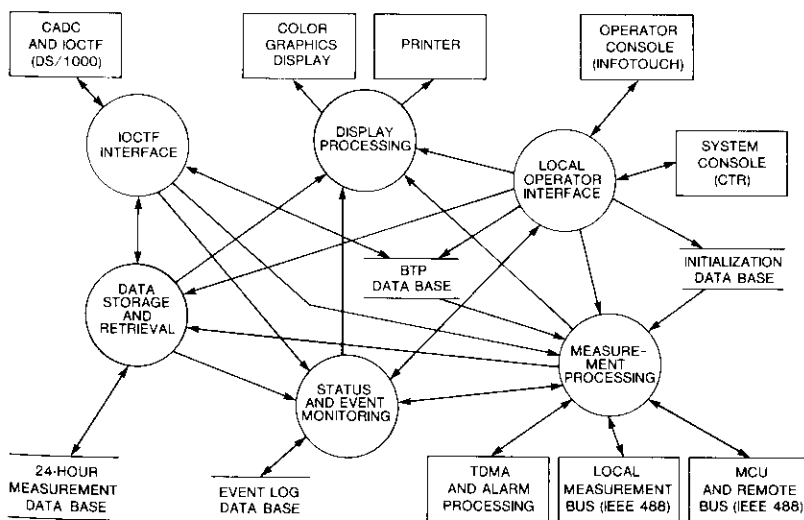
Figure B-1. *TSM Software Architecture*

Jerry S. Barnett received a B.S.E.E. from Iowa State University in 1957 and an M.B.A. from Virginia Polytechnic Institute and State University in 1978. Since joining COMSAT in 1977, he has been a Program Manager at COMSAT Laboratories and at COMSAT Technology Products. His work has involved the design of various monitoring systems for INTELSAT. Previously, Mr. Barnett was employed by Page Communications Engineers, where he was responsible for the design of turnkey tropospheric scatter and microwave communications systems.

C. Richard Thorne received a B.S.E.E. from the University of Maryland in 1969. Since joining COMSAT Laboratories in 1978, he has been a Member of the Technical Staff in the Development Engineering Division and a Department Manager in the Network Technology Division. His work has focused on systems engineering and firmware development in the areas of FDMA and TDMA communications systems monitors, and high-bit-rate TDMA systems. Previously, Mr. Thorne was employed by the Naval Research Laboratory, where he was responsible for software development associated with next-generation electronic warfare systems for naval aircraft.

H. Lewis Parker received a B.S. from Davidson College in 1962 and an M.A. from Duke University in 1966. He was a Research Assistant at Duke University with the Special Research in Numerical Analysis project. Since joining COMSAT in 1969, he has been responsible for numerous software development projects, including the INTELSAT V TDMA System Monitor. He was Project Manager for the development, test, and installation of the TT&C software and hardware for the SBS TT&C stations. He was also responsible for developing TT&C software for the COMSTAR and MARISAT programs for COMSAT General, and for the INTELSAT Communications System Monitor. Mr. Parker is currently a Project Manager with the System Development Division at COMSAT Laboratories. He is a member of the IEEE and the IEEE Computer Society.

Anthony Berntzen joined INTELSAT in 1981 as a Member of the Communications Operations Staff covering all modulation techniques currently used in the INTELSAT system. With the inception of TDMA, he has been primarily involved with TDMA operations and the testing and integration of reference stations, in particular the monitoring stations. Previously, Mr. Berntzen was employed by British Telecom International at Goonhilly Earth Station, where he was involved in all aspects of earth station operations and maintenance, and specialized in cryogenics.
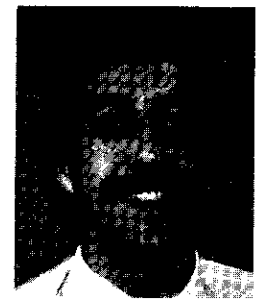
INTELSAT TDMA link design and transmission simulation

M. E. JONES, E. KOH, and D. E. WEINREICH

(Manuscript received June 16, 1986)

Abstract

This paper addresses the key factors involved in the transmission design of the INTELSAT time-division multiple-access (TDMA) system. Linear channel analysis was supplemented with computer and laboratory hardware simulation to evaluate the impairments arising in the actual nonlinear channel. The required system performance standards, a historical review of the system constraints, a transmission model, link budgets, and a detailed discussion of the significant individual link impairments and their evaluation are presented. The simulation data thus obtained should enable system engineers to assess the INTELSAT V/VI performance under a wide variety of operational conditions.

Introduction

The INTELSAT V/VI time-division multiple-access (TDMA) system supports 120-Mbit/s quadrature phase-shift keying (QPSK) transmissions among large earth stations in a global satellite network with up to sixfold frequency reuse in portions of the allocated spectrum. The 80-MHz nominal bandwidth channel is nonlinear, with usable bandwidths from 60 to 72 MHz. The system is efficient, although bandwidth- and interference-limited.

Key factors in the transmission design of the TDMA system as applied to the INTELSAT V/VI channels 1-2, 3-4, and 5-6 transponders (primarily in the C-band hemi and zone antenna coverage configurations) are addressed.

The design process used a linear channel analysis with an initial additive white Gaussian noise (AWGN) assumption for link impairments, supplemented by computer time domain and laboratory hardware simulation, to evaluate the impairments actually encountered in nonlinear channels for which no known analytic solution exists. Only steady-state impairment effects are discussed, under the assumptions that the TDMA preamble design and attendant burst synchronization problems have been treated elsewhere and that the impairments experienced in the data portion of TDMA bursts are the same as if the transmission were continuous. A historical perspective, design constraints, design approach, transmission model, and impairment definition are presented, followed by a discussion of the required performance standards adopted for the system and the system link budgets. The major portion of the paper is devoted to an evaluation of significant system impairments.

The need for forward-error correction (FEC) is identified, the code selection process is discussed, and the selected FEC code and its performance are presented. Examples of overall system performance conclude the paper.

Historical perspective, constraints, and design approach

The early INTELSAT V TDMA transmission link design was somewhat dependent on ongoing operational frequency-division multiplex, frequency modulation, frequency-division multiple-access (FDM-FM-FDMA) systems. The choices made in the basic architecture of communications transponders and earth stations were influenced by FDM-FM-FDMA usage, and by the ever-increasing desire to provide greater transmission capacity. INTELSAT IV and IV-A employed 40-MHz channel spacing with usable channel bandwidths of 30 to 36 MHz. Link budgets and the 36-MHz usable channel bandwidth indicated the capability of supporting 60- to 68-Mbit/s TDMA QPSK signals with Nyquist filtering, with careful attention to channel amplitude and group delay equalization. Experimental tests led to the conclusion that 60-Mbit/s QPSK would be the upper bandwidth-limited bound. Higher than expected nonlinear channel impairments were also encountered, generating concern regarding attainable transmission link margins, especially because of the extensive co-channel interference (CCI) resulting from frequency reuse.

INTELSAT IV-A was the first satellite to support 60-Mbit/s QPSK/TDMA signaling in a large-scale multiple earth station field trial [1] which demonstrated the operational performance of TDMA. The subsequent INTELSAT V system, which employed both 80- and 40-MHz channel spacing, was planned for operational use of 120-Mbit/s QPSK/TDMA with 80-MHz (72-MHz usable)

transponders. Fourfold frequency reuse of the 72-MHz transponders for FDM-FM-FDMA (and potentially for TDMA) was also a significant advance in system architecture which resulted in a TDMA channel design that was both bandwidth- and interference-limited. Thus, during the critical INTELSAT V operational TDMA design period, the basic architecture of the earth station and communications transponders had been sufficiently well defined.

The two most important transmission link choices during the INTELSAT V TDMA design process concerned the modem pulse-shaping filter (to reduce nonlinear channel impairments) and FEC coding, which made it possible to support bandwidth- and interference-limited 120-Mbit/s QPSK TDMA signals.

The INTELSAT V/VI TDMA transmission system design was also complicated by earth station and satellite transponder channel nonlinearities. Closed-form analytic solutions do not exist for the intersymbol interference (ISI) experienced by filtered QPSK signals passing through a nearly saturated traveling wave tube amplifier (TWTA), or the effect of up-link multiple filtered QPSK CCI signals on the wanted signal, all of which are applied ahead of the saturated TWTA. Similarly, the spreading effect of an adjacent channel's filtered QPSK signal on the wanted channel cannot be assessed analytically.

In effect, system analysis started with a linear channel assumption; initial estimates of the additional nonlinear channel impairments were made and then refined through a combination of computer time-domain and laboratory hardware simulation. Although the transponder design that would eventually support the operational system did not exist at the outset of this procedure, pre-TDMA transponder designs were available. In fact, COMSAT Laboratories had constructed laboratory hardware transponder simulators for each operational satellite (INTELSAT IV and IV-A). These simulators employed 36-MHz-bandwidth channels and were capable of supporting 60-Mbit/s QPSK transmission. The INTELSAT IV and IV-A simulators were used for initial channel parameter characterization. Laboratory data could thus be scaled to permit investigations for the desired 120-Mbit/s QPSK system.

Computer simulation was employed throughout the design process. An extensive INTELSAT V TDMA hardware simulation facility was designed, constructed, and used to determine, verify, or refine the channel performance predictions obtained by analysis or computer simulation.

Transmission model and description of impairments

A transmission model of the 120-Mbit/s QPSK/TDMA INTELSAT V/VI system is shown in Figure 1. The significant transmission impairments, in addition to up- and down-link thermal AWGN, include the following:
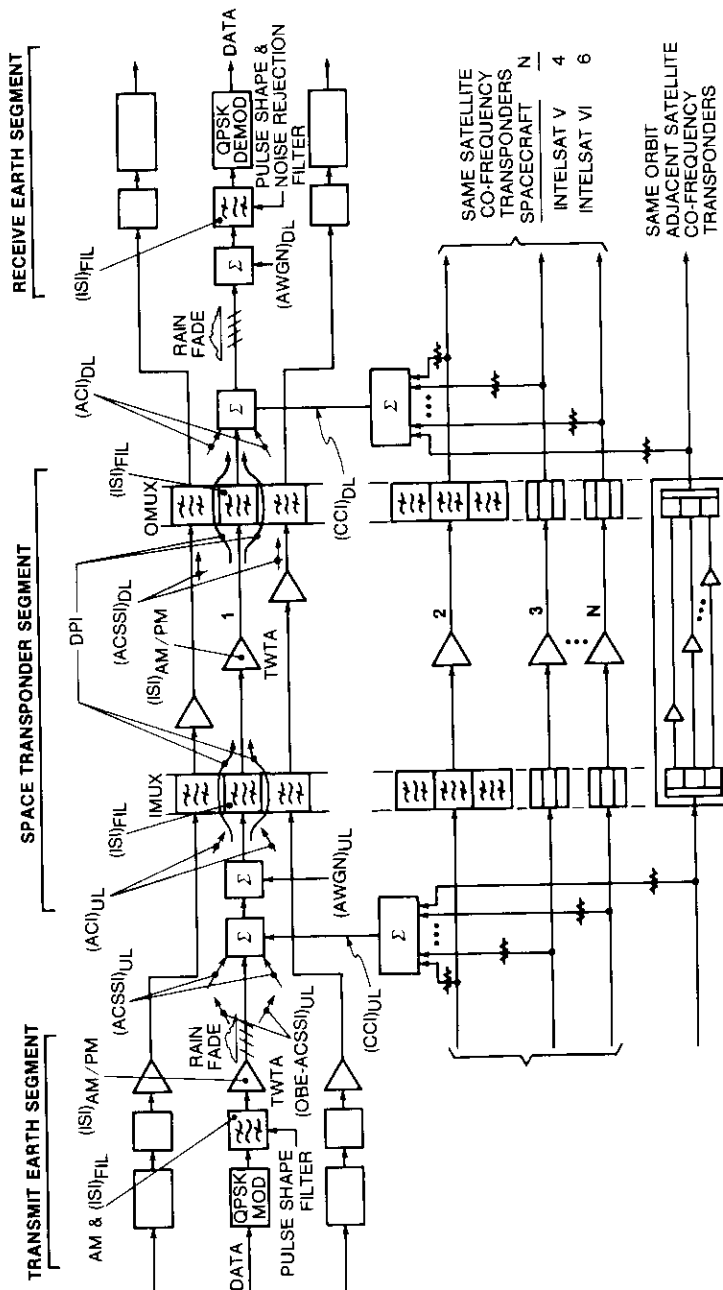
Figure 1. INTELSAT V/VI Transmission Model

a. Wanted channel in-band nonlinear channel ISI due to filtered signal-induced AM followed by TWTA AM/PM conversion.

b. CCI caused by frequency reuse co-frequency transponder coupling from non-ideal feed polarization and/or antenna beam isolation on both up- and down-links. The CCI can increase because of rain-induced cross-polarization isolation reduction of the wanted signal or rain-induced cross-polarization isolation reduction on one or more of the co-channel signals, on the up- and/or down-link.

c. Adjacent channel spectrum spreading interference (ACSSI) caused by TWTA-induced adjacent channel signal spectrum spreading (regrowth) appearing in the wanted channel as CCI on both up- and down-links. (The up-link effect is worse than the down-link and is most severe when the up-link wanted signal is subjected to a rain fade.)

d. Dual-path interference (DPI) caused by the upper and lower extreme edge portions of the wanted signal spectrum propagating through the near edge portions of the adjacent channel transponder input and output multiplexer filters and arriving at the down-link demodulator with amplitude and phase relative to the wanted signal so that destructive interference results.

e. Wanted channel in-band linear ISI due to non-ideal filter amplitude and group delay of modem pulse-shaping filter and any earth station and transponder channel filters having a bandwidth close to that of the transmitted signal spectrum.

f. Adjacent channel interference (ACI) due to strong mainlobe signal components. On the up-link, these components riding through the filter skirts of the wanted signal transponder affect the TWTA operating point, with resulting AM/PM distortion. On the up-link as well as on the down-link, particularly in the presence of rain fading, these components affect the demodulator via the receive filter.

g. CCI due to frequency reuse co-frequency transponder(s) of another communications satellite sharing the same orbit spatially isolated but with the same coupling.

The ACI was already well under control in the case of FDM-FM transponder channel filter designs and in the case of demodulator interference, since the demodulator filter is usually matched to the signal spectrum in order to reject thermal noise efficiently with sharp skirt selectivity. Other satellite CCI was controlled by specifying the minimum permissible carrier-to-interference ratio (C/I) from adjacent satellite systems.

Transmission performance requirements

The transmission design of the TDMA INTELSAT V/VI system is based on performance requirements, summarized in Table 1, which conform to CCIR Recommendation 522 (Geneva, 1982).

The performance objective requires that the available clear-sky carrier-to-noise ratio exceed the carrier-to-noise ratio for the bit error rate (BER) objective of 10^{-6} specified for long-term propagation conditions. The amount of up-link fade, down-link carrier-to-noise degradation, and the allowable up-link carrier-to-CCI ratios should be such that the BER objective of 10^{-3} is not exceeded for the short-term propagation conditions. The short-term BER objective of 10^{-4} for 0.3 percent of the worst month given in CCIR Rec. 522 is not considered because it is not expected to be a limiting factor.

The out-of-band emission constraints shown in Table 1 relate to the e.i.r.p. of the out-of-band emission resulting from spectral spreading of the QPSK carrier due to high-power amplifier (HPA) nonlinearities, as well as the e.i.r.p. of intermodulation products resulting from multicarrier operation of an HPA. These limits are chosen to avoid significantly degrading the performance of adjacent channels.

The maximum acceptable limit of external interference, given in Table 1, is consistent with the current INTELSAT practice in FDM/FM transmission planning. The total external interference contribution should not exceed 10 percent of the thermal noise level at the demodulator for a BER of 1 in 10^6.

TABLE 1. TRANSMISSION DESIGN PERFORMANCE REQUIREMENTS

BER Performance Objective (CCIR Rec. 522)	The BER at the output of the hypothetical reference circuit should not exceed the values of: • 1 in 10^6, 10-min. mean value for more than 20 percent of any month; • 1 in 10^4, 1-min. mean value for more than 0.3 percent of any month; • 1 in 10^3, 1-s mean value for more than 0.01 percent of any year.
Out-of-Band Emission Constraints (earth station transmitting)	$23.0 - 0.02(\alpha - 10)$ dBW/4 kHz at 6 GHz or 12.0 dBW*/4 kHz at 14 GHz, where α is the elevation angle in degrees.
External Interference Criterion (adjacent satellites and terrestrial)	The aggregate interference power level averaged over any 10 min. should not exceed, for more than 20 percent of any month, 10 percent of the total noise power level at the input to the demodulator that would give rise to a BER of 1 in 10^6.

* May be temporarily exceeded by as much as 9 dB when transmitter power control is employed during poor propagation conditions.

TDMA link budget performance

The INTELSAT V/VI systems operate in the 6/4- and 14/11-GHz up-link/down-link frequency bands. The 6/4-GHz frequency band is reused four times through two hemispheric beam coverage regions and two zone beam coverage regions for the INTELSAT V system. The same C-band in the INTELSAT VI system is reused six times through two hemispheric beam and four zone beam coverage regions. The link calculations employ net isolation resulting from the specified isolations between beams for both the up- and down-beams and the earth station, using the full frequency reuse capabilities.

The 14/11-GHz frequency band is reused through spatially separated spot beams. In the INTELSAT V/VI satellites it is also possible to establish transmission paths in the cross-strapped 6/11- and 14/4-GHz frequency bands.

In developing the representative link budgets for the various connections, the INTELSAT V and VI spacecraft specification values are assumed. The actual isolation, e.i.r.p., and G/T values are found to exceed these specification values. Thus, the link calculations presented in this paper are pessimistic relative to operational performance. Tables 2 through 4 illustrate the link calculations using three different versions of INTELSAT V satellites (F1-F4, F5-F9, and F10-F15). The BER performance associated with these link budgets is based on 60-Mbit/s [2],[3] and 120-Mbit/s [4] QPSK transmission performance for the wanted channel only, as determined by laboratory hardware simulation, with an additional allowance of ~0.8 dB at 1×10^{-6} BER for link implementation losses due to modem interoperability, aging, non-ideal modem performance variability, and non-ideal link equalization.

Figure 2 shows theoretical performance, practical modem in-channel measured performance (well-adjusted modem and optimum link equalization), and the adjusted BG-42-65 specification [5] in-channel performance bound. In the link budget tables, the effect of CCI is assumed to be the worst case, in which the interference is AWGN with levels determined by the cross-polarization isolation. The effect of ACSSI and DPI is assumed to be a flat 1-dB loss. (Actually, the AWGN assumption for CCI was pessimistic and the 1-dB loss for ACSSI and DPI was reasonable.)

The available E_b/N_o for the various spacecraft examples ranges from 12.3 to 12.7 dB. From Figure 2, using the BG-42-65 probable performance, it is evident that a clear-sky performance BER of 1×10^{-6} is unattainable for the assumed link conditions. FEC coding studies performed during the design process led to the choice of a rate 7/8 BCH (128,112) block code powerful enough to provide the required clear-sky performance with 2- to 3-dB rain

TABLE 2. 120-Mbit/s TDMA SYSTEM INTELSAT V
(F1–F4)

ITEM	HEMI/HEMI	ZONE/ZONE
Frequency Band (GHz)	6/4	6/4
Occupied Bandwidth (MHz)	60.0	60.0
Up-Link		
• Saturation Flux Density (dBW/m²)	−72.0	−72.0
• Satellite G/T (dB/K)	−11.6	−8.6
• Path Loss (dB)	200.5	200.5
• Input Backoff (dB)	3.0	3.0
• Earth Station e.i.r.p. (dBW)	88.5	88.5
• (C/N) Up-Link (dB)	27.2	30.2
• (C/I) Frequency Reuse (dB)	21.6	21.6
• ($C/N + I$) Up-Link (dB)	20.5	21.0
Down-Link		
• Saturation e.i.r.p. (dBW)	29.0	29.0
• Earth Station G/T (dB/K)	40.7	40.7
• Down-Link Path Loss (dB)	197.0	197.0
• Output Backoff (dB)	0.5	0.5
• (C/N) Down-Link (dB)	23.0	23.0
• (C/I) Frequency Reuse (dB)	21.6	21.6
• ($C/N + I$) Down-Link (dB)	19.2	19.2
Interference		
• (C/I) External Interference (dB)	29.0	29.0
Total ($C/N + I$) (dB)	16.5	16.7
Link Degradations		
• ACSSI, DPI, e.i.r.p. Variations (dB)	1.0	1.0
Total Available ($C/N + I$) (dB)	15.5	15.7
Total Available E_b/N_o (dB)	12.5	12.7
Required E_b/N_o for BER of 1×10^{-6} With Rate 7/8 BCH Code (dB)	9.6	9.6
Margin (dB)	2.9	3.1

TABLE 3. 120-Mbit/s TDMA SYSTEM INTELSAT V
(F5–F9)

ITEM	HEMI/HEMI	ZONE/ZONE
Frequency Band (GHz)	6/4	6/4
Occupied Bandwidth (MHz)	60.0	60.0
Up-Link		
• Saturation Flux Density (dBW/m²)	−74.6	−74.6
• Satellite G/T (dB/K)	−9.0	−6.0
• Path Loss (dB)	200.5	200.5
• Input Backoff (dB)	3.0	3.0
• Earth Station e.i.r.p. (dBW)	85.8	85.8
• (C/N) Up-Link (dB)	27.2	30.2
• (C/I) Frequency Reuse (dB)	21.6	21.6
• ($C/N + I$) Up-Link (dB)	20.5	21.0
Down-Link		
• Saturation e.i.r.p. (dBW)	29.0	29.0
• Earth Station G/T (dB/K)	40.7	40.7
• Down-Link Path Loss (dB)	197.0	197.0
• Output Backoff (dB)	0.5	0.5
• (C/N) Down-Link (dB)	23.0	23.0
• (C/I) Frequency Reuse (dB)	21.6	21.6
• ($C/N + I$) Down-Link (dB)	19.2	19.2
Interference		
• (C/I) External Interference (dB)	29.0	29.0
Total ($C/N + I$) (dB)	16.5	16.7
Link Degradations		
• ACSSI, DPI, e.i.r.p. Variations (dB)	1.0	1.0
Total Available ($C/N + I$) (dB)	15.5	15.7
Total Available E_b/N_o (dB)	12.5	12.7
Required E_b/N_o for BER of 1×10^{-6} With Rate 7/8 BCH Code (dB)	9.6	9.6
Margin (dB)	2.9	3.1

margin. The performance of the selected FEC decoder results in an output BER of 1×10^{-6} for an input symbol error rate of 5×10^{-4}, as shown in Figure 2. The figure also shows that the required E_b/N_o for this FEC operating point is 9.6 dB. The E_b/N_o is referred to the channel QPSK bit rate of 120 Mbit/s. With rate 7/8 FEC, the actual TDMA information transmission rate is 105 Mbit/s.

The link margins for the hemi-to-hemi and zone-to-zone links are about 3 dB with FEC coding. The link margin in the INTELSAT VI system is somewhat lower than those of the INTELSAT V system, as shown in Table 5. The additional degradation in the INTELSAT VI is caused by the lower net C/I resulting from sixfold frequency reuse. The link budgets of Tables 2 through 5 are based on earth terminals with an elevation angle of the order of 10°.

TABLE 4. 120-Mbit/s TDMA System INTELSAT V
(F10–15)

ITEM	HEMI/HEMI	ZONE/ZONE
Frequency Band (GHz)	6/4	6/4
Occupied Bandwidth (MHz)	60.0	60.0
Up-Link		
• Saturation Flux Density (dBW/m²)	−76.6	−76.6
• Satellite G/T (dB/K)	−9.0	−6.0
• Path Loss (dB)	200.5	200.5
• Input Backoff (dB)	3.0	3.0
• Earth Station e.i.r.p. (dBW)	83.8	83.8
• (C/N) Up-Link (dB)	25.2	28.2
• (C/I) Frequency Reuse (dB)	21.6	21.6
• $(C/N + I)$ Up-Link (dB)	20.0	20.7
Down-Link		
• Saturation e.i.r.p. (dBW)	29.0	29.0
• Earth Station G/T (dB/K)	40.7	40.7
• Down-Link Path Loss (dB)	197.0	197.0
• Output Backoff (dB)	0.5	0.5
• (C/N) Down-Link (dB)	23.0	23.0
• (C/I) Frequency Reuse (dB)	21.6	21.6
• $(C/N + I)$ Down-Link (dB)	19.2	19.2
Interference		
• (C/I) External Interference (dB)	29.0	29.0
Total $(C/N + I)$ (dB)	16.3	16.6
Link Degradations		
• ACSSI, DPI, e.i.r.p. Variations (dB)	1.0	1.0
Total Available $(C/N + I)$ (dB)	15.3	15.6
Total Available E_b/N_o (dB)	12.3	12.6
Required E_b/N_o for BER of 1×10^{-6} With Rate 7/8 BCH Code (dB)	9.6	9.6
Margin (dB)	2.7	3.0

Since there are no immediate TDMA operational plans for using the K-band and the C/K-band cross-strapped links, the link calculations are not presented here. However, Reference 6 shows that K-band links have a better margin than C-band links because of the higher satellite e.i.r.p. in K-band spot beams.
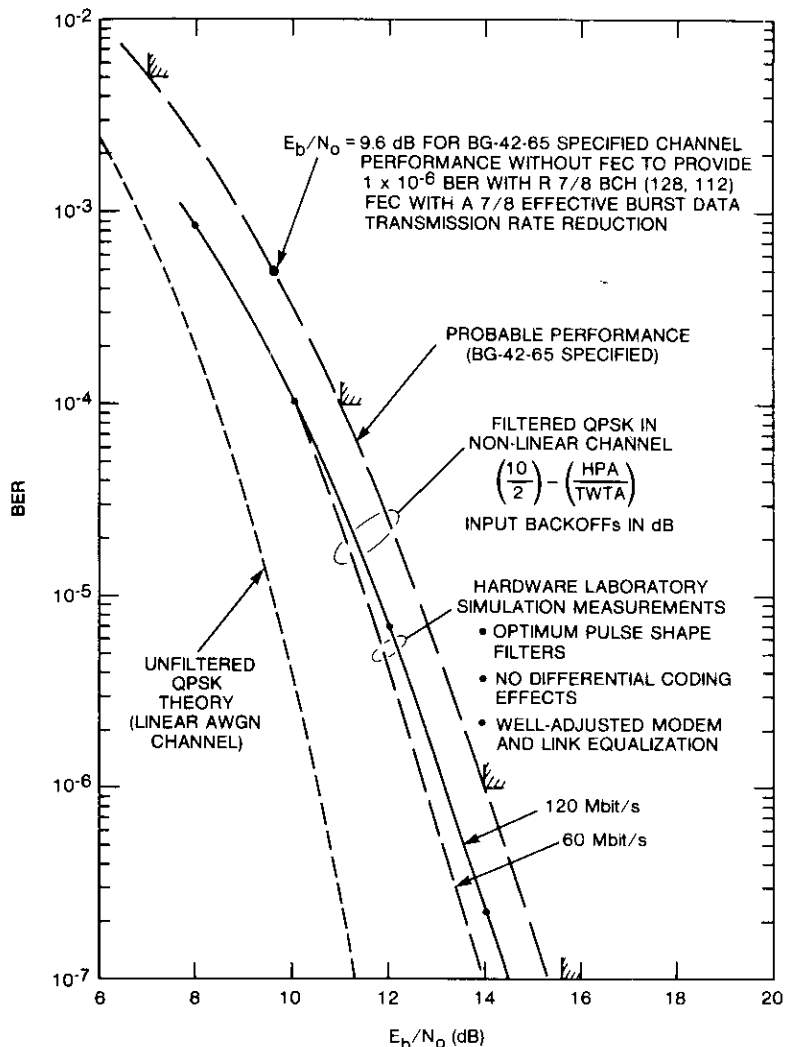
Figure 2. *QPSK Modem Performance in the Nonlinear Channel*

TABLE 5. 120-Mbit/s TDMA SYSTEM INTELSAT VI
(F1–F5)

ITEM	HEMI/HEMI	ZONE/ZONE
Frequency Band (GHz)	6/4	6/4
Occupied Bandwidth (MHz)	60.0	60.0
Up-Link		
• Saturation Flux Density (dBW/m²)	−77.6	−77.6
• Satellite G/T (dB/K)	−9.2	−2.0
• Path Loss (dB)	200.5	200.5
• Input Backoff (dB)	3.0	3.0
• Earth Station e.i.r.p. (dBW)	82.8	82.8
• (C/N) Up-Link (dB)	24.0	31.2
• (C/I) Frequency Reuse (dB)	20.1	21.0
• $(C/N + I)$ Up-Link (dB)	18.6	20.6
Down-Link		
• Saturation e.i.r.p. (dBW)	31.0	31.0
• Earth Station G/T (dB/K)	40.7	40.7
• Down-Link Path Loss (dB)	197.0	197.0
• Output Backoff (dB)	0.5	0.5
• (C/N) Down-Link (dB)	25.0	25.0
• (C/I) Frequency Reuse (dB)	20.5	21.0
• $(C/N + I)$ Down-Link (dB)	19.2	19.5
Interference		
• (C/I) External Interference (dB)	29.0	29.0
Total $(C/N + I)$ (dB)	15.7	16.7
Link Degradations		
• ACSSI, DPI, e.i.r.p. Variations (dB)	1.0	1.0
Total Available $(C/N + I)$ (dB)	14.7	15.7
Total Available E_b/N_o (dB)	11.7	12.7
Required E_b/N_o for BER of 1×10^{-6} With Rate 7/8 BCH Code (dB)	9.6	9.6
Margin (dB)	2.1	3.1

Impairment evaluation

Nonlinear channel impairment [impairment (a)]

Significant efforts in the system design were directed toward the evaluation and subsequent reduction of the nonlinear channel impairment with coherent Nyquist-filtered QPSK digital transmission by modem pulse-shaping filter parameter optimization. Early design plans included bandwidth-efficient Nyquist-filtered QPSK modulation at 60 Mbit/s (30-Msymbol/s channel QPSK

symbol rate) in 36-MHz transponder channels. A relatively sharp 30-percent rolloff raised cosine skew symmetric Nyquist filter function was proposed, with the entire Nyquist function, including $(x/\sin x)$ compensation, located at the modulator on the up-link. For a linear channel assumption, this design would have been compatible with typical INTELSAT IV and IV-A link budgets, even assuming reuse CCI, provided that the channel performance without CCI would be within 1 to 2 dB of the theoretical unfiltered QPSK case. Nyquist filtered QPSK in a linear channel would result in this level of performance. However, in the nonlinear channel, the sharp-skirted filtering associated with 30-percent Nyquist filtering created sufficiently severe AM that the nonlinear AM/PM-induced ISI resulted in a loss from 4 to 5 dB with respect to theoretical unfiltered QPSK [7]. Thus, an intolerable link budget would be encountered when considering all other operational impairments that a fourfold or sixfold frequency reuse TDMA system would experience, as in the then-future 120-Mbit/s QPSK TDMA INTELSAT V/VI systems.

Subsequent work performed in Europe, with bandwidth-efficient TDMA nonlinear channels [8], indicated that reducing the Nyquist skew symmetric rolloff factor ahead of the nonlinearity would significantly reduce the nonlinear channel impairment. Studies were initiated at COMSAT Laboratories using both hardware and software simulation to determine the best way to incorporate this benefit into the INTELSAT TDMA system. The results [2],[3],[6],[9] showed that modified pulse-shaping filters would indeed benefit the INTELSAT TDMA system. Finally, two approaches to pulse-shaping filter design emerged:

a. maintaining the transmit/receive filter function as Nyquist, but with the Nyquist skew symmetric rolloff factor modified in the direction of higher rolloff factor (less severe filter skirt selectivity), and providing some optimum apportionment of the Nyquist function between modulator and demodulator; or

b. departing from a strictly Nyquist approach and broadening the modulator transmit filter function to $1.13 \leq BT \leq 1.15$, where BT is the bandwidth-time product, but keeping the demodulator filter as narrow as possible for good noise rejection.

Eventually, it was found that a broad range of modulator/demodulator pulse-shaping filter designs would produce nearly identical performance in nonlinear satellite channels.

Early hardware simulation studied a series of Nyquist and modified Nyquist filter functions in the nonlinear channel using an INTELSAT IV laboratory transponder simulator and an HPA laboratory hardware simulation (Figure 3) [2]. Table 6 lists the pulse-shaping filter characteristics and configuration
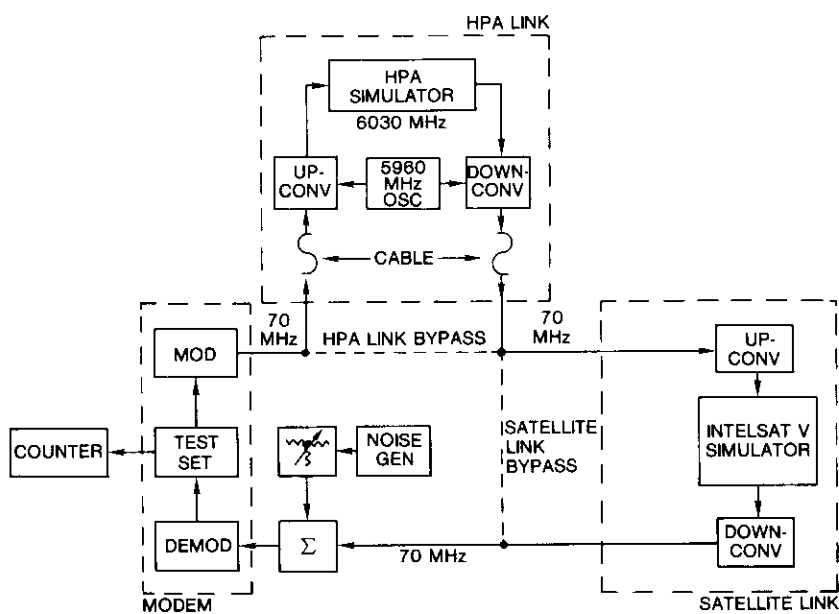
Figure 3. *60-Mbit/s QPSK INTELSAT IV Transmission Test Configuration Functional Block Diagram*

alternatives investigated. Figure 4 shows the modem with pulse-shaping filter locations used for this work. Transmission BER measurements for each of these configurations in the nonlinear channel are summarized in Figure 5. Of the narrowband alternatives, configurations 2, 3, 4, and 5 produced significant performance improvement in comparison to the original 30-percent rolloff Nyquist configuration specified for 60-Mbit/s QPSK INTELSAT TDMA [10].

TABLE 6. HARDWARE STUDY OF MODEM PULSE-SHAPING FILTERS
a. PULSE-SHAPING FILTER CHARACTERISTICS

FILTER	NYQUIST RATE (Msymbol/s)	NYQUIST ROLLOFF (%)	2-dB BANDWIDTH (MHz)	RELATIVE BT*
A	30	30	15.0	1.00
B	30	50	15.0	1.00
C	34	30	17.0	1.13
D	N/A	N/A	17.5	1.15
E	N/A	N/A	31.0	2.07

* B is 2-dB BW; 1/T is 30 Msymbol/s.

TABLE 6. HARDWARE STUDY OF MODEM PULSE-SHAPING FILTERS (cont'd)
b. MODEM PULSE-SHAPING FILTER CONFIGURATION ALTERNATIVES

| CONFIGURATION | TRANSMIT FILTER[a] | | PRESAMPLE RECEIVER FILTER[a,b] | |
	ID	DESCRIPTION	ID	DESCRIPTION
1	A	30-percent rolloff Nyquist, $BT = 1.0$ for 30 Msymbol/s	None	
2	B	50-percent rolloff Nyquist, $BT = 1.0$ for 30 Msymbol/s	None	
3	C	30-percent rolloff Nyquist for 34 Msymbol/s (68 Mbit/s), $BT = 1.13$ for 30 Msymbol/s	A	30-percent rolloff Nyquist, $BT = 1.0$ for 30 Msymbol/s
4	C	30-percent rolloff Nyquist for 34 Msymbol/s (68 Mbit/s), $BT = 1.13$ for 30 Msymbol/s	B	50-percent rolloff Nyquist, $BT = 1.0$ for 30 Msymbol/s
5	D	30-percent rolloff elliptic, $BT = 1.15$ for 30 Msymbol/s	A	30-percent rolloff Nyquist, $BT = 1.0$ for 30 Msymbol/s
6	E	Wide elliptic function, $BT = 2.00$ for 30 Msymbol/s	B	50-percent rolloff Nyquist, $BT = 1.0$ for 30 Msymbol/s
7	B	50-percent rolloff Nyquist, $BT = 1.0$ for 30 Msymbol/s	A	30-percent rolloff Nyquist, $BT = 1.0$ for 30 Msymbol/s

[a] All filters contain an $(x/\sin x)$ spectrum shaping function for the design symbol rate except filters D and E.
[b] The receiver has another wider bandpass filter ($BT = 1.10$) ahead of recovery, demodulating, and sampling functions for all configurations.

Similar results obtained using computer time-domain simulation for a wider array of filter characteristics have been reported in Reference 9. Table 7 gives the filter descriptions for this work, and their performance in the non-linear channel of Figure 6 is shown in Figure 7. The results of Figures 5 and 7 indicate that a wide variety of pulse-shaping filters characterized as either 40- to 50-percent Nyquist at the desired transmission rate or slightly non-Nyquist (30-percent Nyquist for 1.13 to 1.15 times the desired transmission rate) will provide essentially the same performance in the nonlinear channel.
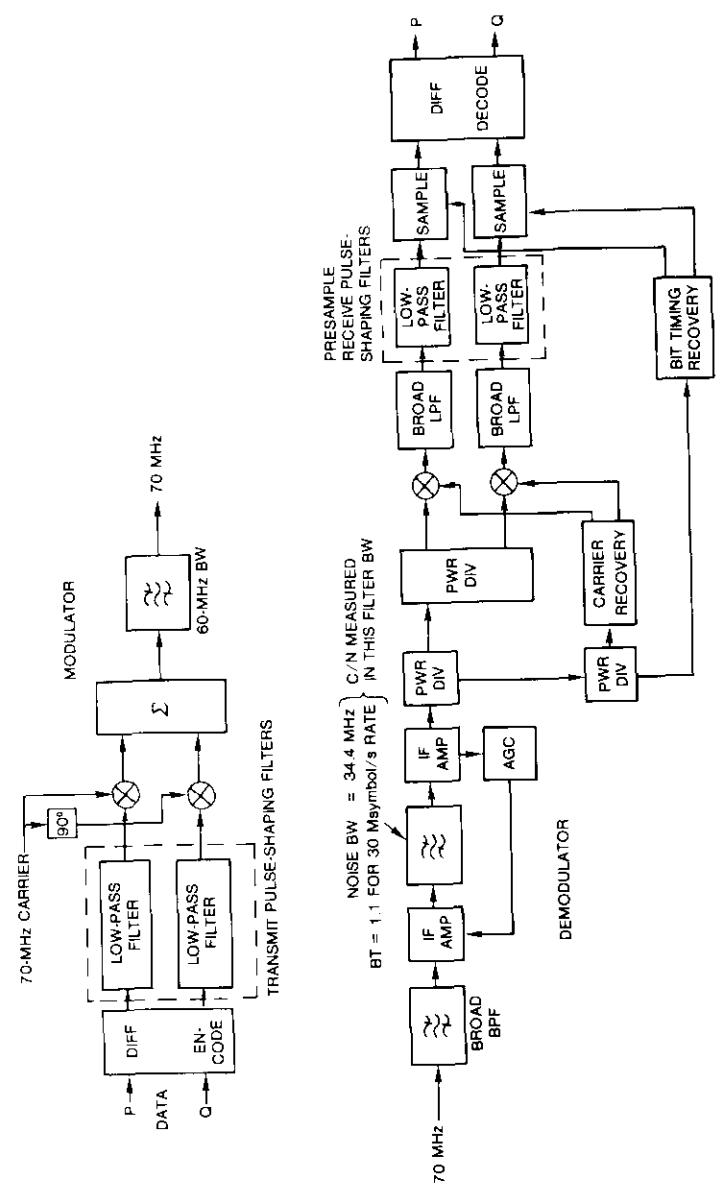
Figure 4. *60-Mbit/s QPSK Hardware Simulation Modem Detail*
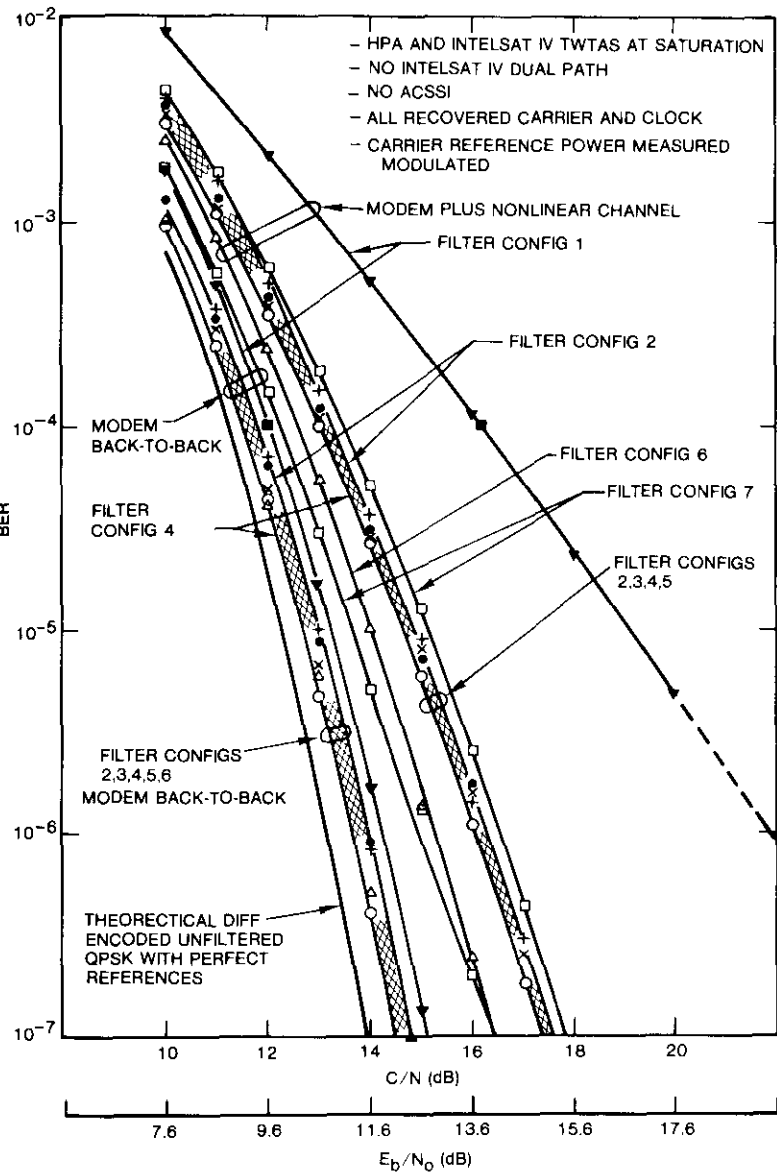
Figure 5. *BER Performance for 60-Mbit/s QPSK Modem Filter Hardware Study*
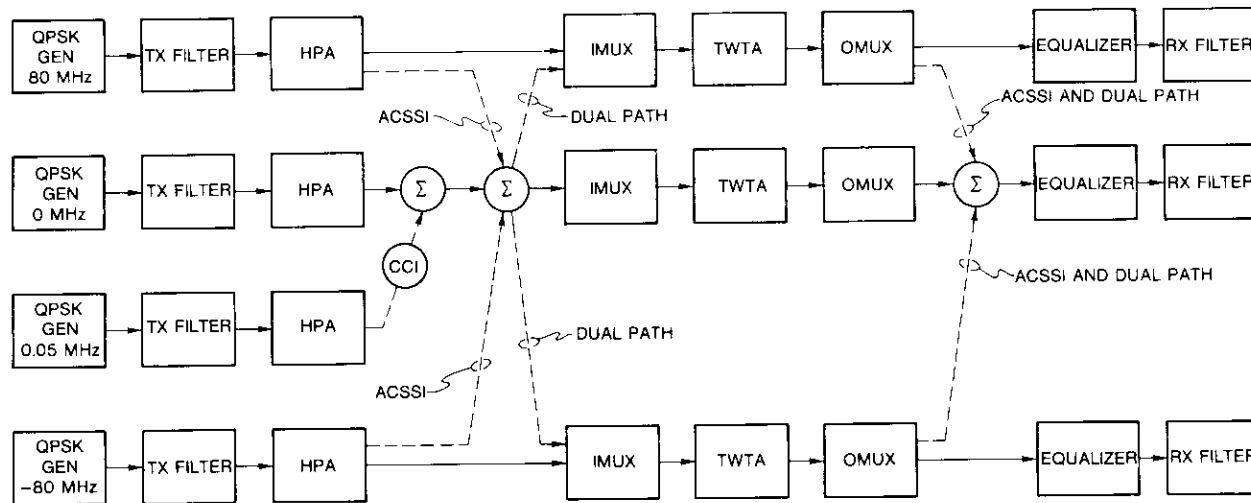
Figure 6. *Typical Computer Time Domain Simulation Block Diagram*

TABLE 7. CANDIDATE MODEM FILTER CHARACTERISTICS FOR COMPUTER SIMULATION STUDY[a]

CASE	BT	TRANSMIT FILTER CHARACTERISTIC	COMPENSATION	BT	RECEIVE FILTER CHARACTERISTIC	COMPENSATION
I	1.0	30% Nyquist	$(x/\sin x)^{1/2}$	1.0	50% Nyquist	$(x/\sin x)^{1/2}$
II	1.0	40% half-Nyquist	$(x/\sin x)^{1/2}$	1.0	40% half-Nyquist	$(x/\sin x)^{1/2}$
III	1.0	40% half-Nyquist	$x/\sin x$	1.0	40% half-Nyquist	None
IV[b]	1.13	30% Nyquist	$(x/\sin x)^{1/2}$	1.0	50% Nyquist	$(x/\sin x)^{1/2}$
V[c]	1.13	30% Nyquist	$x/\sin x$	1.0	50% Nyquist	$(x/\sin x)^{1/2}$
VI	1.13	30% Nyquist	$(x/\sin x)^{1/2}$	1.0	50% Nyquist	without $(x/\sin x)^{1/2}$
VII	1.0	40% half-Nyquist	$(x/\sin x)^{1/2}$	1.0	40% half-Nyquist	$x/\sin x$
VIII	1.0	40% half-Nyquist	$(x/\sin x)^{1/2}$	1.0	50% half-Nyquist	$(x/\sin x)^{1/2}$
IX	1.0	35% half-Nyquist	$(x/\sin x)^{1/2}$	1.0	35% half-Nyquist	$(x/\sin x)^{1/2}$
X[d]		Hardware version of case V				

[a] For cases I through IX, analytical amplitude expression and ideally equalized group delay characteristics are assumed.

[b] Modification of case I with $BT = 1.13$ at the transmit filter.

[c] Recommended in BG-42-65.

[d] Hardware version of case V using measured filter characteristics.
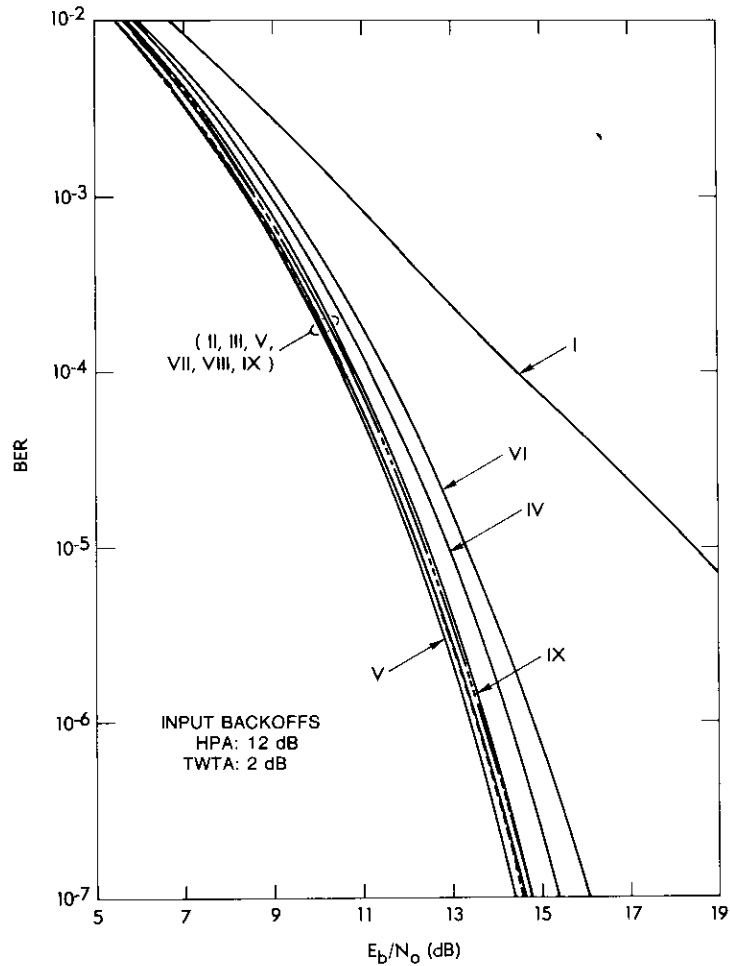
Figure 7. *BER Performance for Computer Simulation Modem Filter Study*

Table 7 and Figure 7 include a candidate modem filter that was selected for the INTELSAT V/VI TDMA system specification. Case III of Table 7 is a Nyquist filter of 40-percent rolloff with (x/sin x) aperture correction at the transmitter, but the Nyquist function is split (square root) between transmitter and receiver. Taking the square root of the function and combining it with full (x/sin x) aperture correction at the transmitter prior to the nonlinearities provides good reduction in filter-generated AM. For modem loopback testing at IF, the filter response is full 40-percent Nyquist, also giving excellent performance.

Further computer simulation work for filter type III was conducted and reported in Reference 6. The rolloff factor was varied to find the optimum value for minimum nonlinear channel impairment. Figure 8 shows that 40-percent rolloff is indeed optimum. Further investigations were conducted for the type III modem filter to determine the effect of varying the receive filter BT product. Figure 9 shows the computed result. A receive filter BT product of 1.0–1.05 is optimum, giving the best balance between thermal noise and filter ISI effects.

Associated with the pulse-shaping filter function choice is the requirement for low earth station HPA sideband regrowth levels falling in the near edge of the upper or lower adjacent channels and causing interference with FDMA signals. Although this requirement does not represent an impairment of the TDMA system, it does represent a constraint on system design. The system parameters that affect out-of-band emission (OBE) are HPA backoff and the modem pulse-shaping filter characteristics. Hardware simulation studies reported in Reference 2 addressed this issue as part of the problem of selecting an optimum filter for minimizing the nonlinear channel BER impairment. After establishing that the behavior of a 35-W helix TWTA is nearly identical to that of a high-power, coupled-cavity earth station HPA [2], the various candidate transmitter pulse-shaping filters were evaluated by direct measurement of spectrum OBE at the output of an HPA simulator using the 35-W helix tube. Figure 10a shows HPA TWTA measurements using filter A of Table 6. Figure 10b shows measurements for the same type of filter (filter A), but designed for 1.15 times the actual transmission rate. Reference 2 shows measured spectra for a 50-percent rolloff Nyquist filter for BT = 1.00 and 1.15, respectively. Analysis of such measurement data in the critical near region of the adjacent channel edges resulted in summary data as shown in Figure 11 for the 30-percent rolloff Nyquist filter type A of Table 6, but operated at $1.0 \leq BT \leq 1.20$, which indicates the OBE level sensitivity to filter BT and adjacent channel frequency location.
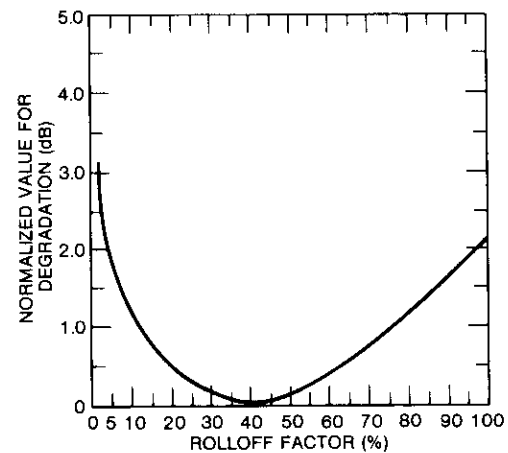
Figure 8. *Filter Type III Nonlinear Channel Impairment vs Filter Rolloff Factor*
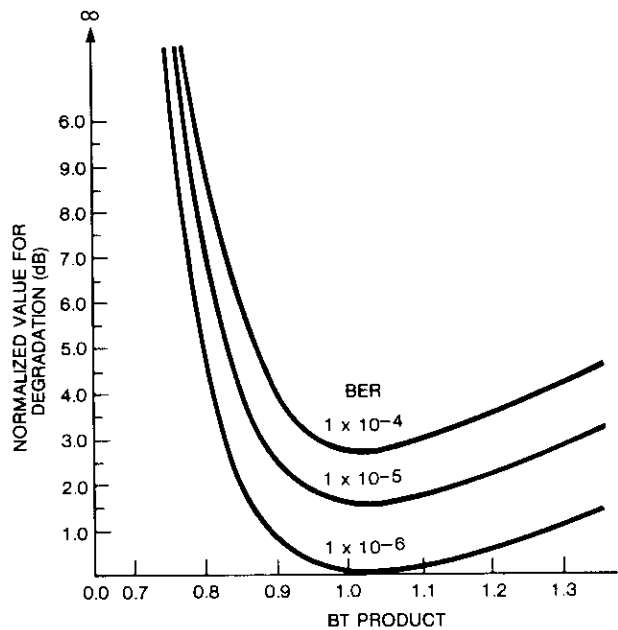
(a) Filter BT = 1.00

Figure 9. *Filter Type III Nonlinear Channel Impairment as a Function of Receiver Filter BT Product*
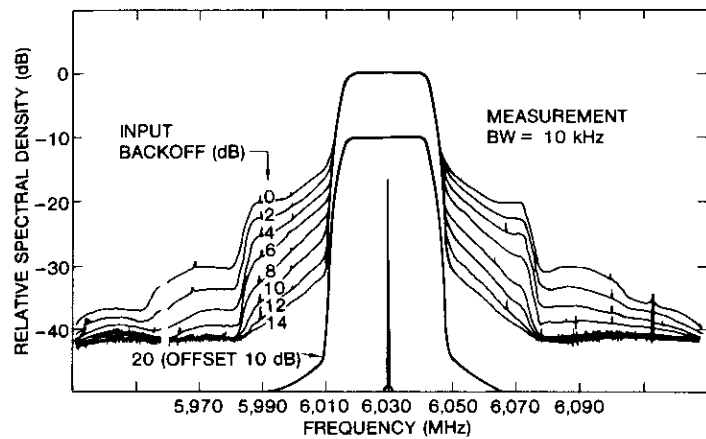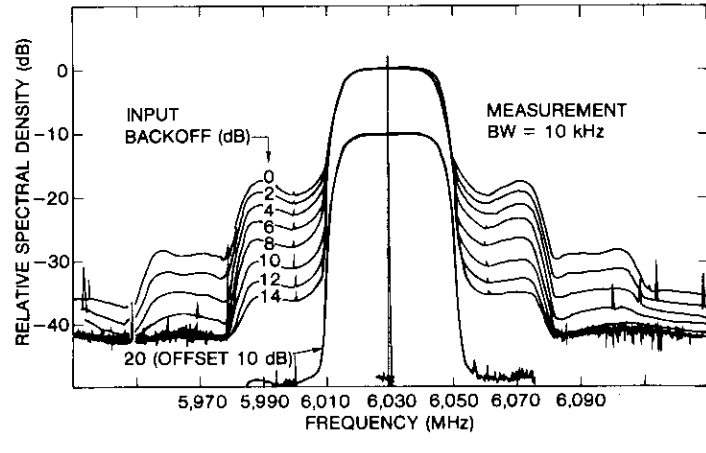
(b) Filter BT = 1.15

Figure 10. *HPA Output Spectra for Filtered QPSK (filter A, 30-percent Nyquist)*
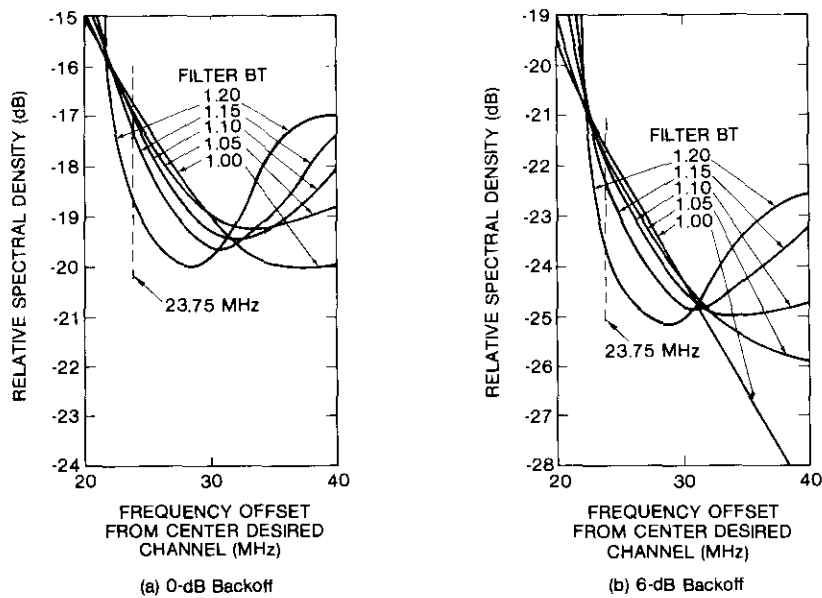
Figure 11. *Summarized HPA Regrowth Spectra for Filtered QPSK (filter A, 30-percent Nyquist)*

The worst-case tolerable power spectral density in the adjacent channel based on interference with an FM signal has been specified as 23.0 dBW/4 kHz for the INTELSAT system (Table 1). The foregoing sideband regrowth levels can be related to an INTELSAT TDMA operational scenario. Assuming a QPSK modulation symbol rate of R_s and an earth station e.i.r.p. of P_T dBW, the power spectral density in 4 kHz at the TDMA signal band center is

$$P_{TBC} = P_T - 10 \log R_s + 10 \log 4 \times 10^3 \text{ (dBW/4 kHz)} \quad .$$

The required level at band center plus or minus a frequency offset corresponding to the usable band edge of the adjacent channels is 23.0 dBW/4 kHz. The sideband levels must be reduced by

$$\Delta P = P_T - 10 \log R_s + 13.0 \text{ (dB)} \quad .$$

For the INTELSAT V/VI TDMA system, $P_T = 89$ dBW. Table 8 presents the relative measured OBE levels.

TABLE 8. RELATIVE MEASURED OBE LEVELS

R_b (Mbit/s)	R_s (Msymbol/s)	ΔP (dB)
60	30	27.2
120	60	24.2

The earlier studies assumed 60-Mbit/s QPSK. For this case, measured sideband power density levels relative to desired signal band center power density for 30- and 50-percent Nyquist filters were determined (as shown in Figures 12a and 12b, respectively) for filter BT products of 1.00 and 1.15. To meet the 27.2-dB sideband reduction would require 10- to 12-dB HPA input backoff for the optimum class of modem pulse-shaping filters determined by the hardware simulation studies. For the actual INTELSAT V 120-Mbit/s QPSK design, the permissible sideband reduction of 24.2 dB could be achieved at an HPA input backoff of 6 to 10 dB.

Similar computer simulation investigations were conducted for the broader class of filters of Table 7 [9]. A typical spectrum plot for a type I modem filter for an HPA input backoff of 12 dB is shown in Figure 13. Table 9 shows the study results of ΔP for 12- and 8.5-dB HPA input backoff for all of the filter types of Table 7. All optimum filter candidates perform equally well, although type III, the square root 40-percent rolloff Nyquist solution (finally selected for the TDMA specification), is slightly worse. This results from the square root of the 40-percent raised cosine Nyquist filter response mainlobe spectrum tending to be higher in the regions where adjacent channel

TABLE 9. 120-Mbit/s QPSK RELATIVE OBE LEVELS (ΔP) AT ADJACENT CHANNEL BAND EDGE: COMPUTER SIMULATION

FILTER TYPE	HPA INPUT BACKOFF	
	12 dB	8.5 dB
I	−30.6	—
II	−33.3	−27.2
III	−32.2	−26.2
IV	−33.1	−27.0
V	−33.2	−27.1
VI	−33.2	−27.1
VII	−33.2	−27.2
VIII	−33.2	−27.2
IX	−33.0	−27.1
X	−31.7	—
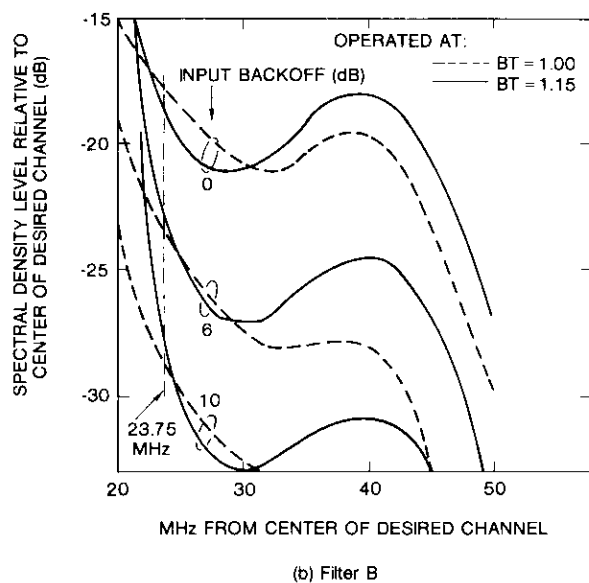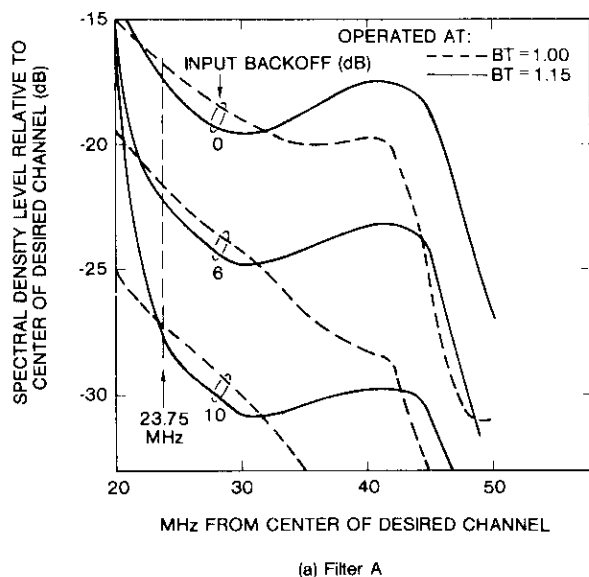
(a) Filter A

(b) Filter B

Figure 12. *HPA Regrowth Spectra Detail Comparison for Filtered QPSK*
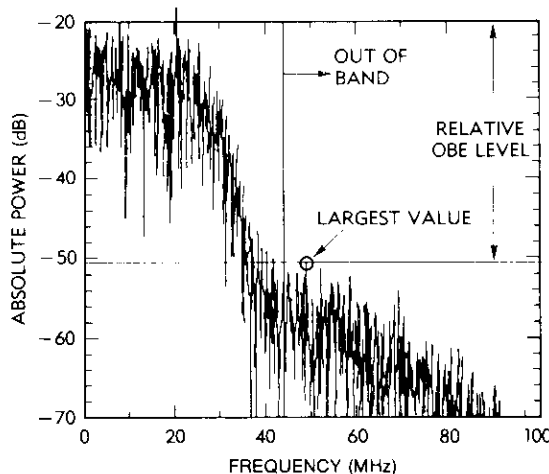
Figure 13. *Computer Simulation of Spectrum of Type I Modem Filters With HPA Input Backoff of 12 dB*

signal density should be reduced. These results are, of course, very dependent on the earth station 89-dBW e.i.r.p. required to maintain the transponder TWTA operating point at or near saturation.

The performance of modem filter type III (Table 7) in the INTELSAT V nonlinear channel has been measured in the laboratory simulation configuration of Figure 14 and using a modem configuration similar to Figure 4, but operating at 120 Mbit/s with an IF of 140 MHz. The results are shown in Figure 15 for various combinations of HPA and INTELSAT V TWTA input backoffs. The values of 10/2 backoff are the system design values. Figure 16 shows the INTELSAT BG-42-65 specified and hardware simulation modulator and demodulator pulse-shaping filter measured responses. Figure 17 shows the measured HPA and INTELSAT V simulator TWTA single-carrier characteristics. The measured HPA TWTA spectrum regrowth characteristics as a function of input backoff are shown in Figure 18. The optimum transponder TWTA backoff that minimizes the channel BER was investigated using the hardware simulation configuration of Figure 14 (with modem filter type III) as a function of HPA input backoff and down-link constant clear-sky E_b/N_o ("earth station size"). The results, shown in Figure 19, indicate that transponder input backoffs of 2 to 0 are optimum. In the operational INTELSAT V system, 3-dB TWTA input backoff is selected because of up-link earth station e.i.r.p. (OBE-related) and transponder gain limitations preceding the TWTA.
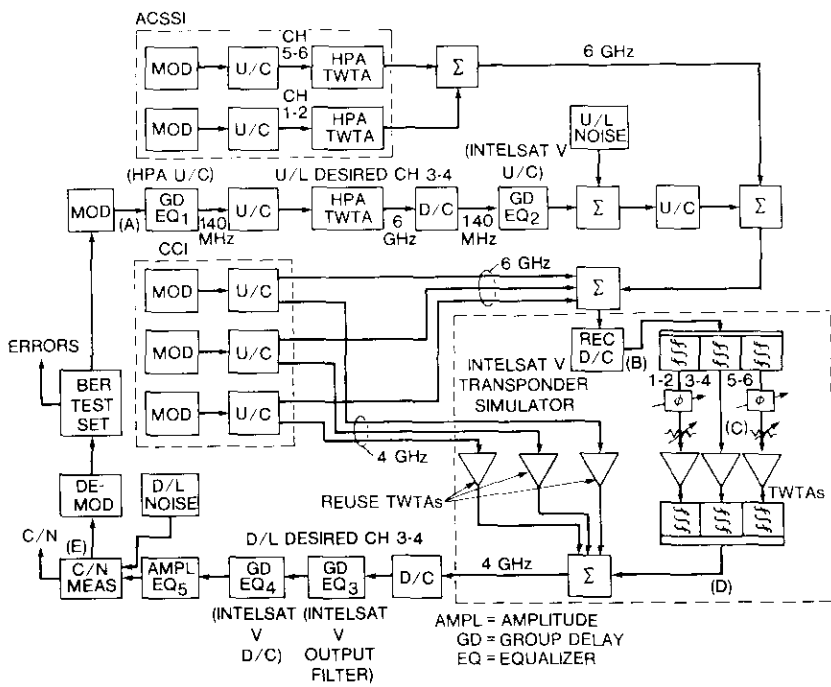
Figure 14. *Simplified Block Diagram of the INTELSAT V Hardware Simulation Experiment*
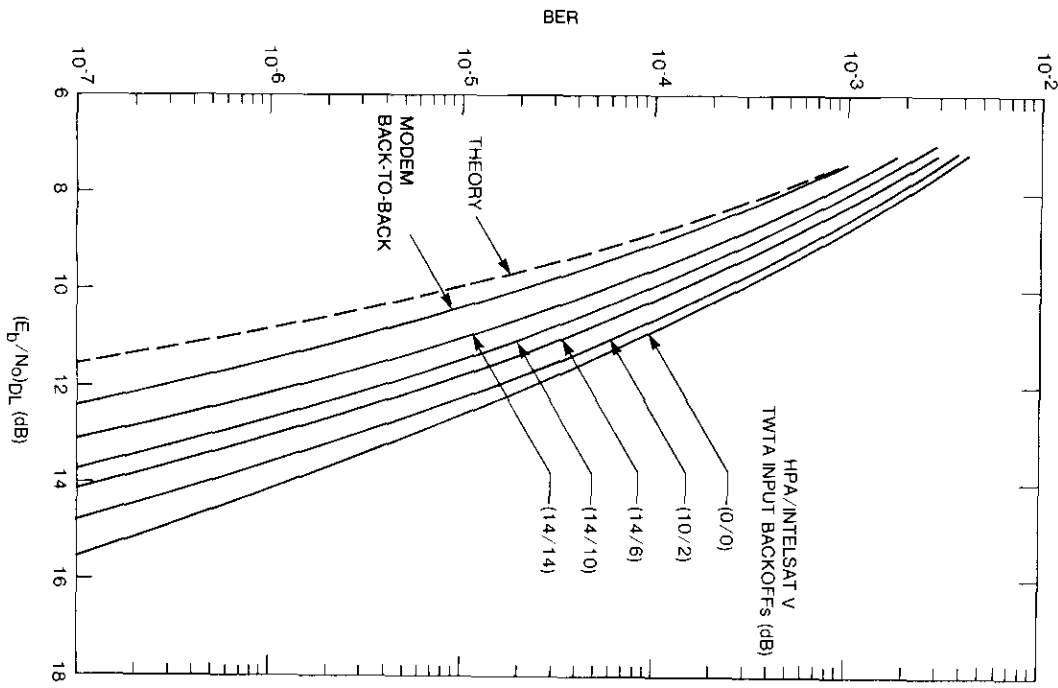
Figure 15. *120-Mbit/s QPSK Modem Filter Type III Performance in INTELSAT V Channel 3-4 Without Interference*
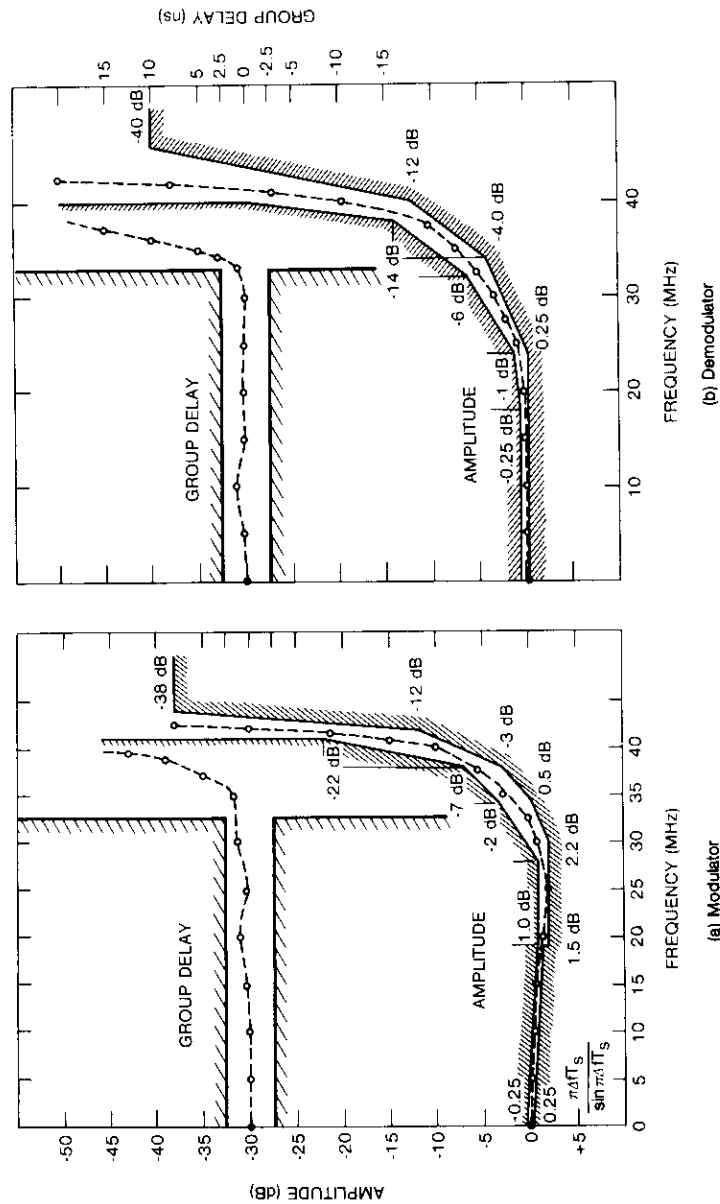
Figure 16. *Typical Specified and Measured Type III Modem Filter Amplitude and Group Delay*
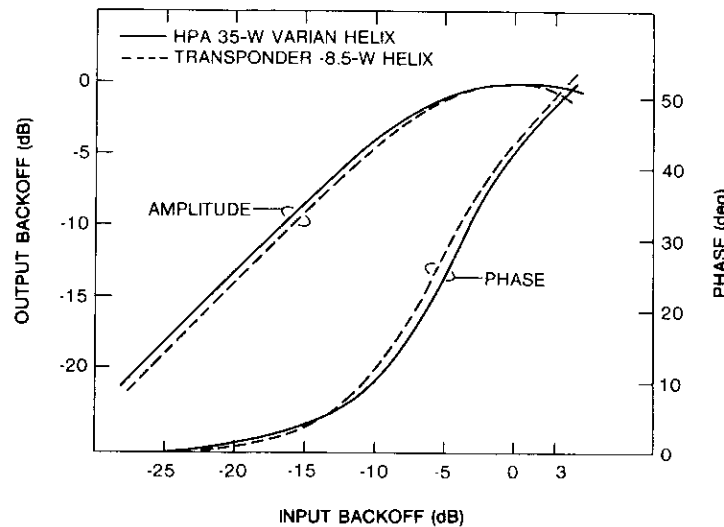
Figure 17. *Desired Channel 3-4 TWTAs Single-Carrier Characteristics*
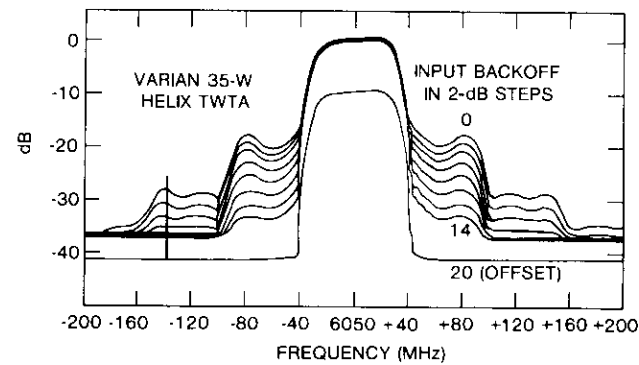
Figure 18. *Channel 3-4 HPA TWTA Spectral Regrowth*
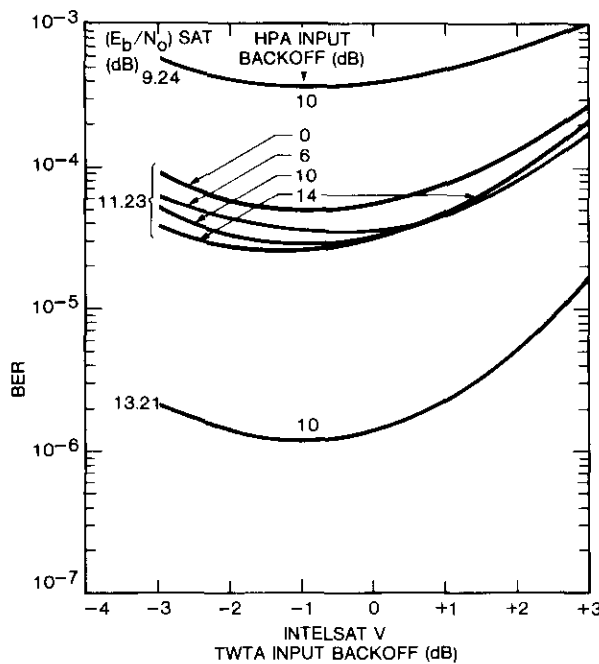
Figure 19. *Channel 3-4 Performance as a Function of HPA and INTELSAT V TWTA Input Backoffs*

Co-channel interference [impairment (b)]

As discussed with reference to the link budget, the initial conservative assumption for CCI was to treat it as AWGN under the assumption that the channel was linear. Simulation studies were then performed to determine the effect of other filtered QPSK co-channel signals. Clearly, the real system CCI model is complicated; the down-link CCI, which is related to the up-link CCI, is a filtered, limited version of the up-link interference for each reuse. Furthermore, each reuse transponder would have a separate receiver and the down-link interference would not, in general, be coherently related to the same reuse up-link interference. Hence, hardware simulation assessment of the up- and down-link effects is complex.

CCI was initially evaluated by employing both hardware and software simulation. Much of the computer simulation work has been reported in References 3, 6, and 9. Figure 20 shows the block diagram for these cases. Significant results from Reference 9, showing comparisons with the hardware
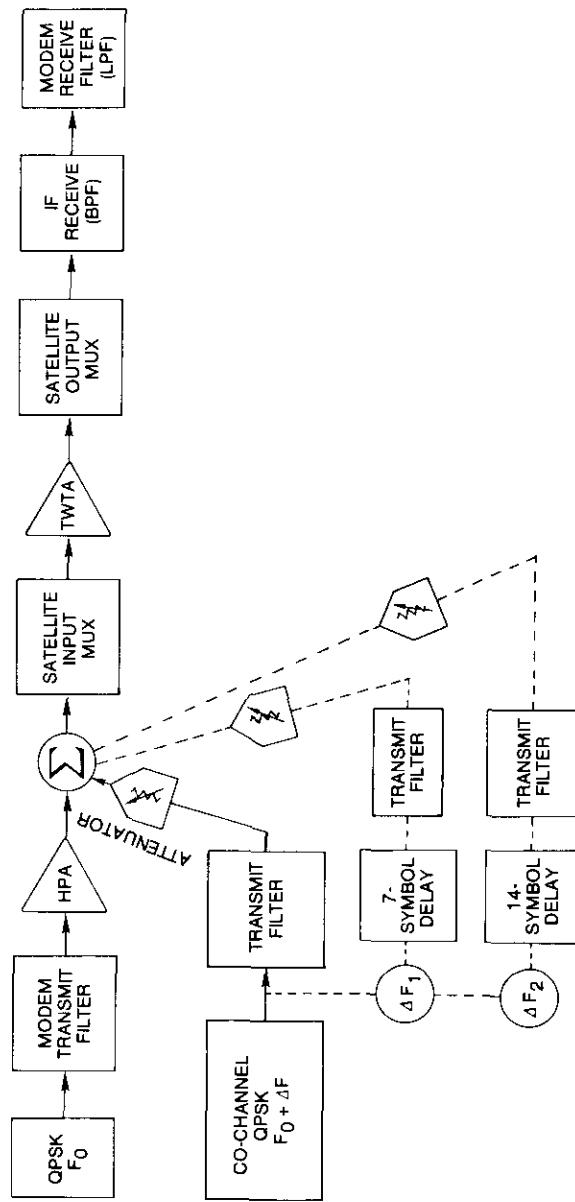
Figure 20. *Hardware/Software Simulation Block Diagram for Up-Link CCI Studies*
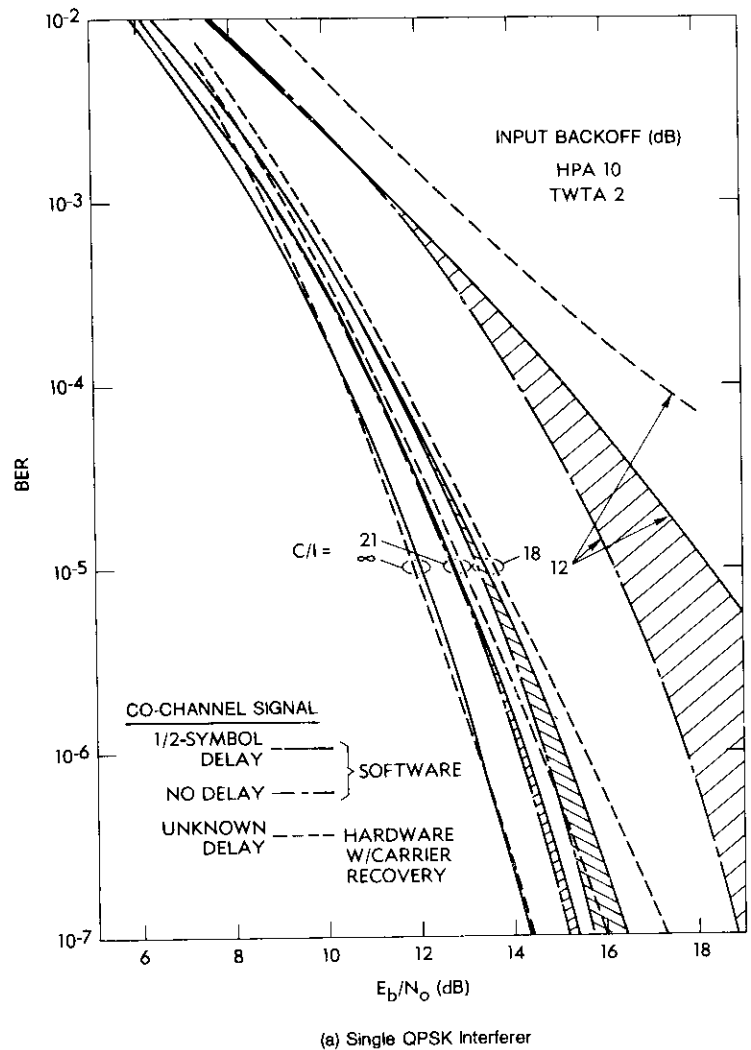
(a) Single QPSK Interferer

Figure 21a. *Hardware/Software BER Performance Comparisons of Satellite System With Up-Link CCI*

(b) Two QPSK Interferers

Figure 21b. *Hardware/Software BER Performance Comparisons of Satellite System With Up-Link CCI (Continued)*

simulation, are given in Figure 21 for one, two, and three QPSK up-link-only CCI signals. For the computer simulation, the interferers had random carrier phases, different PN data sequence seed generators, and either zero or half-symbol delays in the clock pulses among the wanted signal and single or

multiple interferers. For the hardware simulation, the wanted signal was completely independent from the interferers. However, the interferers were generated from a single QPSK modulator source, each additional interferer being generated by successive RF offset and signal envelope delay (7 symbols).

(c) Three QPSK Interferers
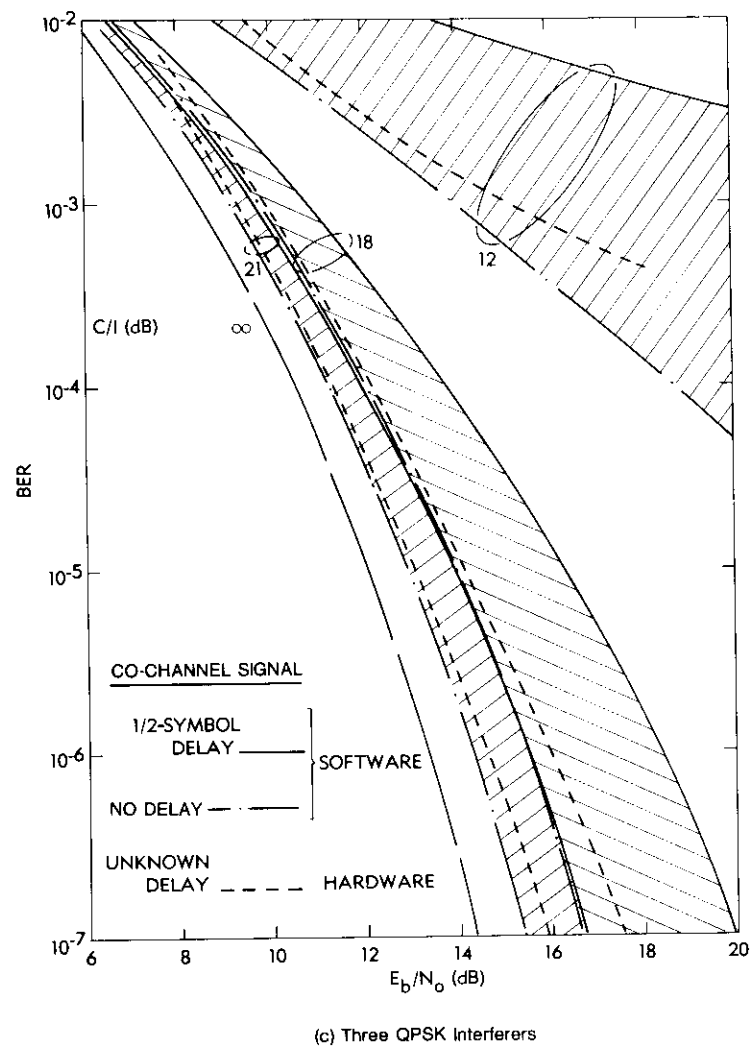
Figure 21c. *Hardware/Software BER Performance Comparisons of Satellite System With Up-Link CCI (Continued)*

Results showed encouraging agreement between simulation disciplines. While the hardware results are believed to be optimistic in most cases, the software results show, as expected, a wide spread in results due to the symbol synchronism assumption.

Additional computer simulation work reported in Reference 6 evaluated one, three, and five up- or down-link QPSK co-channel interferers using the optimum case III (Table 7) pulse-shaping filter in a system configuration similar to that of Figure 6. Results for up-link only or down-link only interference, shown in Figure 22, are similar to the optimistic extremes shown in the computer simulation work of Figure 21.

(a) Up-Link
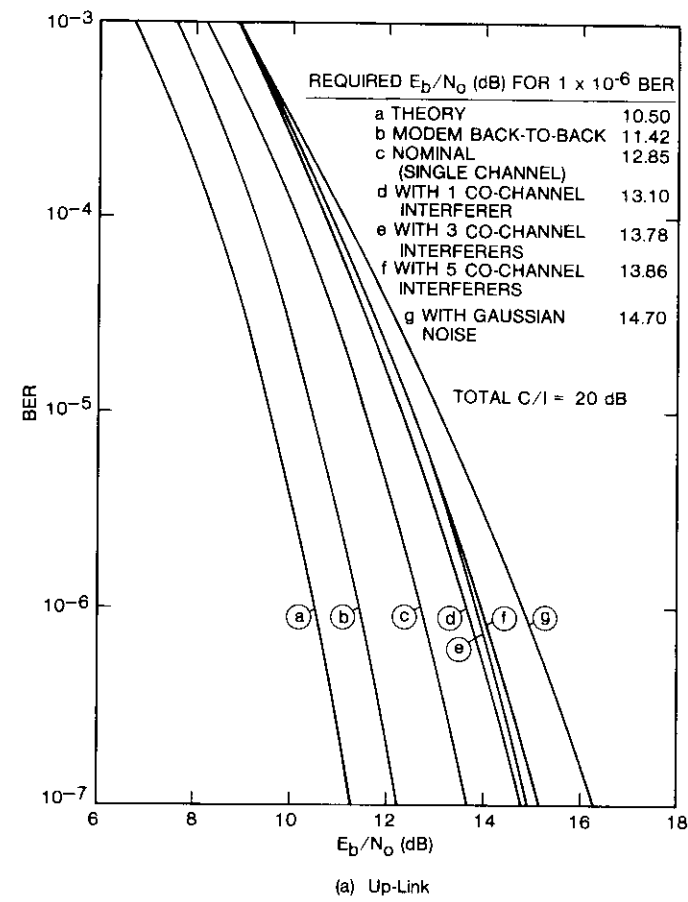
Figure 22a. *Additional Computer Simulation of CCI Performance*

REQUIRED E_b/N_0 (dB) FOR 1 x 10^{-6} BER	
a THEORY	10.50
b MODEM BACK-TO-BACK	11.42
c NOMINAL (SINGLE CHANNEL)	12.65
d WITH 1 CO-CHANNEL INTERFERER	13.69
e WITH 3 CO-CHANNEL INTERFERERS	13.87
f WITH 5 CO-CHANNEL INTERFERERS	13.90
g WITH GAUSSIAN NOISE	14.70

TOTAL C/I = 20 dB

(b) Down-Link
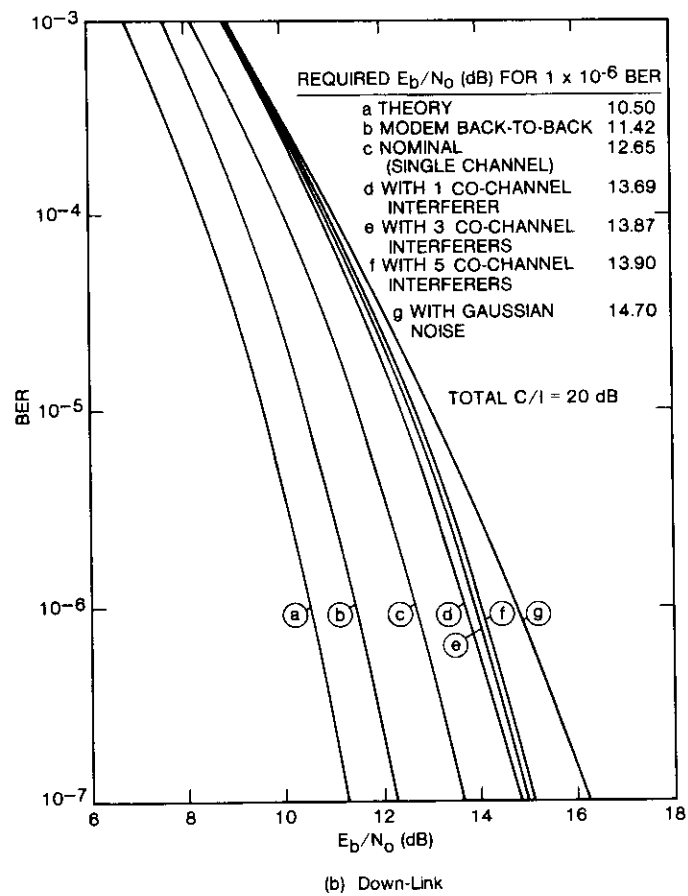
Figure 22b. *Additional Computer Simulation of CCI Performance (Continued)*

Finally, an extensive hardware simulation effort was planned and implemented to evaluate all of the expected TDMA 120-Mbit/s QPSK transmission impairments in the INTELSAT V system. An INTELSAT V transponder simulator was constructed at COMSAT Laboratories using filters and TWTAs identical to those of the spacecraft transponder. Figure 14 is the system simulation block diagram. This system hardware simulation was unique [4]: for the first time, completely independent, similarly filtered 120-Mbit/s QPSK signals were available for the wanted signal, the three CCI signals (INTELSAT V reuse plan),

and the two adjacent channel signals (assumed TDMA loading). Furthermore, the adjacent channels were implemented with TWTAs to simulate the adjacent-channel spreading effect [ACSSI impairment (c)]. The method used to generate and apply the CCI using simulated reuse transponder TWTAs is shown in Figure 14. Up-link (6 GHz) and down-link interference (4 GHz) were generated from the same up-link signal using dual up-converters designed and constructed by COMSAT Laboratories (see Figure 23). As opposed to the real system, these up-converters produced coherent up- and down-link interference signals; in addition, the up- and down-link signal modulation spectra were inverted by virtue of the dual-converter design. Initial investigations were made to determine the effects of a single up-link and a single down-link interferer pair on performance for two configurations:

- down-link co-channel interferer, coherent or non-coherent, and

- down-link spectrum inversion or non-inversion.

Figure 23a shows the configuration for this initial part of the CCI study. The results of BER measurements are shown in Figure 23b for $(C/I)_{UL} = (C/I)_{DL} = 20$ dB, comparing up-link/down-link interference spectrum coherence/noncoherence and inversion/non-inversion. No significant difference was found between these configurations. In a real system, incoherent desired and reuse channels occur by virtue of separate receiver/down-converters in the transponders, but the down-link reuse signal coupled to the desired channel does not experience spectrum inversion with respect to the desired channel spectrum. These initial experiments justified the CCI configuration outlined in Figure 14.

Link performance with band-limited up-link AWGN as interference was measured with this configuration; the results are shown in Figure 24. Also shown is the result of calculating the AWGN interference performance by graphically adding AWGN to the $C/I = \infty$ performance of the modem in the nonlinear channel. The agreement is very good, as previously encountered in the 60-Mbit/s QPSK INTELSAT IV simulation work. In the following QPSK CCI measurements, this method of AWGN analysis is included to support the integrity of the measurements and to show how much more optimistic than an AWGN assumption the particular QPSK interference case will be in a real system. Figure 25 shows the performance results for one, two, and three QPSK co-channel interference signals interfering on either the up-link or down-link, *but not both jointly*. Figure 26 shows the cases of one, two, and three QPSK co-channel interferers on *both* the up- and down-links together.
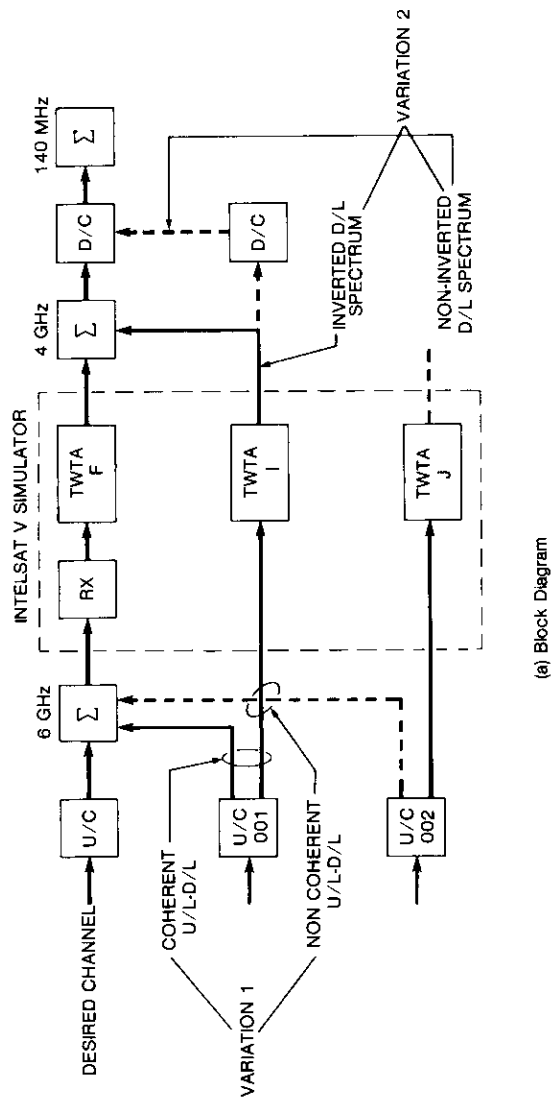
Figure 23a. *Initial Investigation of Simultaneous Single Up-Link and Down-Link CCI Hardware Simulation*
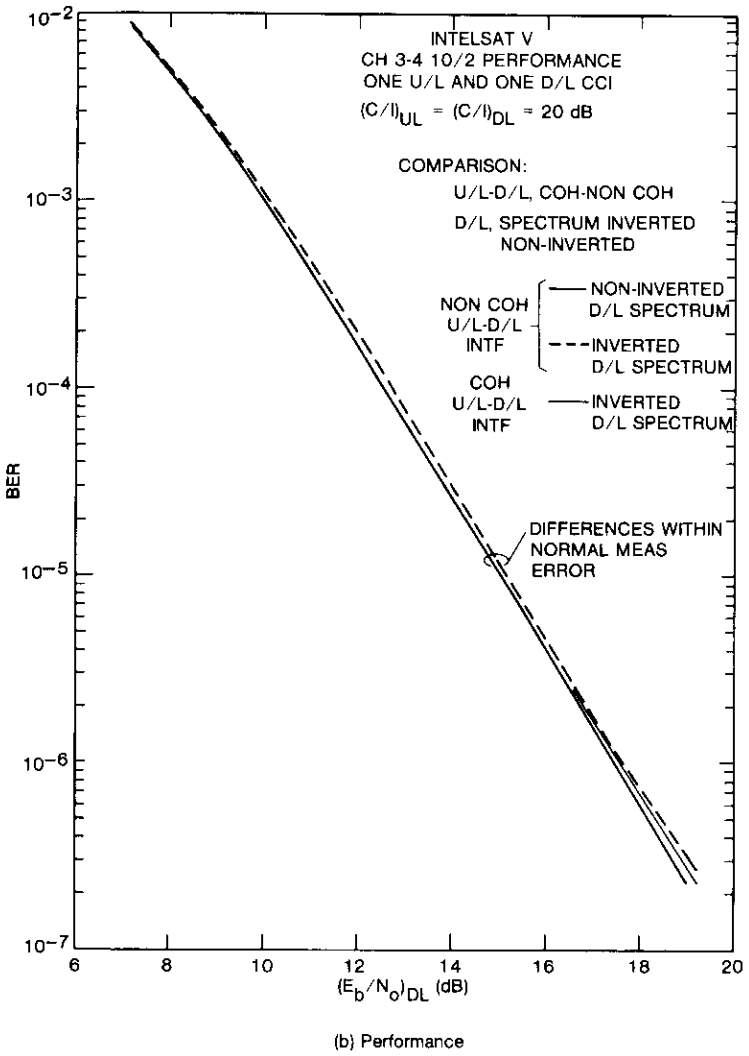
Figure 23b. *Initial Investigation of Simultaneous Single Up-Link and Down-Link CCI Hardware Simulation (Continued)*
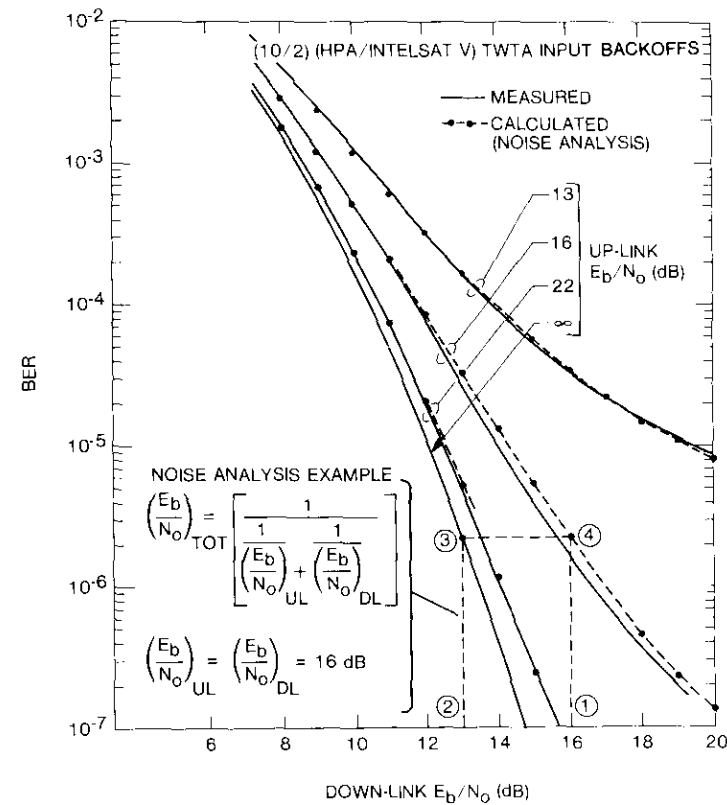
Figure 24. *Performance Impairment Due to Up-Link Thermal Noise*

Adjacent channel spectrum spreading (ACSSI) [impairment (e)]

In the previous link budget discussion, a combined allowance of 1 dB was used for ACSSI and DPI, mainly as the result of computer simulation. For example, Figure 27 shows the result of a three-channel computer simulation using the configuration of Figure 6 with modem filter case III of Table 7 [9]. Figure 28 shows another independent computer simulation investigation of this impairment [6]. Figure 27 would indicate 1 dB or more loss depending on the BER, whereas Figure 28 would indicate 0.5-dB loss for ACSSI.

The validity of the computer simulation was supported by the hardware simulation. The extensive INTELSAT V hardware simulation discussed previously (Figure 14) included ACSSI evaluation. QPSK modulation with independent
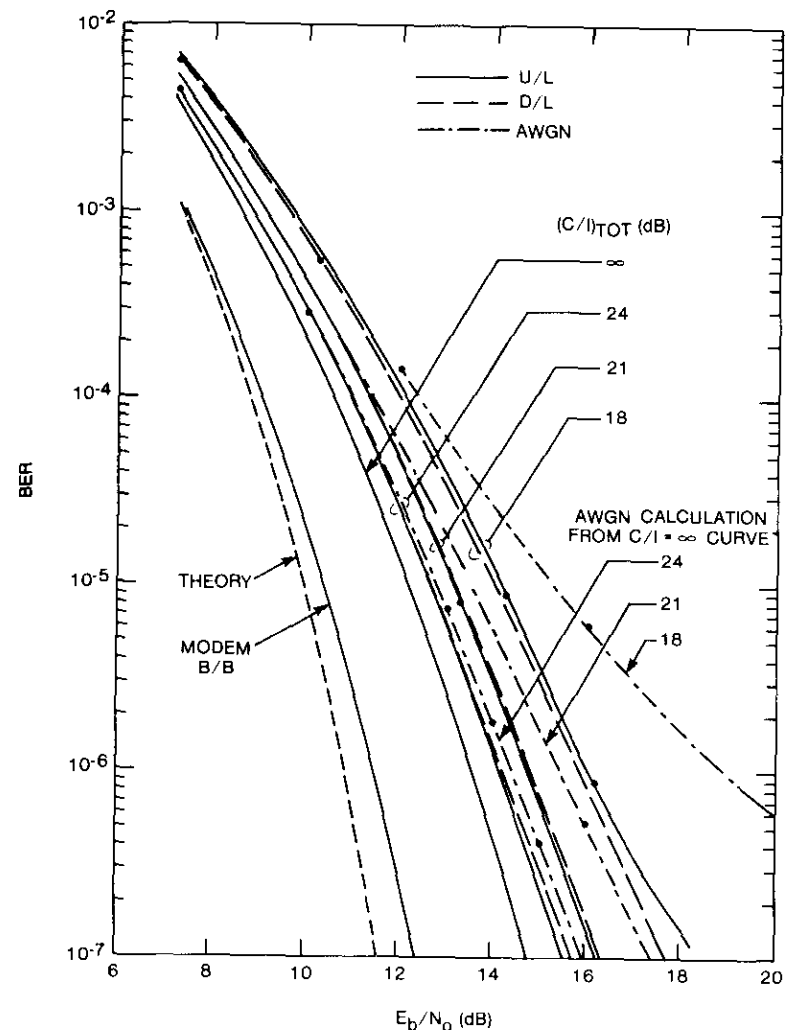
(a) One Up-Link or One Down-Link CCI

Figure 25a. *INTELSAT V Channel 3-4 10/2 Performance With CCI on Either Up-Link or Down-Link*
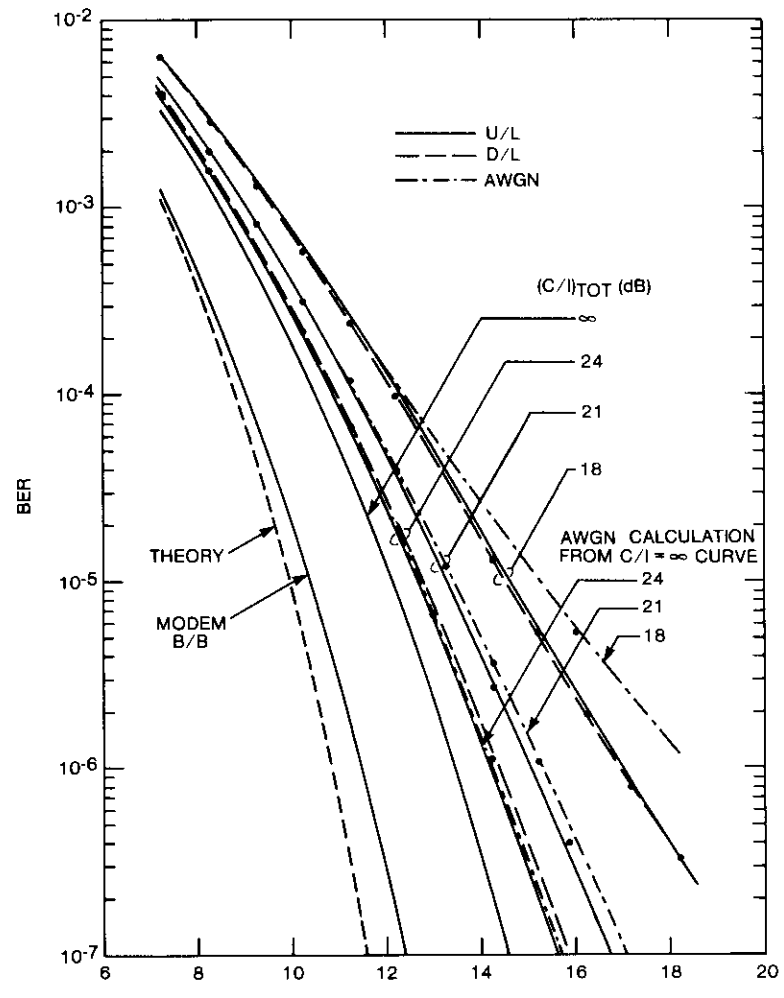
(b) Two Equal Up-Link or Down-Link CCI
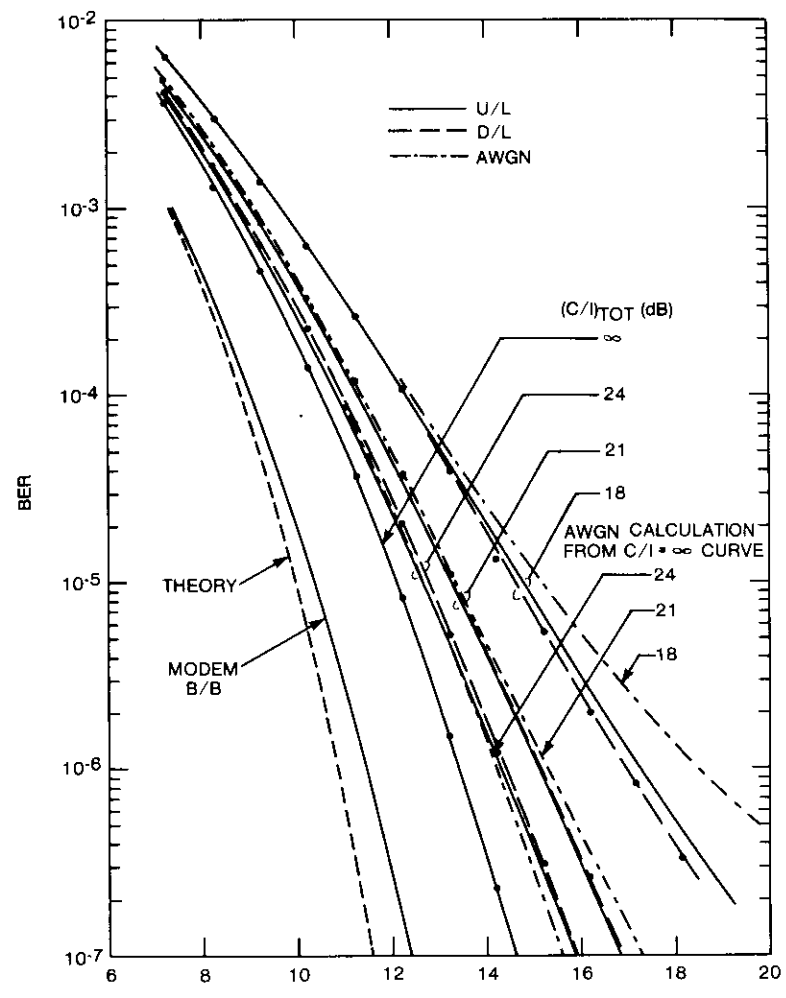
Figure 25b. *INTELSAT V Channel 3-4 10/2 Performance With CCI on Either Up-Link or Down-Link (Continued)*

(c) Three Equal Up-Link or Down-Link CCI

Figure 25c. *INTELSAT V Channel 3-4 10/2 Performance With CCI on Either Up-Link or Down-Link (Continued)*

clocked-PN data generators and case III (Table 7) pulse-shaping filters, together with up-converters and simulated HPA helix TWTAs, was used to achieve realistic sideband spectrum regrowth levels in INTELSAT V laboratory transponder simulator channels 1-2 and 5-6 interfering with the wanted transponder channel 3-4. Figure 29 shows the measured HPA TWTA output spectra as a function of input backoff for these channels. Comparison of the sideband regrowth of Figure 29 with the corresponding detail of the wanted channel HPA output spectrum of Figure 18 indicates some differences in the absolute level and shape of the regrowth sideband power. Interference spectra similar to those of Figure 18 would have been more representative of the adjacent channels of real system high-power, coupled-cavity TWTAs. However, even the slightly non-ideal spectrum regrowth signatures provided the desired result.
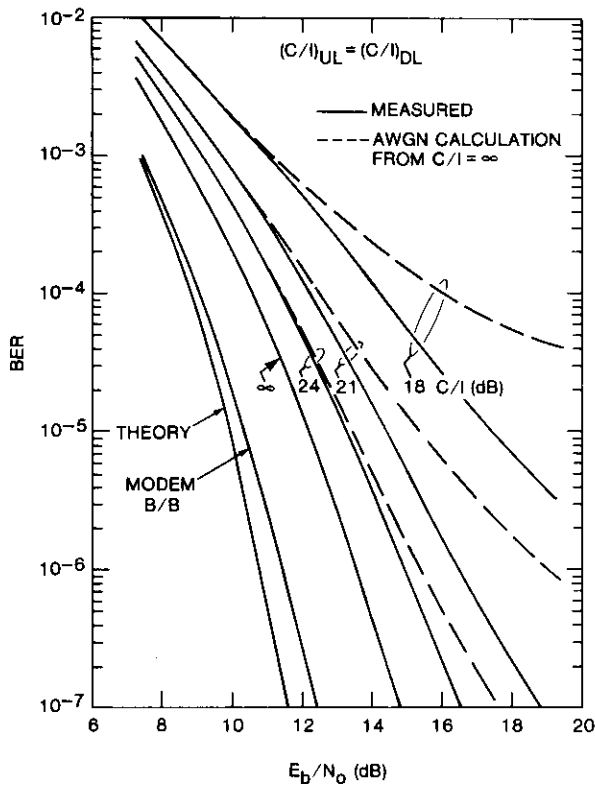
(a) One Up-Link and Down-Link CCI

Figure 26a. *INTELSAT V Channel 3-4 10/2 Performance with CCI on Both Up-Link and Down-Link*

(c) Three Equal Up-Link and Down-Link CCI
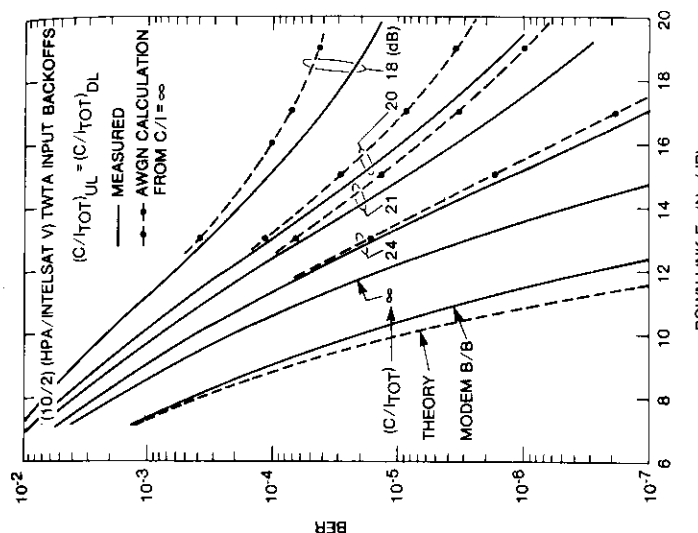
Figure 26c. *INTELSAT V Channel 3-4 10/2 Performance with CCI on Both Up-Link and Down-Link (Continued)*

(b) Two Up-Link and Down-Link CCI
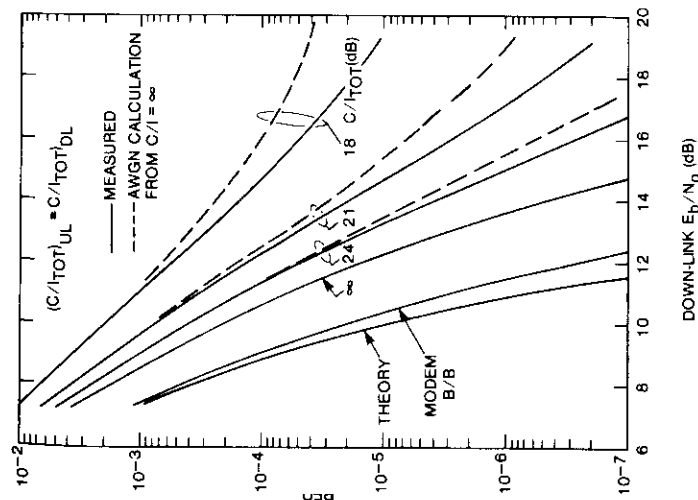
Figure 26b. *INTELSAT V Channel 3-4 10/2 Performance with CCI on Both Up-Link and Down-Link (Continued)*

off for these measurements.) The BER performance measurements show an imbalance in sideband interference between upper and lower adjacent channels (Figures 30a and 30b). This results from the TWTA sideband regrowth differences already noted. Channel 5-6 lower sideband regrowth levels are higher than channel 1-2 upper sideband regrowth levels (Figure 29) and the corresponding performance measurements reflect this imbalance.

These data were used to perform an AWGN analysis. The wanted channel main spectrum lobe and the adjacent channel sideband regrowth levels were graphically integrated within the 60-MHz central portion of each channel, using linear scaling to determine the effective C/I ratios. The adjacent channel input backoff was 10 dB. The resulting C/I ratios are

Channel	C/I (dB)
1-2	25.05
5-6	23.70
1-2 plus 5-6	21.31

Figure 27. *Computer Simulation of INTELSAT V With and Without Two-Channel ACSSI*

ACSSI effects on wanted channel 3-4 performance of each channel separately and both channels combined are presented in Figure 30. These results do not include dual-path effects or any down-link adjacent transponder TWTA ACSSI effects. (The adjacent channel INTELSAT V transponder TWTAs were turned

Figure 28. *Computer Simulation of ACSSI and DPI Effects*
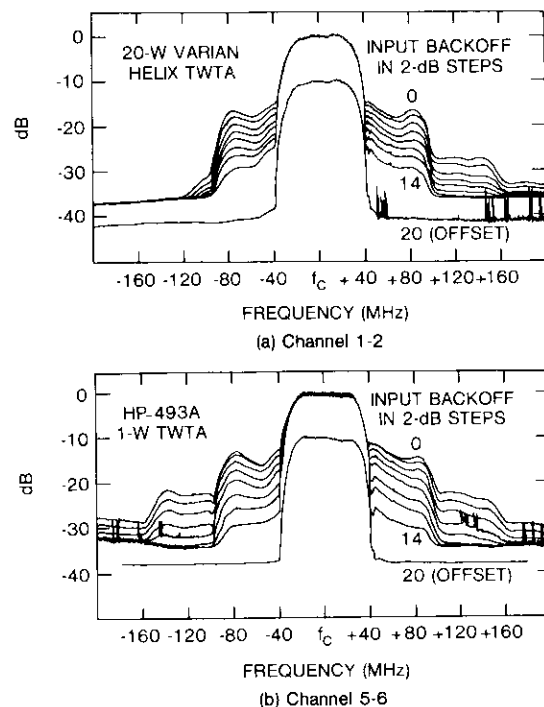
Figure 29. *Adjacent Channel Signal Spectra Showing Sideband Regrowth*

Using these values of C/I ratio, the BER performance was graphically determined from the nonlinear channel performance $(C/I = \infty)$, assuming interference power as thermal AWGN, with the results shown in Figure 30. Clearly, for the levels of regrowth associated with 10-dB HPA input backoff, the interference to the wanted nonlinear channel performance can be treated as AWGN.

Figure 30c indicates that the adjacent channel TWTA regrowth levels (although unbalanced) produced a combined loss of about 1.7 dB at 1×10^{-6} BER. Careful examination of Figures 18 and 29 in the regrowth regions show that, at 10-dB input backoff, the lower regrowth region of channel 5-6, which interferes with channel 3-4, is excessive and nontypical compared to the regrowth regions of the wanted channel 3-4 TWTA, which are more typical of the actual 8- or 12-kW coupled-cavity HPAs. Furthermore, the channel 1-2 upper regrowth sideband (Figure 29), which interferes with channel 3-4 and whose performance is shown in Figure 30a, has a higher

sideband level than the typical TWTA of Figure 18. Therefore, it is more reasonable to assume adjacent channel levels upper bounded by the levels shown by the channel 1-2 plots of Figure 29. (The corresponding computed C/I ratio was 25.05 dB.) The contribution from two such interferences (upper and lower adjacent channels) would be a C/I of 22.05 dB.

Figure 31 is included as an aid to determine the loss effect to the wanted nonlinear channel with specific incremental levels of additive interference expressed as a C/I ratio in a 60-MHz bandwidth. From Figure 31, a C/I ratio
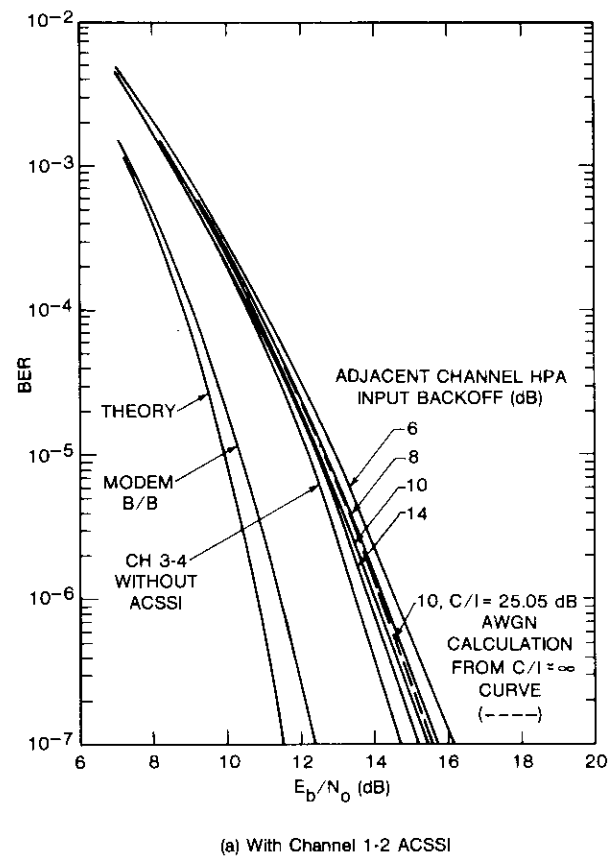
(a) With Channel 1-2 ACSSI

Figure 30a. *INTELSAT V Channel 3-4 10/2 Performance With Up-Link ACSSI*

of 22 dB is seen to incur a loss of about 1.3 to 1.4 dB at 1×10^{-6} BER. Typical sideband levels can be obtained by comparing the channel 1-2 upper sideband level in Figure 29 (-25 dB) to that of Figure 18 (-28 dB) for 10-dB input backoff. The Figure 29 level is approximately 3 dB lower than the corresponding Figure 18 level.* Hence, 28-dB (rather than 25.05 dB) C/I

(b) With Channel 5-6 ACSSI
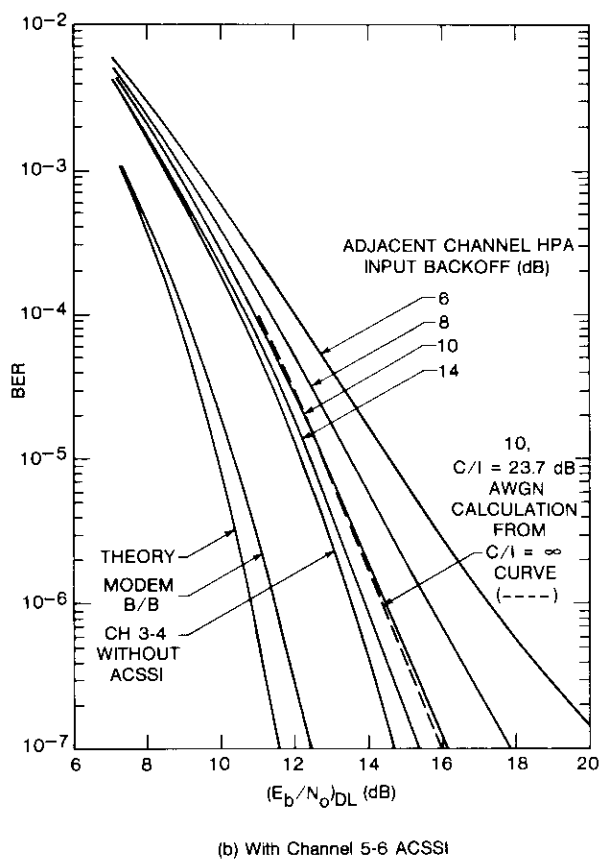
Figure 30b. *INTELSAT V Channel 3-4 10/2 Performance With Up-Link ACSSI (Continued)*

---

* The original laboratory spectral plots are needed to verify the 3-dB difference accurately.

(c) With Channels 1-2 and 5-6 ACSSI and Other Effects, as Noted
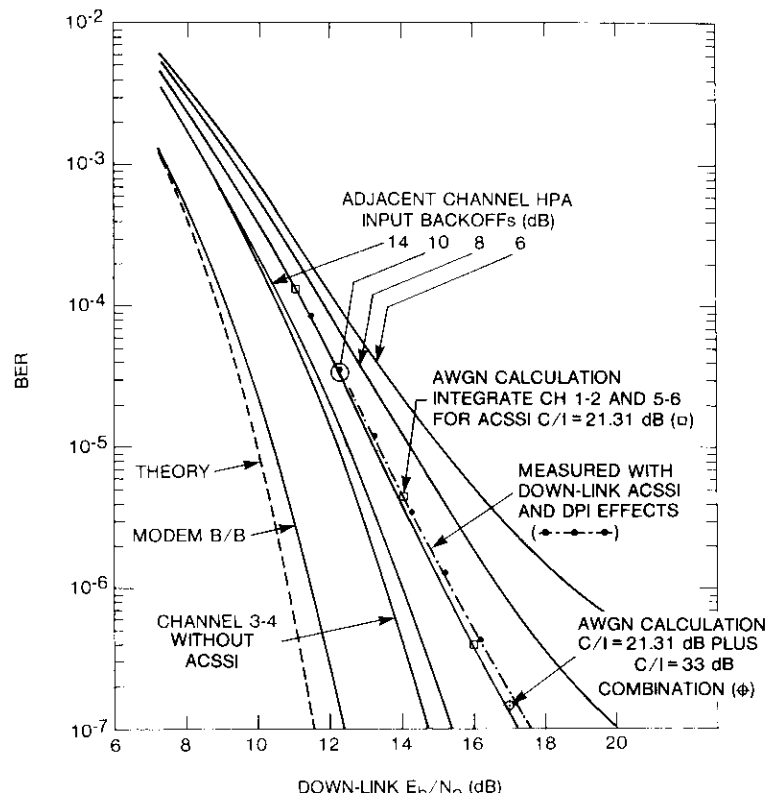
Figure 30c. *INTELSAT V Channel 3-4 10/2 Performance With Up-Link ACSSI (Continued)*

for one ACSSI and 25-dB (rather than 22.05 dB) C/I for two ACSSI interferers would be more likely for the operational system. The resulting loss for $C/I = 25$ dB from Figure 31 would be approximately 0.7 dB.

Dual-path interference (DPI) [impairment (d)]

Early measurements made with an INTELSAT IV laboratory simulator in the configuration shown in Figure 3, with the 60-Mbit/s QPSK modem of Figure 4, indicated that dual-path transmission resulted in some impairment loss. In
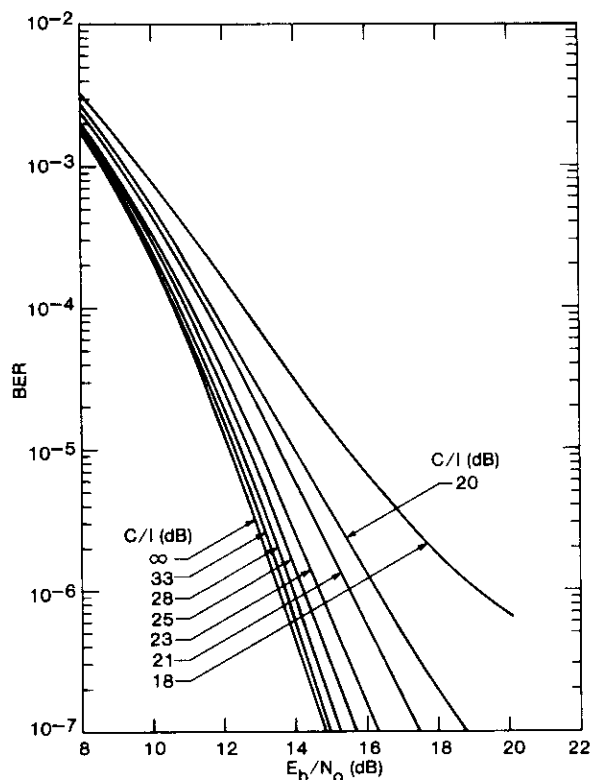
Figure 31. *Modem In-Channel Performance Variation With AWGN Interference Calculation as a Function of C/I*

Reference 2, the minimum and maximum dual-path loss conditions were identified and measured. Although the relative RF phasing of transponder channels in the INTELSAT systems had not been specified, it was observed that a specific phasing condition between adjacent and center wanted channels would result in a worst-case destructive interference at the demodulator.

Attempts were made to evaluate the DPI for INTELSAT V using computer simulation. The evaluation in Reference 9 does not distinguish DPI from ACSSI, and in Reference 6 the effect was found to be negligible (see Figure 28).

The extensive INTELSAT V hardware simulation work included this impairment evaluation. Figure 14 shows the arrangement of the transponder simulator adjacent channels 1-2 and 5-6 with phase shifters and attenuators which allowed the determination of maximum and minimum dual-path effects.

Optimum pulse-shaping filters (case III of Table 7) were used in the modem. The transponder channels were prepared by adjusting the small-signal gains of channels 1-2, 3-4, and 5-6 to be equal with the channel 1-2 and 5-6 phase shifters in place. Additional attenuation of 6 dB was introduced into the signal path of channels 1-2 and 5-6 to study the effects simulating the presence of signals in these channels that saturate the TWTAs. Each phase shifter needed to be adjusted methodically to search out the minimum and maximum effects of dual path on the BER of the desired channel. Due to the lack of a phasing specification between channels, it is impossible to predict the average effect prior to pre-launch or in-orbit measurements.

Figure 32 shows the measured results of the INTELSAT V hardware simulation. BER was measured for channel 3-4 with HPA and transponder TWTA operating input backoff of (10/2) and (0/0) dB. It is important to note that these results were obtained for "silent" adjacent channels (channels without signal loading). For the case of adjacent channels loaded with QPSK/TDMA signals, up-link (primarily) and down-link ACSSI effects will mask the effect of DPI alone.

These results showed that, for the (0/0) input backoff channel 3-4 link operating conditions, the worst-case phasing dual-path effects are large for the equal small-signal, three-channel gain condition. When the adjacent channel gain is reduced by 6 dB, the (0/0) worst-case phasing dual-path effect is reduced considerably. This same (0/0) link condition showed essentially no dual-path effect for the best-case phasing adjustment. For the normally expected (10/2) input backoff link operating conditions, the worst-case dual-path phasing produces moderate effects (equal small-signal, three-channel gain conditions) and essentially no effect for the best-case phasing adjustment. Although not measured, it can be inferred from the (0/0) link condition that reducing the small-signal gain of the adjacent channels by 6 dB would produce essentially no dual-path effect for the worst-case phasing adjustment in the case of (10/2) link operating conditions.

These impairment losses are lower than previous dual-path measurements made at 60 Mbit/s [2]. System parameters affecting this impairment are primarily the input and output transponder filter multiplexer characteristics and the demodulator adjacent channel rejection filter characteristics, and secondarily, the modem pulse-shaping filter design, the HPA spectral regrowth characteristics, and possibly the demodulator carrier and clock recovery circuits.

The overall system down-link effect of both adjacent channels loaded with TDMA signals which include the dual-path effect as well as any down-link ACSSI was studied as indicated in the previous section on ACSSI impairment
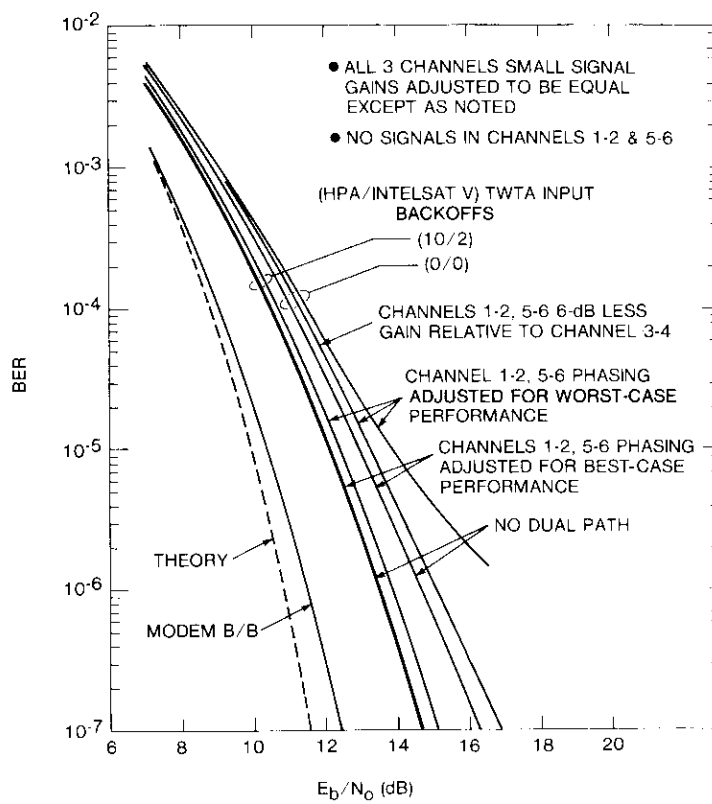
Figure 32. *INTELSAT V Channel 3-4 Performance With Channel 1-2 and Channel 5-6 DPI Effects*

evaluation. The phasing of the adjacent channels was adjusted to give the worst-case dual-path effect as explained above. The adjacent channel TWTAs were turned off to measure the up-link ACSSI effect and then turned on to include dual-path and down-link ACSSI. Figure 30c shows the result for 10-dB HPA input backoffs. The combined effect of DPI and down-link ACSSI (thought·to be mainly dual path) is small. An AWGN analysis shows this effect to be equivalent to a noise interferer having a C/I of 33 dB producing an E_b/N_o degradation of approximately 0.1 dB at a BER of 1×10^{-6}. The combined effect of up-link and down-link ACSSI (0.7 dB) plus DPI (0.1 dB) justifies the assumption of 1.0 dB used in the link budget work.

Channel equalization distortion ISI [impairment (e)]

A very important issue for the INTELSAT V TDMA transmission system was the precision required in the link amplitude and group delay responses. This issue was addressed in part through the INTELSAT V laboratory hardware simulation effort.

The link shown in Figure 14 includes up- and down-link group delay and amplitude equalizers to bring the various portions of the link into compliance with prescribed INTELSAT specifications or, in the case of the transponder output filter, to achieve an improvement in the filter group delay characteristic with reasonable equalization complexity.

The equalization of the HPA simulator of Figure 14 was required due to the characteristics of the single up-conversion bandpass filter. A very small single-stage parabolic correction (equalizer 1 of Figure 14) was required to correct this filter. The HPA simulator up- and down-converters shown in Figure 14 are not part of the actual operational system.

The equalization of the second up-converter (the only up-converter in the actual system) was required as a result of the first IF bandpass filter in the up-converter. A two-stage all-pass group delay equalizer was designed (equalizer 2 of Figure 14) with the aid of a COMSAT Laboratories computer program. The overall up-link responses were observed from interface (A) to interfaces (B) and (C) (Figure 14). The response of interface (A) to (B) represents the entire "earth station transmit chain" response. The measured "transmit chain" amplitude and group delay responses have been plotted on the INTELSAT TDMA specification masks and are shown in Figure 33.

The response of the channel 3-4 transponder input multiplexer filter (not included in Figure 33) is shown in Figure 34a. This filter has a measure of internal group delay equalization required by INTELSAT V transponder specifications.

The down-link is somewhat more complicated than the up-link. Two group delay equalizers had to be designed and constructed, one for INTELSAT V channel 3-4 output filter correction (not equalized by INTELSAT V transponder specifications) and one for the down-link down-converter (equalizers 3 and 4, respectively, of Figure 14). Equalizer 3 employed a three-stage all-pass configuration and equalizer 4 employed a two-stage configuration. The correction required for the transponder output filter is not specified. Figure 34b shows the amplitude and group delay response of the channel 3-4 transponder output filter without group delay equalization. A reasonable tradeoff between corrected group delay and equalizer complexity was chosen, resulting in a three-stage design for equalizer 3. An amplitude slope correction of
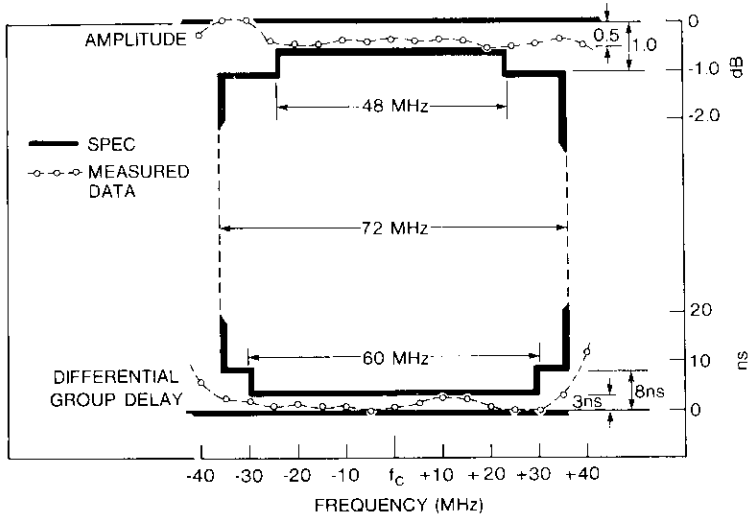
Figure 33. *Channel 3-4 Up-Link Amplitude and Group Delay Responses*

+0.5 dB/80 MHz was found to be necessary for the down-link in addition to the group delay correction, resulting in part from the non-ideal all-pass characteristics of the cascaded group delay equalizers 3 and 4. This resulted in equalizer 5 of Figure 14.

Figure 35 shows the amplitude and group delay responses plotted on the INTELSAT TDMA specification masks for the "earth station receive chain" (without equalizer 3) demonstrating the degree of compliance achieved [interface (D) to (E) of Figure 14].

Finally, the overall tandem HPA and transponder channel 3-4 amplitude and group delay responses (including equalizer 3) measured at two combinations of HPA and transponder TWTA input backoffs are shown in Figure 36 [interface (A) to (E) of Figure 14]. The link equalization achieved is evident from these figures.

However, the question remains as to how good equalization has to be or, conversely, how sensitive is BER to link equalization degradation. BER performance measurements have been made for linear group delay, parabolic group delay, and linear amplitude slope of varying degrees of distortion on the up- or down-link of an INTELSAT V 72-MHz channel having the initial equalization perfection described above. The results are summarized in Tables 10 through 12 for linear amplitude slope, linear group delay slope, and parabolic group delay distortion types, respectively.
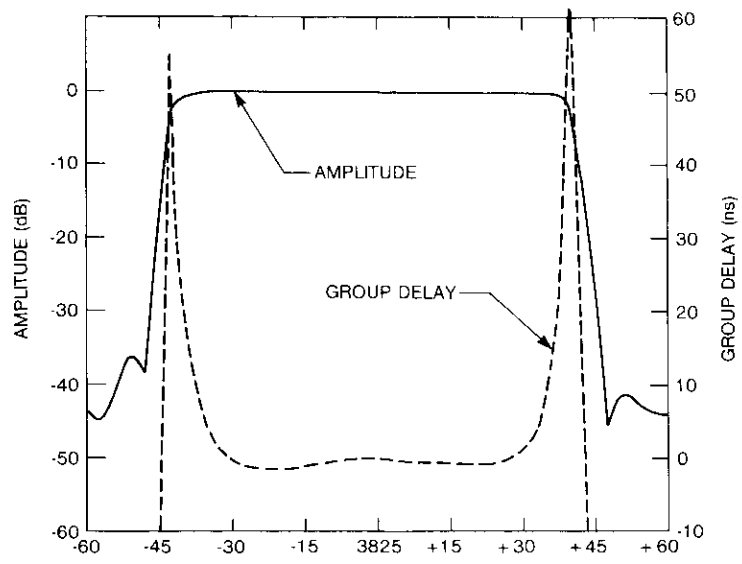
(a) Input
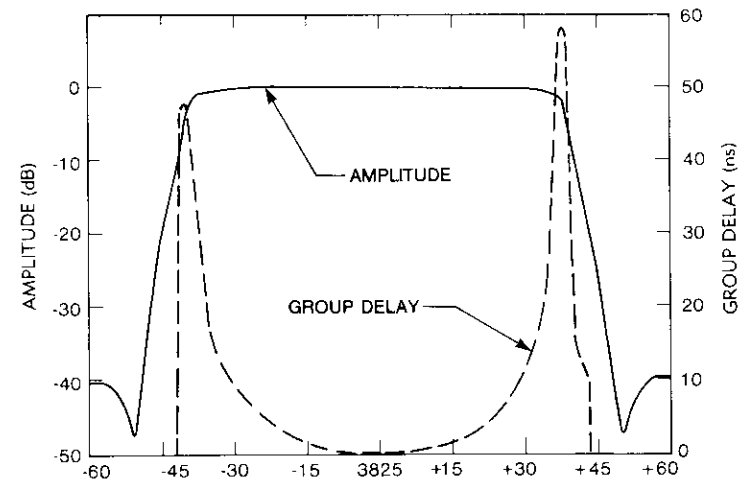
(b) Output

Figure 34. *Channel 3-4 Transponder Input and Output Filters Amplitude and Group Delay Responses*
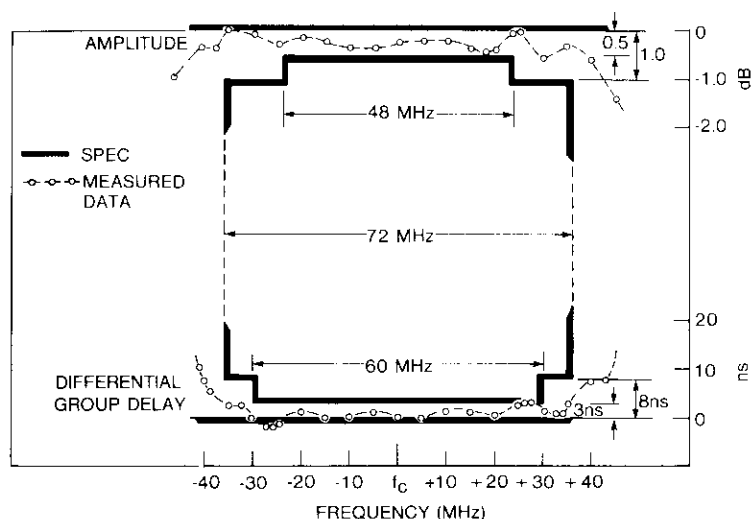
Figure 35. *Channel 3-4 Down-Link Amplitude and Group Delay Responses*

Forward error correction coding

FEC coding is required on links that experience the full reuse CCI. A study was conducted to identify candidate error correction codes and assess their impact on the INTELSAT TDMA system [11]. The primary performance goals were to improve an uncoded BER of 7×10^{-5} under clear-sky conditions to better than 1×10^{-6} and to improve an uncoded BER of 3×10^{-3} under CCI conditions arising from rain-induced depolarization to better than 1×10^{-3}. Errors produced by CCI were concluded to be sufficiently random to permit the use of random error correcting codes to achieve the desired performance goals. This fact was subsequently confirmed in hardware testing of models of a coder/decoder (codec) selected on the basis of the study results.

Block codes were found better suited to TDMA operation than convolutional codes, which require the extra complexity of convolutional encoder parity bit flushing at the end of a burst. Furthermore, the convolutional decoders need the insertion of dummy information bits corresponding to the flushed parity bits. The time required to process the numerous dummy bits restricts the minimum spacing of adjacent bursts. Block codes are also shorter than comparable self-orthogonal convolutional codes and offer better BER performance.
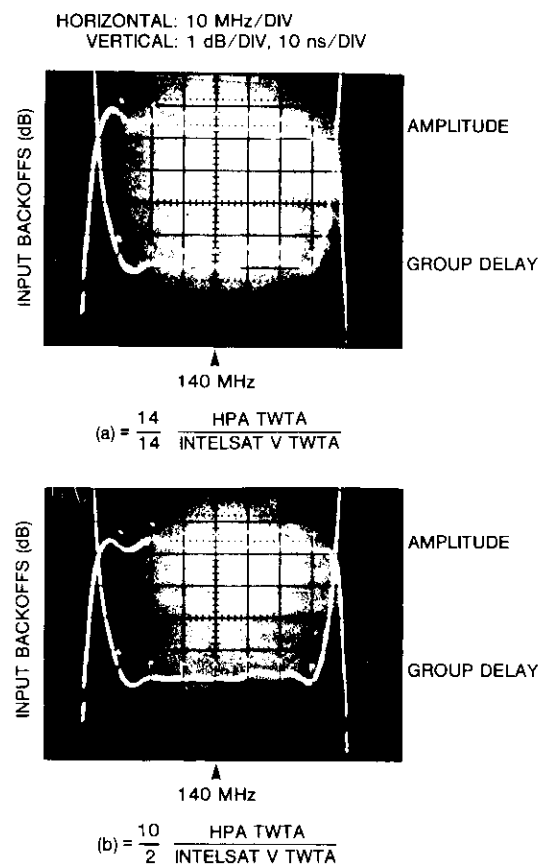
Figure 36. *Channel 3-4 Overall Link Responses*

Universal application of a single coding and decoding method throughout the system appeared most desirable since a larger number of links require coding and all requirements can be met with a high-rate code and moderate codec complexity. Placement of the codec between the multiplexer/demultiplexer and scrambler/descrambler permits a single codec operating in a burst mode to process all bursts. Unique word detection was recommended for ambiguity resolution since differential decoding doubles the BER. Furthermore, if the differential decoder is located ahead of the FEC decoder, the resulting paired errors produce further decoding degradation, while positioning the differential decoder after the FEC decoder requires additional overhead bits since ambiguity is not resolved prior to FEC decoding.

TABLE 10. LINEAR AMPLITUDE SLOPE DISTORTION

DISTORTION ± (dB/72 MHz)	E_b/N_o DEGRADATION FROM IDEAL (dB)	
	UP-LINK	DOWN-LINK
0	2.50	2.50
1	2.65	2.65
2	3.10	3.05
3	3.75	3.65
4	4.70	4.50
5	6.15	5.35
6	7.75	6.50

TABLE 11. LINEAR GROUP DELAY SLOPE DISTORTION

DISTORTION ± (ns/72 MHz)	E_b/N_o DEGRADATION FROM IDEAL (dB)	
	UP-LINK	DOWN-LINK
0	2.50	2.50
2	2.60	2.63
4	2.90	2.93
6	3.25	3.43
8	3.85	4.10
10	4.80	5.13
12	6.25	6.50

TABLE 12. PARABOLIC GROUP DELAY DISTORTION

DISTORTION ± (ns/36 MHz)	E_b/N_o DEGRADATION FROM IDEAL (dB)	
	UP-LINK	DOWN-LINK
0	2.60	2.65
+2	2.70	2.90
+4	2.80	3.00
+6	2.95	3.30
+8	3.30	3.70
+12	4.00	4.55
+16	4.80	5.40
0	2.60	2.65
−2	2.55	2.60
−4	2.62	2.62
−6	2.70	2.67
−8	2.85	2.80
−12	3.35	3.25
−16	4.00	3.95

A code rate of 7/8 is a nearly optimum tradeoff between efficiency and decoder complexity. Efficiency improves only slightly for rates above 7/8, while decoding complexity increases greatly. For rates below 7/8, decoders become much simpler, but efficiency suffers significantly because of the increased percentage of parity bits. The recommended block code was the rate 7/8 (128,112) BCH code. The final performance specification of the decoder is given in Table 13. Figure 37 is the decoder input/output error rate characteristic. This figure can be used to transform any of the previous uncoded BER performance measurements, or calculations, to performance with coding. Note, however, that all measurement data based on hardware simulation in this paper include modem differential coding for phase ambiguity resolution. These hardware simulation BER results must therefore be divided by two for use in determining both uncoded and coded performance in the INTELSAT V/VI system.

TABLE 13. FEC PERFORMANCE REQUIREMENTS WITHOUT DIFFERENTIAL ENCODING

LINK CONDITION	INPUT BER	OUTPUT BER
Clear-Sky	5×10^{-4}	1×10^{-6}
Rain Degraded	6×10^{-3}	1×10^{-3}

System performance

The overall transmission performance of the INTELSAT V system with all impairments present will now be discussed with emphasis on two areas:

a. Results of the extensive INTELSAT V laboratory hardware simulation with all or partial impairments present. This work yields steady-state results assuming all signal and interference levels at some selected constant value.

b. Results of a BER/error-free second (BEEFS) program that computes estimates of BER and percent error-free seconds (EFS) applied to a worst-case INTELSAT TDMA link based on known earth station location rain fade statistics.

Laboratory hardware measured system performance

The following describes results of performance measurements made with a composite system of interference types and levels using the extensive INTELSAT V hardware simulation configuration of Figure 14 to represent what could be expected in the INTELSAT V TDMA operating system. Because of the
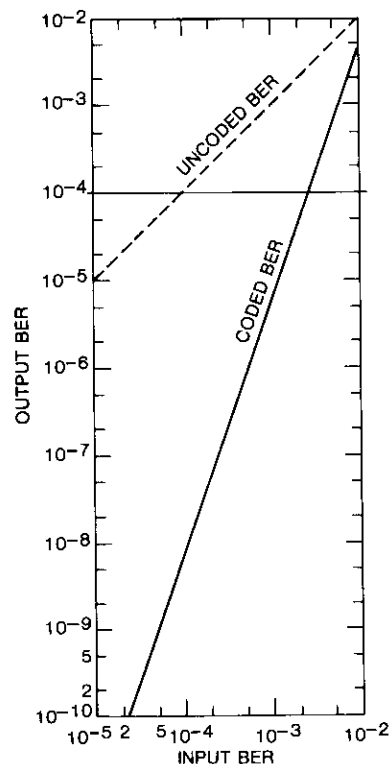
Figure 37. *BER Performance of FEC Rate 7/8
(128,112) BCH Code*

large number of variables involved, the variation of parameter values had to be limited to avoid an unmanageable number of combinations. For application of these results to INTELSAT system planning, it should be re-emphasized that they include differential coding/decoding and do not include any FEC coding. To use any of these results for the INTELSAT application, which does not employ differential coding/decoding for carrier phase ambiguity resolution, the BERs shown must be reduced by a factor of two.

Table 14 defines the configuration and conditions for a nominal INTELSAT system. Figure 38 shows the resulting BER performance with all interference present and with selected interference components present. In addition, an AWGN analysis has been calculated assuming that all interference levels are AWGN and can be added on a power basis to obtain an equivalent $(E_b/N_o)'_{DL}$.

TABLE 14. COMPOSITE NOMINAL INTELSAT SYSTEM CASE

Desired Channel	3–4; HPA/INTELSAT V TWTA input
Backoffs	10/2 (dB)
Up-Link Noise	$E_b/N_o = 24.2$ dB
Up-Link CCI	
Three Equal Interference Sources	$C/I = 21.6$ dB
External Interference	$C/I = 32.2$ dB[a]
Total Interference	$C/I = 21.24$ dB
ACSSI	
HPA Input Backoffs	10 dB
Carrier Frequencies	± 80 MHz from ch 3–4
Carrier Levels	Equal to ch 3–4 level at INTELSAT V receiver output
TWTA Input Backoffs	3.8 dB[b]
Down-link CCI[c]	
Three Equal Interference Sources	$C/I = 21.6$ dB
External Interference	$C/I = 32.2$ dB[a]
Total Interference	$C/I = 21.24$ dB
Down-Link Noise E_b/N_o	Variable (Nominal value expected, $E_b/N_o = 19.7$ dB)

[a] Provided by increasing the level obtained with three equal interference sources.

[b] An inadvertent error used through all of the full-scale work but which has no impact on results since adjacent channel TWTA spectrum spreading is well filtered on the down-link, producing no ACSSI. The up-link ACSSI is set by the HPA backoff.

[c] Co-channel INTELSAT V TWTAs at 2-dB input backoff.

ACSSI has been accounted for by integrating the appropriate adjacent channel spectrum regrowth measured for channels 1-2 and 5-6 in a 60-MHz bandwidth as explained earlier. The desired signal power has been determined by integrating the modulated signal power for channel 3-4 in a 60-MHz bandwidth. In order to perform this calculation, C/I ratios are assumed to be equivalent to E_s/N_o (signal-to-noise ratio in 60-MHz bandwidth) and the linear addition of all interference is accomplished with interference measured in the same bandwidth, as follows:

- *Up-link*

  Thermal Noise $(E_b/N_o)_1 = 24.2$ dB

  $(E_s/N_o)_1 = 27.2$ dB

  CCI $(E_s/N_o)_2 = 21.24$ dB

  ACSSI $(E_b/N_o)_3 = 21.31$ dB (total ch 1-2 and ch 5-6)

• *Down-link*

Thermal Noise $(E_b/N_o)_4 = 19.7$ dB (nominal value expected)

$(E_s/N_o)_4 = 22.7$ dB

CCI $(E_s/N_o)_5 = 21.24$ dB
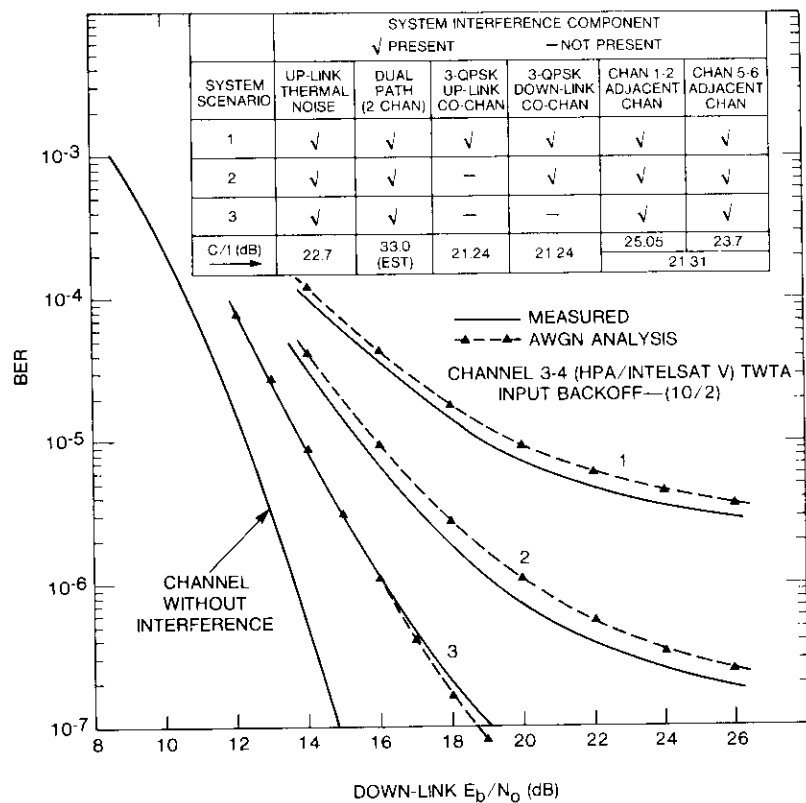
Figure 38. *Channel 3-4 Static BER Performance With Three Multiple Interference Scenarios*

The total equivalent down-link power ratio is given by

$$(E_s/N_o)_{TOTEQ} = \cfrac{1}{\cfrac{1}{(E_s/N_o)_1} + \cfrac{1}{(E_s/N_o)_2} + \cfrac{1}{(E_s/N_o)_3} + \cfrac{1}{(E_s/N_o)_4} + \cfrac{1}{(E_s/N_o)_5}}$$

Substituting and performing the indicated operations for $(E_s/N_o)_4 = 22.7$ dB results in

$$(E_s/N_o)_{TOTEQ} = 15.28 \text{ dB}$$

or

$$(E_b/N_o)_{TOTEQ} = 12.28 \text{ dB}$$

From Figure 38, the channel without interference performance curve is used to determine the BER for $(E_b/N_o)_{DL} = 12.28$ dB and the result is plotted as a point at the actual case 1 down-link E_b/N_o of 19.7 dB $[(E_s/N_o)_4 = 22.7$ dB].

Using this AWGN analysis approach, comparative noise performance was developed and plotted for all of the system interference scenarios listed in Figure 38. The results show very good agreement with actual measured performance but also reveal that the AWGN analysis is slightly pessimistic for multiple interference cases. The value of E_b/N_o used in Figure 38 is down-link thermal noise only referred to 120 Mbit/s.

Table 15 shows the tabulated link BER for system scenario 1 with (hardware simulation measurement cases) and without (operational system case) differential coding and with the rate 7/8 (128, 112) BCH FEC decoding (applying Figure 37). Note that with FEC the margin to a threshold performance of 1×10^{-6} (10.7-dB E_b/N_o) from a clear-sky E_b/N_o of 20 dB (23-dB C/N in 60 MHz, Tables 2 through 5) appears to be 9.3 dB. However, it should be understood that rain degradation causes a loss in wanted signal level plus a cross-polarization isolation depolarization effect, both of which increase CCI. The total impairments would be an increase in thermal noise, an increase in CCI (decrease in co-channel C/I), and an increase in ACSSI. It is not possible to determine the true statistical link margin from these steady-state laboratory simulation measurements.

TABLE 15. SYSTEM PERFORMANCE DERIVED FROM SIMULATION
MEASUREMENTS (SCENARIO 1)

DOWN-LINK THERMAL NOISE ONLY E_b/N_o[a] (dB)	MEASURED BER WITH DIFFERENTIAL CODING	BER WITHOUT DIFFERENTIAL CODING	BER WITHOUT DIFFERENTIAL CODING BUT WITH FEC
8.0	6.0×10^{3}	3.0×10^{3}	2.2×10^{4}
10.0	1.6×10^{3}	8.0×10^{4}	4.0×10^{6}
10.7[b]	1.0×10^{3}	5.0×10^{4}	1.0×10^{6}
12.0	4.0×10^{4}	2.0×10^{4}	6.8×10^{8}
14.0	1.1×10^{4}	5.5×10^{5}	1.5×10^{9}
16.0	3.6×10^{5}	1.8×10^{5}	$<10^{9}$
20.0[c]	7.0×10^{-6}	3.5×10^{-6}	$<<10^{-9}$

[a] Referred to 120 Mbit/s.

[b] Link threshold FEC output BER $= 1 \times 10^{6}$.

[c] Typical down-link clear-sky E_b/N_o $(C/N = 23$ dB in 60 MHz, Tables 2 through 4 for INTELSAT V).

It is important to note that the measured results show significant flaring of BER as a function of down-link E_b/N_o and might at first glance be questioned. However, using the nonlinear channel modem performance $C/I = \infty$ result, which of itself does not significantly flare out, produces a flared result as a result of the AWGN analysis. It is the degree of interference being characterized closely by AWGN that causes the flare. It is *not* a measurement error.

Now it is easily seen how FEC is necessary to reduce the relatively high error rates resulting from a scenario 1 system configuration, for example, to the acceptable values given in Table 15.

True link rain degraded system performance using the BEEFS computer program

The BEEFS program developed by COMSAT Laboratories computes an estimate of BER, percent EFS, and percent error-free deciseconds (EFDS) performance for INTELSAT TDMA links. This program was developed to assess INTELSAT TDMA links for use in data transmission networks such as the integrated services data network (ISDN).

The program combines detailed link parameters, rain impairment effects, and laboratory measured BER data to obtain performance for very small percentages of time. (The desired performance objective for the links being analyzed initially has been a BER of 10⁻⁶ or better for 99.2 percent of the time, and a percent EFS of 99.36 percent, normalized to a 64-kbit/s channel.)

The BEEFS program combines the following elements to compute BER and percent EFS and EFDS for specific INTELSAT TDMA links:

a. A description of the satellite, including its location and its transmission characteristics in the direction of INTELSAT earth stations, including co- and cross-polarized antenna characteristics.

b. A description of the location and link characteristics of the INTELSAT earth stations involved.

c. A rain impairment model for up- and down-link rain impairments at each earth station.

d. For each run, the identity of the specific earth stations and transponders that are the up-link and down-link for the desired carrier and the co-channel and adjacent channel interferers.

e. A laboratory measurements-derived model based on the work presented in this paper that gives BER as a function of up- and down-link thermal noise, CCI, and ACSSI, and the transponder operating point for INTELSAT 120-Mbit/s TDMA transmission.

f. A model that converts BER to percent EFS and EFDS. The program has been developed to handle C-band, K_u-band, and C-band/K_u-band cross-strapped links.

The principal output of this program is a plot of BER vs percent time, and values of percent EFS and EFDS.

To assess the rain fading condition in the INTELSAT V and VI TDMA system, a representative link in the Indian Ocean Region primary path (IOR PRI) INTELSAT V network was studied using the BEEFS program. The analysis was performed for the link from Fucino to Yamaguchi, which has severe rain statistics. The other three co-frequency transponders were loaded with cross-polarized TDMA carriers from Raisting to Jatiluhur, Jatiluhur to Raisting, and Yamaguchi to Fucino. Figure 39a, which shows the BER from the clear-sky condition to 99.999-percent availability without FEC coding for the worst month precipitation modeling, indicates that the clear weather BER is better than 1×10^{7}. Figure 39b shows the BER vs link availability for the same link with FEC coding. With FEC coding, the clear-sky error rate improves to better than 1×10^{17}. Figure 39 demonstrates that the INTELSAT TDMA system meets the current CCIR Recommendation 522 and the new draft recommendation for ISDN.
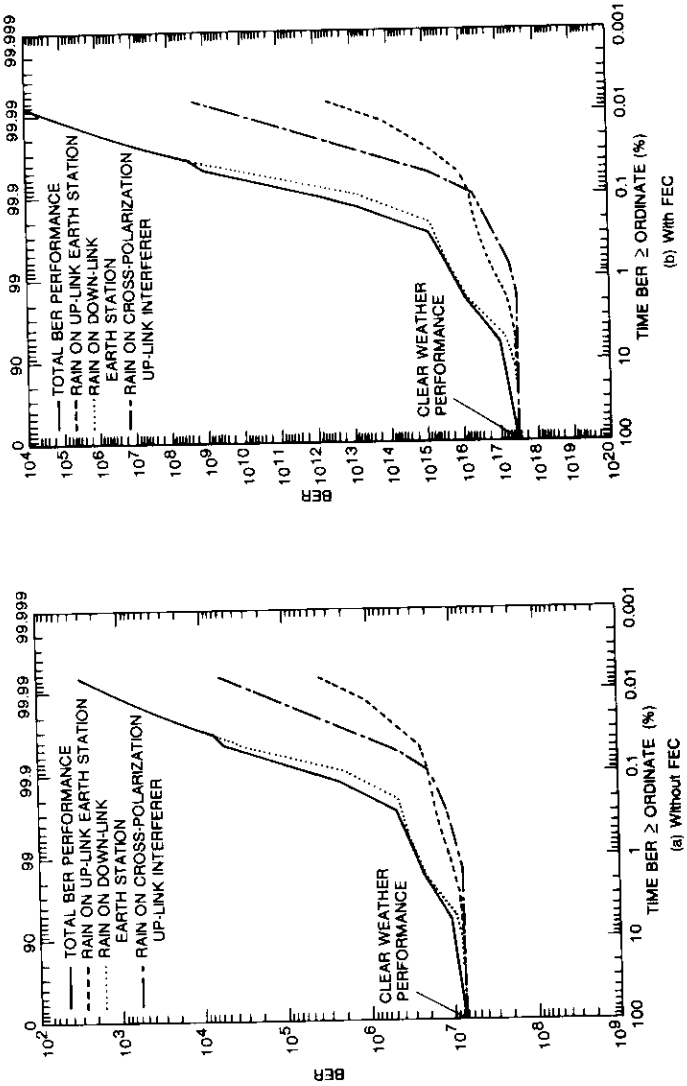
Figure 39. *Rain-Degraded Dynamic BER Performance*

Conclusions

The INTELSAT V/VI TDMA link transmission design has been reviewed in detail. The major focus of the paper dealt with the development of pulse-shaping modem filters for the nonlinear channel, with the resulting in-band BER performance and related earth station OBE in adjacent channels, and the evaluation of system impairments. FEC coding was reviewed and overall system performance was presented using both static hardware simulation measurements and a statistical dynamic modeling program (BEEFS).

Emphasis was placed on hardware simulation for the evaluation of the modem filters; co-channel, adjacent channel, dual path, and channel equalization distortion; and for the realistic assessment of HPA out-of-band emission spectrum characteristics and levels.

Overall system performance of the nonlinear channel with system interference elements was determined with good accuracy by treating all interference components as AWGN and adding them to the measured modem performance in the nonlinear channel (without interference). For one or two co-channel interferers, this approach will give more pessimistic results than for three to five co-channel interferers with C/I_{TOT} values on the order of 20 dB.

Acknowledgments

References

[1] S. J. Campanella *et al.*, "The INTELSAT TDMA Field Trial," *COMSAT Technical Review*, Vol. 9, No. 2A, Fall 1979, pp. 293–340.

[2] M. E. Jones and M. R. Wachs, "Optimum Filtering for QPSK in Bandwidth-Limited Nonlinear Satellite Channels," *COMSAT Technical Review*, Vol. 9, No. 2A, Fall 1979, pp. 465–507.

[3] C. Devieux and M. E. Jones, "A Practical Optimization Approach for QPSK/TDMA Satellite Channel Filtering," *IEEE Transactions on Communications*, Vol. COM-29, No. 5, May 1981, pp. 556–566.

[4] M. E. Jones, "Laboratory Hardware Simulation Measurements of 120-Mbit/s QPSK/TDMA Transmission Performance in the INTELSAT V System," Sixth International Conference on Digital Satellite Communications, Phoenix, Arizona, September 19–23, 1983, *Conference Record*, 1-A-1–1-A-8.

[5] INTELSAT, "TDMA DSI System Specification: TDMA/DSI Traffic Terminals," Specification BG-42-65 (Rev. 2), June 23, 1983.

[6] E. Koh *et al.*, "Transmission Analysis for the INTELSAT VI 120-Mbit/s TDMA System," Sixth International Conference on Digital Satellite Communications, Phoenix, Arizona, September 19–23, 1983, *Conference Record*, pp. 1-A-9–1-A-17.

[7] M. E. Jones and M. R. Wachs, "Measured 60-Mbit/s 4-Phase PSK Signal Impairments Through Earth Station HPA and Satellite Transponder," National Telecommunications Conference, Dallas, Texas, November–December 1976, *Conference Record*, Vol. II, pp. 21.2-1–21.2-5.

[8] L. Lundquist, M. Shum, and S. Fredricsson, "Pulse Shaping in Bandwidth-Limited Design Satellite Systems," *IEEE Transactions on Communications*, Vol. COM-26, No. 4, April 1978, pp. 478–483.

[9] P. Chang, R. J. Fang, and M. E. Jones, "Performance Over Cascaded and Band-Limited Nonlinear Satellite Channels in the Presence of Interference," IEEE International Conference on Communications, Denver, Colorado, June 14–18, 1981, *Conference Record*, pp. 47.3.1–47.3.10.

[10] INTELSAT, "System Specification of the INTELSAT Prototype TDMA System," Specification BG-1-18 (Rev. 2), March 1974.

[11] T. Muratani *et al.*, "Application of FEC Coding to the INTELSAT TDMA System," Fourth International Conference on Digital Satellite Communications, Montreal, Canada, October 23–25, 1978, *Conference Record*, pp. 108–115.

Milton E. Jones received a B.S.E.E. in 1951 and an M.S.E.E. in 1956 from Newark College of Engineering (now New Jersey Institute of Technology). He worked for International Telephone and Telegraph Federal Laboratories, where he was involved in missile guidance communications systems. While employed at Computer Sciences Corporation, he performed system studies for the U.S. Defense Satellite Communication System development. In 1975, he joined COMSAT Laboratories as a member of the Systems Applications and Simulation Department, where he was principally involved in hardware simulation studies for the evaluation of satellite link transmission impairments. He is currently a member of the Transmission Processing Department engaged in modulation-related transmission systems studies and applications. Mr. Jones is a member of IEEE and Tau Beta Pi.

Eui K. Koh received a B.S.E.E. from the Hanyang University, Seoul, Korea, in 1967, and M.E.E. and Ph.D. degrees in Electrical Engineering from the Catholic University of America, Washington, D.C., in 1972 and 1983, respectively. Since joining INTELSAT in 1979, he has been involved in high-speed digital satellite communications system studies. Currently, as a Senior Engineer in the Communications Engineering Department, he is involved in the development of the IBS/TDMA system and the TDMA performance evaluation program. Prior to joining INTELSAT, from 1974 to 1977, he was with the American Satellite Corporation, where he conducted transmission impairment studies in the nonlinear satellite channel environment. From 1976 to 1979, he was employed by M/A-COM DCC in Germantown, Maryland, and SBS in McLean, Virginia. He is a member of IEEE.
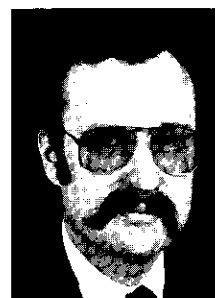
David E. Weinreich received a Bachelor of Engineering degree from Stevens Institute of Technology in 1968 and an M.S.E.E. from George Washington University in 1980. He joined COMSAT Laboratories in 1973 as a Member of the Technical Staff in the Systems Simulation Laboratory. Throughout his career at COMSAT, he has been involved in the hardware modeling of satellite communications systems. This work has included optimization of video transmission parameters, interference effects, high-speed digital transmission, optimization of maritime satellite system parameters, and design and construction of hardware satellite simulators. He is currently Manager of the Systems Simulation and Evaluation Department, where he directs satellite system modeling and the evaluation of new transmission techniques. Prior to joining COMSAT, Mr. Weinreich was employed as a Senior Applications Engineer by General DataComm Industries of Danbury, Connecticut, and as a Communications Engineer by the American Electric Power Service Corporation of Canton, Ohio.

Since 1981, Mr. Weinreich has represented the U.S. at meetings of CCIR Study Group 4. He is currently a member of Interim Working Party 4/2 on the application of satellite systems to integrated services digital networks. He is a member of IEEE and AIAA.
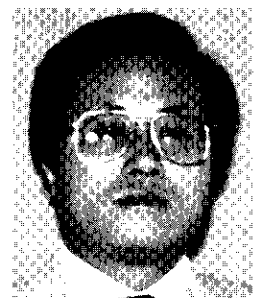
*TDMA traffic terminal verification and testing**

R. P. RIDINGS, J. F. BOMAR, AND F. L. KHOO

(Manuscript received September 5, 1985)

Abstract

COMSAT has performed system integration testing to prepare the U.S. Signatory's time-division multiple-access (TDMA) traffic terminal for use in the INTELSAT TDMA network. Tests were developed to verify compliance with the INTELSAT TDMA/DSI Traffic Terminals Specification BG-42-65 and to ready the traffic terminal for INTELSAT network testing and live traffic. The tests were conducted after manufacturer on-site acceptance testing and before INTELSAT network testing. This paper describes the tests, special test equipment, and related data.

Introduction

COMSAT has installed two 120-Mbit/s time-division multiple-access (TDMA)/digital speech interpolation (DSI) traffic terminals for the U.S. Signatory at the Etam, West Virginia, earth station to operate in the INTELSAT TDMA network accessing the Major Path 2 (MP2) and Primary satellites. COMSAT has also installed a third TDMA terminal at the new earth station in Roaring Creek, Pennsylvania. This terminal was originally planned for operation over the Major Path 1 (MP1) satellite; however, there are currently no plans for MP1 TDMA network operation.

The system integration tests described in this paper verified that the MP2 terminal [1] is in compliance with INTELSAT Traffic Terminals Specification BG-42-65 [2]. The test plan was designed to be run in-station without the

127

use of the satellite, the INTELSAT reference terminal, or the traffic terminals of other signatories. However, satellite loop tests were conducted because the satellite was already in a hemi-loopback configuration for INTELSAT testing of the Etam MP2 reference terminal.

The tests were performed with the traffic terminal operating in the loop configurations shown in Figure 1. The traffic terminal was controlled by a built-in reference burst generator when testing in the IF and RF loop configurations, and by the Etam reference terminal when testing in the satellite loop configuration. Testing in the transmultiplexer loop does not
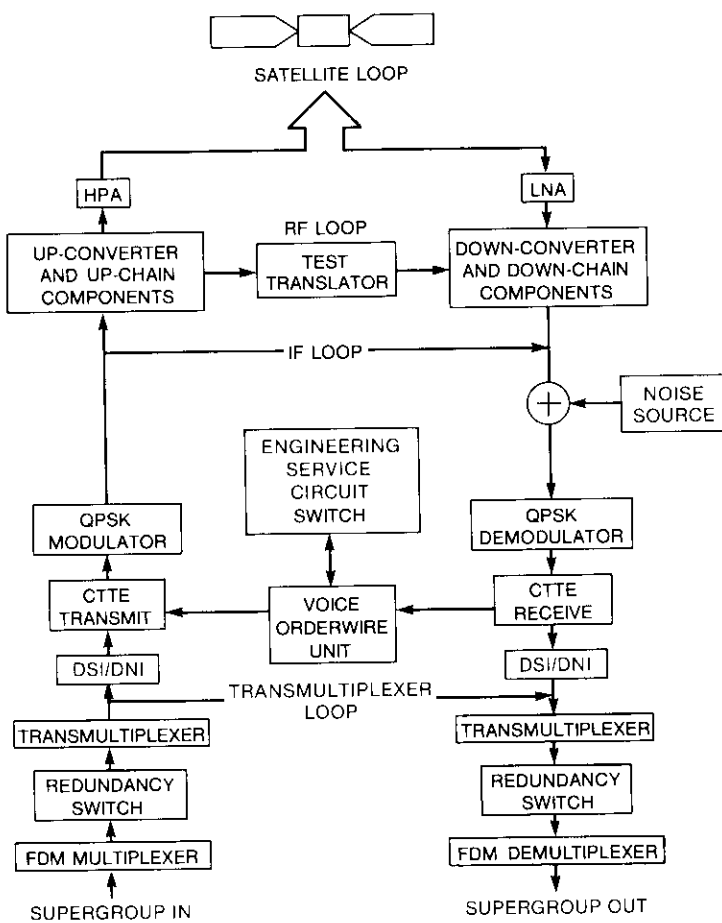
Figure 1. *Loop Test Configurations*

require a reference burst controller. The tests included equipment alignment (equalization, gain, etc.), acquisition and synchronization, baseband performance, verification of burst time plan (BTP) management, system monitoring and control, and redundancy switching control.

Tests were also conducted using the COMSAT Laboratories experimental TDMA traffic terminal [3] and the INTELSAT reference station emulator (RSE) [4],[5]. This permitted end-to-end baseband testing between two traffic terminals, verification that the INTELSAT DSI specifications were properly implemented, and extensive exercise of the acquisition and synchronization protocols by the RSE.

Traffic terminal overview

Three components of the U.S. Signatory's TDMA traffic terminal will be discussed: baseband equipment, RF equipment, and the operations and maintenance center (OMC). As shown in Figure 2, baseband terrestrial supergroup traffic is routed through the redundancy switch to the transmultiplexer, where it is digitized into the CEPT pulse-code modulation (PCM) 2.048-Mbit/s format. The traffic is then compressed by the DSI module into an allocated number of satellite channels and routed through the DSI interface to the common TDMA terminal equipment (CTTE). The CTTE multiplexes the traffic into TDMA bursts, which are transmitted at a bit rate of 120.832 Mbit/s using quadrature phase-shift keying (QPSK) modulation. The return traffic is demultiplexed from the received TDMA bursts and routed through the DSI interface to the proper DSI module. The DSI module directs the received traffic into the CEPT 2.048-Mbit/s bit streams. The digitized traffic is then converted back to analog supergroups by the transmultiplexer and routed through the redundancy switch to the frequency-division multiplex (FDM) equipment.

The RF up-links and down-links are illustrated in Figure 3. Redundant equalizers and up-converters feed traffic to one of three high-power amplifiers (HPAs) via redundant interfacility link (IFL) amplifiers. The RF down-link consists of redundant low-noise amplifiers (LNAs) which interface with redundant equalizers and down-converters. The status interface unit (SIU) monitors the status of the equalizers, IFLs, HPAs, and LNAs and feeds this information to the OMC where it is monitored at the status, alarm, and control (SAC) panel.

Figure 4 shows the OMC, which consists of an HP-1000/A600 computer with a 67-Mbyte hard disk, a printer, an operator console, and a real-time operating system. Two HP-9816 microcomputers used as operator terminals interface to the computer: one for operation and one for maintenance. Operation includes
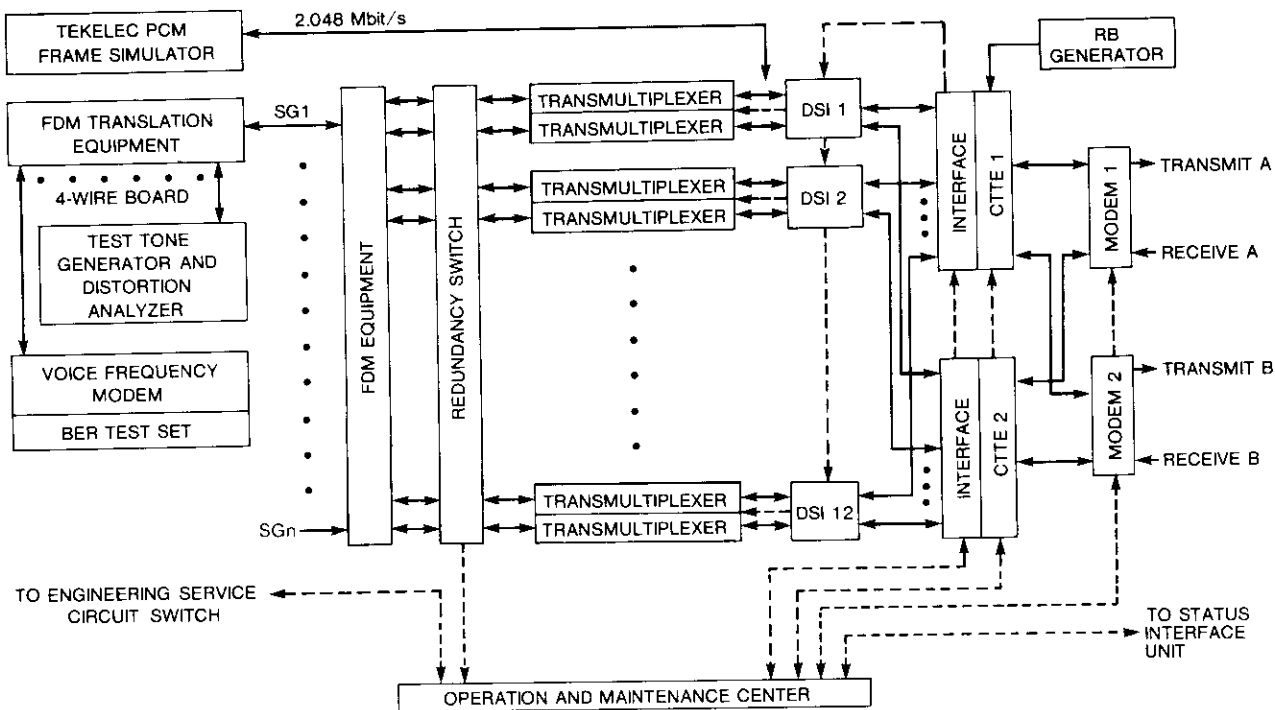
Figure 2. *TDMA Traffic Terminal Baseband Equipment*
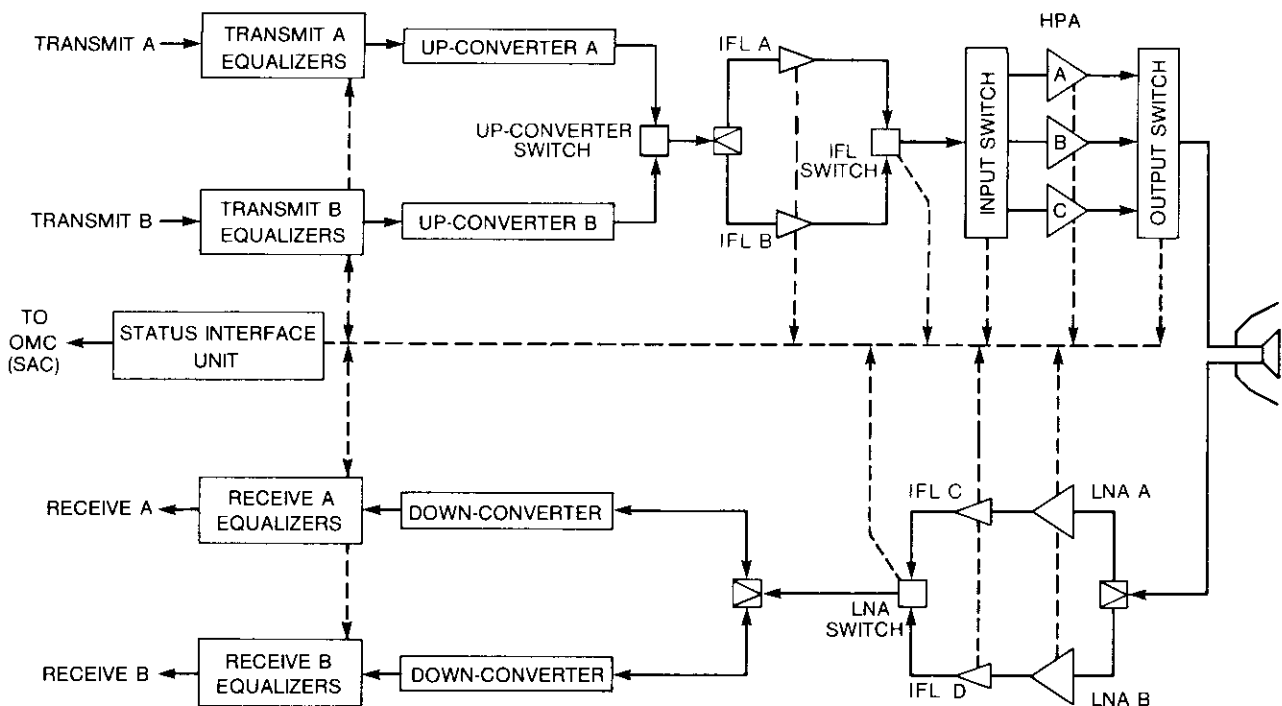
Figure 3. *TDMA Traffic Terminal IF/RF Equipment*
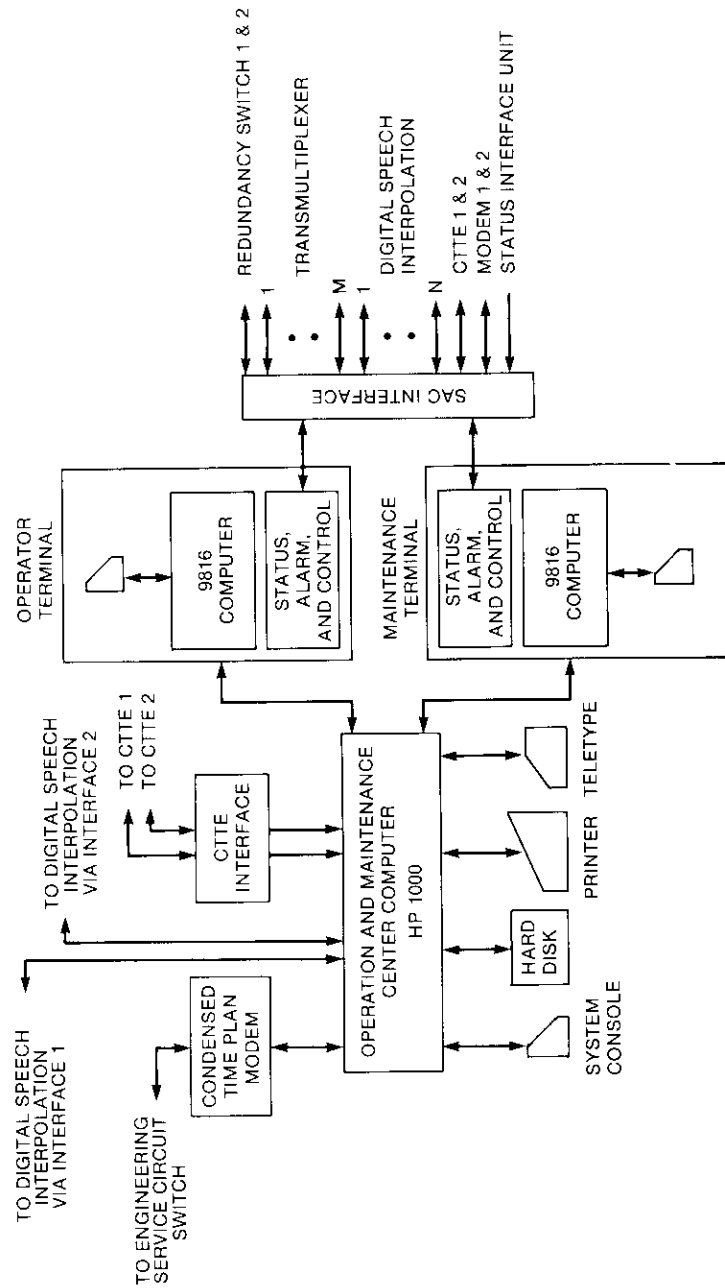
Figure 4. TDMA Traffic Terminal Operation and Maintenance Center

real-time monitoring, control, and data collection; maintenance includes diagnostic testing of off-line equipment and the entry of master time plan (MTP) information. Each operator terminal is provided with a SAC unit which displays equipment status and alarm conditions, implements automatic redundancy switching, and allows for manual control of equipment status (on-line, standby, maintenance, and fail). The OMC computer monitors the CTTEs via their respective CTTE interfaces, and the remaining equipment via the SAC interface. The computer provides real-time displays for monitoring and control, data collection, and MTP entry. It also receives the condensed time plan (CTP) from the INTELSAT Operations Center (IOC) using X.25 protocols, verifies checksums, and converts the CTP to machine-readable format (BG-42-65, Subsection 7.7.3). In case of hard disk failure or computer failure, backup configurations are available that permit CTP reception and operation of the terminal with a limited number of monitoring functions.

The SAC unit receives the status from each of the individual units carrying traffic and commands the appropriate redundancy switch when a fault occurs. The redundancy configuration for the DSI and transmultiplexers is a 1-for-N scheme. Two 120-channel transmultiplexers and one 240-channel DSI module switch as a single unit whenever a failure occurs in the DSI or a transmultiplexer. The redundancy switch redirects four supergroups to the redundant transmultiplexers, and the CTTE/DSI interface is automatically remapped to the redundant DSI module. The remaining equipment switches in a 1-for-1 redundancy scheme. The CTTE and the CTTE/DSI interfaces switch together, the modulator and up-converter switch together, and the demodulator and down-converter switch together. The RF equipment redundancy switching is controlled independently of the TDMA system, and status is provided through the SIU for display at the SAC panel.

Traffic terminal tests

The traffic terminal tests are partitioned into the following categories (see Table 1):

* equipment alignment,
* acquisition and synchronization,
* baseband tests,
* BTP management, and
* operation and maintenance.

Equipment alignment

The transmultiplexer, modem, RF chain, and orderwire circuits were aligned by setting signal levels and equalizing certain equipment in accordance with INTELSAT specifications.

TABLE 1. TDMA SYSTEM INTEGRATION TESTS (U.S. SIGNATORY)

TEST TITLE	REFERENCE	
	SSOG [6] Vol. 3, Book 2	BG-42-65
Equipment Alignment		
Transmultiplexer Signal Level Adjustments	—	—
Modem		
• Demodulator Recovered Carrier and Clock Phase Adjustment	2.2	—
• Modulator IF Frequency and Stability	2.7	—
• Electrical Path Length Equalization	2.10	3.5
• Carrier and Clock Cycle Skips	2.9	3.3.3.3
• BER and Unique Word Miss Detection	2.4, 2.5, 2.6	3.3.3.1, 3.3.3.2
RF Equipment		
• Earth Station e.i.r.p.	6.2	2.2
• Gain	3.2	2.8
• Frequency Tolerance	3.7, 6.7	2.1.1, 2.1.2
• Amplitude and Group Delay	3.3, 6.3	2.5
• Electrical Path Length Equalization	3.4, 6.4	2.6
• Satellite Equalization	3.6, 6.6	2.5.2
Voice Orderwire		
• Insertion Loss	9.2.1	7.2
• Frequency Response	9.2.2	7.2
• Channel Noise	9.2.3	7.2
Acquisition and Synchronization		
• RSE Tests	—	6.0, 7.8
• Reference Burst Generator Tests	5.0	6.0
• Satellite Loop Tests	—	6.0
Baseband Tests		
• Channel BER	10	—
• Test Tone *S/N*	—	—
• Channel Check Test Alarm	—	8.5.5
• Speech Detection	—	8.6
• Speech Detector—Echo Canceller Interaction	—	—
• 14.4-kbit/s Modem Data BER	—	—
BTP Management		
• CTP Reception	9.4.2	7.7.2
• Local CTP Generation	—	—
• MTP Generation	—	7.7
Operation and Maintenance		
• Monitor and Control	—	—
• Fault Detection and Redundancy Switching	—	3.5, 6.5

TRANSMULTIPLEXER

The transmultiplexer was designed with the level of the supergroup pilot fixed at −20 dBm0 so that setting the supergroup level automatically sets the levels in the system. The transmit level was adjusted to give the specified input level at the analog-to-digital converters, and the receive level was adjusted to give the specified level at the supergroup distribution frame. The performance of the transmultiplexer was verified during the baseband tests.

MODEM

The following modem adjustments and performance measurements were conducted:

• demodulator recovered carrier and clock phase adjustment,
• modulator frequency and stability,
• electrical path length equalization,
• carrier and clock slips, and
• bit error rate (BER) and unique word (UW) miss detection.

The demodulator recovered carrier was adjusted in IF loop for the optimum eye pattern, and the clock was adjusted for midbit sampling. Modulator frequency and stability were verified by measurement over a 24-hour period, indicating a frequency deviation of less than 1 part in 10^7. Electrical path lengths were adjusted in the factory by trimming coils of coaxial cable provided in the modem for that purpose and tested on-site by COMSAT. The delay variation between any modulator/demodulator combination was equalized to within 7.2 ns. Carrier and clock slip measurements were conducted in the IF loop configuration with the modem in continuous transmission mode and are plotted as a function of E_b/N_o in Figure 5. The BER and UW miss detection were measured in both the IF loop (Figure 6a) and the satellite loop (Figure 6b).

RF UP- AND DOWN-CHAINS

The following measurements were conducted to verify alignment of the RF up-chains and down-chains:

• earth station e.i.r.p. for TDMA,
• gain,
• frequency tolerance,
• amplitude and group delay responses,
• electrical path length equalization, and
• satellite equalization.
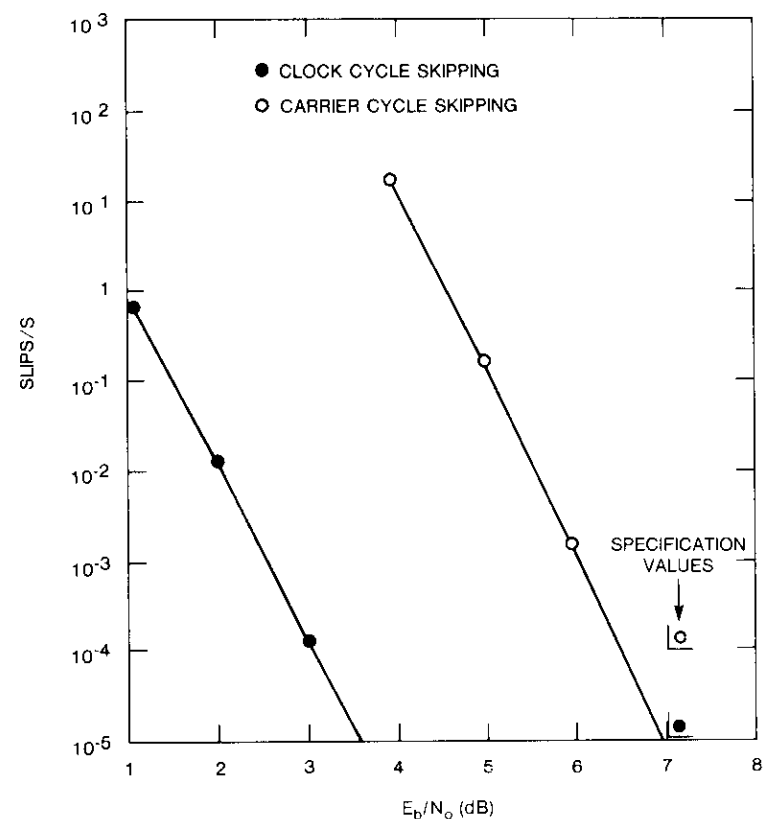
Figure 5. *Carrier and Clock Cycle Slipping vs* E_b/N_o

The TDMA e.i.r.p. was adjusted at the up-converter RF output by using a continuously variable potentiometer with a 30-dB range. Since the IFLs and HPAs operate in the multicarrier mode, no gain adjustments were made beyond the up-converter. Down-link gain adjustments were made at the RF input and the IF output of the down-converter.

Up-converter frequency translation accuracy and stability were measured by injecting a continuous IF carrier and measuring the output frequency of the up-converter over a 24-hour period. Down-converter frequency translation and stability were measured by injecting a continuous RF carrier and measuring the frequency at the IF output over a 24-hour period. The worst-case frequency deviation, measured for both up-converters and down-converters, was less than 1 part in 10^8.
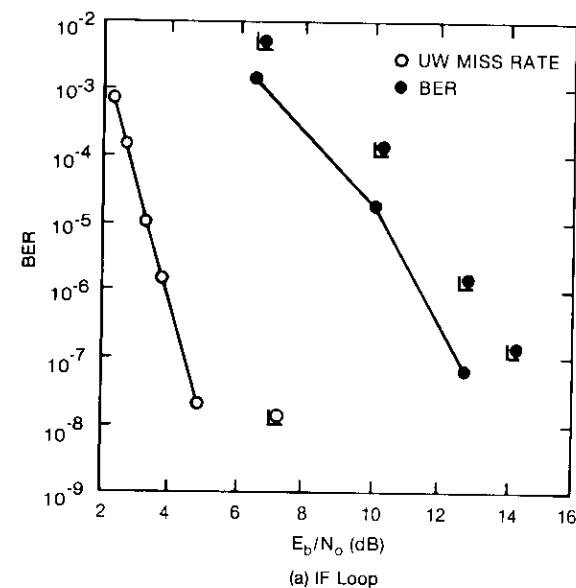
(a) IF Loop
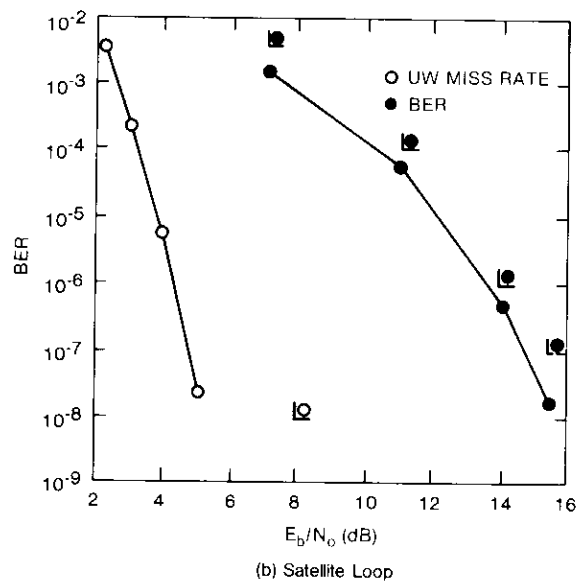
(b) Satellite Loop

Figure 6. *Modem BER Performance*

Amplitude and group delay were adjusted by using a conventional microwave link analyzer (MLA) operating in the continuous mode. Up-link alignment was achieved by placing the MLA transmitter at the equalizer input and the receiver at the antenna feed. For down-link alignment, the MLA transmitter was placed at the antenna feed and the receiver at the equalizer output. Amplitude equalization was implemented using fixed modules of positive or negative linear slope ranging from 1 to 4 dB, and linear group delay equalization was accomplished using fixed modules of positive or negative slope ranging from 2 to 8 ns. Parabolic group delay equalization was performed with fixed modules of curvature ranging from 1 to 4 ns over the 80-MHz band. Final trimming of the equalization was achieved by a four-tap variable transversal equalizer. Figure 7 shows amplitude and group delay as a function of frequency for both the up-link and down-link.

Electrical path lengths were equalized because a redundancy switch can cause a jump in burst timing which must be minimized in order to maintain

(a) Up-Converter A, IFL A, HPA A

(b) Down-Converter A, LNA/IFL D
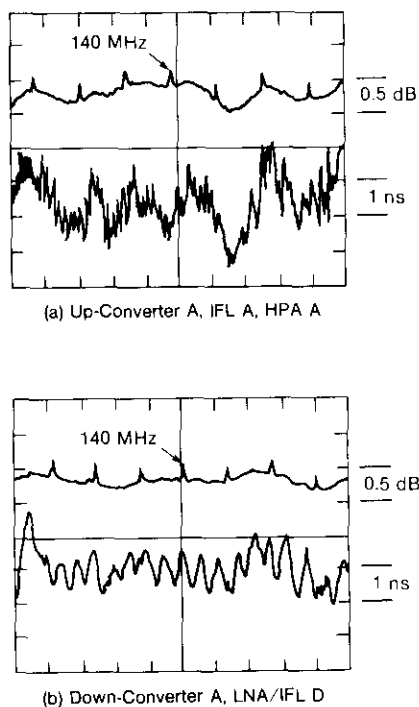
NOTE: MARKERS AT 10 MHz

Figure 7. *Up-Link Amplitude and Group Delay Response*

burst reception within the specified aperture. Measurements were made for the 12 combinations of up-links and 4 combinations of down-links (Figure 3). The down-link electrical path length was measured from the antenna feed port to the demodulator input, and the worst-case difference between any two paths was 8 ns. Likewise, the up-link electrical path was measured from the modulator output to the transmit feed port, and the worst-case difference between any two paths was 13 ns.

The design of the satellite channel equalizers is the same as that described for the up-link and down-link equalizers. Figure 8 gives the amplitude and group delay measured in the satellite loop configuration.

(a) Equalizers Set to the Approximate INTELSAT Mask

(b) Response Modified by Adjusting Down-Link Satellite Equalizer
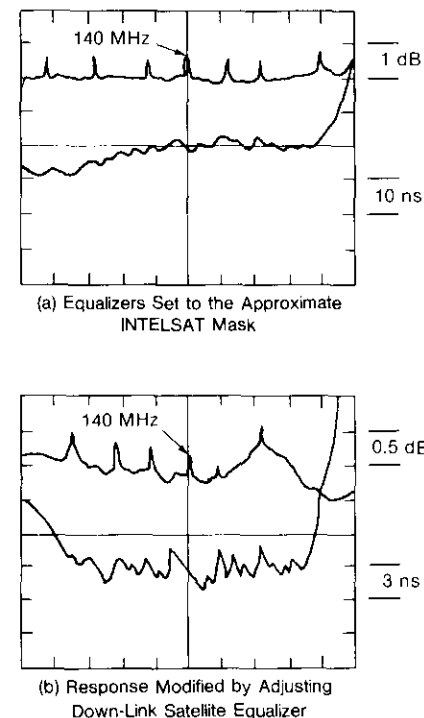
NOTE: MARKERS AT 10 MHz

Figure 8. *Overall Satellite Loop Response*

ORDERWIRE CODECS

The delta-modulation orderwire codecs were aligned at the factory by the manufacturer and their performance was verified by the following tests:

- insertion loss,
- frequency response, and
- channel noise.

Insertion loss was measured at 1,020 kHz and adjusted to 0 ± 0.1 dB, and frequency response was obtained by measuring the amplitude of a -10-dBm0 test tone transmitted at the frequencies given in Figure 9. Channel noise measurements consisted of C-message weighted idle channel noise (-73 dBm0) and test tone signal-to-noise ratio (S/N) vs input signal level (see Table 2).
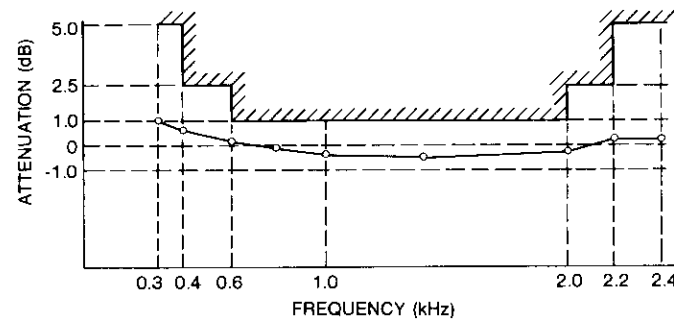
Figure 9. *Delta Codec Frequency Response*

TABLE 2. DELTA CODEC TEST TONE S/N

INPUT SIGNAL* LEVEL (dBm0)	C-MESSAGE WEIGHTED S/N (dB)
-38	19
-35	22
-28	26
-20	29
-18	30
-10	30
-8	30
0	28
$+2$	15

*Frequency = 1,020 Hz.

Acquisition and synchronization

Tests were performed to verify the operation of the acquisition and synchronization protocols specified by INTELSAT. These tests were critical

because protocol failure can cause interference to traffic bursts or reference bursts that share the same transponder. COMSAT tested the protocols using the RSE, the reference burst generator, and the Etam MP2 reference terminal.

The RSE was developed by COMSAT Laboratories for INTELSAT to validate the acquisition and synchronization protocols of traffic terminals under both normal and anomalous operating conditions [4],[5]. The RSE transmits reference burst(s) and receives the traffic terminal's principal burst via an IF interface. Tests are implemented in the RSE by programming the reference burst status and UW bit errors. The response of the traffic terminal is monitored by reading the principal burst's service channel messages and observing the CTTE front panel indicators. Test scenarios are programmed into the RSE to test the following protocols:

- search mode acquisition (SMA),
- gated mode acquisition (GMA),
- steady-state reception (SSR),
- burst timing synchronization (BTS),
- reference burst identification (RBID),
- burst qualified (BQ),
- receive frame synchronization (RFS),
- transmit frame acquisition (TFA),
- transmit frame synchronization (TFS),
- do not transmit (DNTX),
- selective do not transmit (SDNTX),
- BTP change,*
- service channel evaluation.

An example of the RSE operation can be explained using the SSR test, which verifies that the traffic terminal declares loss of SSR status when four consecutive UWs are missed, followed by 512 frames without the occurrence of four consecutive UW detects. The test procedure consists of the following three steps:

   a. The RSE synchronizes the traffic terminal to the primary reference burst (PRB) and receives the traffic terminal's principal burst.
   b. The RSE programs six bit errors† in the PRB's UW for 512 consecutive frames and verifies continued reception of the principal traffic burst.
   c. The RSE programs six bit errors in all the PRB UWs and verifies

---

* In the BTP change test, the RSE compensated for the satellite delay and monitored for traffic burst UW misses, thereby executing a BTP change with verification of no interruption to traffic.
† Six bit errors in the UW will cause a UW miss, since the error threshold is 5.

ceased transmission of the principal traffic burst (the operator verifies ceased transmission of all other traffic bursts).

The built-in reference burst generator implements the following INTELSAT Satellite Systems Operations Guide (SSOG) nontransmitting protocol tests (Reference 6, Section 5):

- acquisition and steady-state reception (ASSR) evaluation,
- RFS evaluation,
- TFA evaluation,
- SDNTX evaluation,
- DNTX response evaluation, and
- BTP change.

These tests are conducted to requalify the CTTE following a failure. After requalification the CTTE is placed in the standby mode, fully operational with its transmit bursts terminated at the up-converter switch. Operation is verified from the CTTE status displays and by measuring the transmit burst length and frame position using an oscilloscope.

The Etam MP2 reference terminal acquired and synchronized the Etam traffic terminal in the satellite loop configuration. The reference terminal monitored traffic burst position in the frame, the delay number (D_n) returned in the service channel, and UW misses. Acquisition was successfully completed multiple times and synchronization was maintained over a 24-hour period.

Baseband tests

The objective of the baseband tests was to verify transmultiplexer and DSI performance. These tests consisted of the following:

- channel BER,
- test tone S/N,
- channel check test,
- speech detection,
- echo canceller-speech detector interaction, and
- 14.4-kbit/s modem BER.

Tests with the COMSAT Laboratories experimental TDMA traffic terminal were conducted to allow end-to-end BER and S/N measurements between two DSI modules and to verify the channel check test procedure. The RSE was used for acquiring and synchronizing the two terminals.

Test configurations used to evaluate DSI/DNI channel performance can be explained with reference to Figure 2. The first baseband test measured the

test tone S/N and in-band data (2,400 and 4,800 bit/s) BER, interfaced at the four-wire board with the terminal looped at the digital side of the trans-multiplexer. The second baseband test repeated the measurements with the terminal in IF loop. Both tests were conducted for 24 hours without DSI loading and without additive noise. The test tone S/N was displayed on a strip-chart recorder, and the BER was recorded hourly. All BER measurements were zero, and the test tone S/N was the same in both tests (40 dB, C-message weighted). This verified that no degradation was introduced in the DSI/DNI channel by the digital portion of the traffic terminal.

Following these tests, DSI/DNI channel BER measurements were performed in IF loop using the Tekelec PCM test set without DSI loading and with additive noise. The test verified that BER vs E_b/N_o in the DSI channel was the same as that measured in the modem test. The BER was then measured with forward error correction (FEC) to verify the improvement due to coding. Figure 10 shows BER vs E_b/N_o with and without FEC.
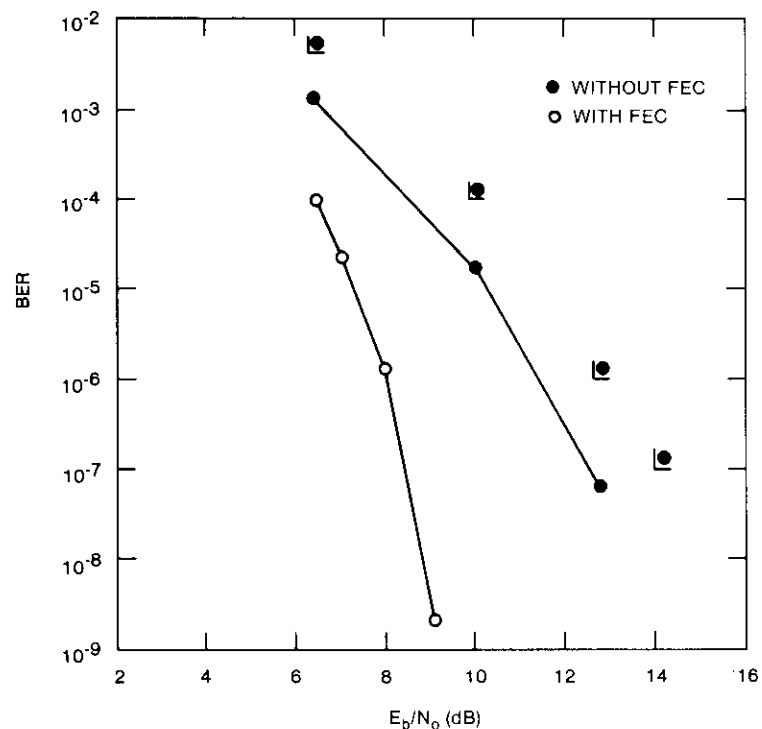
Figure 10. *DSI Channel BER Performance (IF loop with DSI loading)*

The test configuration using the COMSAT Laboratories TDMA traffic terminal and the RSE is depicted in Figure 11. The two traffic terminals and the RSE were connected at IF with additive noise. The DNI channels were evaluated by measuring BER (using two Tekelec units), and the DSI channels by measuring test tone S/N. The DSI modules were loaded by a speech activity simulator located in the COMSAT Laboratories DSI module; loading at the Etam traffic terminal was achieved by looping the received channels, except for the channels under test.

BER vs E_b/N_o was measured for DNI channels, with and without FEC, and the results were the same as those obtained in IF loop (Figure 6a). The test tone S/N was measured in the DSI channel with DSI loading and without additive noise. The C-message weighted S/N was nominally 40 dB, except during periods of overload when the S/N dropped to approximately 34 dB. In this case the measured noise is due mostly to quantization distortion.

The COMSAT experimental traffic terminal was used to verify the channel check test procedure. This procedure confirms DSI channel assignment and continuity between DSI modules by transmitting a 1,000-Hz square wave which is on for 500 frames and off for 4,500 frames. Reception of this signal was verified at both the Etam terminal and the experimental terminal. Whenever the channel check test signal is not properly received, an alarm message is sent to the transmitting station. To ascertain that the alarm message was sent, DSI loading was increased until the test signal was frozen out.

The speech detector was tested using prerecorded speech to verify that no perceptible degradation was introduced by speech clipping, speech chopping, or noise spurts between words caused by false speech detection. The prerecorded speech was transmitted through the DSI channel with the system operating in satellite loop, and was received and recorded for later evaluation by trained listeners.

The speech consisted of phonetically balanced (PB) words spoken by male and female talkers, with levels of -20 and -30 dBm0 and additive noise ranging from -70 to -48 dBm0. The DSI was forced into constant overload, thereby requiring each speech spurt to be detected by the speech detector before assignment to a satellite channel. A second recording was made of the PB words (same signal and noise levels) transmitted over a DNI channel (no speech detector). The trained listeners found that the PB words from both the DNI and DSI channels were of the same quality, except for slight clipping noticed on a few words when the speech level was -30 dBm0 and the noise level was -48 dBm0.

The DSI was tested to evaluate the interaction between the speech detector and an echo canceller [5],[7]. In the presence of receive speech, the echo

Figure 11. *COMSAT Laboratories Traffic Terminal Test Setup*
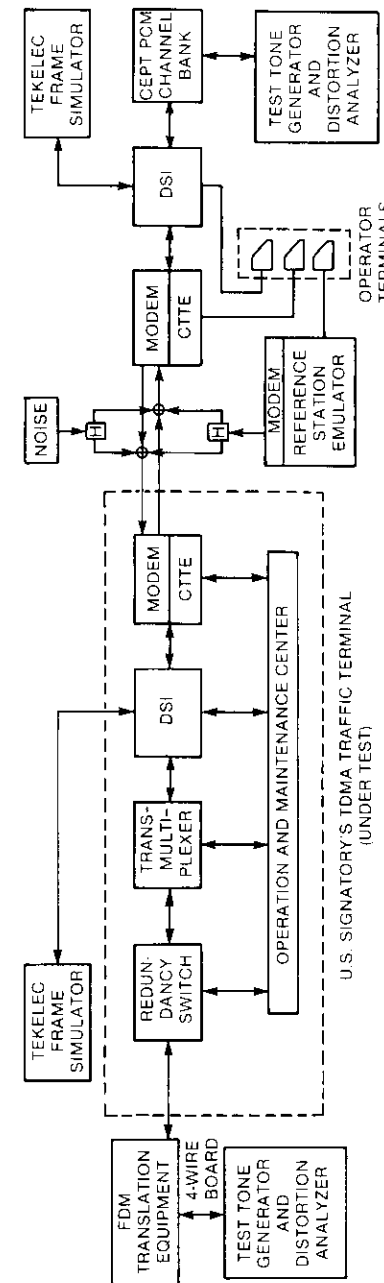
canceller center clipper operation reduces noise power at the DSI channel input, forcing the adaptive threshold in the speech detector to adjust to a lower level. When receive speech ends, center clipper action is removed, causing a sudden increase in the noise power which may result in a false detection and the transmission of a noise spurt. This increases the probability of overload and freeze-out, thereby degrading the quality of the voice channel. This interaction was tested using the COMSAT Laboratories experimental terminal connected at IF to the Etam terminal (Figure 11). Noise (-55, -50, and -45 dBm0) was inserted at the send side of the Etam terminal, and recorded PB words (-20 and -30 dBm0) were inserted at the send side of the COMSAT Laboratories terminal. Activity in the channel was monitored at the receive side at the COMSAT Laboratories terminal. The results indicated that activity due to speech detector and echo canceller interaction was insignificant because of the speed of threshold adaptation and the minimum allowable threshold level. Activity resulting from false triggering was further minimized because of the shorter hangover time specified by INTELSAT for signals of short duration.

The BER performance of the traffic terminal configured in the IF loop mode with additive noise was measured with 14.4-kbit/s of modem data. The tests were conducted using a Fujitsu 1926L modem and a BER test set. The results are given in Table 3.

TABLE 3. 14.4-kbit/s MODEM BER PERFORMANCE

CHANNEL BER	14.4-kbit/s BER	FEC
6.8×10^{6}	1.2×10^{4}	No
6.3×10^{-7}	6.3×10^{-5}	No
1.3×10^{-7}	3.0×10^{6}	No
7.0×10^{-9}	4.1×10^{7}	No
2.7×10^{4}	8.9×10^{-6}	Yes
5.0×10^{5}	$< 1 \times 10^{-7}$	Yes

Burst time plan management

The operational parameters of the TDMA traffic terminal are provided by INTELSAT in the BTP, which consists of the CTP and the MTP. The CTP contains information that identifies controlling and noncontrolling reference bursts, transmit and receive burst timing, the transponder number for each burst, the number of sub-bursts per burst, sub-burst length, and orderwire maps. The MTP contains information to configure IF/RF equipment and DSI/DNI equipment and to identify voice and teletype (TTY) orderwires.

In normal operation, the CTP is generated by INTELSAT and sent from the IOC to the traffic terminals over an engineering service circuit (ESC). The CTP reception at the Etam traffic terminal was verified by receiving the INTELSAT CTP from the IOC. After reception, the CTP is automatically returned over the ESC to the IOC for verification. Implementation of the CTP was verified by measuring the burst positions and burst lengths using an oscilloscope.

During the testing at Etam, it was necessary that CTPs be generated by the test personnel. The OMC permits operator entry of the CTP, storage on floppy disk, and down-loading to the CTTE under operator control. Prior to conducting the acquisition and synchronization tests and baseband tests, CTP generation and implementation by the CTTE had to be verified. This was achieved by down-loading the CTP from the OMC computer, performing normal acquisition and synchronization using the reference burst generator, and measuring burst positions and burst lengths using an oscilloscope. The acquisition and synchronization tests required two CTPs for the BTP change. The CTP for baseband testing allowed the CTTE to receive its own transmitted bursts, and the CTP for interfacing with the COMSAT Laboratories experimental terminal allowed one sub-burst of traffic between terminals. The CTPs were generated with and without FEC. The CTP for the RSE was programmed by the operator at the RSE operator terminal.

The procedure for MTP generation is local entry at the OMC operator terminal, with the operational MTPs specified by INTELSAT and the test MTPs specified by the test personnel. Test MTPs configure the DSI modules as required for the baseband tests. In normal operation, the MTP is down-loaded automatically during CTP reception from the IOC; however, test MTPs are stored on floppy disks with their corresponding CTP and are down-loaded by operator command.

Operation and maintenance

Operation and maintenance of the traffic terminal is performed at the OMC. The OMC testing described in this section includes system monitoring and control, fault detection, and redundancy switching.

System monitoring and control are implemented from the operator terminals and at the OMC computer console. Testing was accomplished by controlling and monitoring the terminal from the OMC during system testing. Particular attention was given to the real-time CTTE acquisition and synchronization display because this display must allow the operator to quickly determine CTTE status in case of an alarm.

An equipment fault can be detected by either on-line or off-line diagnostic testing. Each piece of equipment performs these tests, and the results are

sent to the OMC. On-line diagnostic testing requires that a fault be forced into the unit to produce the desired failure. Three types of alarms are sent to SAC: minor 1, indicating a nontraffic problem; minor 2, indicating loss of interface signal from another unit; and major, indicating loss of traffic in the unit. Each piece of equipment was tested to verify that the correct alarm message was displayed at the SAC panel and that the fault message was displayed at the operator terminals. The equipment was then manually switched to the maintenance mode to verify off-line diagnostic testing.

If a failure occurs in an on-line unit, causing a major alarm, the SAC will automatically switch the alarm unit to the failed mode and the standby unit on-line. Redundancy switching was tested by forcing a major fault and measuring the switchover time by observing the duration of the traffic outage. Measurement was made by monitoring a test tone signal in the traffic channel at the four-wire board using a storage oscilloscope. This test was conducted in the satellite loop configuration; however, if the satellite loop were not available, the test could have been performed in the RF loop configuration. Table 4 gives the worst-case redundancy switching times.

TABLE 4. MEASURED REDUNDANCY SWITCHING TIMES

EQUIPMENT	TRAFFIC OUTAGE TIME (WORST CASE) (ms)
Transmultiplexer/DSI	150
CTTE	3
Modulator/Up-Converter	2-100 (adjustable)
Demodulator/Down-Converter	2-100 (adjustable)
Transmit IFL	125
HPA	275
LNA/Receive IFL	140

Specialized test equipment

The following specialized equipment was used in testing the TDMA traffic terminal:

- modem test set,
- MLA or burst mode link analyzer (BMLA),
- Tekelec PCM frame simulator,
- reference burst generator,
- RSE, and
- COMSAT Laboratories experimental traffic terminal.

The modem tests were conducted using a modem test set supplied by the manufacturer of the TDMA equipment. The test set was designed to implement the INTELSAT modem test procedure (BG-42-65, Attachment A). The RF amplitude and group delay equalization was performed by using a conventional MLA which requires continuous transmission. This was possible since the transponder was not otherwise loaded; however, during normal operation a BMLA (SSOG, Section 4, Annex 1) will be necessary to prevent interference to other bursts in the transponder. The Tekelec PCM frame simulator (TE-820) was used for baseband testing since the PCM DSI test set specified by INTELSAT (BG/temp-48-1732, Rev. 1) was unavailable. The reference burst generator is a special test unit supplied with the Etam traffic terminal to verify normal acquisition and synchronization operation. The RSE was used to verify the acquisition and synchronization protocols under both normal and anomalous operating conditions.

Testing with the COMSAT Laboratories experimental traffic terminal verified compatibility between two TDMA/DSI terminals developed by different manufacturers. The RSE and the experimental TDMA traffic terminal were essential in the early phases of system testing as there was no reference station or other traffic terminal available to operate with the Etam MP2 traffic terminal.

Conclusions

The results of COMSAT traffic terminal system integration testing verified that the U.S. Signatory's traffic terminal complied with INTELSAT Specification BG-42-65. The INTELSAT SSOG tests and the AT&T subjective tests were successfully completed, and the terminal entered service in October 1985. The Etam MP2 traffic terminal has performed exceptionally well, and the same system integration tests have since been conducted for the primary traffic terminal at Etam and the traffic terminal at Roaring Creek.

The COMSAT testing identified problems for correction before INTELSAT SSOG and AT&T subjective testing and provided the operators with the experience necessary to evaluate procedures and recommend improvements. Testing with the INTELSAT RSE and the COMSAT Laboratories experimental traffic terminal uncovered minor problems that could not be identified with other available test equipment.

The newness of the TDMA equipment and the differences between it and the communications equipment previously installed at the earth station meant that highly knowledgeable personnel were required in order to integrate and ready the terminal for operation. The test team consisted of three full-time engineers trained in TDMA traffic terminal operation, earth station personnel,

and specialized technical support from COMSAT Laboratories. The high degree of cooperation that existed between the manufacturers and COMSAT enabled prompt correction of problems found during testing.

Acknowledgments

References

[1] M. C. Benjamin and W. M. Bogaert, "COMSAT's TDMA Traffic Terminal," International Journal of Satellite Communications, Vol. 3, Nos. 1 and 2, January–June 1985, pp. 15–25.

[2] INTELSAT, "TDMA/DSI System Specification: TDMA/DSI Traffic Terminals," Specification BG-42-65 (Rev. 2), June 23, 1983.

[3] R. P. Ridings, R. R. Lindstrom, and T. R. Dobyns, "An Experimental TDMA Traffic Terminal," COMSAT Technical Review, Vol. 15, No. 2B, Fall 1985, pp. 399–422.

[4] J. A. Lunsford and T. R. Dobyns, "A Reference Station Emulator for Testing INTELSAT TDMA/DSI Terminals," COMSAT Technical Review, Vol. 15, No. 2B, Fall 1985, pp. 511–525.

[5] R. Ridings et al., "Verification Tests of a Prototype INTELSAT TDMA/DSI Terminal," Sixth International Conference on Digital Satellite Communications, Phoenix, Arizona, September 19–23, 1983, Proc., pp. II-14–II-23.

[6] INTELSAT, "TDMA/DSI Test and Maintenance Procedures," (draft), Satellite Systems Operations Guide, Vol. 3, Book 2, April 1, 1985.

[7] J. H. Rieser and M. Onufry, "Terrestrial Interface Architecture (DSI/DNI)," COMSAT Technical Review, Vol. 15, No. 2B, Fall 1985, pp. 483–509.

Robert P. Ridings received a B.S.E.T. degree from the Capitol Institute of Technology in 1969, and a B.S.E.E. and M.S.E.E. from George Washington University in 1973 and 1979, respectively. He joined COMSAT Laboratories in 1969, and is currently a Senior Scientist in the Network Technology Division working on the Advanced Communications Technology Satellite (ACTS) TDMA ground segment. Prior to this, he was responsible for the design of digital speech interpolation systems and TDMA systems. He was Program Manager for the development and testing of the COMSAT experimental TDMA traffic terminal and the reference station emulator, and was Test Manager for the COMSAT MP2 TDMA traffic terminal located at the Etam, West Virginia, earth station.

John F. Bomar received a B.S.E.E.T. degree from the Capitol Institute of Technology in 1976. He joined COMSAT in 1981 and is currently working on the INTELSAT Business Services earth station implementation for COMSAT International. Previously, he was involved with implementation of the INTELSAT TDMA/DSI system at the Etam and Roaring Creek earth stations. Prior to joining COMSAT, Mr. Bomar was employed as an Electronics Engineer at E-Systems, Melpar Division, and as a Member of the Technical Staff at Litton Industries, Amecom Division.
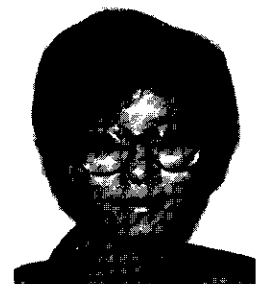
F. Lin Khoo received a B.S.E.E. from George Washington University in 1983 and is currently pursuing an M.S.E.E. in Communications at the same institution. She joined the COMSAT World Systems Division in 1983 and was involved in the design, implementation, and testing of the COMSAT TDMA/DSI system; development and testing of a status interface unit for TDMA RF equipment; performance evaluation of the TDMA Traffic Terminal Operations and Maintenance Center; and development of real-time software for the burst power monitor system. Ms. Khoo joined INTELSAT in 1986 as a Member of the Technical Staff in the Satellite Evaluation and Control Department, where her responsibilities include operation of the communications subsystems of all in-orbit INTELSAT satellites, reconfiguration of the subsystems to support operational and test requirements, subsystem performance evaluation, and investigation of subsystem anomalies in orbit. She is a member of Tau Beta Pi and Eta Kappa Nu.

Generation of burst time plans for the INTELSAT TDMA system*

P. A. TRUSTY, C. A. KING, AND P. W. ROACH

(Manuscript received October 24, 1985)

Abstract

In the INTELSAT time-division multiple-access (TDMA) system, the burst time plan (BTP) contains the assignments of traffic and reference bursts, common acquisition windows, and test slots to time slots within the TDMA frame for a given network. Generation of the BTP involves the processes of sub-burst formation, burst formation, reference burst assignments, and burst scheduling. BTP information is transferred to the individual reference and traffic stations in the form of a master time plan (MTP) and a condensed time plan (CTP). This paper describes algorithms which have been developed for each of the BTP generation processes, as well as those algorithms and procedures used to generate the MTPs and CTPs. A software system which implements these algorithms is also discussed.

Introduction

In the INTELSAT time-division multiple-access (TDMA) system, a community of transponders is synchronized to a common time period called the TDMA frame. During the frame, each accessing station transmits its traffic

within preassigned time intervals in one or more high-rate streams of bits referred to as bursts. The INTELSAT TDMA system is characterized by the use of transponder hopping, digital speech interpolation (DSI) techniques for voice channel compression, and forward error correction (FEC) coding.

A network which uses two transponders on an Atlantic Ocean region satellite is currently operating in the INTELSAT TDMA system. A second network which uses transponders on an Indian Ocean region satellite began operation in December 1985. Another TDMA network will become operative in the future on another Atlantic Ocean region satellite.

The implementation of these networks has required considerable coordination and planning by the international signatories and the executive organ of INTELSAT. Traffic prediction and management, the design and acquisition of equipment, network configuration and control, and training in the concepts of TDMA system operation have been addressed in great detail in order to facilitate the development of these networks.

Traffic management deals with the process of collecting traffic requirements from each system user; allocating the space segment efficiently while meeting the traffic requirements of each user; recognizing the equipment constraints of each user and complying with all INTELSAT TDMA system conditions and constraints; coordinating a time for the synchronous reconfiguration of the network for adding new traffic and/or stations; and providing each station with the timing and control information necessary for transmitting and receiving its traffic and configuring its baseband equipment.

The projections of traffic requirements given to INTELSAT by the users are entered in the INTELSAT traffic data base (ITDB) from which the burst time plan (BTP) is generated. The BTP is the entire body of timing assignments for a specific TDMA network, including the time slot assignments for all transmitted traffic and the control information for all network terminals. After the network BTP is reviewed and agreed upon by the system users at an annual operations representatives meeting, baseband worksheets are used to support generating the baseband equipment configuration for each station. The baseband assignments and BTP timing assignments for each individual terminal are then formatted into a master time plan (MTP) and a condensed time plan (CTP) and sent to the stations to allow them to prepare for the changeover to the new BTP.

Generation of a BTP requires a voluminous amount of information about the individual stations and the constraints and requirements of the INTELSAT TDMA system. This paper describes those considerations which are applicable to the process of generating a BTP, and the algorithms which are implemented in a set of software used by INTELSAT for this purpose.

Overview of the INTELSAT TDMA system

An INTELSAT TDMA network consists of four reference stations, traffic stations, and the INTELSAT Operations Center TDMA Facility (IOCTF). The reference stations monitor the status and timing of the system and provide the traffic terminals and other reference terminals with timing and control information. The traffic stations transmit voice signals using DSI techniques at baseband, and also transmit digital noninterpolated (DNI) voice and data traffic. A description of the components of the INTELSAT TDMA system and its operation is given in Reference 1.

Network timing

All network traffic transmission and reception is synchronized to a common 2-ms time frame [120,832 quadrature phase-shift keying (QPSK) symbols]. Each traffic and reference station is assigned time slots within the frame during which it will transmit or receive. The duration of each time slot depends on the amount and type of traffic contained in the burst being transmitted or received. Burst length is determined by the number of satellite channels in the burst, the preamble length, and whether or not the burst is FEC encoded. Each satellite channel is 64 symbols long. Time slots are also reserved in the frame for terminal acquisition and network testing functions. An appropriate amount of guard time separates the bursts within a transponder.

The BTP contains the time slot assignments for the entire network. Each BTP is identified by a unique number. When network traffic changes, a new BTP is distributed to all network terminals from the IOCTF, and a scheduled, synchronous changeover is made to the new BTP by all of the network terminals.

MTPs and CTPs for each traffic and reference terminal and for the TDMA system monitors (TSMs) are derived from the BTP. The MTP and CTP contain the subset of BTP information which is relevant to a particular terminal. This includes the terminal transmit and receive burst time slot assignments, orderwire assignments, and controlling transponder information. The MTP is written in an operator-readable format, while the CTP is in a binary format and is loaded into the TDMA terminal. A later section describes MTPs and CTPs in detail.

System startup and terminal acquisition

In each hemi region, one reference terminal is assigned to transmit a primary reference burst, RB1, into each transponder, and the other reference terminal is assigned to transmit the redundant reference burst, RB2, in each transponder. The four reference stations are assigned specific roles in the BTP

for startup purposes. These roles are master primary, secondary to the master primary, primary, and secondary to the primary.

The criteria used to assign startup roles to the reference terminals are based on the transponder configuration. In a loop configuration, a reference terminal with access to the loopback transponder is appointed the master primary role. This terminal controls all of the network reference terminals and thus is able to ensure that transmission into all transponders is synchronous at the satellite. A reference station in the opposite coverage region is appointed primary. The two redundant stations are assigned the corresponding secondary roles.

In the nonloopback configuration, a reference station in either coverage region may be assigned the master primary role. In this mode, reference terminals in each hemi region monitor and control the terminals in the opposite hemi region, which results in two sets of synchronized transmission groups in the network.

At system startup, the master primary station, under the control of the IOCTF, transmits the first burst. In normal operation this role is assigned to a station transmitting RBIs. The master primary station establishes, maintains, and controls network timing. Once normal operation has been established, the roles of master primary and secondary to the master primary may be interchanged. The roles of primary and secondary to primary may also be interchanged.

Role of the BTP software

The software system, which was developed at COMSAT Laboratories to generate the BTP, models an INTELSAT TDMA network and uses the network traffic matrix to assign time slots for each station to transmit and receive its traffic. The software implements algorithms which form traffic and reference bursts, generate timing and control assignments for reference terminals and the TSMs, assign orderwires between all terminals and the IOCTF, and generate baseband channel mapping assignments. In addition, a network configuration data base is maintained using the software. This data base contains information concerning all earth stations using or planning to use a particular INTELSAT satellite. The information includes such assignments as terminal identification numbers, the control channel address for receiving control and delay information for each terminal, and the satellite name and number.

After the network BTP has been determined, the software generates MTPs for each terminal. These MTPs are sent to the administrations responsible for the earth stations for review and approval. The CTPs are loaded into the terminals and are executed after the changeover to the new BTP.

The software also generates baseband worksheets for each country, based on the BTP assignments. These worksheets are used by the administrations to inform INTELSAT of the baseband channel mapping at their earth stations. This information can be used to modify the mapping generated by the software algorithms.

Several test CTPs can be generated from the software which are compatible with the operational BTP and can be used in various testing procedures without interfering with TDMA operation.

Algorithms applied in generating the INTELSAT TDMA system BTP

This section describes each of the algorithms used in generating a BTP. The algorithms fall into three major categories: burst scheduling algorithms, network control assignment algorithms, and intrasystem communications assignment algorithms.

Scheduling the network traffic

In generating an INTELSAT TDMA BTP, all network terrestrial traffic is first grouped into sub-bursts. The sub-bursts are then grouped into bursts which will eventually be scheduled for transmission at an assigned time in the frame. All generated bursts and their return bursts are assigned to specific terminals at the earth stations. Bursts transmitted by the reference terminals are generated and assigned to each accessible transponder. Each reference and traffic terminal in the network is assigned to receive reference bursts from one or two specific transponders. Test slots and idle time slots are assigned for each transponder, and common acquisition windows (CAWs) are assigned in transponders where necessary. The test slots, CAWs, traffic and reference bursts, and idle time slots are then scheduled in the frame.

The remainder of this section describes the individual network BTP generation algorithms in the sequence in which they are invoked when generating the burst schedule.

SUB-BURST FORMATION

The network terrestrial traffic matrix consists of the numbers of 64-kbit voice and nonvoice channels for each traffic link, and the transmit and receive transponders for these links. Each traffic link is grouped into sub-bursts which will be assigned to individual terrestrial interface modules (TIMs) at the station. The traffic links are assumed to be symmetrical. Figure 1 shows a typical traffic matrix.

SAMPLE BURST TIME PLAN
TDMA TRAFFIC MATRIX

V = VOICE CHANNELS
NV = NONVOICE CHANNELS

	AAA V	NV	MMM V	NV	NNN V	NV	RRR V	NV	TTT V	NV	YYY V	NV	ZZZ V	NV	TOTAL TX	NV
BBB	14	2	57	3	63	1	71	3	88	5	33	2	422	11	748	27
CCC	28	0	24	2	7	2	11	3	16	4	6	2	24	0	116	13
DDD	15	2	32	3	6	1	12	1	30	3	40	3	49	3	184	16
EEE	21	2	24	1	19	3	11	3	32	3	33	4	203	13	343	29
FFF	25	2	26	1	0	0	6	1	54	3	16	2	48	3	175	12
JJJ	0	0	0	0	17	1	33	4	0	0	57	6	0	0	107	11
KKK	12	1	29	1	10	1	20	2	19	2	37	2	61	7	188	16
GGG	8	1	28	1	0	0	10	1	33	1	10	0	110	5	199	7
HHH	23	2	35	1	0	0	17	3	22	1	15	1	105	2	217	13
III	37	4	36	4	13	1	20	4	24	3	24	0	72	2	226	15
LLL	6	1	26	1	0	0	20	2	27	3	21	1	57	2	157	10
TOTAL RCV	189	17	317	18	135	9	231	27	345	27	292	23	1151	48		

TRAFFIC FOR TRANSPONDER 11 | — | 2660 V | 169 NV

NOTE: EACH ROW IDENTIFIES THE NUMBER OF VOICE AND NON-VOICE CHANNELS TRANSMITTED BY THE STATION IDENTIFIED IN THE FIRST COLUMN TO EACH OF THE RECEIVE STATIONS DESIGNATED IN THE REMAINING COLUMN HEADINGS.

Figure 1. *Sample Traffic Matrix*

The function of the sub-burst formation algorithm is to assign the input terrestrial traffic to DSI and DNI modules while minimizing the number of TIMs required at the station. The algorithm makes efficient use of both transponder capacity and earth station equipment.

Voice traffic is primarily assigned to DSI sub-bursts. DSI techniques take advantage of the characteristic pauses in speech to interpolate the terrestrial voice channels into a reduced number of satellite channels. The DSI gain is the ratio of the number of input channels into the TIM to the number of satellite channels out of the TIM. The DSI gain increases as the number of terrestrial voice channels into the TIM increases. Currently, the maximum DSI gain used in the INTELSAT TDMA/DSI system is 2.25 [2]. The maximum input capacity of a DSI module is 240 terrestrial voice channels, and the maximum satellite channel output is 128 channels.

Portions of each DSI sub-burst may contain nonvoice traffic or noninterpolated voice traffic. If there is a sufficient amount of such traffic, it is typically assigned on DNI sub-bursts. DSI and DNI sub-bursts can be single or multidestinational, with a maximum of eight destinations per sub-burst.

Single-destination sub-bursts are formed when there is sufficient traffic between two stations to use the full capacity of the DSI module, thus achieving maximum DSI gain and efficient use of the receive terminal since it will only be receiving its own traffic. A multiple-destination sub-burst is formed by combining small groups of voice channels to different destinations to maximize the DSI gain on that sub-burst and minimize the number of TIMs required at the transmit station.

The voice channels for each link from the transmit stations are assigned first. For each transmit station, possible full-capacity (240-channel), single-destination DSI sub-bursts are formed first; that is, let

n_i = number of voice channels between station A and station B_i, where the subscript i designates a specific receive station.

Then,

m_i = number of full-capacity, single-destination sub-bursts
= $[n_i/240]$, where $[x]$ is the greatest integer less than or equal to x.

The remaining less-than-240-channel portions of the links from station A (i.e., $r_i = n_i - (m_i \cdot 240)$ are then grouped to form multiple-destination sub-bursts. These links are grouped by simply adding together the r_i assigned to the same transponder until the capacity of the DSI module is exceeded, in which case a new DSI sub-burst is formed.

After the voice traffic for all stations has been assigned, any DSI sub-bursts carrying less than 14 channels are reassigned as DNI sub-bursts. Statistically there is no appreciable DSI gain with so few channels, and the DNI units are less expensive than the DSI units. This reassignment is contingent upon equipment availability at the earth station and whether or not the return voice channels can be transmitted as noninterpolated.

The nonvoice channels are assigned using the same basic logic. The full-capacity, single-destination DNI sub-bursts are formed first. Remaining links are assigned to existing DNI sub-bursts (creating multiple-destination DNI sub-bursts), to existing multiple-destination DSI sub-bursts, or a new DNI sub-burst is formed.

An alternate algorithm for sub-burst formation assigns both the voice and nonvoice traffic on each link to sub-bursts before proceeding to the next link. Using this option, less than full-capacity voice and nonvoice portions of a link must be assigned to the same DSI sub-burst before the voice portions of additional links can be assigned.

TRAFFIC BURST FORMATION

Each traffic burst consists of a preamble followed by one or more sub-bursts carrying the voice and data traffic. Figure 2a provides the format of a traffic burst. The preamble is 280 symbols long and consists of a carrier and bit timing recovery sequence, a unique word, a service channel, and voice and teletype (TTY) orderwire channels.

The traffic burst formation process groups all single-destination sub-bursts from a station to a common destination into one burst. A maximum of eight sub-bursts can be assigned to any one burst. Each multiple-destination sub-burst is assigned to a separate burst to make efficient use of receive station equipment, since a receive terminal must "listen" to each designated received burst from the preamble up through the end of the last sub-burst carrying traffic to that terminal. If several sub-bursts to different destinations were combined, the receive terminal would be required to process unused sub-bursts and its capacity would be reduced.

The bursts are then converted from satellite channels to symbols (64 symbols per channel) and are selectively FEC encoded. The preamble is assigned to the burst, and each burst is assigned a unique number in the network. For example, if two fully loaded DSI sub-bursts had been formed from station A to station B, they would be combined to form one burst. Each fully loaded DSI sub-burst contains 108 satellite channels using a DSI gain of 2.2. The length of this burst without FEC is

$$\ell = p + 2 \times 108 \times 64$$
$$= 280 + 13,824$$
$$= 14,104 \text{ symbols}$$

where p is the 280-symbol preamble. If the burst is to be FEC encoded, the length becomes

$$\ell_{FEC} = \left[\frac{\ell - p}{g}\right] \cdot (c + g) + k + p$$
$$= 16,080 \text{ symbols} = 246 \times 64 + 56 + 280$$

where
g = FEC information group size = 56 symbols
c = FEC check group size = 8 symbols
k = 0 if $(\ell - p) = |(\ell - p)/g| \cdot g$

otherwise, $k = (\ell - p) - [(\ell - p)/g] g + c$

and where $[x]$ = greatest integer $\leq x$.

* NOT TO SCALE.
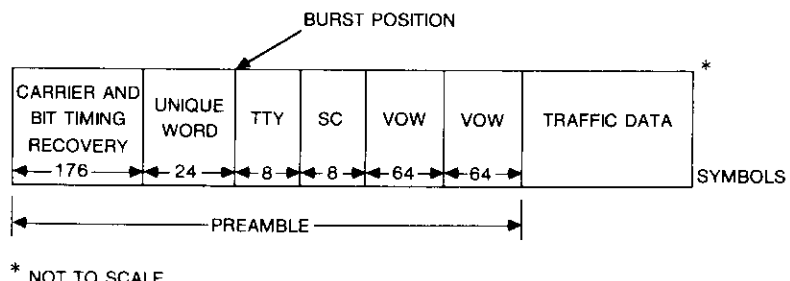
(a) Traffic Burst
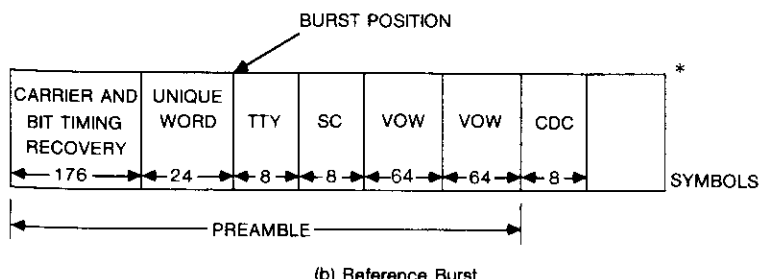
(b) Reference Burst

Figure 2. *Burst Description*

REFERENCE BURST FORMATION

A reference burst must be transmitted by a reference terminal into every transponder in its coverage region during each 2-ms frame. Reference bursts are also given unique numbers consistent with the traffic burst numbering scheme. Figure 2b shows the format of a reference burst. Each reference burst is 288 symbols long, with a 280-symbol preamble followed by an 8-symbol control and delay channel (CDC). The CDC carries information from the reference terminal to its controlled reference and traffic terminals.

Two reference bursts, RB1 and RB2, are transmitted into each transponder each frame from the two reference stations in the coverage region. In multitransponder operations, the reference bursts transmitted into the transponders by one reference terminal can be scheduled at different transmission times within the frame and are identical in content. The only exception to this may be in the contents of the CDC if more than one cycle is being used.

TEST SLOTS AND CAWs

A vacant slot, referred to as a test slot, is reserved in each transponder for system tests and the testing of redundant equipment. By using the vacant slot, testing of this type will not interrupt normal traffic. A test slot is assigned in each transponder in the network and is considered an additional entity to be scheduled in the time frame for that transponder. The nominal length of a test slot is 3,000 symbols.

CAWs are generated in transponders where terminals must acquire sequentially, and are considered an additional entity to be scheduled in those transponders. These windows are used for acquisition by terminals that have allocated slot durations in the frame which are less than the system requirement. Reference terminals and traffic terminals with small bursts will typically acquire in these windows. The nominal duration of a CAW is 5,024 symbols. A maximum of one CAW is scheduled in any transponder, and no more than four users are assigned to any CAW.

COUPLING OF SUB-BURSTS AS TRANSMIT AND RETURN PAIRS

As each sub-burst is formed, it has associated with it a unique sub-burst number, one or more destinations, and groups of terrestrial channels to each destination. After all sub-bursts have been formed, each destination on a sub-burst is coupled with a return sub-burst from that destination to ensure that return traffic on a link is assigned to be received by the same terminal that transmitted the sub-burst. The first unassigned sub-burst transmitted by each destination station, which contains the same number of terrestrial voice channels as are being transmitted to the destination being processed, is specified as the return sub-burst for the voice channels of that destination.

The two sub-burst numbers are coupled as returns for that group of terrestrial voice channels. By the same procedure, the nonvoice channels to each destination are assigned to a return sub-burst.

A single-destination sub-burst can have one return sub-burst carrying its return terrestrial channels, both voice and data, or two return sub-bursts, one carrying return voice channels and one carrying data. Similarly, a multidestination sub-burst can have as many as two return sub-bursts specified for each destination.

CALCULATION OF REQUIRED TERMINALS

The number of TDMA terminals required at each earth station is determined based on various parameters associated with the transmit and receive bursts at the station. Several factors determine the necessary number of TDMA terminals: the number of transponders the station transmits into and receives from, the number of bursts transmitted and received, the number of sub-bursts transmitted and received, and the total number of symbols transmitted and received. The terminal capacities per frame are 4 transmit and 4 receive transponders, 16 transmit bursts, 32 receive bursts, 32 transmit and 32 receive sub-bursts, and a total transmit and receive capacity of 120,832 symbols per frame. For station A, let

t = number of bursts transmitted
r = number of bursts received
s_t = number of sub-bursts transmitted
s_r = number of sub-bursts received
j_t = number of transponders in which the station transmits
j_r = number of transponders from which the station receives traffic
m_t = total number of QPSK symbols transmitted by the station (including burst preambles and guard time)
m_r = total number of QPSK symbols received

then

n = number of TDMA terminals required at station A
= max($[t/16]$, $[r/32]$, $[s_t/32]$, $[s_r/32]$, $[j_t/4]$, $[j_r/4]$, $[m_t/120,832]$, $[m_r/120,832]$)

where $[x]$ is the smallest integer greater than or equal to x.

ASSIGNMENT OF BURSTS TO TERMINALS

Before bursts are assigned to terminals, the number of terminals required at each earth station is determined. Linked burst groups are then formed at

each station. These groups consist of transmitted and received bursts at a station which must be assigned to the same terminal because they carry coupled sub-bursts.

Figure 3 illustrates a linked group for earth station A. Transmit burst 1 has receive burst 2 as its return. Since two sub-bursts of burst 2 have sub-bursts on transmit burst 3 as a return, this burst is also included in the group. Burst 4, which contains the other return sub-burst for burst 3, completes the linked grouping.
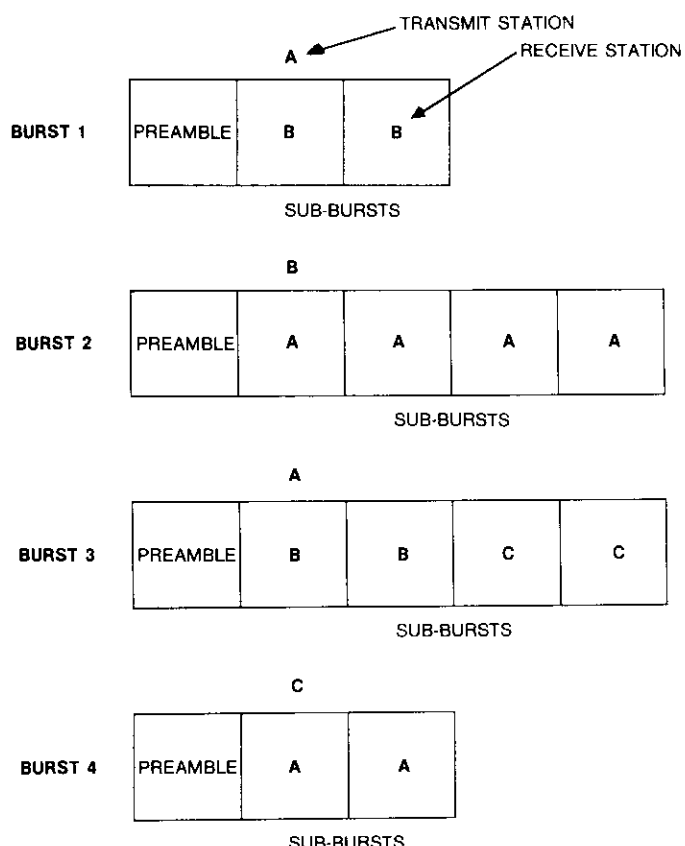
Figure 3. *Linked Burst Group*

After all linked groups have been formed, groups are assigned to terminals at the earth station using two criteria: first, minimizing receive transponder hopping at each terminal, and then if possible distributing the total receive symbols evenly between the terminals. In rare cases, an additional terminal

must be added at the earth station in order for all transmit and receive bursts in a group to be assigned to the same terminal. For example, if station A is transmitting three equal-sized bursts into three transponders where each burst is approximately two-thirds of a frame in duration (80,000 symbols), three terminals are required even though theoretically two terminals would provide sufficient capacity (*i.e.*, 3 bursts × 80,000 symbols/burst = 240,000 symbols, where the capacity of two terminals is equal to 241,664). Figure 4 illustrates this case. Since bursts 1, 2, and 3 must all be transmitted simultaneously for at least one-third of the frame, regardless of how the bursts are scheduled, no one terminal can transmit any two of these bursts.
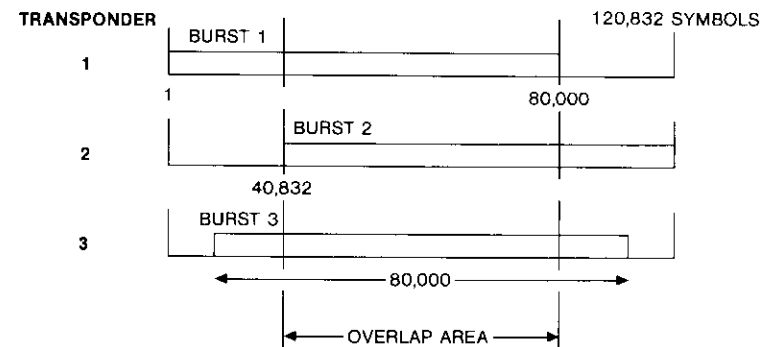
Figure 4. *Illustration of Three Terminal Requirements*

PRIORITY ASSIGNMENTS

Priority factors are computed for all traffic and reference bursts, test slots, and CAWs which have been generated. These priority factors determine the sequence in which these entities will be scheduled (in order of descending priorities).

The highest priority factors are given to those bursts which will be the most difficult to schedule. Factors which influence how difficult the burst will be to schedule are burst size, number of transponder hops required of the assigned transmit and receive terminals, and transmit and receive fill factors for the terminals. The transmit fill factor is the total number of symbols sent by the terminal transmitting the burst, divided by the number of symbols per frame. The receive fill factor is the sum of all the assigned receive symbols at all of the burst's destination terminals, divided by the

frame length in symbols. The priority factor, p, for a burst i is calculated as

$$p_i = b(t_h \cdot t_f + r_h \cdot r_f)$$

where b = burst size in symbols

  t_h = number of transmit transponder hops made by the terminal transmitting i

  r_h = sum of receive transponder hops made by all terminals receiving burst i, divided by the number of terminals receiving burst i

  t_f = transmit terminal fill factor

  r_f = receive terminal fill factor.

Three primary factors influence the complexity of reference burst scheduling and are considered when computing reference burst priority factors. First, the reference station may be colocated with a traffic station, in which case both stations may share a high-power amplifier; therefore, the transmit parameters of the colocated traffic terminal are considered. Second, receive terminal fill factors and the number of receive terminal hops made by the reference burst destinations are considered. However the third factor, the reference burst size, generally causes the reference bursts to have a low scheduling priority factor.

The items considered in determining test-slot scheduling priority factors are the average number of transponder hops, the average transmit terminal fill factor, and the average receive terminal fill factor of the constrained test-slot users. Constrained test-slot users are those who cannot transmit bursts and use the test-slot simultaneously.

Priority factors are also determined for CAWs. Acquisition slot size is the only parameter considered in determining the CAW scheduling priority factor.

SCHEDULING ALGORITHM

The burst scheduling process locates a slot for each traffic and reference burst, CAW, and test slot in the frame, while avoiding transmit and receive terminal overlap and intraframe collision. Transmit or receive overlap occurs when any one terminal is scheduled to transmit or receive more than one burst at any given instant. Intraframe collision occurs when two or more bursts are transmitted into the same transponder simultaneously.

The bursts, test slots, and CAWs are scheduled at the earliest acceptable location in the frame, with the exception of the RB2 reference bursts. The last symbol of the unique word of each traffic and reference burst is required to be positioned on a modulo 16 location in the frame. The first symbol of each acquisition window and test slot is also scheduled on a modulo 16

location. The RB2s are scheduled at the earliest acceptable location after the center of the frame in order to bias the algorithm to provide maximum spacing between the reference bursts in a frame.

The hierarchy by which the bursts, test slots, and acquisition windows are scheduled is as follows:

  a. The RB1s in the designated timing and reference transponders (TRTs) are scheduled. The start of frame (SOF) for synchronized transponders is defined as the burst position of these reference bursts.

  b. All bursts occupying more than half of the frame are scheduled in such a way as to minimize transmit and receive overlap for the terminals assigned to these large bursts.

  c. The remaining bursts, test slots, and CAWs are scheduled in order of descending priority factors.

When a burst, test slot, or acquisition window is encountered that cannot be scheduled, this entity is flagged and the remaining entities continue to be scheduled.

The priorities of any unscheduled entities are adjusted after the first scheduling attempt is complete. The scheduling algorithm is then reinvoked, with the previously unscheduled bursts, test slots, and acquisition windows having the highest priorities. This priority adjustment rescheduling attempt is an iterative process that repeats until all bursts have been scheduled or until a specified number of attempts have been made.

Figure 5 is a plot of a burst schedule. Details of this burst schedule are provided in Table 1.

CALCULATION OF EQUIPMENT REQUIREMENTS

The basic traffic station equipment required in order to implement a TDMA system consists of the TIMs, common TDMA traffic equipment (CTTE), and up-link and down-link converters. Calculation of the number of CTTEs for each station was discussed in a preceding section. The TIMs at each station can be either DSI modules or DNI modules. The number of DSI modules and the number of DNI modules are determined for each traffic station based on a one-to-one correspondence with the DSI and DNI sub-bursts assigned to each terminal at the earth station. An up-link or down-link converter is assigned for each transmit or receive transponder used by each traffic station.

CHANNEL NUMBERING

Channel numbers are assigned to identify the traffic elements throughout the system. Terrestrial channel (TC) numbers are assigned to identify the
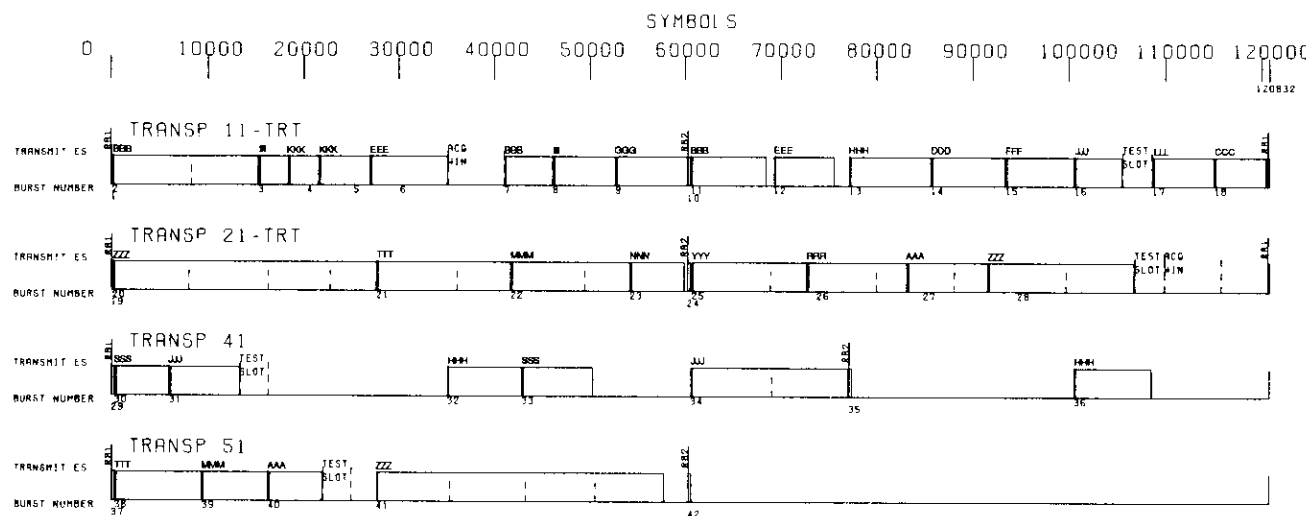
Figure 5. *Sample Plot of TDMA Burst Schedule*

TABLE 1. TDMA BURST SCHEDULE

BURST NUMBER		TRANSPONDER NUMBER	BEGINNING SYMBOL	BURST POSITION	END SYMBOL	LENGTH
1	RB1	11	−199	0	88	288
2		11	153	352	15280	15128
3		11	15353	15552	18416	3064
4		11	18489	18688	21624	3136
5		11	21689	21888	27016	5328
6		11	27081	27280	35120	8040
ACQUISITION WINDOW		11	35200	———	40767	5568
7		11	41097	41296	46136	5040
8		11	46201	46400	52704	6504
9		11	52777	52976	60224	7448
10	RB2	11	60297	60496	60584	288
11		11	60649	60848	68464	7816
12		11	69321	69520	75600	6280
13		11	77209	77408	85680	8472
14		11	85753	85952	93424	7672
15		11	93497	93696	100584	7088
16		11	100649	100848	105536	4888
TEST SLOT		11	105616	———	108615	3000
17		11	108713	108912	115064	6352
18		11	115129	115328	120456	5328
19	RB1	21	−199	0	88	288
20		21	153	352	27720	27568
21		21	27785	27984	41744	13960
22		21	41817	42016	54240	12424
23		21	54313	54512	59936	5624
24	RB2	21	60297	60496	60584	288
25		21	60793	60992	72776	11984
26		21	72841	73040	83216	10376
27		21	83289	83488	91616	8328
28		21	91689	91888	106816	15128
TEST SLOT		21	106896	———	109895	3000
ACQUISITION WINDOW		21	109968	———	115535	5568
29	RB1	41	41	240	328	288
30		41	393	592	6088	5696
31		41	6153	6352	13384	7232
TEST SLOT		41	13456	———	16455	3000
32		41	35209	35408	42952	7744
33		41	43017	43216	50392	7376
34		41	60681	60880	77128	16448
35	RB2	41	77193	77392	77480	288
36		41	100665	100864	108624	7960
37	RB1	51	41	240	328	288
38		51	393	592	9456	9064
39		51	9529	9728	16392	6864
40		51	16457	16656	22080	5624
TEST SLOT		51	22160	———	25159	3000
41		51	27801	28000	57856	30056
42	RB2	51	60409	60608	60696	288

voiceband channels in each station-to-station traffic link. International channel (IC) numbers sequentially identify the terrestrial channels as input into a DSI or DNI module. Satellite channel (SC) numbers identify the output channels of a DSI or DNI module. On DSI sub-bursts, satellite channel 0 is specified as the assignment channel, carrying dynamic SC-to-IC mapping information. An additional satellite channel is assigned as a supervisory channel for the exchange of terrestrial traffic alarm information over the TDMA/DSI system. DSI check channels are assigned for testing of the DSI modules. Figure 6 shows a typical configuration for BTP channel numbering.
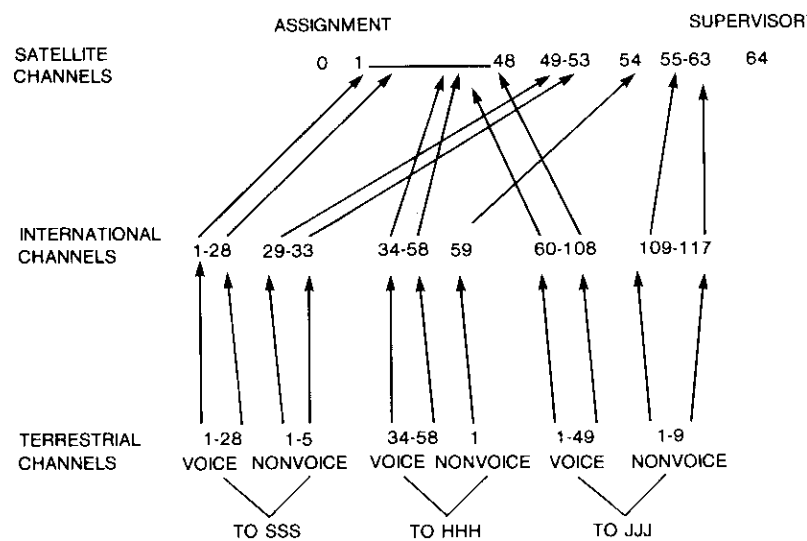
Figure 6. *Channel Numbering on DSI Multidestination Sub-Burst From Station AAA to Stations SSS, HHH, and JJJ*

Voice and data TC numbers are assigned for the channels in each station-to-station traffic link defined in the input traffic matrix. The voice channels on each link are numbered beginning with channel 1 and incremented by 1 for each voice channel on the link until all voice channels have been assigned numbers. The data channels are also numbered beginning with channel 1 and incremented by 1 for each transmitted data channel until all data channels have been assigned numbers for that particular link. Numbering continues for each link, beginning with 1 for the voice channels and 1 for the data channels, until all links have been processed. As each set of TC numbers to a sub-burst destination is assigned, the return sub-burst is found and the same TC numbers are assigned to the return link on the return sub-burst to ensure

correct baseband channel mapping into the TIMs at the transmit and receive earth stations. The IC numbers are assigned as input to a DSI or DNI module. Each IC corresponds to one input terrestrial channel. Each noninterpolated DNI sub-burst in the BTP can have up to 128 terrestrial channels assigned to it, and each interpolated DSI sub-burst can have up to 240 terrestrial channels.

The IC numbers are assigned on the sub-burst and are associated with groups of terrestrial channels. Each sub-burst is assigned IC numbers sequentially, beginning with the number 1 and incremented by 1 for each assigned terrestrial channel in the first destination until all terrestrial channels to all destinations have been counted.

SC numbers are assigned first to the satellite channels generated from the interpolated pool of terrestrial channels, then to the satellite channels generated from the assigned noninterpolated voice channels, and finally to the noninterpolated data channels. The satellite channels are numbered from 0 to 127. Channel 0 is used as an assignment channel for DSI sub-bursts and as a dummy assignment channel in DNI sub-bursts that receive return channels from DSI sub-bursts. If a supervisory channel is required, it is considered an additional noninterpolated channel and is assigned the highest SC number on the sub-burst.

The DSI check channels convey a special checking procedure which tests the end-to-end assignments by requesting assignments and, when an assignment is not received, setting an alarm at the transmit terminals. These channel numbers are assigned beginning with 192, in increments of 1, for each destination of the sub-burst.

THE BTP NUMBER

Every BTP is assigned a unique five-digit decimal number which follows one of two patterns. Plans to be used for normal system operation have BTP numbers with a first digit of 0. The second digit identifies the operating network, the third and fourth digits identify the generation, and the final digit is the issue number of that plan. Plans which are generated for special test purposes have numbers with the network identifier as the first digit, and the remaining four digits are used for internal identification.

Acquiring the satellite and control of the system

The INTELSAT TDMA system requires a highly accurate system of control in order to ensure exact synchronization of bursts sharing the transponder in a TDMA frame. There must also be a procedure to start up the network. Startup roles and redundant startup roles are assigned for all reference stations. Each reference station follows a procedure at startup based on its assigned role.

The principal burst transmitted by every earth station is designated as the burst used for acquisition. Synchronization information is delivered to each terminal via the CDC on a controlling reference burst specified in the BTP. This section describes the algorithms which are invoked to determine all control-related information in the BTP for use in the MTPs and CTPs.

REFERENCE STATION ROLE ASSIGNMENT AND REFERENCE STATION REPLACE-MENT MATRIX

The algorithm that assigns startup roles to the reference stations uses criteria for startup that are based on the transponder configuration of the network. These criteria were described in detail in the preceding section on system startup and terminal acquisition. The reference station replacement matrix provides information indicating the roles of each of the reference terminals during normal operation and in the event of failure of any reference terminal for the given BTP.

After startup roles have been assigned, a unique reference station replace-ment matrix is associated with each reference terminal and included in the MTP and CTP for that terminal. Each matrix is generated by listing all of the reference terminals in a designated order, followed by the type of network configuration (loop or nonloop) and the highest possible role the reference station could have at startup. The order in which the reference terminals are listed is determined by the assigned startup role for the terminal whose matrix is being generated. The highest role assigned is either master primary or primary. For example, the redundant reference station to the master primary is assigned master primary as its highest role, since it would be required to take on that role in the event of master primary station failure or outage.

ASSIGNMENT OF REFERENCE BURSTS TO TERMINALS FOR CONTROL

A traffic terminal must receive a set of reference bursts from the reference terminals in each coverage region into which it transmits, regardless of the number of transponders it accesses. One set of reference bursts (RB1 and RB2) controls the SOF for the terminal and monitors each burst received in its coverage region, sending selective-do-not-transmit (SDNTX) messages for these bursts. These reference bursts are referred to as the controlling reference bursts for the terminal. The second set of RB1 and RB2, referred to as noncontrolling reference bursts, monitors bursts transmitted into the other coverage region and sends SDNTX messages for those bursts. The RB1 and RB2 must be received from the same transponder. Each traffic terminal is assigned to receive the reference bursts (for each coverage region) in the transponder from which it is receiving the most traffic. Reference terminals are assigned to receive all reference bursts in all of their receive transponders.

A traffic terminal receiving only one set of reference bursts is assigned these bursts as controlling reference bursts. If a traffic terminal receives two sets of reference bursts, the reference bursts assigned in the loopback transponder are designated to carry control information.

In a nonloop configuration, each set of reference terminals controls the other, and the bursts transmitted into the designated TRTs are arbitrarily selected as controlling bursts. In a loop configuration, bursts from the reference stations transmitting into the loopback transponder are assigned as controlling bursts for all four reference stations, since the loopback stations will then monitor and adjust their own bursts to achieve a higher degree of timing accuracy.

Several constraints exist for assigning controlling reference bursts. Each reference terminal can control a maximum of 56 terminals, with up to 28 being controlled by one transponder.

PARALLEL OR SEQUENTIAL ACQUISITION ASSIGNMENTS

Terminals can acquire the system either sequentially, using a CAW, or in parallel, using the assigned transmit principal burst slot in the frame. One burst transmitted by each terminal is assigned as the principal burst to be transmitted during acquisition. Only the preamble of this principal burst (the short burst) is transmitted into the center of the acquisition slot until the terminal has been synchronized. All acquisition slots must be scheduled at least 320 symbols from any sync window in order to avoid inaccurate control information resulting from an acquisition window and sync window overlap.

When the principal burst of a terminal is longer than 5,840 symbols, an acquisition slot can be assigned within the burst slot in the frame. Several terminals can acquire in parallel in this manner. Otherwise, the terminal is assigned to acquire sequentially in a CAW. A maximum of four terminals can be assigned to use the same CAW. They acquire using the CAW one at a time, or sequentially [3].

PRINCIPAL BURST ASSIGNMENT

Principal bursts are assigned for every terminal in the BTP, based on the controlling reference burst assignment. The longest burst transmitted by the terminal into a transponder received by the controlling reference bursts is assigned as the principal burst for the terminal. The reference terminals' principal bursts are arbitrarily assigned in the first transmit transponder monitored by the controlling reference station.

CONFIGURATION OF ACQUISITION WINDOWS WITHIN THE PRINCIPAL BURST SLOT

Figure 7 illustrates the algorithm used to configure an acquisition slot for a terminal acquiring in its assigned principal burst slot in the frame. The

CENTER OF ACQUISITION WINDOW = 92,368 + 5,024/2 = 94,880

* NOT TO SCALE.
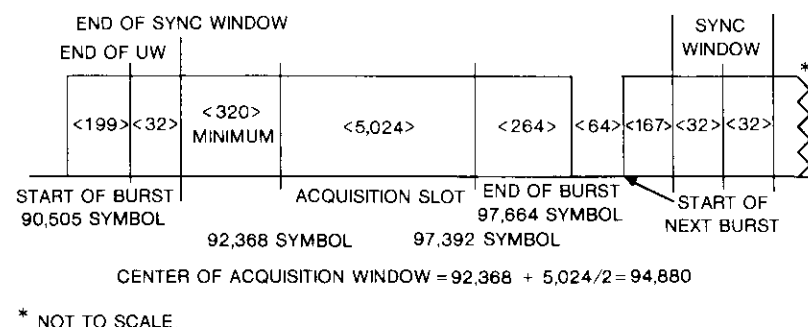
Figure 7. Assignment of Acquisition Slot in a Principal Burst

acquisition window is a 5,024-symbol-long slot located within the burst slot. The end of the acquisition slot is positioned 264 symbols from the scheduled end symbol of the burst to ensure that adequate space (*i.e.*, at least 320 symbols) is allowed between the acquisition window and the sync window of a following burst. The start of the acquisition slot is then adjusted forward within the burst slot to the first modulo-16 position available. A check is made that the start of the acquisition slot is at least 320 symbols from the sync window of the burst to avoid acquisition window and sync window collision within the burst. The center of the acquisition window is then calculated by adding half its length (2,515 symbols) to the adjusted start of the window.

SDNTX TRANSPONDER ASSIGNMENT

Whenever a burst has been declared lost, for example because it has lost synchronization, the reference terminal monitoring that burst initiates the SDNTX procedure for the terminal transmitting the burst. This procedure requires the terminal to switch to redundant equipment or shut down transmission of that one particular burst in order to protect the system. An algorithm associates an SDNTX transponder with each burst in the BTP. The set of reference stations receiving the burst, and the terminal transmitting the burst, are identified. The transponder from which the transmitting terminal receives reference bursts from that set of reference stations is assigned as SDNTX transponder for the transmit burst.

CDC ASSIGNMENTS

Control and delay information is sent to each controlled terminal by destination-addressed messages over the CDC. The duration of each message

is one multiframe (16 contiguous frames), and the messages are repeated once in each control frame (32 multiframes) [3]. This information includes the control codes and transmit delay information to be used by the controlled terminals for acquisition and synchronization, the reference station status code, the start-of-superframe (every 16.384 s) code, and the BTP number. A unique multiframe number within the control frame (the CDC address) is assigned to each terminal. Address 0 is used for transmission of the status code, and addresses 29, 30, and 31 are reserved for testing purposes. The reference terminals generate control information in two cycles, A and B. Reference terminals can maintain these two CDC address cycles, allowing them to control up to 56 terminals when using more than one transponder. Each CDC address cycle can be used to control up to 28 terminals, and only one cycle may be used in each transponder.

ASSIGNMENT OF BURST POSITION

A detailed description of the format of the burst preamble can be found in Reference 1. Figure 2 illustrates the components in the preamble. The last symbol of the unique word in the preamble of each burst marks the position of the burst in the frame. Burst position is calculated by adding 199 symbols to the scheduled starting symbol of the burst.

Communications on the TDMA network

Voice and TTY orderwire channels are contained in the preambles of all bursts and are used to facilitate communications in the network between operators and for network control. There are terrestrial communications lines between the reference stations and the IOCTF.

FORMAT OF THE PREAMBLE

Figure 2 gives the format of the preamble for the reference and traffic bursts. The preamble consists of a carrier and bit timing sequence, the unique word, voice and TTY orderwires, and a service channel. A detailed description of the burst preamble is provided in Reference 1. Orderwires in the preamble provide voice and data communications between earth stations and downloading of the CTPs to terminals.

ORDERWIRE ASSIGNMENTS

Orderwires are assigned between all stations with assigned traffic links. Each traffic station is also assigned an orderwire to one set of reference stations, and orderwires are assigned between reference stations receiving each other's bursts. The traffic stations communicate with the IOCTF via additional orderwires assigned through the reference stations.

Ten orderwires are available on each burst: two for voice and eight for TTY. The voice orderwires are numbered P1 and P2, and the TTY orderwires C1 through C8. Each earth station pair is assigned one voice orderwire and one TTY orderwire. Each traffic terminal can transmit up to 16 voice and 32 TTY orderwires, and can receive up to 32 voice and 64 TTY orderwires. The algorithm for assigning orderwires minimizes the total number of orderwires assigned and tries to distribute evenly the total number of orderwires assigned to each set of reference stations.

For each traffic terminal, the set of reference stations for orderwire communications to the IOCTF is selected using the following criteria. If the terminal receives only one set of reference bursts, the reference stations transmitting those bursts are selected. If the terminal receives reference bursts from both coverage regions, the reference stations switching the least number of IOCTF orderwires are selected. If possible, orderwires are assigned to the IOCTF on two separate traffic bursts received by those reference stations. The P1 and C1 orderwires assigned through the reference station transmitting RB2s are designated as orderwires to IOCB. Those assigned through the reference station transmitting RB1s are designated as IOCA orderwires. Whichever reference station is designated as the primary switches the orderwires to the IOCTF.

When IOCTF orderwires are assigned on two separate bursts from each traffic terminal, the orderwires are selected in the following manner. If the principal burst is received by these reference stations, it is selected as one of the bursts for IOCTF orderwires. The burst which can be received by these reference stations and has the greatest number of destinations is then located. If this burst also happens to be the principal burst at the terminal, then the burst with the next greatest number of destinations is located. If the principal burst has more destinations than this second transmit burst, IOCB orderwires are assigned on P1 and C1 of the principal burst; otherwise, IOCA orderwires are assigned. The second burst is then assigned IOCA or IOCB, whichever remains. If the principal burst is not received by the selected reference stations, then the two transmitted bursts with the greatest number of destinations received by these reference stations are chosen for the IOCTF orderwire assignments.

Orderwires to the reference station pair are assigned on P2 and C2 of the second transmit burst. These orderwires are not assigned on the principal burst from the terminal unless necessary. If the terminal receives bursts from all four reference stations, P2 and C2 orderwires to the second reference station pair are assigned on the transmit burst with the greatest number of destinations which is received by that reference station pair.

One voice (P2) and one TTY (C2) orderwire are assigned to each of the traffic destinations on the burst with the greatest number of destinations. The burst with the next greatest number of unassigned orderwire destinations is selected for the next orderwire assignments. This process continues until all orderwire assignments have been made.

The P2 and C2 orderwires are assigned between all reference stations able to receive each other, and from the reference stations to all received traffic stations on the reference bursts previously assigned to be received by these stations. Return P1 and C1 orderwires from the IOC to the traffic station destinations are assigned on the received reference bursts from the reference stations designated for IOCTF orderwire switching.

TERRESTRIAL LINES BETWEEN REFERENCE STATIONS AND THE IOCTF

All four reference stations have direct terrestrial lines to the IOCTF. Communications between the traffic stations and the IOCTF are relayed via orderwires assigned on the reference bursts and switched at the reference stations.

Manual maintenance of the network assignments

A number of manual assignments are made in the BTP which are maintained and updated by the operations planners at INTELSAT. Decimal terminal numbers are manually assigned to all traffic and reference terminals and TSMs in the network. Binary equivalents of the decimal terminal numbers are also used in the MTPs and CTPs. A short terminal number is obtained by using the 6 least-significant binary digits from the binary equivalent of the decimal terminal number. A long terminal number contains the 8 least-significant binary digits.

Four CDC addresses are assigned to each terminal. These addresses are multiframe numbers used to address the individual terminals. The actual addresses used in a particular BTP are determined by the cycle (A or B, as previously described) used in the transponder from which the terminal receives its controlling reference bursts, and by the coverage region of the reference stations transmitting these bursts.

Three special terminal numbers are assigned on all networks. Terminal number 31 is assigned as a universal test terminal. Terminal numbers 29 and 30 are used for system control purposes.

A table of coded earth station names and corresponding International Telecommunications Union (ITU) country codes is maintained for each satellite network. The coded earth station name consists of a three-character abbreviation of the earth station name, followed by a dash and two-character antenna code. Each satellite is assigned a name, based on its present role,

and an identifying number. These identifiers are used to extract the correct traffic levels from the ITDB for inclusion in the BTP. They are also used to identify the MTPs and CTPs.

Each BTP is assigned a unique five-digit BTP number which identifies the network, generation, and issue number of the plan.

MTP and CTP descriptions

The following subsections describe the functions of the MTPs and the different types of CTPs. The information provided in these terminal-specific time plans is also described.

Purpose of the MTPs and CTPs

The MTPs and CTPs provide the TDMA station with all of the information it will need to configure itself in order to participate in the network when the network switches over to a new BTP. Stations may need to reconfigure or introduce such items as baseband equipment, frequency converters, and amplifiers in order to accommodate the new traffic assignments. Orderwire assignments and baseband channel arrangements between the individual traffic links are formalized and verified through the time plans. The CTP binary information is loaded into the terminal to provide the transmit and receive timing information for that terminal.

The MTPs are typically sent to the administrations responsible for each earth station weeks or months before the BTP change is scheduled to take place. The CTP is transmitted from the IOCTF to the terminal via orderwires anywhere from 2 weeks to minutes before the BTP change will occur.

Operational MTPs and corresponding operational and test CTPs are defined for the reference, traffic, and TSM terminals and have specific functions. Each of these formatted time plans will be described later in this section. The operational MTPs and CTPs are defined in pairs; that is, for every operational MTP there is a corresponding set of operational and test CTPs.

CTP format

The machine-readable CTPs are coded using the 5-bit International Telegraph Alphabet (ITA) No. 2 [4]. Each CTP contains a variable number of information blocks, depending on the CTP type and the amount of traffic to be transmitted and received by the terminal. A unique three-digit code number defines each block type. The code number range varies with the CTP terminal type.

Each CTP block ends with a binary five-digit checksum which is calculated by the following procedure. The checksum is set to zero at the start of each code block of the CTP. As each line of the block is generated, the checksum is incremented by summing the ITA character codes from that line, including control characters such as line feeds, spaces, and carriage returns. The five

least significant bits of this sum are retained. The checksum is provided as the last line of each block and is used to verify the accuracy of the CTP transmission as received by the TDMA station. The checksums for each block are recomputed by the receive station and compared against the received checksums. If any discrepancies are found, the IOCTF retransmits the CTP.

Traffic terminal operational time plans

The traffic terminal operational MTP includes information on controlling and noncontrolling reference bursts; transponder, sub-burst, orderwire, and schedule information for each transmit burst and receive burst at the traffic terminal; acquisition information; transmit and receive baseband arrangements; and a summary of the transmit burst configurations, the receive burst configurations, and the equipment requirements at the earth station.

The traffic terminal operational CTP consists of a series of information blocks indicating received reference burst information, unique word position, length, transponder assignment, and orderwire maps for all transmit and receive bursts at a terminal. Preamble and postamble blocks begin and end each CTP, identifying the BTP number and terminal number, and indicating the total number of blocks in the CTP.

Examples of a typical traffic terminal MTP and corresponding operational CTP are presented as an appendix to this paper.

Reference terminal operational time plans

The reference terminal MTP contains transponder, terminal, burst, and orderwire information for the terminal's controlling pair of reference bursts, controlled reference bursts, and any other received pair of reference bursts. The reference station replacement matrix is provided. There is burst and orderwire information for each transmit burst; terminal, transponder, sub-burst, and orderwire acquisition information for each traffic burst controlled by the reference terminal; and information on all other received traffic bursts. The CAW and test slot assignments are also provided. The CDC addresses are provided for all terminals controlled by the reference station.

The reference terminal CTP contains information blocks for controlling, controlled, and any other received reference bursts; the reference station replacement matrix; information for all reference bursts transmitted by the terminal; blocks with terminal number, unique word position, and acquisition information for all traffic bursts controlled by the reference terminal; CDC addresses of all controlled terminals; information for all other received traffic bursts; and the positions for CAWs. "Preamble" and "postamble" blocks begin and end each CTP. These blocks identify the BTP number and reference terminal number, and give the total number of CTP blocks.

System monitor operational time plan

The TSM MTP provides transponder, terminal, and burst information for all reference bursts transmitted or received by its monitored reference terminal. It provides a list by transponder of all traffic bursts received by its monitored reference terminal. This list gives the transmit terminal and the number, length, and position of each burst. Descriptions of idle time slots, CAWs, and test time slots for all transponders transmitted into or received by the monitored reference terminal are also provided.

The TSM CTP consists of blocks providing the burst position, number, transponder, and transmit terminal for all reference bursts transmitted or received by the monitored reference terminal and for all traffic bursts received by the monitored reference terminal. Idle time slots are given for all transmit and receive transponders. "Preamble" and "postamble" blocks provide the BTP number, TSM identification, and the total number of blocks in the CTP.

Abridged CTPs

Abridged CTPs (ACTPs) for traffic, reference, or TSM terminals consist of a preamble and postamble block providing the BTP number, terminal number, and a block count of 2. The ACTP is used by the IOCTF to verify the content of the CTP in the background memory for the specified terminal. Upon receiving an ACTP from the IOCTF, the terminal substitutes the BTP number from the ACTP into the CTP in its background memory and returns the complete CTP to the IOCTF.

Test CTPs

The INTELSAT Satellite Systems Operations Guide (SSOG) [5] describes the testing procedures carried out in the system. Test CTPs are generated to facilitate some of the SSOG procedures when the TDMA system is being used in the testing.

Test-2 CTPs (T2-CTPs) are used by traffic terminals in a contrived loop configuration [6] to evaluate the correct functioning of the DSI/DNI units in conjunction with the terminal's CTTE. The traffic terminal receives one set of real reference bursts to identify the start of frame; however, it does not transmit into the TDMA system, but into a contrived loopback mode to test the traffic path through the terminal. Information for this CTP is generated by assigning one full-size sub-burst to each DSI or DNI unit at the terminal; forming maximum-configuration FEC encoded test bursts from these sub-bursts; scheduling these test bursts in the transponder from which the traffic terminal receives its controlling reference bursts in the operational CTP; and scheduling simulated reference bursts in this transponder. The CTP is then generated using preamble and postamble blocks, a block with the simulated

controlling reference bursts, a block with a test burst assigned as the principal burst, and using the test bursts for both transmit and receive burst and sub-burst information blocks.

After the off-line tests have been conducted and the T2-CTPs utilized, a new terminal is sent a test-1 CTP (T1-CTP) to test its on-line response to the reference terminal's control information. The T1-CTPs are identical to the operational traffic terminal CTPs except that each transmit burst has only one sub-burst consisting of two satellite channels. The traffic terminal's response to the acquisition and synchronization procedures and SDNTX messages is tested. Once it has been determined that the terminal is qualified, it is taken out of the TDMA system, sent its operational CTP, and it reacquires the system using this CTP.

Test-abridged CTPs (TACTPs) are identical to ACTPs except that the BTP number differs. A TACTP is used to support a traffic terminal in conducting the transmit frame acquisition test, phase 1 [3]. TACTPs can be generated for every traffic, reference, and TSM terminal in the network.

Baseband worksheets

Baseband worksheets are used to request changes in the automatic baseband and orderwire assignments for terminals in a proposed BTP. These worksheets may be generated for each traffic station. The assigned transponder and destinations for each transmit burst are provided for each station. The number of assigned channels for each sub-burst of the burst is also provided. Orderwire assignments can be requested and channel numbering on each sub-burst can be specified.

BTP software system description

The software system which generates the BTP and the MTPs and CTPs consists of four programs implemented in FLECS, a high-order structured FORTRAN language. Figure 8 illustrates the data flow between these programs. The software is oriented toward the operational planner and the communications engineer. The programs are command-driven through a user-oriented command language. Each command generates a BTP assignment, executes one of the algorithms described in previous sections, or overrides part of an algorithm.

The input commands may be categorized as control commands, specification commands, analysis commands, modification commands, or output commands. Control commands interface the program with on-line user files and control the program flow. Specification commands define the TDMA network which is to be considered. Some of these commands have a direct impact on
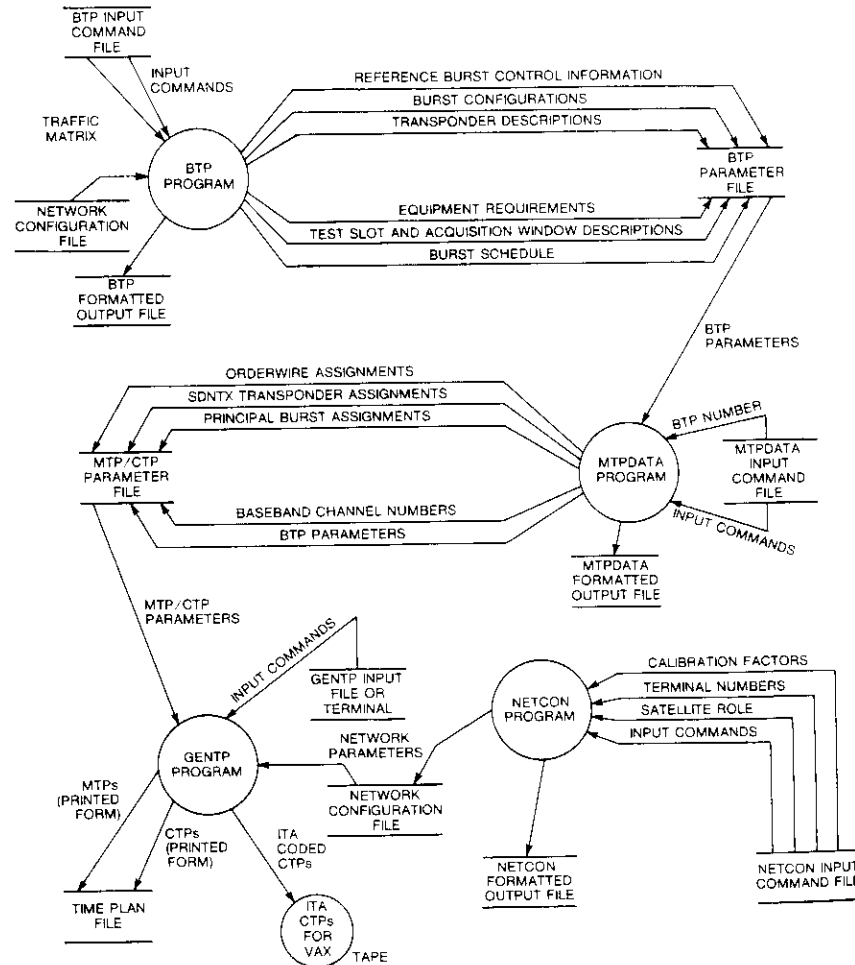
Figure 8. *BTP/MTP/CTP Software System Data Flow*

the analysis commands, which are used to initiate the automatic algorithms in the various programs. Modification commands allow the user to modify assignments made by the automatic algorithms, while output commands generate printed output.

Functions of the four programs

The BTP program implements the previously described algorithms to form and schedule sub-bursts, traffic bursts, and reference bursts; schedule test

slots and CAWs; couple sub-bursts with returns; determine required equipment; assign bursts to terminals; and assign reference bursts to terminals for control. Output from the program consists of tables of various assignments, a plot of the frame schedule for each transponder, and a binary file of parameters generated by the assignments.

The MTPDATA program is dependent upon the assignments generated by the BTP program. It requires the binary BTP output parameter file as an input. The MTPDATA program implements the algorithms for assigning orderwires, SDNTX transponders, principal bursts, and channel numbers.

The NETCON program has no analysis functions. Its purpose is to generate a table describing the network configuration, including satellite name, participating stations, terminal identification numbers, and specific CDC addresses, along with a binary file of these same parameters which can be used by the GENTP program to generate the MTPs and CTPs. The binary file can also be accessed by the BTP program if specific terminal numbers are desired in BTP output. An input file, which is generally fixed over long periods of time, consists of a series of commands specifying assignments for the particular satellite and network configuration.

The GENTP program formats the MTPs and CTPs and generates output files in both printed and binary form from corresponding ITA code. It is dependent upon the output generated by the MTPDATA and NETCON programs. The GENTP program implements the algorithms for acquisition slot configuration, DSI check channel numbering, ITA conversion, checksum generation, and generation of T2-CTP test burst parameters. For each block of the CTP, data are converted into ITA standard code line by line, the checksum is calculated, and the entire coded block is written to an output file. This ITA file is written to magnetic tape and read by the IOCTF operator onto the background processor (BGP), where it is stored until it is disseminated to the network terminals.

Use of the BTP system in planning

Incorporated into the design of the BTP software system is the ability to selectively override the automatic algorithms to reconcile a generated BTP with existing operational constraints or to reduce the changes between successive time plan assignments which may occur using the automatic algorithms.

When BTPs are being generated, first the automatic algorithms are invoked and the resulting burst schedule and assignments are reviewed. The operations planners are then able to override certain results of the automatic algorithms in order to modify the final plan generated. Various modification commands are used in both the BTP and MTPDATA programs for this purpose.

In the BTP program, terrestrial channels can be moved from one sub-burst to another, bursts can be divided or merged, interpolated channels can be switched to noninterpolated and vice versa, and bursts, test slots and CAWs can be moved in the frame or distributed within the frame more evenly. Selected bursts can be assigned a scheduled starting symbol, and the program will schedule all other entities around them using the automatic scheduling algorithm but exempting these selected bursts. Bursts can be manually formed, and the program will then schedule these bursts and make all other assignments.

In the MTPDATA program, orderwires can be manually assigned or deleted on specified bursts, principal bursts can be specified for terminals, channel numbers and SDNTX transponders can be selectively reassigned, and baseband configurations can be input.

Development phases of the BTP software system

Development of the BTP software began with the system design and implementation of the BTP program in 1981, employing user commands designed to implement the automatic algorithms and selectively override several of these algorithms. The MTPDATA, NETCON, and GENTP programs were initiated in 1982.

The use of the FLECS FORTRAN preprocessor simplified the task of developing a large software system and resulted in a well-ordered, readable set of software which has readily accommodated software maintenance and enhancements. The software has been implemented in a modular manner, which permits the addition of new functions or the replacement of existing functions with little effect on the other system components.

As the planning stages of the INTELSAT TDMA system progressed, various options were added to the software to selectively override the automatic algorithms in order to comply with additional operational constraints or requests from participating earth stations to minimize changes to equipment configurations. For example, it was found that if at least one reference burst in each transponder is not located at the same position in the frame in consecutive BTPs, difficulties arise in maintaining synchronization of the system during a BTP change. Therefore, the capability to manually fix the scheduled start of a burst was added to the BTP program. Baseband channel mapping was another area in the BTP where requests for minimizing changes between succeeding time plans resulted in the creation and distribution of baseband worksheets and the implementation of commands in the MTPDATA program to override automatic mapping at specific earth stations.

As commands to override the automatic algorithms proliferated in the software, so did the probability of a user-generated error in the resulting

operational CTPs. The most recent enhancement of the software has been the implementation of an extensive error-checking system throughout the software to prevent the release of an erroneous CTP which, if used, could cause system failure.

Conclusions

Traffic management in the INTELSAT TDMA system involves a large number of coordinated timing and control assignments which must be related specifically to each participating terminal. Channel mapping and orderwire assignments must also be provided for each terminal. The entire body of these assignments is referred to as the BTP. After a BTP has been generated, a procedure for gaining approval of (or processing modifications of) the BTP from participating administrations is necessary. A software system has been developed at COMSAT Laboratories, in close cooperation with the operations planners at INTELSAT, which automatically generates these assignments for a complete TDMA network. This software system enables planners to override selected assignments based on requests from participating administrations, and analyzes these overrides to ensure that the resulting BTP will be compatible with INTELSAT's TDMA specifications.

Acknowledgments

References

[1] B. A. Pontano, S. J. Campanella, and J. L. Dicks, "The INTELSAT TDMA/DSI System," *COMSAT Technical Review*, Vol. 15, No. 2B, Fall 1985, pp. 369–398.

[2] J. H. Rieser and M. Onufry, "Terrestrial Interface Architecture (DSI/DNI)," *COMSAT Technical Review*, Vol. 15, No. 2B, Fall 1985, pp. 483–509.

[3] G. Forcina and R. Bedford, "TDMA Terminal Acquisition and Synchronization," *COMSAT Technical Review*, Vol. 15, No. 2B, Fall 1985, pp. 467–482.

[4] CCITT, "Operational Provisions Applying to Printing Telegraph Systems," Recommendation F.1, Div. C, VIIIth Plenary Assembly, Malaga-Torremolinos, 1984, *Red Book*, Vol. II.4.

[5] INTELSAT, "TDMA/DSI Test and Maintenance Procedures" (Draft), *Satellite Systems Operations Guide*, Vol. 3, April 1, 1985.

[6] INTELSAT, "TDMA/DSI Traffic Terminals," Specification BG-42-65 (Rev. 2), June 23, 1983.

Appendix. Sample traffic terminal time plans

This appendix describes an MTP and CTP for a selected traffic terminal. Portions of the operational MTP are presented at the end of this appendix, followed by portions of the operational CTP for a traffic terminal in country "AAA" participating in a TDMA network. Since the terminal in this example receives a large number of bursts, portions of the receive burst assignments have been deleted for the sake of brevity. The BTP and MTP are consistent with the example BTP figures and tables which have been presented throughout this paper. It should be noted that this BTP has been generated for illustrative purposes only and will not be implemented in the network.

The network being illustrated uses four transponders: two with hemi-beam coverages on up-link and down-link and two with zone-beam coverages on up-link and down-link. There is no loopback transponder; therefore, all traffic and reference terminals are controlled by the reference stations in the opposite coverage region. One set of reference stations is located in each of the zone coverage regions. These stations are referred to as WZ1 and WZ2 in the West zone and EZ1 and EZ2 in the East zone.

Traffic terminal MTP example

The MTP consists of a cover page and a number of pages containing the traffic and control information for this terminal. Each information page contains a header with the page number, station name, and terminal number. The BTP number, date of MTP generation, traffic terminal identification, and network identification are contained on the cover page.

Page 2 of the MTP contains the controlling reference burst information for this terminal. The controlling reference bursts are in transponder 11 and are burst numbers 1 and 10. Burst 1 is the TRT reference burst (RB1) transmitted by EZ1 and is positioned at symbol 0, the SOF. Terminal 196 will receive controlling information from this burst during acquisition from its CDC. Four orderwires are active for terminal 196 on this burst: P1 and C1 are the voice and TTY orderwires from the IOCTF, and P2 and C2 are the voice and TTY orderwires from the controlling reference station, EZ1.

The bursts and orderwire addresses which contain the return orderwires to complete the links are listed beside each of the receive orderwires. These are the bursts on which terminal 196 will transmit orderwires to the IOCTF and EZ1. Burst 10 is the secondary reference burst (RB2) and contains essentially the same information as the RB1. The reference station passes an alternate IOCTF orderwire (IOCB) and its own orderwire (EZ2).

Page 3 shows the transmit burst information for terminal 196's principal burst, which is used for acquisition. The principal burst, number 27, will be transmitted into transponder 21. The time slot assignment, burst duration, and FEC indicator and transponder containing the reference bursts which will provide the SDNTX message are provided next.

The orderwire assignments reflect that the principal burst is assigned as many orderwires as possible. All terminals receiving this burst will be assigned a voice and TTY orderwire. IOCB rather than IOCA has been assigned on this burst, since the burst has the greatest number of destinations of any transmit burst. The return orderwire assignments are indicated.

Burst 27 consists of two multiple-destination sub-bursts. The individual sub-burst information is supplied at the bottom of page 3. The sub-burst start symbol specifies the number of symbols after the last symbol of the preamble unique word where the sub-burst begins. The sub-burst length is given in uncoded symbols. Each traffic link assignment on the sub-burst is specified by the receive stations, number of voice and non-voice terrestrial channels, and the return burst and sub-burst assignments.

One other burst, number 40, is transmitted by terminal 196. This burst carries the necessary orderwire information to the reference stations, the IOCTF, and the remaining traffic terminals.

Page 5 begins the information for the traffic bursts received by terminal 196. A total of 13 bursts will be received in response to the 2 bursts transmitted by terminal 196. The receive orderwire assignments and traffic assignments correspond with the transmit burst assignments. The receive burst information continues through page 17 of the MTP; however, pages 6 through 16 have been omitted in this example.

Pages 18 and 19 contain the transmit baseband arrangements. The channel numbers identify the interpolated and non-interpolated traffic being transmitted by terminal 196 from the baseband arrangement through the satellite. The channels are assigned per sub-burst. The description type indicates *I* for interpolated channels, *P* for preassigned or noninterpolated channels, and *S* for a supervisory channel. Multiple stations can share the supervisory channel, as shown in the MTP.

Pages 20 through 23 contain the baseband arrangements for the received traffic bursts; however, pages 21 through 23 have been omitted in this example. The first burst, 5, is transmitted by station KKK and contains 12 voice channels, one nonvoice channel, and the supervisory channel for station AAA (terminal 196). This is the traffic being returned for burst 27, as shown on page 18. The assigned channel numbers match for the symmetric link, but the international channel numbers and size of the satellite channel interpolated pool may differ.

A summary of the transmit and receive information, along with an equipment summary, is provided at the end of the MTP.

CTP example

This subsection describes the traffic terminal CTP for BTP 51111 for station AAA (terminal 196) which corresponds to the MTP previously discussed. The readable CTP which is normally sent to the users is shown in its EBCDIC format. The CTP which is

electronically transmitted to the terminal from the IOCTF is translated entirely into the 5-bit ITA Number 2 code.

Like the MTP, the traffic terminal CTP begins with a cover page containing identifying information, and the remainder of the CTP has a numbered header on each page. The cover page information header and page titles are not part of the ITA-encoded CTP. The information block which begins the CTP is ITA-encoded but is not included in a checksum. The traffic terminal strips this information upon reception of the CTP.

The traffic terminal operational CTP code blocks are numbered between 00 and 99. Codes 00 and 99 are the preamble and postamble blocks which carry the critical time plan identification information. The preamble block is the first block to be check-summed. The checksum 01001 was derived by doing a binary addition of the ITA equivalent for each character in that block, including control characters such as line feed, space, and carriage return. The 5 least significant bits were saved and each was translated into its ITA equivalent for the CTP. The block count indicates that there are 34 information blocks in this CTP.

The code 10 block provides the critical information for receiving the controlling reference bursts. The burst positions are T1I and T2I for RB1 and RB2, respectively. The orderwire activity is shown in the binary map, where a 1 indicates an active orderwire. The leftmost bits represent the voice orderwires, P1 and P2, followed by the TTY orderwires, C1 through C8, in bits 3 through 10.

Codes 30 through 51 contain the critical subset of the MTP transmit and receive burst parameters needed for terminal operation. Each CTP block corresponds directly with the more detailed MTP descriptions. Pages 5 through 7 of receive burst parameters have not been included in this example.

```
                    SAMPLE BURST TIME PLAN


                    DATE:  17 OCT 85
```

```
MASTER TIME PLAN

BURST TIME PLAN NUMBER 51111
TRAFFIC TERMINAL – AAA
TERMINAL NUMBER – 196
SATELLITE – XXX XXX
END OF PLAN —        SAMPLE
```

CONTROLLING REFERENCE BURSTS

BURST(NO.)	TRANSPONDER	FREQUENCY	START OF BURST	BURST POSITION
RB1 1	11(EH TO WH)	5970.000 MHZ	-199 SYM.	0 SYM.

LENGTH	REFERENCE STATION
288 SYM.	EZ1

RECEIVE ORDERWIRES (ORIGINATOR/RETURN BURST/OW#)

```
P1 (IOCA    / 40- P1 )
P2 (EZ1     / 40- P2 )
C1 (IOCA    / 40- C1 )
C2 (EZ1     / 40- C2 )
C3  -
C4  -
C5  -
C6  -
C7  -
C8  -
```

BURST(NO.)	TRANSPONDER	FREQUENCY	START OF BURST	BURST POSITION
RB2 10	11(EH TO WH)	5970.000 MHZ	60297 SYM.	60496 SYM.

LENGTH	REFERENCE STATION
288 SYM.	EZ2

RECEIVE ORDERWIRES (ORIGINATOR/RETURN BURST/OW#)

```
P1 (IOCB    / 27- P1 )
P2 (EZ2     / 40- P2 )
C1 (IOCB    / 27- C1 )
C2 (EZ2     / 40- C2 )
C3  -
C4  -
C5  -
C6  -
C7  -
C8  -
```

TRANSMIT BURST INFORMATION

PRINCIPAL BURST

BURST(NO.)	TRANSPONDER	FREQUENCY	START OF BURST	BURST POSITION
27	21(WH TO EH)	5970.000 MHZ	83289 SYM.	83488 SYM.

LENGTH	FEC	TRANSPONDER FOR SDNTX	SATELLITE CHANNELS
8328 SYM.	ON	11(EH TO WH)	110

TRANSMIT ORDERWIRES (DESTINATION/RETURN BURST/OW#)

```
P1   IOCB   ( 10- P1 )
P2   BBB    ( 11- P2 )CCC    ( 18- P2 )DDD    ( 14- P2 )
P2   EEE    ( 12- P2 )FFF    ( 15- P2 )KKK    (  5- P2 )
P2   GGG    (  9- P2 )HHH    ( 13- P2 )III    (  8- P2 )
P2   LLL    ( 17- P2 )
C1   IOCB   ( 10- C1 )
C2   BBB    ( 11- C2 )CCC    ( 18- C2 )DDD    ( 14- C2 )
C2   EEE    ( 12- C2 )FFF    ( 15- C2 )KKK    (  5- C2 )
C2   GGG    (  9- C2 )HHH    ( 13- C2 )III    (  8- C2 )
C2   LLL    ( 17- C2 )
C3   -
C4   -
C5   -
C6   -
C7   -
C8   -
```

SUB-BURST	TYPE	START (SYM)	LENGTH (SYM)	DSI ALARM CHAN	RCV STATIONS WITH CONFIGURED CHANNELS AND RETURN BURST/SUB-BURST		
1	DSI	81	4096	192	BBB	- 14V	(BURST 11 SUB-BURST 1)
					BBB	- 2NV	(BURST 11 SUB-BURST 1)
				193	DDD	- 15V	(BURST 14 SUB-BURST 1)
					DDD	- 2NV	(BURST 14 SUB-BURST 1)
				194	EEE	- 21V	(BURST 12 SUB-BURST 1)
					EEE	- 2NV	(BURST 12 SUB-BURST 1)
				195	FFF	- 25V	(BURST 15 SUB-BURST 1)
					FFF	- 2NV	(BURST 15 SUB-BURST 1)
				196	KKK	- 12V	(BURST 5 SUB-BURST 1)
					KKK	- 1NV	(BURST 5 SUB-BURST 1)
				197	HHH	- 23V	(BURST 13 SUB-BURST 1)
					HHH	- 2NV	(BURST 13 SUB-BURST 1)
2	DSI	4177	2944	192	CCC	- 28V	(BURST 18 SUB-BURST 1)
				193	GGG	- 8V	(BURST 9 SUB-BURST 1)
					GGG	- 1NV	(BURST 9 SUB-BURST 1)
				194	III	- 37V	(BURST 8 SUB-BURST 1)
					III	- 4NV	(BURST 8 SUB-BURST 1)
				195	LLL	- 6V	(BURST 17 SUB-BURST 1)
					LLL	- 1NV	(BURST 17 SUB-BURST 1)

TRANSMIT BURST INFORMATION

OTHER TRANSMIT BURST

BURST(NO.)	TRANSPONDER	FREQUENCY	START OF BURST	BURST POSITION
40	51(WZ TO EZ)	5970.000 MHZ	16457 SYM.	16656 SYM.

LENGTH	FEC	TRANSPONDER FOR SDNTX	SATELLITE CHANNELS
5624 SYM.	ON	11(EH TO WH)	73

TRANSMIT ORDERWIRES (DESTINATION/RETURN BURST/OW#)

P1	IOCA	(1- P1)				
P2	EZ1	(1- P2)EZ2		(10- P2)HHH	(36- P2)	
P2	JJJ	(31- P2)SSS		(30- P2)		
C1	IOCA	(1- C1)				
C2	EZ1	(1- C2)EZ2		(10- C2)HHH	(36- C2)	
C2	JJJ	(31- C2)SSS		(30- C2)		
C3	–					
C4	–					
C5	–					
C6	–					
C7	–					
C8	–					

SUB-BURST	TYPE	START (SYM)	LENGTH (SYM)	DSI ALARM CHAN	RCV STATIONS WITH CONFIGURED CHANNELS AND RETURN BURST/SUB-BURST
1	DSI	81	4672	192	HHH – 33V (BURST 36 SUB-BURST 1)
					HHH – 1NV (BURST 36 SUB-BURST 1)
				193	JJJ – 55V (BURST 31 SUB-BURST 1)
					JJJ – 9NV (BURST 31 SUB-BURST 1)
				194	SSS – 34V (BURST 30 SUB-BURST 1)
					SSS – 5NV (BURST 30 SUB-BURST 1)

RECEIVE BURST INFORMATION

BURST(NO.)	TRANSPONDER	FREQUENCY	START OF BURST	BURST POSITION
5	11(EH TO WH)	5970.000 MHZ	21689 SYM.	21888 SYM.

LENGTH	FEC	SATELLITE CHANNELS	TRANSMIT NAME/TERMINAL
5328 SYM.	ON	69	KKK / 208

RECEIVE ORDERWIRES (ORIGINATOR/RETURN BURST/OW#)

P1	–	
P2	KKK	(27 – P2)
C1	–	
C2	KKK	(27 – C2)
C3	–	
C4	–	
C5	–	
C6	–	
C7	–	
C8	–	

SUB-BURST	TYPE	START (SYM)	LENGTH (SYM)	DSI ALARM CHANNEL	CONFIGURED CHANNELS AND (RETURN BURST/SUB-BURST)
1	DSI	81	4416	194	12 V (BURST 27 SUB-BURST 1)
					1NV (BURST 27 SUB-BURST 1)

RECEIVE BURST INFORMATION

BURST(NO.)	TRANSPONDER	FREQUENCY	START OF BURST	BURST POSITION
36	41(EZ TO WZ)	5970.000 MHZ	100665 SYM.	100864 SYM.

LENGTH	FEC	SATELLITE CHANNELS	TRANSMIT NAME/TERMINAL
7960 SYM.	ON	105	HHH / 199

RECEIVE ORDERWIRES (ORIGINATOR/RETURN BURST/OW#)

```
P1  -
P2 HHH    ( 40 - P2 )
C1  -
C2 HHH    ( 40 - C2 )
C3  -
C4  -
C5  -
C6  -
C7  -
C8  -
```

SUB-BURST	TYPE	START (SYM)	LENGTH (SYM)	DSI ALARM CHANNEL	CONFIGURED CHANNELS AND (RETURN BURST/SUB-BURST)
1	DSI	81	6720	193	33 V (BURST 40 SUB-BURST 1)
					1NV (BURST 40 SUB-BURST 1)

TRANSMIT BASEBAND ARRANGEMENTS

BURST NO. 27

SUB-BURST NO.   1 TYPE-DSI

RECEIVE STATION				ASSIGNED CHANNELS		INTERNATIONAL CHANNELS		SATELLITE CHANNELS		TYPE
BBB	AAA	-BBB	,V,	1-	14	1-	14	0-	51	I
BBB	AAA	-BBB	,NV,	1-	2	15-	16	52-	53	P
DDD	AAA	-DDD	,V,	1-	15	17-	31	0-	51	I
DDD	AAA	-DDD	,NV,	1-	2	32-	33	54-	55	P
EEE	AAA	-EEE	,V,	1-	21	34-	54	0-	51	I
EEE	AAA	-EEE	,NV,	1-	2	55-	56	56-	57	P
FFF	AAA	-FFF	,V,	1-	25	57-	81	0-	51	I
FFF	AAA	-FFF	,NV,	1-	2	82-	83	58-	59	P
KKK	AAA	-KKK	,V,	1-	12	84-	95	0-	51	I
KKK	AAA	-KKK	,NV,	1-	1	96-	96	60-	60	P
HHH	AAA	-HHH	,V,	1-	23	97-	119	0-	51	I
HHH	AAA	-HHH	,NV,	1-	2	120-	121	61-	62	P
BBB	AAA	-BBB							63	S
DDD	AAA	-DDD							63	S
EEE	AAA	-EEE							63	S
FFF	AAA	-FFF							63	S
KKK	AAA	-KKK							63	S
HHH	AAA	-HHH							63	S

SUB-BURST NO.   2 TYPE-DSI

RECEIVE STATION				ASSIGNED CHANNELS		INTERNATIONAL CHANNELS		SATELLITE CHANNELS		TYPE
CCC	AAA	-CCC	,V,	1-	28	1-	28	0-	38	I
GGG	AAA	-GGG	,V,	1-	8	29-	36	0-	38	I
GGG	AAA	-GGG	,NV,	1-	1	37-	37	39-	39	P
III	AAA	-III	,V,	1-	37	38-	74	0-	38	I
III	AAA	-III	,NV,	1-	4	75-	78	40-	43	P
LLL	AAA	-LLL	,V,	1-	6	79-	84	0-	38	I
LLL	AAA	-LLL	,NV,	1-	1	85-	85	44-	44	P
CCC	AAA	-CCC							45	S
GGG	AAA	-GGG							45	S
III	AAA	-III							45	S
LLL	AAA	-LLL							45	S

PAGE 19
STATION   AAA
TERMINAL   196

TRANSMIT BASEBAND ARRANGEMENTS

BURST NO. 40

SUB-BURST NO.   1 TYPE-DSI

RECEIVE STATION				ASSIGNED CHANNELS	INTERNATIONAL CHANNELS	SATELLITE CHANNELS	TYPE
HHH	AAA	-HHH	.V.	1- 33	1- 33	0- 56	I
HHH	AAA	-HHH	.NV.	1- 1	34- 34	57- 57	P
JJJ	AAA	-JJJ	.V.	1- 55	35- 89	0- 56	I
JJJ	AAA	-JJJ	.NV.	1- 9	90- 98	58- 66	P
SSS	AAA	-SSS	.V.	1- 34	99- 132	0- 56	I
SSS	AAA	-SSS	.NV.	1- 5	133- 137	67- 71	P
HHH	AAA	-HHH				72	S
JJJ	AAA	-JJJ				72	S
SSS	AAA	-SSS				72	S

PAGE 20
STATION   AAA
TERMINAL   196

RECEIVE BASEBAND ARRANGEMENTS

BURST NO. 5

SUB-BURST NO.   1 TYPE-DSI

TRANSMIT COUNTRY				ASSIGNED CHANNELS	INTERNATIONAL CHANNELS	SATELLITE CHANNELS	TYPE
KKK	KKK	-AAA	.V.	1- 12	1- 12	0- 58	I
KKK	KKK	-AAA	.NV.	1- 1	13- 13	59- 59	P
KKK	KKK	-AAA				68	S

BURST NO. 8

SUB-BURST NO.   1 TYPE-DSI

TRANSMIT COUNTRY				ASSIGNED CHANNELS	INTERNATIONAL CHANNELS	SATELLITE CHANNELS	TYPE
III	III	-AAA	.V.	1- 37	1- 37	0- 70	I
III	III	-AAA	.NV.	1- 4	38- 41	71- 74	P
III	III	-AAA				84	S

BURST NO. 9

SUB-BURST NO.   1 TYPE-DSI

TRANSMIT COUNTRY				ASSIGNED CHANNELS	INTERNATIONAL CHANNELS	SATELLITE CHANNELS	TYPE
GGG	GGG	-AAA	.V.	1- 8	1- 8	0- 89	I
GGG	GGG	-AAA	.NV.	1- 1	9- 9	90- 90	P
GGG	GGG	-AAA				97	S

BURST NO. 11

SUB-BURST NO.   1 TYPE-DSI

TRANSMIT COUNTRY				ASSIGNED CHANNELS	INTERNATIONAL CHANNELS	SATELLITE CHANNELS	TYPE
BBB	BBB	-AAA	.V.	1- 14	1- 14	0- 92	I
BBB	BBB	-AAA	.NV.	1- 2	15- 16	93- 94	P
BBB	BBB	-AAA				102	S

PAGE 24
STATION AAA
TERMINAL   196

TERMINAL SUMMARY
(TRANSMIT)

	TPDR 21	TPDR 51
TRANSMIT BURSTS	1	1
TRANSMIT SUB-BURSTS	2	1
TRANSMIT VOICE OW	2	2
TRANSMIT TTY CH.	2	2

TRANSMIT BURST CONFIGURATIONS

BURST NO.	TPDR	SUB-BURST NO./TYPE	CONFIGURED CH. TOTAL (NON-VOICE)	SATELLITE CHANNELS	UN-CODED SYMB.	DSI ALARM CHAN	RCV-STA TOTAL CH. (NON-VOICE)	
27	21	1-DSI	121(11)	64	4096	192 BBB	16(	2)
						193 DDD	17(	2)
						194 EEE	23(	2)
						195 FFF	27(	2)
						196 KKK	13(	1)
						197 HHH	25(	2)
		2-DSI	85(6)	46	2944	192 CCC	28(	0)
						193 GGG	9(	1)
						194 III	41(	4)
						195 LLL	7(	1)
40	51	1-DSI	137(15)	73	4672	192 HHH	34(	1)
						193 JJJ	64(	9)
						194 SSS	39(	5)

PAGE 25
STATION AAA
TERMINAL   196

TERMINAL SUMMARY (CONT.)
RECEIVE

	TPDR 11	TPDR 41
RECEIVE BURSTS	12	3
RECEIVE SUB-BURSTS	10	3
RECEIVE VOICE OW	14	3
RECEIVE TTY CH.	14	3

RECEIVE BURST CONFIGURATIONS

TX. STA.	BURST NO.	TPDR	SUB-BURST NO./TYPE	CONFIGURED CH. TOTAL (NON-VOICE)	SAT. CHAN	UN-CODED SYMB.	DSI ALARM CHAN	RCV-STA TOTAL CH. (NON-VOICE)	
KKK	5	11	1-DSI	136 (9)	69	4416	194 AAA	13(	1)
III	8	11	1-DSI	167 (13)	85	5440	194 AAA	41(	4)
GGG	9	11	1-DSI	206 (7)	98	6272	194 AAA	9(	1)
BBB	11	11	1-DSI	214 (9)	103	6592	193 AAA	16(	2)
EEE	12	11	1-DSI	156 (16)	82	5248	194 AAA	23(	2)
HHH	13	11	1-DSI	230 (13)	112	7168	194 AAA	25(	2)
DDD	14	11	1-DSI	200 (16)	101	6464	194 AAA	17(	2)
FFF	15	11	1-DSI	187 (12)	93	5952	194 AAA	27(	2)
LLL	17	11	1-DSI	167 (10)	83	5312	194 AAA	7(	1)
CCC	18	11	1-DSI	129 (13)	69	4416	194 AAA	28(	0)
SSS	30	41	1-DSI	134 (19)	74	4736	193 AAA	39(	5)
JJJ	31	41	1-DSI	187 (16)	95	6080	193 AAA	64(	9)
HHH	36	41	1-DSI	153 (59)	105	6720	193 AAA	34(	1)
EZ1	1	11	RB1			288			
EZ2	10	11	RB2			288			

TERMINAL SUMMARY (CONT.)

EQUIPMENT REQUIREMENTS

TERM.	U/L	D/L	S-DEST. DSI	M-DEST. DSI	S-DEST. DNI	M-DEST. DNI
1	2	2	0	3	0	0

DATE: 17 OCT 85

CONDENSED BURST TIME PLAN

BURST TIME PLAN NUMBER 51111

STATION — AAA   TERMINAL — 196

PAGE 2
STATION   AAA
TERMINAL   196

TRAFFIC TERMINAL
CONDENSED BURST TIME PLAN (CTP)

DESCRIPTION

17.10.85	DATE OF TRANSMISSION
10.45.58	TIME OF TRANSMISSION
IOC	ORIGINATOR CODE
510	SATELLITE IDENTITY

CODE 00	PREAMBLE BLOCK
51111	BURST TIME PLAN NUMBER
196	TERMINAL NUMBER
0034	BLOCK COUNT
01001	CHECK SUM

CODE 10	CONTROLLING REFERENCE BURSTS
11	CONTROL TRANSPONDER NUMBER
000000	T11 FOR RB1 IN SYMBOLS
1111000000	ORDERWIRE MAP FOR RB1
060496	T2I FOR RB2 IN SYMBOLS
1111000000	ORDERWIRE MAP FOR RB2
00001	CHECK SUM

CODE 30	PRINCIPAL BURST PARAMETERS
21	TRANSPONDER NUMBER
0027	BURST NUMBER
083488	LOCATION OF UW FROM SOTF
008328	DURATION OF BURST IN SYMBOLS
1	FEC INDICATOR: 1 = FEC, 0 = NO FEC
11	TRANSPONDER NUMBER FOR SDNTX
1111000000	ORDERWIRE MAP
01001	CHECK SUM

CODE 31	SUB-BURST OF PRINCIPAL BURST
1	TRANSMIT SUB-BURST NUMBER
000081	START OF SUB-BURST FROM UW
4096	LENGTH OF SUB-BURST IN SYMBOLS
00111	CHECK SUM

PAGE   3
STATION   AAA
TERMINAL   196

TRAFFIC TERMINAL
CONDENSED BURST TIME PLAN (CONT.)

DESCRIPTION

CODE 31	SUB-BURST OF PRINCIPAL BURST
2	TRANSMIT SUB-BURST NUMBER
004177	START OF SUB-BURST FROM UW
2944	LENGTH OF SUB-BURST IN SYMBOLS
11011	CHECK SUM

CODE 40	OTHER TRANSMIT BURST PARAMETERS
51	TRANSPONDER NUMBER
0040	BURST NUMBER
016656	LOCATION OF UW FROM SOTF
005624	DURATION OF BURST IN SYMBOLS
1	FEC INDICATOR: 1 = FEC, 0 = NO FEC
11	TRANSPONDER NUMBER FOR SDNTX
1111000000	ORDERWIRE MAP
00000	CHECK SUM

CODE 41	SUB-BURST OF TRANSMIT BURST
1	TRANSMIT SUB-BURST NUMBER
000081	START OF SUB-BURST FROM UW
4672	LENGTH OF SUB-BURST IN SYMBOLS
11100	CHECK SUM

CODE 50	RECEIVE BURST PARAMETERS
11	TRANSPONDER NUMBER
0005	BURST NUMBER
021888	LOCATION OF UW FROM SORF
005328	DURATION OF BURST IN SYMBOLS
1	FEC INDICATOR: 1 = FEC, 0 = NO FEC
0101000000	ORDERWIRE MAP
10111	CHECK SUM

CODE 51	RECEIVE SUB-BURST PARAMETERS
1	SUB-BURST NUMBER
000081	START OF SUB-BURST FROM UW
4416	DURATION OF SUB-BURST IN SYMBOLS
01001	CHECK SUM

PAGE   4
STATION   AAA
TERMINAL   196

TRAFFIC TERMINAL
CONDENSED BURST TIME PLAN (CONT.)

DESCRIPTION

CODE 50	RECEIVE BURST PARAMETERS
11	TRANSPONDER NUMBER
0008	BURST NUMBER
046400	LOCATION OF UW FROM SORF
006504	DURATION OF BURST IN SYMBOLS
1	FEC INDICATOR: 1 = FEC, 0 = NO FEC
0101000000	ORDERWIRE MAP
00001	CHECK SUM

CODE 51	RECEIVE SUB-BURST PARAMETERS
1	SUB-BURST NUMBER
000081	START OF SUB-BURST FROM UW
5440	DURATION OF SUB-BURST IN SYMBOLS
00011	CHECK SUM

CODE 50	RECEIVE BURST PARAMETERS
11	TRANSPONDER NUMBER
0009	BURST NUMBER
052976	LOCATION OF UW FROM SORF
007448	DURATION OF BURST IN SYMBOLS
1	FEC INDICATOR: 1 = FEC, 0 = NO FEC
0101000000	ORDERWIRE MAP
10001	CHECK SUM

CODE 51	RECEIVE SUB-BURST PARAMETERS
1	SUB-BURST NUMBER
000081	START OF SUB-BURST FROM UW
6272	DURATION OF SUB-BURST IN SYMBOLS
01011	CHECK SUM

CODE 50	RECEIVE BURST PARAMETERS
11	TRANSPONDER NUMBER
0011	BURST NUMBER
060848	LOCATION OF UW FROM SORF
007816	DURATION OF BURST IN SYMBOLS
1	FEC INDICATOR: 1 = FEC, 0 = NO FEC
0101000000	ORDERWIRE MAP
10011	CHECK SUM

```
                                              PAGE   8
                                              STATION   AAA
                                              TERMINAL    196


                        TRAFFIC TERMINAL
                CONDENSED BURST TIME PLAN (CONT.)

                        DESCRIPTION

CODE 50                 RECEIVE BURST PARAMETERS
41                      TRANSPONDER NUMBER
0031                    BURST NUMBER
006352                  LOCATION OF UW FROM SORF
007232                  DURATION OF BURST IN SYMBOLS
1                       FEC INDICATOR: 1 = FEC, 0 = NO FEC
0101000000              ORDERWIRE MAP
10011                   CHECK SUM



CODE 51                 RECEIVE SUB-BURST PARAMETERS
1                       SUB-BURST NUMBER
000081                  START OF SUB-BURST FROM UW
6080                    DURATION OF SUB-BURST IN SYMBOLS
10000                   CHECK SUM



CODE 50                 RECEIVE BURST PARAMETERS
41                      TRANSPONDER NUMBER
0036                    BURST NUMBER
100864                  LOCATION OF UW FROM SORF
007960                  DURATION OF BURST IN SYMBOLS
1                       FEC INDICATOR: 1 = FEC, 0 = NO FEC
0101000000              ORDERWIRE MAP
10000                   CHECK SUM



CODE 51                 RECEIVE SUB-BURST PARAMETERS
1                       SUB-BURST NUMBER
000081                  START OF SUB-BURST FROM UW
6720                    DURATION OF SUB-BURST IN SYMBOLS
01110                   CHECK SUM



CODE 99                 POSTAMBLE BLOCK
51111                   BURST TIME PLAN NUMBER
196                     TERMINAL NUMBER
0034                    BLOCK COUNT
01101                   CHECK SUM
```

Penny A. Trusty received a B.S. in Mathematics from the College of William and Mary in 1960. Since joining COMSAT in 1982, she has been involved in the development of the software system which generates traffic schedules for the INTELSAT TDMA system. Prior to joining COMSAT, Mrs. Trusty was employed by NASA as a Technical Editor.

Christine A. King received a B.S. in Applied Mathematics and an M.S.E.E. from George Washington University in 1978 and 1985, respectively. She joined COMSAT in 1976 and is currently Manager of the Systems Analysis Software Department at COMSAT Laboratories, where she manages the development of computer programs for the analysis and simulation of communications systems. Her experience includes the design and implementation of several INTELSAT and COMSAT software models, including the INTELSAT TDMA Burst Time Plan Software System. She has authored several papers on TDMA burst scheduling. Ms. King is a member of IEEE.

Peter W. Roach is a Senior Operations Planner with INTELSAT, where he is currently responsible for the development of operational plans for INTELSAT satellites in the Indian and Pacific Ocean Regions for all modulation systems, including TDMA. Before joining INTELSAT in 1979, he was with the foreign service staff of Cable and Wireless PLC, where he was involved with providing and operating a wide range of international terrestrial and satellite telecommunications services.

Advantages of TDMA and satellite-switched TDMA in INTELSAT V and VI

S. J. CAMPANELLA, B. A. PONTANO, and J. L. DICKS

(Manuscript received September 12, 1985)

Abstract

Because time-division multiple-access (TDMA) terminals share a common carrier in
the time domain, the number of up- and down-conversion chains needed to implement
a network with TDMA is significantly reduced compared to the number needed with
frequency-division multiple-access (FDMA). A cost model based on counting the
number of up- and down-conversion chains for TDMA and FDMA is presented. From
this model, the number of stations for which TDMA implementation costs become
lower than those for FDMA is determined. The model is applied to a single earth
coverage beam system, to the INTELSAT V multiple-beam system with static connections,
and to the INTELSAT VI multiple-beam system with either static or dynamically switched
connections.

It is shown that dynamically switched TDMA will provide enhanced beam-to-beam
connectivity, allow adjustment of beam-to-beam traffic capacity in increments of a
single voice channel, and permit the TDMA network to operate with two rather than
four reference stations in each ocean region. The other advantages of TDMA discussed
include single-carrier-per-transponder operation, which doubles the available tran-
sponder power compared to FDMA; the ability to accommodate traffic capacity
variations by changing burst location and duration; and the capability of dynamic
switching among multiple beams, which in the future may evolve to hopping-beam
TDMA systems.

Introduction

Time division multiple access (TDMA) has been introduced in the INTELSAT V system to carry traffic over digital links implemented by earth stations that time-share 120.832-Mbit/s digital carriers, which are relayed back to earth through nominal 72-MHz bandwidth satellite transponders. In INTELSAT V satellites, the transponders interconnect a multiple-beam arrangement comprising two hemi beams and two northern zone beams using static interconnections [1]. In INTELSAT VI satellites, the transponders will interconnect a multiple-beam arrangement comprising two hemi beams, two northern zone beams, and two southern zone beams using either static, or static and dynamic, interconnections [2].

As the number of beams on a satellite increases, the number of transponders also increases. With static interconnection, the number increases as the square of the number of beams, while with dynamic switching it increases linearly. INTELSAT VI will have available two 6 × 6-port dynamic microwave switch matrices interconnecting six beams in two transponder frequency banks, with each bank containing six transponders. This ensures full, flexible, and efficient interconnectivity among the six beams of the hemi/zone beam configuration [3]. To achieve the same connectivity with static switching, 36 transponders would be required.

The INTELSAT 120.832-Mbit/s TDMA system has been designed to provide efficient communications service via multibeam satellites, with cooperative interaction among traffic terminals and dedicated reference stations [4]. The system can operate with the static interconnections of INTELSAT V and INTELSAT VI satellites, as well as with the dynamically switched interconnections of INTELSAT VI.

TDMA will result in lower total earth station costs compared to a system employing frequency division multiple access (FDMA), provided that a sufficient number of stations use TDMA. These costs can be expressed in terms of the number of up- and down-conversion chains needed to implement the total system. An up-link conversion chain consists of a modem, an IF-to-RF frequency converter, and an intermediate amplifier needed to drive the high-power amplifier (HPA). A down-conversion chain consists of a low-noise amplifier (LNA), an RF-to-IF frequency converter, and a demodulator. In most applications, the HPA and LNA are common to a multiplicity of up-link and down-link conversion chains and are not duplicated.

A system that minimizes the total number of up- and down-link conversion chains required to achieve a given connectivity will also minimize overall system cost. Cost advantage is realized when the number of earth stations exceeds a threshold below which FDMA is less expensive and above which

TDMA is less expensive. This paper presents an analysis of the INTELSAT V and VI multibeam systems which leads to expressions for the total number of up- and down-chains in the system and assigns to them the actual costs experienced for TDMA and FDMA implementations. (A single-beam system is analyzed for comparison purposes.)

The benefits resulting from the introduction of the dynamic microwave switch matrix are also discussed. The principal advantage of dynamic switching stems from the higher fill efficiency of the system, which is achieved when traffic routing in capacity increments of whole transponders is replaced with fully flexible traffic routing in single-voice-channel increments. For a six-beam system using only six transponders, each 6 × 6 dynamic switch on INTELSAT VI provides all 36 interconnectivities needed. With static connections, full interconnectivity among six beams would require the use of 36 transponders, which is impractical. A static configuration with fewer transponders would constrain or eliminate selected connectivities, depending on the choice of static routing. An additional benefit of the dynamic switch is improved connectivity between TDMA reference and traffic stations. As a result, the number of reference stations, and hence the cost of the reference station system, can be reduced.

INTELSAT V beam connectivities

INTELSAT V has five beams at C-band. Figure 1 shows typical earth coverages provided for the Atlantic Ocean Region (AOR). The transponder frequency plan of Figure 2 shows that the earth coverage beam is separated from the hemi and zone beams by frequency diversity, and the hemi beams are separated from the zone beams by polarization diversity. K_u-band transponders are also available for two spot beams. Some C-band transponders can be used in either the hemi and zone beams or in the earth coverage beam. Cross-strapping between hemi, zone, and spot beams is accomplished by static switching. The hemi and zone beams are used principally for trunk telephone service, while the earth coverage beam is used principally for services such as television, single-channel-per-carrier data, and thin-route telephony. This discussion deals exclusively with trunk telephony at C-band.

The hemi and zone beams can be represented schematically as shown in Figure 3. Regions bounded by the perimeter of a beam at its earth intersection are referred to as *beam cells*. Interconnectivity from east to west and west to east can be accomplished with a minimum of four links: two (A and B) connecting zone beams 1 and 2, and two (C and D) connecting hemi beams 3 and 4. North-south interconnectivity may be accomplished by loopbacks E and F to the west and east hemi beams. Thus, at least six links are needed
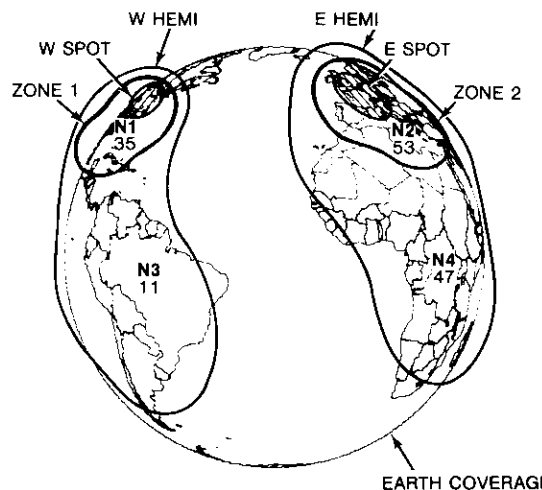
Figure 1. *INTELSAT V AOR Beam Coverages*
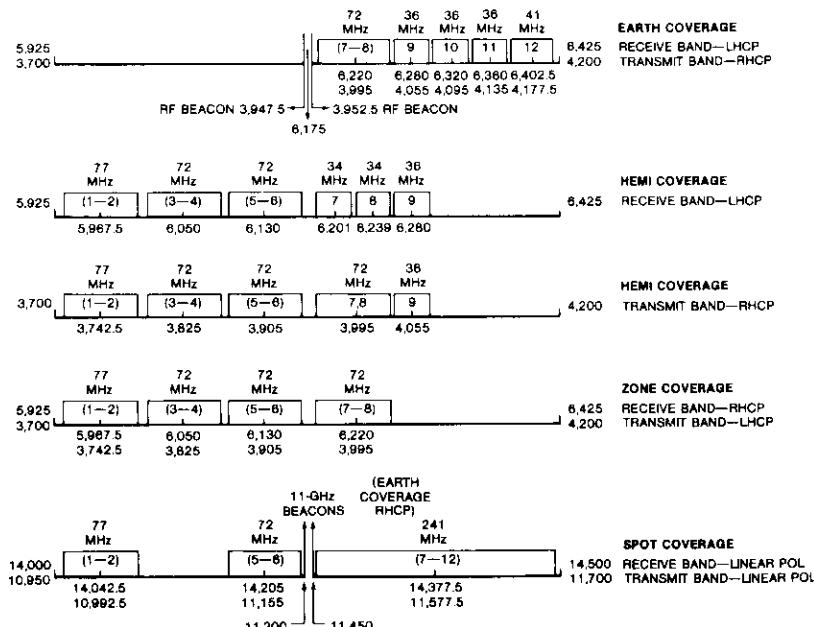
Figure 2. *INTELSAT V Transponder Frequency Plan*
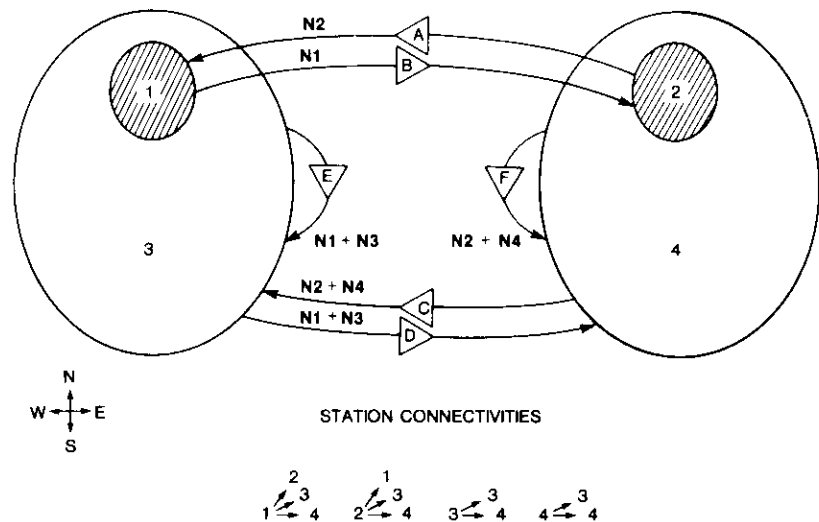
Figure 3. *INTELSAT V Beam Cells and Minimum Connectivities*

to provide communications among all earth stations. If all possible intercon-nectivities among the four beams were implemented, 16 links would be required; however, the overlap of the INTELSAT V beam permits the number of links to be reduced to six.

Links A and B can be assigned the full bandwidth of beams 1 and 2, respectively; links C and F can share the capacity of beam 4; and links D and E can share the capacity of beam 3. When the bandwidth of an interconnecting link exceeds that of a single transponder, multiple transponders operating in parallel are needed. Single transponders capable of delivering the required power over a wideband link are undesirable because of reliability considerations, inefficient transponder utilization caused by the output backoff needed to avoid intermodulation distortion among multiple carriers per transponder, and lack of flexibility to accommodate variations in traffic flow. To implement the hemi and zone beams of both INTELSAT V and VI satellites, multiple C-band transponders each with a nominal bandwidth of 72 MHz are used.

The FDMA or TDMA stations operating in regions where beam cells overlap have access to the capacity of the overlapping beams and may place carriers in each destination beam. Stations residing in beam cell 1 can communicate with those in beam cells 2, 3, and 4 via links B, E, and D, respectively (and those in beam cell 3 can communicate with those in beam cells 3 and 4 via

links E and D, respectively) by transmitting and receiving on appropriate frequencies and polarizations. Each link requires one or more transponders, depending on the routing plan. Transponder assignments are controlled by ground-commanded static switches. Similar arrangements can be made in the reverse direction for stations residing in beam cells 2 and 4. Loopback connections within the zone beams are not included, since the little traffic they would carry is accommodated by hemi-beam loopbacks.

To achieve full interconnectivity, each station in a beam cell must transmit at least one FDMA carrier or one TDMA burst to stations in each destination beam cell. The number of carriers, up-conversion chains, and down-conversion chains needed in the system to achieve full interconnectivity is a function of the number of beams and the multiple-access method used (FDMA or TDMA).

INTELSAT V FDMA operation

Up-link conversion chains

With N stations operating in a single-beam system (one up-beam connected to a congruent down-beam) with continuous FDMA carriers, each station would have to transmit at least one carrier and receive $N - 1$ carriers. This leads to a system requiring N up-link conversion chains and $N(N - 1)$ down-link conversion chains. For a multiple-beam satellite such as INTELSAT V, full network connectivity requires a larger number of carriers. This requirement can be estimated as follows.

Consider the multibeam configuration shown in Figure 3 for serving a community of N stations using continuous FDMA carriers. A convention will be adopted for counting stations in the system in a manner independent of beam cell overlapping. This convention assigns the number of stations in terms of regions bounded between the perimeter of a beam cell and the perimeter of contained beam cells. With reference to Figure 3, let the number of stations only in beam cell 1 be N_1, the number only in beam cell 2 be N_2, the number only in beam cell 3 but not in beam cell 1 be N_3, and the number only in beam cell 4 but not in beam cell 2 be N_4. Stations residing in regions of beam overlap are members of each overlapping cell and are assumed to operate on both polarizations. Thus, the number of stations in beam cell 1 is N_1, in beam cell 2 is N_2, in beam cell 3 is $N_1 + N_3$, and in beam cell 4 is $N_2 + N_4$.

To implement the connectivity shown in Figure 3 among all stations, those in beam cells 1 and 2 would each transmit three carriers. Those in beam cell 3 but not in beam cell 1, and those in beam cell 4 but not in beam cell 2,

would each transmit two carriers. Thus, the total number of FDMA carriers needed in the INTELSAT V system to provide full connectivity is

$$3(N_1 + N_2) + 2(N_3 + N_4) \quad . \tag{1}$$

Since each FDMA carrier must originate from a dedicated up-conversion chain, the above expression also gives the number of up-link conversion chains.

Currently in the INTELSAT AOR system [5], the beam cell station number variables are $N_1 = 35, N_2 = 53, N_3 = 11$, and $N_4 = 47$. Using expression (1), the number of carriers (and hence up-conversion chains) needed to implement full FDMA connectivity in INTELSAT V is 380. If all of these stations were operated in a single earth coverage beam equipped with a sufficient number of transponders, 146 carriers would be required. Thus, multibeam operation increases the number of carriers needed for FDMA operation by the ratio 2.6. In general, the increase in the number of up-link carriers, and consequently up-conversion chains, caused by partitioning any network into multiple beams will always be much greater for FDMA than for TDMA transmission.

For extrapolation purposes, it will be convenient to assign a fixed distribution of stations among the beams. Assuming that future INTELSAT V earth station growth will occur with the present geographic distribution ($N_1 = 0.24N$, $N_2 = 0.36N$, $N_3 = 0.08N$, and $N_4 = 0.32N$, where N is the total number of stations in the network), and substituting these values into expression (1), the number of carriers and hence the number up-link conversion chains for the multibeam INTELSAT V network is $2.6N$. If a uniform geographic distribution were assumed (corresponding to $N_1 = N_2 = N_3 = N_4 = N/4$), the result would be $2.5N$. Thus, the number of carriers is relatively insensitive to large variations in earth station distribution.

Because of the large number of carriers needed for continuous FDMA operation, each transponder must handle several carriers. This results in inefficient use of the transponder because of the need to back off the output power by 4 dB or more.

Down-link conversion chains

Consider now the number of down-conversion chains needed for continuous FDMA at the receive end. The matrix presented in Table 1 gives the number of FDMA carriers from the originating beam cell to the destination beam cell, using the counting convention previously adopted. The table also gives the number of stations in the destination beam cell that will receive the carriers, as well as the number of receive down-link conversion chains in each destination beam cell (obtained by summing the products of column elements in the matrix and the number of stations in the destination beam).

TABLE 1. NUMBER OF DOWN-LINK CONVERSION CHAINS FOR
INTELSAT V FDMA

		To Beam Cell			
		1	2	3	4
From Beam Cell	1	0	N_1	0	0
	2	N_2	0	0	0
	3	0	0	$N_1 + N_3$	$N_1 + N_3$
	4	0	0	$N_2 + N_4$	$N_2 + N_4$
Number of Destinations		N_1	N_2	$N_1 + N_3 - 1*$	$N_2 + N_4 - 1*$
Totals to Beam Cell	1	N_1N_2			
	2	N_1N_2			
	3	$(N_1 + N_3)(N - 1)$			
	4	$(N_2 + N_4)(N - 1)$			

* 1 subtracted for loopback connections only.

Table 1 was developed as follows: from beam cell 1, N_1 stations transmit N_1 multidestinational carriers to N_2 stations in beam cell 2, yielding N_1N_2 down-link conversion chains for stations in beam cell 2. Similarly, in the direction from beam cell 2 to beam cell 1, there are N_2N_1 down-link conversion chains for the stations in beam cell 1. From beam cell 3, $N_1 + N_3$ stations transmit $N_1 + N_3$ multidestinational carriers that are received by $N_2 + N_4$ stations in beam cell 4, yielding a total of $(N_1 + N_3)(N_2 + N_4)$ down-link conversion chains. In addition, since loopback connections are allowed in beam cell 3, $N_1 + N_3$ stations transmit $N_1 + N_3$ carriers that are received by $N_1 + N_3 - 1$ stations, yielding an additional $(N_1 + N_3)(N_1 + N_3 - 1)$ down-link conversion chains. Similarly, in the reverse sense of beam cells 3 and 4, there are $(N_2 + N_4)(N_1 + N_3)$ down-link conversion chains for traffic from beam cell 4 to beam cell 3 and $(N_2 + N_4)(N_2 + N_4 - 1)$ for loopback traffic in beam cell 4. The sum of the individual beam cell contributions gives the total number of receive down-conversion chains in the INTELSAT V FDMA system, as

$$N(N - 1) + 2N_1N_2 \qquad (2)$$

where $N = N_1 + N_2 + N_3 + N_4$.

Using the present distribution of stations for the INTELSAT AOR system, and inserting the appropriate numbers into expression (2) results in 24,880 down-link conversion chains to achieve full interconnectivity with FDMA in the INTELSAT V multiple-beam system, as compared to 21,170 chains needed if the same stations were served by earth coverage beams. The latter value is obtained from the expression $N(N - 1)$, with $N = 146$. Thus, introduction of the multibeam INTELSAT V increases the number of down-link conversion chains needed for full interconnectivity by the ratio 1.17 compared to earth coverage beam operation.

Assuming that growth occurs with the present geographic distribution as described previously, and substituting the resulting variable assignments into expression (2), the expression for the number of down-conversion chains becomes $N(1.17N - 1)$. Using the uniform earth station distribution assumption, expression (2) reduces to the expression $N(1.125N - 1)$. These results show that the number of down-conversion chains is relatively insensitive to large changes in earth station distribution.

INTELSAT V TDMA operation

Up- and down-link conversion chains

With TDMA, the access domain is time rather than frequency. Transponder power is used more efficiently because, with only one carrier per transponder present at a given time, the large power output backoff needed for multiple FDMA carriers is avoided. Typically with TDMA, each transponder handles only one carrier, centered in the assigned frequency band, which can operate with 1 dB of output power backoff using 120-Mbit/s QPSK modulation* in the nominal 72-MHz transponder bandwidth of INTELSAT V or VI. This carrier is shared among all earth stations by means of individual, non-overlapping traffic bursts.

Each TDMA station transmits traffic bursts into one or more transponders from a single modulator, up-converter, and HPA chain, using frequency hopping or polarization hopping to gain access to the various transponders according to a traffic burst time plan. Frequency hopping, which provides increased connectivity, can be accomplished by means of a frequency-agile local oscillator inserted in the up- or down-chain, or by separate up- and

---

* When a QPSK-modulated carrier is filtered to achieve a bandwidth-symbol period product (WT) near unity, significant amplitude ripple is generated at the symbol rate. This ripple interacts with the AM-to-PM nonlinearity typical of TWTA used in transponders, causing the QPSK signal to become phase modulated, and thus impairing phase recovery at the demodulator. Because TWTA distortion is higher near saturation, about 1 dB of output backoff is required in order to achieve optimum performance.

down-conversion chains. Polarization hopping can be accomplished by switching the up-converter between two HPAs and the down-converter between two LNAs, or by switching between separate up- and down-conversion chains.

The bit rate of the shared carrier must be high enough to accommodate the sum of the traffic of all stations served, and yet not so high as to constitute a disadvantage in terms of earth station e.i.r.p. requirements. In INTELSAT V and VI, the carrier bit rate in each 72-MHz transponder is 120.832 Mbit/s to conservatively carry 3,000 64-kbit/s digital speech interpolated, pulse-code modulated voice channels shared among as many as 28 earth stations. To operate in the hemi and zone beams, a typical TDMA station must be able to deliver an e.i.r.p. of 84 to 87 dBW using a Standard-A antenna (G/T = 40.7 dB/K). Each station transmits only on one carrier frequency by means of a single up-conversion chain, and the entire system can be implemented with N such up-link conversion chains for either single-beam or multibeam operation. However, in some cases separate up-conversion chains may be used, as previously mentioned, to hop between transponders.

Because TDMA bursts serve a role analogous to that of carriers in FDMA, the number of traffic bursts in a TDMA system equals the number of carriers in a comparable FDMA system. Thus, expression (1) can be used to determine the total number of bursts needed in a given system. Furthermore, only one receive-side down-link conversion chain is required per TDMA station, yielding a total of N for the entire system, since a single receive chain can extract traffic from many multidestinational traffic bursts. In a statically interconnected multiple-beam system such as INTELSAT V, the TDMA stations must be equipped for transponder hopping on the receive side or the transmit side, or both. Transponder hopping can be significantly reduced and even eliminated by using dynamic satellite switching.

Comparison of up- and down-conversion chain requirements for INTELSAT V

Compared to FDMA, TDMA reduces the number of up-link conversion chains needed from the value determined by expression (1) to N, and the number of down-link conversion chains from the value determined by expression (2) to N. Using the current INTELSAT AOR earth station distribution numbers given previously, the number of up-link conversion chains is reduced by the ratio 2.6 (380/146), and down-link chains by the ratio 170 (24,880/146) if TDMA is introduced throughout the system. If a total of N stations are distributed uniformly, the reduction ratio is 2.5 for the number of up-link conversion chains and approximately $1.125N$ for the number of down-conversion chains for INTELSAT V. These are significant reductions in the

number of up- and down-link conversion chains and constitute a significant advantage for TDMA.

INTELSAT VI beam connectivities

INTELSAT VI has seven beams at C-band. Figure 4 shows typical antenna coverages provided for the AOR. Compared to the antenna coverages for INTELSAT V, there are two additional zone beams for east and west coverages in the southern hemisphere. INTELSAT VI achieves sixfold frequency reuse of the C-band spectrum. The transponder frequency plan for INTELSAT VI, shown in Figure 5, is similar to that for INTELSAT V, with the addition of transponders for the two new zone beams. Only the two hemi and four zone beams at C-band are of concern here.
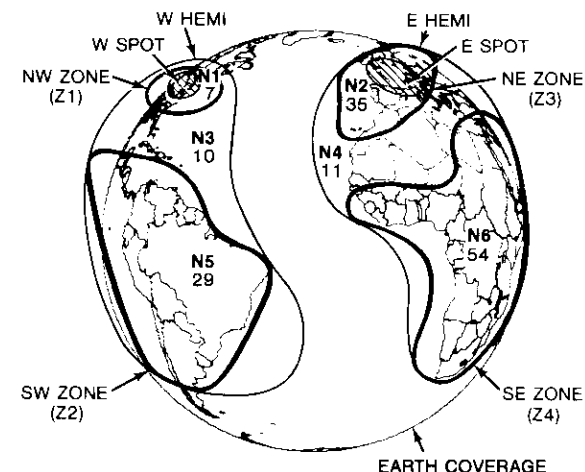
Figure 4. *INTELSAT VI AOR Beam Coverages*

Referring to the schematic diagram of the INTELSAT VI hemi and zone beams shown in Figure 6, the number of links for accomplishing east/west, west/east, north/south, and south/north connectivities increases from 6 for the five beam cells of INTELSAT V to 16 for the six beam cells of INTELSAT VI. The increase is due to the 10 additional links (*viz.*, G, H, I, J, K, L, Q, R, S, and T) needed to connect the two additional southern hemisphere zone beams (beams 5 and 6 in Figure 6.) In effect, the number of interconnecting links increases from one to three for the northern zone beams, and the two additional southern zone beams bring in six additional interconnecting links.

Thus in INTELSAT VI, the higher number of carriers required for continuous FDMA operation would necessitate an increase in the number of up- and down-link conversion chains needed to implement the total system. However, the TDMA case requires no increase in the number of carriers or the number of up- and down-conversion links.
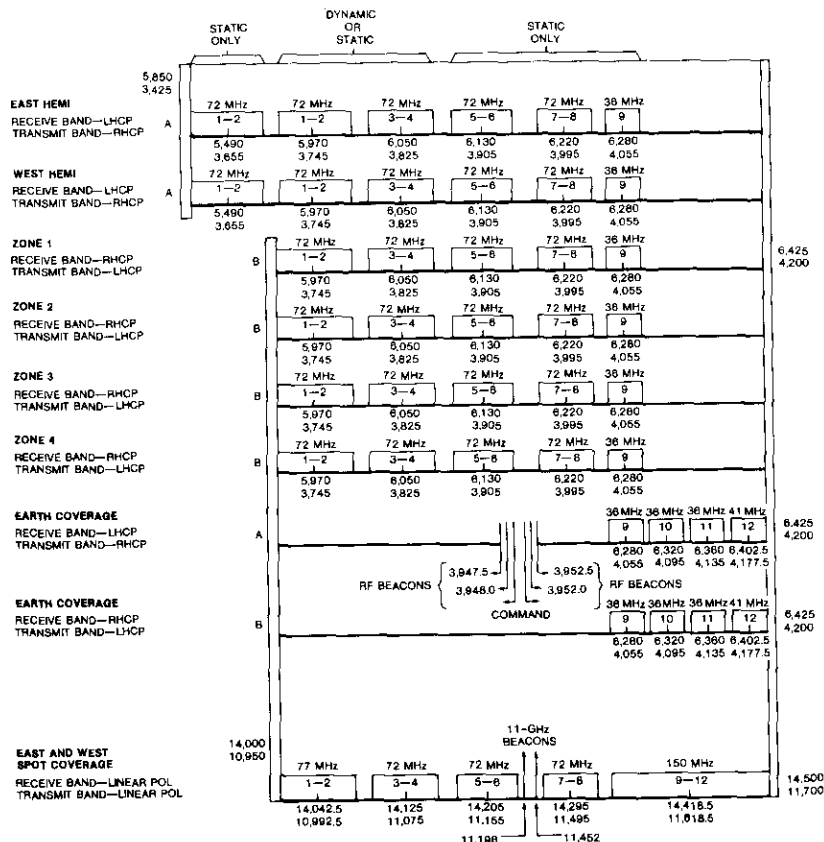
Figure 5. *INTELSAT VI Transponder Frequency Plan*

INTELSAT VI static switching

INTELSAT VI can operate with all transponders statically interconnected, or with a combination of static and dynamic interconnections. With static on-board connections, each beam-to-beam interconnecting path of a multiple-beam satellite requires a dedicated transponder. The beam-to-beam assignments
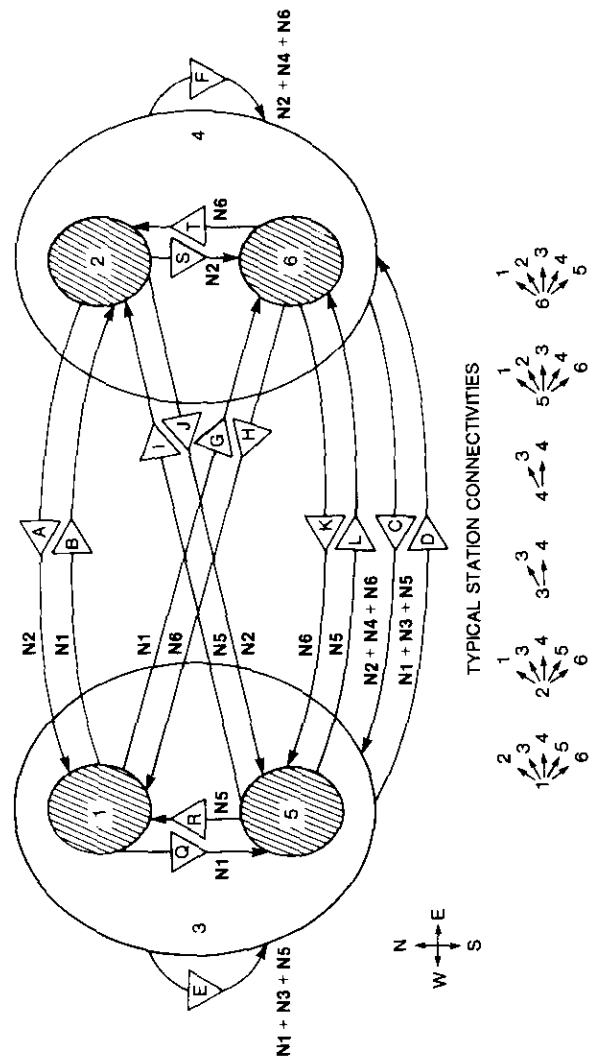
of such transponders can be modified by a static switch to accommodate changes in traffic flow during the lifetime of the satellite. As the number of beams increases, the minimum number of interconnecting links increases as the square of the number of beams. Because each beam has a finite spectrum assigned to it which must be shared among the beams to which it connects, the bandwidth for each connection decreases in inverse proportion to the number of beams.

At C-band, INTELSAT VI has six beams as compared to four for INTELSAT V (excluding the global beam). The consequent increase in the minimum number of static interconnecting links is evident by comparing Figures 3 and 6. A minimum of 6 links are required for INTELSAT V and 16 for INTELSAT VI. This illustrates the rapid increase in such paths as the number of beams increases, even with overlapping beams. (With non-overlapping beams, the minimum number of interconnecting links for a four-beam system would be 16 and for a six-beam system, 36.)

Static switching of transponders among the beam interconnections on INTELSAT V and VI provides the capability to redirect capacity to match traffic and network growth. At C-band, INTELSAT V has 20 switchable transponders available, while INTELSAT VI has 32. However, the higher number of interconnectivities required on INTELSAT VI results in less flexibility to match the traffic flow pattern by static switching because fewer transponders are available per interconnecting link (approximately three per interconnecting link for INTELSAT V, compared to approximately two for INTELSAT VI). The use of more than one satellite in a system relieves link congestion when static switching is used.

The introduction of dynamic satellite switching on INTELSAT VI will greatly improve interconnection flexibility by permitting unconstrained assignment of the capacity of two banks, each of six transponders, among the six beams. TDMA traffic bursts can be adjusted in single 64-kbit/s voice channel increments. In combination with satellite switching, this permits beam-to-beam traffic to be routed in single-voice-channel increments. Other advantages of dynamic satellite switching will be discussed in detail in a later section.

INTELSAT VI FDMA operation

Up-link conversion chains

In order to estimate the number of FDMA carriers needed to achieve the INTELSAT VI spacecraft connectivity shown in Figure 6, a procedure similar to that used for INTELSAT V was developed. Consider the beam cell connectivity of Figure 6 and a community of N FDMA stations distributed as follows. Let the number of stations in beam cells 1, 2, 5, 6, and 3 but not in 1 or 5, and

the number in beam cell 4 but not in 2 or 6, be N_1, N_2, N_5, N_6, N_3, and N_4, respectively. In terms of this definition, the number of stations in beam cell 3 is $N_1 + N_3 + N_5$, and in beam cell 4 is $N_2 + N_4 + N_6$. Let $N = N_1 + N_2 + N_3 + N_4 + N_5 + N_6$. For the connectivity among all stations shown in Figure 6, those in beam cells 1, 2, 5, and 6 each transmit five carriers, and those in beam cell 3 but not in 1 or 5, and in beam cell 4 but not in 2 or 6, each transmit two carriers. Thus, the total number of FDMA carriers in the INTELSAT VI system is

$$5(N_1 + N_2 + N_5 + N_6) + 2(N_3 + N_4) . \qquad (3)$$

Expression (3) also gives the number of up-link conversion chains needed to achieve the interconnectivity shown in the INTELSAT VI beam cell configuration of Figure 6.

For the present AOR earth station distribution, $N_1 = 7$, $N_2 = 35$, $N_3 = 10$, $N_4 = 11$, $N_5 = 29$, and $N_6 = 54$. Compared to the INTELSAT V case previously described, INTELSAT VI has significantly reduced the coverages for northern zone beams in order to provide increased capacity to the high-intensity traffic generated in North America and Europe. By substitution into expression (3), the number of carriers and hence the number of up-conversion chains needed to implement full FDMA connectivity is 667, while for earth coverage beam operation the number would be 146. Thus, with INTELSAT VI, the number of up-conversion chains is increased by the ratio 4.57 (667/146) in comparison with an earth coverage beam system, and by the ratio 1.76 (667/380) in comparison with the INTELSAT V multibeam system.

The following assignments for the variables of expression (3) represent the current geographic distribution of earth stations in the INTELSAT VI beam cells: $N_1 = 0.05N$, $N_2 = 0.24N$, $N_3 = 0.07N$, $N_4 = 0.07N$, $N_5 = 0.20N$, and $N_6 = 0.37N$. Substituting these into expression (3), the number of carriers and hence the number of up-conversion chains for FDMA in INTELSAT V becomes $4.58N$, which is also the number of traffic bursts needed if the system is totally implemented with TDMA. For a uniform geographic distribution of earth stations ($N_1 = N_2 = N_3 = N_4 = N_5 = N_6 = N/6$), the number of up-conversion chains is $4N$. Once again, the results are relatively independent of earth station distribution.

Down-link conversion chains

Consider next the number of receive-side down-conversion chains needed to implement interconnectivity of INTELSAT VI for the beam cell connectivities

shown in Figure 6, using continuous FDMA. The matrix shown in Table 2 gives the number of carriers from originator beam cell to destination beam cell, the number of stations that receive the carriers, and the resulting number of receive-side down-link conversion chains for each beam cell. The total number of INTELSAT VI FDMA down-chains is

$$N(N - 1) + 2N_1(N_2 + N_5 + N_6) + 2N_2(N_5 + N_6) + 2N_5N_6 \quad . \quad (4)$$

Substituting into expression (4) the same values for the variables for the present earth station distribution as were used for calculating the number of down-conversion chains for INTELSAT VI, the number of down-conversion chains is 31,764. From a previous calculation for INTELSAT V using the same present earth station distribution, the number was 24,880. Thus, introduction of the six-beam INTELSAT VI has increased the number of down-conversion chains needed for FDMA transmission by 28 percent. The number of down-conversion chains needed for all TDMA transmission is only 146.

Extrapolating the future growth distribution of stations in the INTELSAT VI beams based on the present distribution (as previously discussed) of expression (4), the expression for the number of FDMA down-conversion chains reduces to $N(1.5N - 1)$. This expression will be used later to compare the cost of all FDMA and all TDMA implementations of service in INTELSAT VI. If the geographic distribution is assumed to be uniform, the above expression becomes $N(1.33N - 1)$, illustrating that the result is relatively insensitive to large variations in geographic distribution.

INTELSAT VI dynamic switching

In Figure 5, the 72-MHz transponders of the second and third columns (transponder banks) of the frequency plan can be configured by using either static switches or two separate 6 × 6 dynamic matrix switches. The remaining columns are configured by static switches only. Figure 7 is a schematic diagram of the dynamic matrix switch configuration used for each transponder bank. Each of the six transponders supports the 120.832-Mbit/s transmission rate of the INTELSAT BG-42-65 TDMA system [6].

Each dynamic microwave switch matrix is capable of providing full, flexible connectivity among the satellite's six beams. For redundancy, each switch is implemented using 10 rows and 6 columns. The 10 rows are connected to the 6 up-beams through a 6 × 10 redundancy switch to permit routing around switch element failures [7]. The six columns of each matrix switch are connected to six transponders and their six down-beams. Each switch matrix thus serves a total capacity of 432 MHz.

TABLE 2. NUMBER OF DOWN-LINK CONVERSION CHAINS FOR INTELSAT VI FDMA

	To Beam Cell									
From Beam Cell		1	2	3	4	5	6			
	1	0	N_1	0	0	N_1	N_1			
	2	N_2	0	0	0	N_2	N_2			
	3	0	0	$N_3 + N_4 + N_5$	$N_3 + N_5 + N_6$	0	0			
	4	0	0	$N_3 + N_4 + N_6$	$N_2 + N_4 + N_6$	0	0			
	5	N_5	N_5	0	0	0	N_5			
	6	N_6	N_6	0	0	N_6	0			
Column Sums		$N_2 + N_5 + N_6$	$N_1 + N_5 + N_6$	$N_1 + N_3 + N_5 - 1^*$	$N_2 + N_3 + N_4 + N_6 - 1^*$	$N_1 + N_2 + N_6$	$N_1 + N_2 + N_5$			
Number of Destination Stations		N_1	N_2	N_3	N_4	N_5	N_6			
Totals to Beam Cell	1	$N_1(N_2 + N_5 + N_6)$								
	2	$N_2(N_1 + N_5 + N_6)$								
	3	$(N - 1)(N_1 + N_3 + N_5)$								
	4	$(N - 1)(N_2 + N_3 + N_4 + N_6)$								
	5	$N_5(N_1 + N_2 + N_6)$								
	6	$N_6(N_1 + N_2 + N_5)$								

* 1 subtracted for loopback connections only.

Figure 7. *INTELSAT VI SS/TDMA Connectivities*

In the INTELSAT 120-Mbit/s TDMA system, each transponder conservatively provides a capacity of 3,000 64-kbit/s pulse-code modulated, digital speech interpolated voice channels. Consequently, each switch matrix will provide a capacity of 18,000 voice channels. This arrangement imposes no constraints on traffic routing interconnectivities among the six beam cells of INTELSAT VI, other than those inherent in the need to fill the beams themselves.

Connectivities among the up- and down-beams are programmed as a sequence of switch states occurring in a frame period equal to that of the TDMA system (2 ms). Each switch state is an array of row-to-column connections of the switch matrix selected to provide a specific set of connectivities among all six beams. This array persists for an epoch of sufficient duration to carry the traffic bursts assigned to those connectivities [7]. Figure 8 illustrates a typical sequence of switch states. For an M-beam system, $M!$ unique switch states are possible, and a sequence of $M^2 - 2M + 2$ switch states is theoretically sufficient to route any arbitrary traffic pattern with better than 95-percent fill efficiency [8], [9]. For INTELSAT VI, this relation yields 28 switch states. Actually, INTELSAT VI has been provided with 64 programmable switch states.
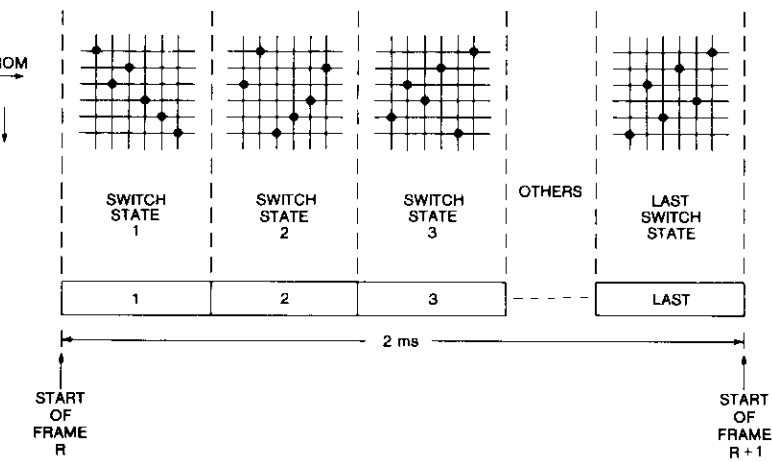
Figure 8. *Typical Switch-State Time Plan For 6 × 6 Beams*

INTELSAT VI TDMA and SS/TDMA operation

Up- and down-link conversion chains

The number of up- and down-link conversion chains needed to implement the INTELSAT VI system with TDMA or satellite-switched TDMA (SS/TDMA) is *N*, since only one such chain is required at each earth station regardless of the number of beams. However, in some installations additional up- and down-conversion chains may be required for transponder hopping among statically connected beams. A second TDMA terminal with additional up- and down-conversion chains may be required at some stations if more than eight traffic bursts need to be transmitted. In INTELSAT VI, the number of TDMA traffic bursts is the same as the number of carriers needed for continuous FDMA operation, as given by expression (3).

Comparison of up- and down-link chain requirements for INTELSAT VI

Compared to FDMA, the use of TDMA reduces the number of up-link conversion chains from the value determined by expression (3) to *N*, and the number of down-link conversion chains from the value determined by expression (4) to *N*. Based on the earth station numbers previously given, the number of up-link conversion chains is reduced by the ratio 4.57 (667/146), and the number of down-link chains by the ratio 217 (31,764/146) if TDMA is introduced throughout the system. When *N* stations are uniformly distributed, the reduction factor is 4 for the number of up-link conversion chains and approximately $1.33N$ for the number of down-conversion chains. These are significant reductions in the number of up- and down-link conversion chains and constitute an even greater advantage for TDMA in INTELSAT VI as compared with the INTELSAT V case.

Cost analysis of FDMA and TDMA implementations

The differences in implementing the INTELSAT V and VI systems with either all FDMA or all TDMA stations have been evaluated in terms of estimates of the number of up- and down-link chains needed in the earth segment for each case. Table 3 summarizes the results for FDMA and TDMA implementations of a single earth coverage beam system and of the multibeam configurations of INTELSAT V and VI. The estimates of the number of up- and down-link conversion chains are based on the assumption that, for the single earth coverage beam, all *N* stations use the beam, and for the multibeam INTELSAT V or VI, *N* stations using the system are distributed among the

beams according to the present geographic distribution in the INTELSAT AOR system. As previously shown, the results are relatively insensitive to variations in station distribution.

TABLE 3. SUMMARY OF REQUIRED NUMBER OF UP- AND DOWN-CONVERSION CHAINS

SYSTEM	EARTH COVERAGE BEAM	INTELSAT V MULTIBEAM	INTELSAT VI MULTIBEAM
Up-Chains			
FDMA	N	$2.6N$	$4.58N$
TDMA	N	N	N
Down-Chains			
FDMA	$N(N-1)$	$N(1.125N-1)$	$N(1.5N-1)$
TDMA	N	N	N

For TDMA, in addition to the cost of up- and down-conversion chains, the cost of reference stations must be added. For a single-beam earth coverage system, two reference stations are typically needed per satellite to provide redundancy. For the statically routed multiple beams of INTELSAT V and VI, because of the combination of restricted visibility in the beams and redundancy, four reference stations are needed per satellite, two in each zone beam. The stations in the east beam require primary and secondary reference bursts from two reference stations located in the west, and those in the west require a similar pair of reference bursts from two reference stations located in the east. However, if the dynamic satellite switch of INTELSAT VI is used, the visibility limitation is eliminated and only two reference stations are required for the entire system.

Expressions for the cost of FDMA and TDMA implementations are obtained by introducing cost variables for the individual up- and down-conversion chains. Let the up- and down-conversion chain costs for FDMA be designated as *CFU* and *CFD*, for TDMA as *CTU* and *CTD*, and for the TDMA reference stations *CTR1* for the single earth coverage beam, and *CTR2* and *CTR3* for the multibeam INTELSAT V and VI systems, respectively. Using the numbers of up- and down-conversion chains given in Table 3, the following cost expressions are obtained for systems with *N* stations:

- *Single Earth Coverage Beam*

$$\text{Cost of TDMA} = N\,(CTU + CTD) + CTR1 \tag{5a}$$

$$\text{Cost of FDMA} = N(CFU) + N(N-1)CFD \tag{5b}$$

- *INTELSAT V Multibeam*

Cost of TDMA $= N(CTU + CTD) + CTR2$ (6a)

Cost of FDMA $= (2.6N)CFU + N(1.125N - 1)CFD$ (6b)

- *INTELSAT VI Multibeam*

Cost of TDMA $= N(CTU + CTD) + CTR3$ (7a)

Cost of FDMA $= (4.58N)CFU + N(1.5N - 1)CFD$ (7b)

In general, because the cost of individual TDMA up- and down-conversion chains is much higher than for FDMA, and since TDMA requires that reference stations be shared by all users, the total cost of a TDMA network will exceed that of an FDMA network when the number of terminals, N, is small. However, the number of down-conversion chains needed for FDMA increases as N^2, while for TDMA the increase is as N. Hence, as N increases, the cost difference between an FDMA and TDMA network diminishes and eventually a crossover point is reached. The number of stations at which this crossover occurs is

$$NCOX = (Q/2)\left(1 + \sqrt{1 + P/Q^2}\right)$$ (8)

where $Q = B^{-1}[(CTU + CTD)/CFD) + C - A(CFU/CFD)]$

$P = 4B^{-1}(CTRX)/CFD$

and the parameters A, B, and C are given by the following expressions for each case:

- *Earth Coverage, $(X = 1)$*
  $A = 1, B = 1, C = 1$

- *INTELSAT V, $(X = 2)$*
  $A = 2.6, B = 1.125, C = 1$

- *INTELSAT VI, $(X = 3)$*
  $A = 4.58, B = 1.5, C = 1$.

To assign cost elements to the above relations, the assumptions presented in Tables 4 and 5 are made regarding the costs of the TDMA and FDMA up- and down-conversion chains. Common costs such as the antenna and its feeds, LNAs, intermediate amplifiers, and buildings are excluded, since they influence both cases equally. TDMA is burdened with an additional HPA cost

to account for the larger HPA needed to support its higher peak-power requirement. It is also burdened with costs for wide-band equalizers on both up- and down-links because of its wide-band signal, as well as costs for an operations and maintenance center (OMC), ground control equipment (GCE) for frequency conversion, and transponder hopping and special test equipment (such as a burst mode link analyzer, burst BER test set, burst power meter, and path delay measurement equipment). The cost of installation and test is also included. The TDMA costs are combined for the up- and down-link chains.

TABLE 4. TDMA COSTS: UP- AND DOWN-LINKS COMBINED*

ITEM	AMOUNT ($K)
Common TDMA Terminal Equipment and Modems	170
HPA Enhancement	200
OMC	215
Equalizers	70
GCE	100
Special Test Equipment	200
Installation and Test	200
Total TDMA (CTU + CTD)	1,155

* Excludes earth station equipment costs which are common to both TDMA and FDMA operation.

TABLE 5. FDMA COSTS: UP- AND DOWN-LINKS SEPARATED*

ITEM	AMOUNT ($K)
Up-Link Chain	
Modulator/Coder	15
GCE and OMC	20
Installation and Test	15
Total Up-Link (CFU)	50
Down-Link Chain	
Demodulator/Decoder	15
GCE and OMC	30
Installation and Test	15
Total Down-Link (CFD)	60

* Excludes earth station equipment costs which are common to both TDMA and FDMA operation.

The tables also include the cost of TDMA reference stations, which is assumed to be $2 million each. For the earth coverage system, two reference stations are used; for the INTELSAT V and VI multibeam systems with static switching, four reference stations are used; and for the INTELSAT VI multibeam system with dynamic switching, two reference stations are used (modified for dynamic satellite switch acquisition and synchronization at an additional cost of $500K each). The FDMA costs are substantially lower for the modulator, FEC coder, demodulator, FEC decoder, GCE, OMC, and installation and test. All costs given are for redundant equipment. No adjustment is included for terrestrial interfaces, since in the future both TDMA and FDMA will carry digital traffic and use similar digital interfaces.

Using the costs given in Tables 4 and 5, the values of the cost parameters are

$$CTU + CTD = 1,155K$$

$$CFU = 50K$$

$$CFD = 60K .$$

The variable $CTRX$, representing the cost of the reference stations, must also be assigned. For each statically switched satellite used in the system, the value assigned to $CTRX$ is $8 million, since each satellite requires a compliment of four reference stations. For each dynamically switched satellite used in the system, the value assigned to $CTRX$ is $5 million, since each satellite requires two reference stations, each equipped with a special satellite switch acquisition and synchronization unit costing $500K.

Substituting the appropriate values into the equations for $CNOX$, the number of stations at the crossover point depends on the type of satellite and the number of satellites in the system.

The results, presented in Table 6, show that TDMA implementation costs become lower than those of FDMA for a moderate number of stations. For a three-satellite INTELSAT V system, the earth segment cost of TDMA is less than that of FDMA when the number of earth stations is greater than 29, with a loading of approximately 10 stations per satellite. For a three-satellite INTELSAT VI system with dynamic switching, the number of stations at crossover is 20 and the loading per satellite is approximately 7. The present INTELSAT AOR system already has 146 stations, and only a fraction of these need to be equipped for TDMA operation to achieve earth segment costs lower than those for FDMA.

Figure 9 further illustrates the cost of TDMA and FDMA versus the number of earth stations and crossovers for the cases of INTELSAT V and VI, both

with static switching, and for the case of INTELSAT VI using a single satellite with dynamic switching. Note the cost crossover points that correspond to values given in Table 6. Also, the earth segment costs of FDMA implementation are greater for INTELSAT VI than for INTELSAT V because of the greater connectivity of INTELSAT VI. The reverse is true for TDMA when dynamic switching is used in INTELSAT VI because the number of reference stations is reduced from four to two.

TABLE 6. NUMBER OF STATIONS AT CROSSOVER

SATELLITE TYPE	X	NUMBER OF SATELLITES		
		1	2	3
Earth Coverage	1	23	25	27
INTELSAT V	2	23	26	29
INTELSAT VI, Static	3	17	21	23
INTELSAT VI, Dynamic	3	15	18	20
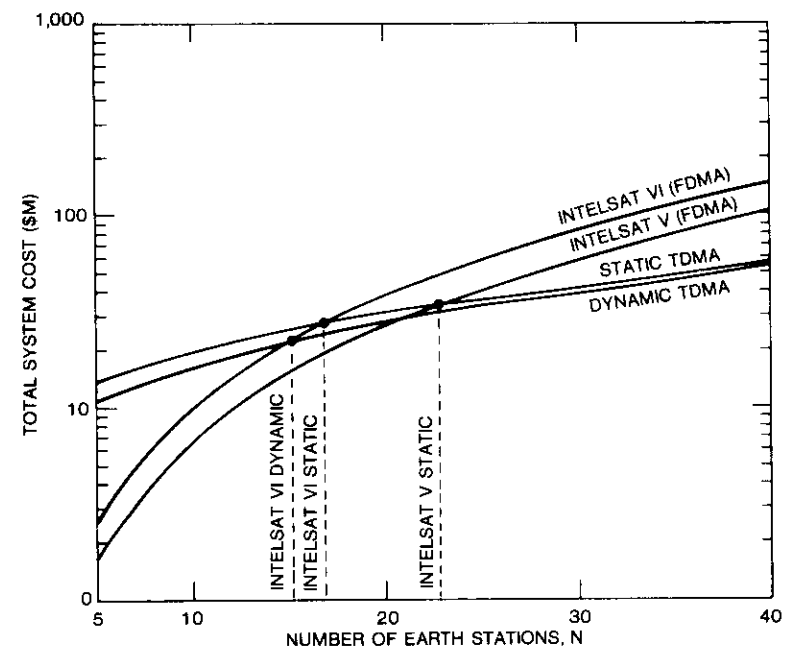
Figure 9. *Earth Station Costs vs Number of Stations for One Satellite*

It is important to observe the influence of point-to-point trunking on the above estimates. Today, a relatively small number of stations (fewer than 10) carry high-volume point-to-point traffic between North America and Europe; and in the future high-capacity, single-carrier-per-transponder digital links might be used. Even so, the stations which remain involved in multidestinational satellite service would be served most economically by a TDMA network. It is likely that the stations which use the high-capacity point-to-point trunks would also wish to be part of the multidestinational network and would participate in both.

Other SS/TDMA advantages

Interconnectivity advantage

The principal value of dynamic on-board switching lies in its ability to achieve full connectivity among multiple beams with significantly fewer on-board interconnecting links, and hence fewer transponders, than are needed by static switching. Each $M \times M$ dynamic switch matrix can provide full interconnectivity among M beams with M transponder links, whereas with a static switch matrix, a transponder must be dedicated to each of M^2 links. Thus, compared to a static switch, a dynamic switch matrix reduces the number of transponders needed by $M(M - 1)$.

This advantage can be illustrated by considering INTELSAT VI. Its six hemi/zone multiple beams can be fully interconnected by each of its 6×6 dynamic switch matrices using only six transponders. With a static switch, the same connectivity requires 36 transponders. Thus, in achieving full connectivity, dynamic switching saves 30 transponders. Only 32 transponders are actually provided on INTELSAT VI for the hemi/zone multiple beams; however, the combination of beam overlap and the fact that traffic is concentrated on certain routes makes it possible to achieve efficient traffic fill using as few as 16 interconnections, as shown in Figure 6.

Conceivably, a single $M \times M$ dynamic switch matrix with M transponders of very wide bandwidth and sufficient power could serve an entire system; however, this would require an extremely high bit rate (1 Gbit/s for the 500 MHz available at C-band), which appears impractical with today's technology.

An additional advantage of dynamic switch connectivity is that it eliminates the need for a station to perform transponder hopping in order to gain access to the various down-beams of a multibeam system. This has a direct and favorable influence on the cost of the earth segment.

Traffic routing advantage

With the dynamic switch matrix, the capacity on individual interconnecting links is adjustable in small increments by modifying the duration of the dwell times of the interconnecting switch states. By comparison, the capacity provided by static interconnections is adjustable principally in 80-MHz increments. This inflexibility of static interconnection results in a loss of traffic fill efficiency which is referred to as the granularity effect. Dynamic satellite switching avoids this limitation and is able to fine-tune the interconnecting link capacities.

To demonstrate the consequences of granularity, consider a four-beam system connected as shown in Figure 10. The traffic must satisfy the following relations:

$$0 \ + \ T_{12} \ + \ T_{13} \ + \ T_{14} \ = \ T \ , \text{ beam cell 1}$$

$$T_{12} \ + \ 0 \ + \ T_{23} \ + \ T_{24} \ = \ T \ , \text{ beam cell 2}$$

$$T_{13} \ + \ T_{23} \ + \ 0 \ + \ T_{34} \ = \ T \ , \text{ beam cell 3}$$

$$T_{14} \ + \ T_{24} \ + \ T_{34} \ + \ 0 \ = \ T \ , \text{ beam cell 4} \qquad (9)$$

where T_{ij} refers to the traffic between beam cells i and j, respectively ($T_{ij} = T_{ji}$ for symmetric traffic), and T is the total traffic capacity of a beam. Each equation represents the total traffic originating or terminating in the cell, which must equal T for 100-percent fill efficiency. The relationships must be satisfied for either the static or dynamic switches.

With the dynamic switch, the individual elements, T_{ij}, can be adjusted in increments of a single voice channel to match traffic requirements, while
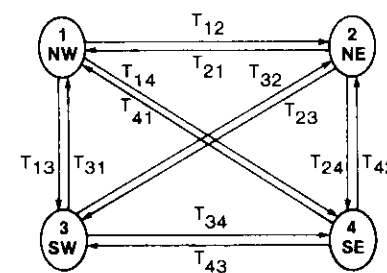
Figure 10. *Traffic Coefficients For a Four-Beam Network*

with the static switch, the adjustment is in increments of the full capacity of an interconnecting link transponder. Furthermore, when the traffic equations are solved for an increment of ΔT in any one of the coefficients, a net cumulative change of $4\Delta T$ occurs in all the coefficients. This is illustrated by determining the consequence of changing the capacity of element T_{12} to $T_{12} + \Delta T$ and rebalancing each node equation to equal T. Thus,

$$0 \quad + (T_{12} + \Delta T) \quad + (T_{13} - a\Delta T) \quad + (T_{14} - b\Delta T) = T$$
$$(T_{12} + \Delta T) \quad + \quad 0 \quad + (T_{23} - c\Delta T) \quad + (T_{24} - d\Delta T) = T$$
$$(T_{13} - a\Delta T) + (T_{23} - c\Delta T) + \quad 0 \quad + (T_{34} + e\Delta T) = T$$
$$(T_{14} - b\Delta T) + (T_{24} - d\Delta T) + (T_{34} + e\Delta T) + \quad 0 \quad = T \quad (10)$$

where the following relations among the parameters a, b, c, d, and e must exist for the equations to remain satisfied:

$$a + b = 1$$
$$c + d = 1$$
$$a + c = e$$
$$b + d = e \quad .$$

Solving these parameter relations yields

$$e = 1$$
$$a + b + c + d = 2 \quad . \quad (11)$$

If the traffic element T_{12} is incremented by an amount ΔT, then an increment of ΔT is induced in T_{34} and a sum of $2\Delta T$ is induced in the remaining coefficients, yielding a total of $4\Delta T$ for all of the changes. In general, by summing the traffic at all nodes of an M-beam network, it can be shown that the total adjustment in traffic on the links between nodes due to an adjustment of ΔT on any link is $M\Delta T$. Thus, if a traffic planner makes a traffic adjustment of ΔT on any link, accompanying adjustments must be made on other links which total M times the amount of the first adjustment. In the worst case, if the planner cannot make the adjustments, a peak mismatch of $M\Delta T$ between capacity and traffic can occur. If ΔT is made small, the problem is greatly reduced.

Consequently, if the traffic on one of the links of a statically switched six-beam system is to be adjusted by its smallest increment, which is a full

transponder, then associated adjustments equal to the capacity of five additional transponders must accompany this adjustment. Traffic planners are faced with a relatively difficult problem in matching capacity to traffic and may have to compromise by inefficient loading on some links.

For the hemi/zone beam system of INTELSAT VI, the peak mismatch between capacity and traffic could be six 72-MHz transponders of capacity out of a total capacity of 2,088 MHz, or 21 percent. However, if dynamic satellite switching is used, the smallest increment of adjustment is reduced to the capacity of one voice channel, and this is adjusted simply by changing the duration of a switch state on board the satellite. For a six-beam system, the peak mismatch is six voice channels. With this capability, the traffic planner's task is much simpler and the resulting loading on the links is more efficient.

Summary and conclusions

As the number of stations sharing a network increases and the number of beam-to-beam interconnectivities increases, the economic advantage of time-sharing TDMA up- and down-link conversion chains quickly becomes apparent. Comparative analyses of the increase in up- and down-link chains for FDMA and TDMA network implementation were carried out for single-beam, INTELSAT V multibeam, and INTELSAT VI multibeam networks. The results of the analyses were combined with cost estimates of FDMA and TDMA up- and down-chains to determine the number of stations at which the cost of an FDMA network exceeds that of a TDMA network. The influence of space segments comprising one, two, and three satellites was also examined because the number of satellites influences TDMA costs by adding reference stations.

In general, the number of stations at which cost crossover occurs decreases significantly as the number of multiple beams increases. INTELSAT VI, with dynamic satellite switching, requires the least number of stations for the crossover to occur: 15 for one, 18 for two, and 20 for three satellites, respectively. INTELSAT VI with static switching is next with 17 for one, 21 for two, and 23 for three satellites, respectively. INTELSAT V requires 23 for one, 26 for two, and 29 for three satellites, respectively, which differs little from the requirements for the earth coverage beam case.

Even though the analyses were carried out for pure TDMA or FDMA networks, they are also applicable to networks which are partly TDMA and partly FDMA. The part of the network using TDMA will experience the TDMA-type costs, while the part using FDMA will experience the FDMA-type costs.

The benefits of SS/TDMA were also analyzed. Use of the on-board satellite switch has the principal advantage of providing full beam-to-beam interconnectivity in a multibeam system with a relatively small number of transponders.

The satellite switch, operating jointly with TDMA, permits the traffic capacity among beams to be adjusted in single-voice-channel increments. This avoids the waste of the equivalent of several transponders of capacity which can occur when static switching is used. The theoretical worst-case loss can be as much as 21 percent of the total available capacity. With the dynamic satellite switch, the capacity of a route can be adjusted in increments of one 64-kbit/s voice channel, which essentially eliminates such waste.

Additional benefits of the dynamic satellite switch were presented. Dynamic switching makes it possible to operate the system with as few as two reference stations in each ocean region, rather than the four presently required. It also eliminates the need for transponder hopping by traffic stations, with attending overall cost reductions.

References

[1] J. C. Fuenzalida, P. Rivalan, and H. J. Weiss, "Summary of the INTELSAT V Communications Performance Specifications," *COMSAT Technical Review*, Vol. 7, No. 1, Spring 1977, pp. 311–326.

[2] N. M. F. Wong, "INTELSAT VI—A 50-Channel Communications Satellite With SS-TDMA," International Satellite Communications Conference, Ottawa, Canada, June 14–17, 1983, *Proc.*, pp. 20.1.1–20.1.9.

[3] S. J. Campanella and R. J. Colby, "Network Control for TDMA and SS-TDMA in Multiple-Beam Satellite Systems," Fifth International Conference on Digital Satellite Communications, Genoa, Italy, March 1981, *Proc.*, pp. 335–343.

[4] B. A. Pontano *et al.*, "A Description of the INTELSAT TDMA/DSI System," Fifth International Conference on Digital Satellite Communications, Genoa, Italy, March 1981, *Proc.*, pp. 327–334.

[5] *INTELSAT Facts and Figures.* INTELSAT Headquarters, Washington, D.C., 1985.

[6] INTELSAT, "TDMA/DSI System Specification: TDMA/DSI Traffic Terminals," Specification BG-42-65 (Rev. 2), June 23, 1983.

[7] S. J. Campanella and T. Inukai, "Satellite Switch State Time Plan Control," Sixth International Conference on Digital Satellite Communications, Phoenix, Arizona, September 19–23, 1983, *Proc.*, pp. X-16–X-26.

[8] Y. Ito *et al.*, "Analysis of a Switch Matrix for an SS-TDMA System," *Proc. IEEE*, Vol. 65, No. 3, March 1977, pp. 411–419.

[9] T. Inukai, "An Efficient SS/TDMA Time Slot Assignment Algorithm," *IEE Transactions*, Vol. COM-27, No. 10, October 1979, p. 1449.

S. J. Campanella received a B.S.E.E. from the Catholic University of America in 1950, an M.S.E.E. from the University of Maryland in 1956, and a Ph.D. in Electrical Engineering from the Catholic University of America in 1965. He is currently Chief Scientist and Vice President of COMSAT Laboratories. Previously, he served as Executive Director of the Communications Technology Division. He has contributed significantly to technologies for TDMA network control, satellite-switched TDMA, and TDMA terminal development and has been responsible for the research and development of numerous other satellite communications innovations such as echo cancellers, digital speech interpolation, demand-assigned TDMA, and synchronous burst time plan control. Most recently, his efforts have been devoted to advanced satellite communications concepts involving on-board baseband processing, multiple hopping beams, and intersatellite links. Dr. Campanella is a Fellow of the IEEE and AAAS. He teaches at George Washington University and holds numerous patents in digital processing techniques.

Benjamin A. Pontano received a B.S.E.E. degree from Carnegie-Mellon University in 1965, and M.S.E.E. and Ph.D. degrees from the Pennsylvania State University in 1967 and 1970, respectively. He originally joined COMSAT Laboratories in 1969, and was appointed Manager of the Laboratory Simulation Branch. He rejoined COMSAT Laboratories in 1984, and is currently a Principal Scientist engaged in the study of future satellite systems for domestic and international applications. During the interim, Dr. Pontano was with INTELSAT for over 10 years, where he was actively involved in development of the INTELSAT TDMA system and design of the INTELSAT VI spacecraft system.

Jack L. Dicks received a B.S. degree in Mathematics and Engineering Physics from Sir George Williams College in Montreal, Canada. He joined the Engineering Division of INTELSAT in 1978 as Manager of the Communications Engineering Department. In this position, he has been responsible for all aspects of the communications systems design and development for both the INTELSAT V and VI satellites and associated earth stations throughout the system. This involved the introduction of many new transmission techniques, both analog and digital, the most notable being development of the 120-Mbit/s TDMA system, which is now being succeeded by SS/TDMA. He has represented INTELSAT on numerous occasions at such ITU forums as the CCIR, and most recently participated in WARC-ORB 85.

Before joining INTELSAT, Mr. Dicks was with COMSAT for 10 years where he was primarily responsible for transmission planning for the INTELSAT III, IV, IV-A, and V satellites. Prior to this, he was on the engineering staff at Teleglobe Canada, responsible for the planning, installation, and testing of submarine cable systems and the introduction of the Mill Village earth station.

CTR Notes

Subjective evaluation of the INTELSAT TDMA/DSI system

M. ONUFRY AND S. J. ENGELMAN

Introduction

Subjective evaluation tests of the 64-kbit/s pulse-code modulation (PCM) digital speech interpolation (DSI) system were conducted in the fall of 1985 between COMSAT Laboratories in the U.S. and Martlesham Laboratories of British Telecom International (BTI) in the U.K. as part of the preoperational testing of the INTELSAT time-division multiple-access (TDMA) network via the Atlantic Major Path 2 satellite. The performance of the DSI system under controlled stressed loading conditions was assessed by using an active talker type of subjective evaluation. A mean opinion score (MOS) was used to measure performance. The conditions evaluated included a DSI gain of 2.0 for 60 terrestrial input channels. DSI gains of 2.3 and 2.5 for 120 terrestrial input channels, three local loop-loss conditions, and a 64-kbit/s PCM noninterpolated reference circuit. The equipment configuration, the description of the test program, and the subjective test results are presented.

A customer call-back test on the INTELSAT TDMA/DSI system was conducted by AT&T Communications in late 1985 and early 1986. An appendix to this note presents excerpts from the AT&T Bell Laboratories TDMA/DSI field trial report summarizing the customer call-back test results.

Equipment configuration

Figures 1 and 2 are block diagrams of the equipment configurations used in the U.S. and the U.K. Conversational tests were conducted between COMSAT Laboratories in the U.S. and Martlesham Laboratories in the U.K. using four-wire terrestrial leased lines between both laboratories and the earth stations. The test circuits were carried over the satellite using the TDMA/DSI equipment at each earth station.

The equipment configurations at the earth stations were quite different. On the U.S. side, the test circuit was analog into the earth station, multiplexed up to supergroup

Michael Onufry is Manager of the Voice Band Processing Department in the Communications Techniques Division at COMSAT Laboratories.

Stephen J. Engelman is Manager of International Standards with INTELSAT Satellite Services at COMSAT.
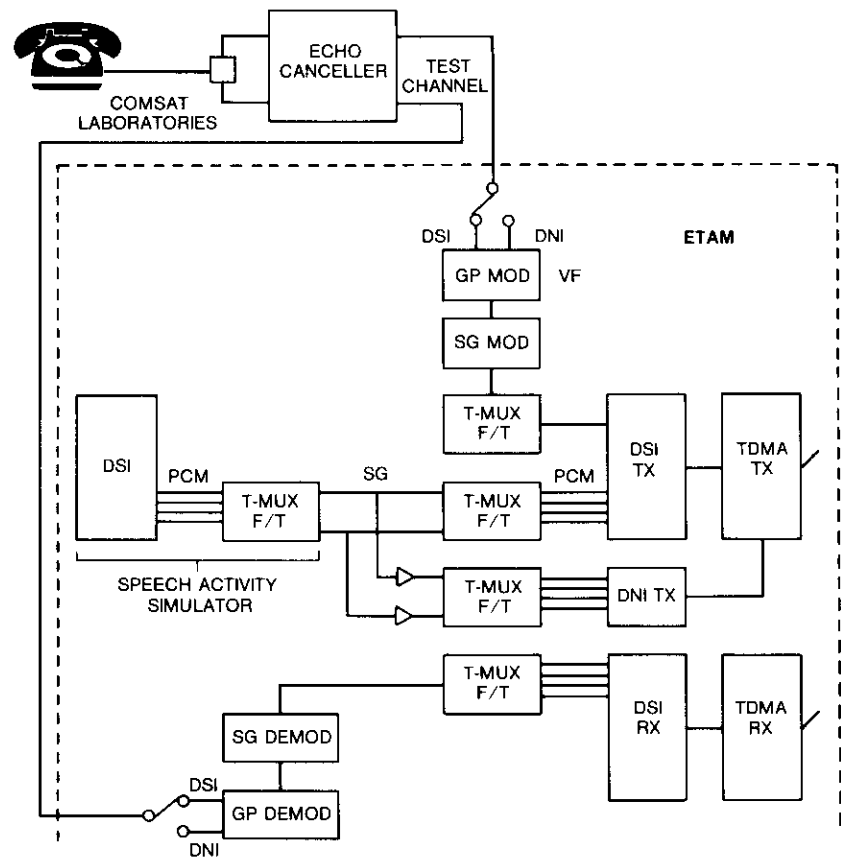
Figure 1. *U.S. Circuit Configuration*

level, and then applied to a transmultiplexer for conversion to PCM. On the U.K. side, the test circuit was digital into the earth station and carried on a 2.048-Mbit PCM primary multiplex.

The TDMA/DSI equipment at the earth stations was provided by various manufacturers. The U.S. TDMA/DSI equipment at Etam, West Virginia, was manufactured by Nippon Electric Company (NEC), while the U.K. equipment at Madley was manufactured by M/A-COM. Echo control at the U.S. circuit end was provided by a Telesystems EC 4542 echo canceller located at COMSAT Laboratories, and conformed to CCITT Recommendation G.165. Echo control at the U.K. end was provided by an echo suppressor conforming to either CCITT Recommendation G.161 or G.164.

The DSI systems used in the test were loaded with simulated traffic generated by a speech load activity simulator which is part of a DSI system developed at COMSAT

BTI TEST
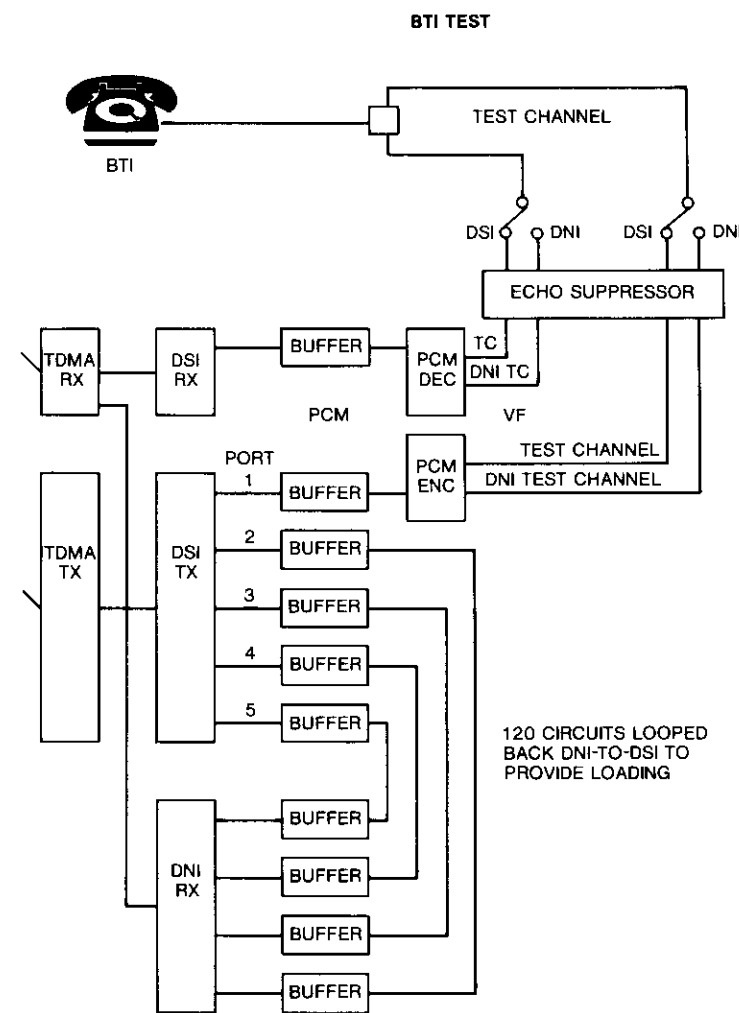
Figure 2. *U.K. Circuit Configuration*

Laboratories. The U.S.-generated loading signals were bridged and sent to the U.K. on a separate DNI sub-burst to load the U.K.-to-U.S. link. Hence the test conditions were symmetrical in that identical DSI system configurations and loading conditions were used in each direction. A switch at voice frequency band level permitted selection of DSI or digital noninterpolated (DNI) test conditions. During each day, the test variables were local loop losses.

Experiment design

A 12 × 12 Graeco-Latin Square experiment design was used. A total of 12 test subjects were employed at each test location, with each subject participating in the experiment on three different days. Subjects participated in four conversations per day, each conversation under a different circuit condition. The test circuit was switched from DSI to DNI operation during the test window (9:00–12:00 a.m. eastern daylight time), as dictated by the test sequences for each day and subject. The DSI system was operated with one DSI test condition per day, so that no complex DSI system configuration changes were made during the test window.

To stimulate conversation between subjects who had never met, each was given an identical set of four picture cards and presented with the task of establishing a mutually agreeable order of preference (i.e., first, second, third, and fourth) for displaying the picture on the cards in a public place, such as the company cafeteria. The card sets were generally of similar scene content to encourage descriptive conversation. The cards within each set at each circuit end were numbered; however, to avoid the possibility of the subjects using the number designations to reduce conversational effort, the numbers within the sets for the same scene did not match.

Table 1 presents details of the complete 12 × 12 Graeco-Latin Square experiment design. The capital letters identify the picture card set used for a specific test condition. The rows represent subjects and the columns represent test sequences. Column 0 represents a training sequence which uses a picture card set designated as M to familiarize the subject with the procedures prior to actual testing. The subjects participated on three different occasions evaluating 12 circuit conditions, as indicated in the top rows of the table. The notation used for table entries can be understood by considering the entry in the first row, third column (for subject 1, sequence 2), as shown below

$$A1/2.0$$
$$\text{short}$$

The letter A identifies picture card set A, the 1 specifies circuit condition 1, and the number 2.0 defines the DSI gain used. The word *short, medium,* or *long* indicates the length of the local loop between the test telephone and the two- to four-wire hybrid. Where no DSI gain number is given (such as D4, H8, and L12 for subject 1), a DNI circuit is used. All subjects were trained using a DNI condition with card set M.

Test conditions are identified in Table 2. Circuit condition 0 signifies a training condition used to familiarize subjects with the procedures used in the experiment. Table 3 presents the test subject schedule. Three participants each day for 12 days were needed to complete the experiment. For each DNI/DSI condition, tests were conducted for low, medium, and high local loop losses, which correspond respectively to short, medium, and long local loops.

Test results

After completing their conversational task, the subjects were requested to express their opinion of the circuit quality as excellent, good, fair, poor, or bad. Opinion

TABLE 1. EXPERIMENTAL DESIGN

SUBJECT	0	INITIAL PARTICIPATION				SECOND PARTICIPATION				FINAL PARTICIPATION			
		1	2	3	4	5	6	7	8	9	10	11	12
1	MO	D4 Short	A1/2.0 Short	B2/2.0 Medium	C3/2.0 Long	F6/2.3 Medium	E5/2.3 Short	G7/2.3 Long	H8 Medium	L12 Long	I10/2.5 Medium	J9/2.5 Short	K11/2.5 Long
2	MO	B3/2.0 Long	C2/2.0 Medium	D1/2.0 Short	A4 Short	H5/2.3 Short	G6/2.3 Medium	E8 Long	F7/2.3 Long	J11/2.5 Long	L9/2.5 Short	K10/2.5 Medium	I12 Long
3	MO	A2/2.0 Medium	D3/2.0 Long	C4 Short	B1/2.0 Short	G8 Medium	H7/2.3 Long	F5/2.3 Short	E6/2.3 Medium	I10/2.5 Medium	K12 Long	L11/2.5 Long	J9/2.5 Short
4	MO	C1/2.0 Short	B4 Short	A3/2.0 Long	D2/2.0 Medium	E7/2.3 Long	F8 Medium	I6/2.3 Medium	G5/2.3 Short	K9/2.5 Short	I11/2.5 Long	J12 Long	L10/2.5 Medium
5	MO	I8 Medium	I5/2.3 Short	I6/2.3 Medium	K7/2.3 Long	B10/2.5 Medium	A9/2.5 Short	C11/2.5 Long	D12 Long	I4 Short	F2/2.0 Medium	E1/2.0 Short	G3/2.0 Long
6	MO	I7/2.3 Long	K6/2.3 Medium	I5/2.3 Short	J8 Medium	D9/2.5 Short	C10/2.5 Medium	A12 Long	B11/2.5 Long	F3/2.0 Long	H1/2.0 Short	G2/2.0 Medium	E4 Short
7	MO	I6/2.3 Medium	L7 Long	K8 Medium	I5/2.3 Short	C12 Long	D11/2.5 Long	B9/2.5 Short	A10/2.5 Medium	E2/2.0 Medium	G4 Short	H3/2.0 Long	F1/2.0 Short
8	MO	K5/2.3 Short	I8 Medium	I7/2.3 Long	K6/2.3 Medium	A11/2.5 Long	B12 Long	D10/2.5 Medium	C9/2.5 Short	G1/2.0 Short	E3/2.0 Long	F4 Short	H2/2.0 Medium
9	MO	H12 Long	E9/2.5 Short	I9/2.5 Long	G1/2.0 Medium	J2/2.0 Medium	I1/2.0 Short	K3/2.0 Long	L4 Short	D8 Medium	B6/2.3 Medium	A5/2.3 Short	C7/2.3 Long
10	MO	F11/2.5 Long	G10/2.5 Medium	H9/2.5 Medium	I10/2.5 Medium	L1/2.0 Short	K2/2.0 Medium	I4 Short	J3/2.0 Long	B7/2.3 Long	D5/2.3 Short	C6/2.3 Medium	A8 Medium
11	MO	E10/2.5 Medium	H11/2.5 Long	G12 Long	H10/2.5 Medium	K4 Short	L3/2.0 Medium	J1/2.0 Short	I2/2.0 Medium	A6/2.3 Medium	C8 Medium	D7/2.3 Long	B5/2.3 Short
12	MO	G9/2.3 Short	F12 Long	E11/2.5 Long	I3/2.0 Long	I3/2.0 Long	J4 Short	L2/2.0 Medium	K1/2.0 Short	C5/2.3 Short	A7/2.3 Long	B8 Medium	D6/2.3 Medium

TABLE 2. CIRCUIT CONDITIONS FOR THE SUBJECTIVE EVALUATION

CIRCUIT CONDITION NUMBER	DSI RATIO	LOCAL LOOP CONFIGURATION
0	DNI	Medium
1	2.0 (60/30)	Short
2	2.0 (60/30)	Medium
3	2.0 (60/30)	Long
4	DNI	Short
5	2.3 (120/52)	Short
6	2.3 (120/52)	Medium
7	2.3 (120/52)	Long
8	DNI	Medium
9	2.5 (120/48)	Short
10	2.5 (120/48)	Medium
11	2.5 (120/48)	Long
12	DNI	Long

TABLE 3. TEST SUBJECT SCHEDULE

DAY	DSI PLAN	SUBJECTS[a]		
1	2.0	1_1	2_1	3_1
2	2.3	2_2	5_1	7_1
3	2.5	5_2	9_1	10_1
4	2.0	4_1	9_2	10_2
5	2.3	1_2	6_1	8_1
6	2.5	6_2	7_2	11_1
7	2.0	5_3	7_3	11_2
8	2.3	3_2	4_2	9_3
9	2.5	1_3	8_2	12_1
10	2.0	6_3	8_3	12_2
11	2.3	10_3	11_3	12_3
12	2.5	2_3	3_3	4_3
13[b]	2.0			
14[b]	2.3			
15[b]	2.5			

[a] Each subject participates in the experiment on three separate days. The designation 2_1 subject number 2, first day of participation; 6_3 means subject number 6, third day of participation, etc.
[b] Make-up days.

scores of 4, 3, 2, 1, or 0, respectively, were assigned to the subject responses, and an MOS was computed across all subjects for each test condition. The results are summarized in Table 4, which includes columns for the MOS, its standard deviation, and the observed percentage of difficulty for the DNI/DSI conditions tested for the U.S. and U.K. subjects.

TABLE 4. SUBJECTIVE EVALUATION SUMMARY

TEST CONDITIONS	U.S. SUBJECTS RESPONSE			U.K. SUBJECTS RESPONSE		
	MOS	STANDARD DEVIATION	DIFFICULTY (%)	MOS	STANDARD DEVIATION	DIFFICULTY (%)
DNI						
Low	2.75	1.01	25.0	2.75	0.60	41.2
Medium	3.25	0.72	—	3.17	0.60	8.3
High	2.92	0.76	8.3	2.08	0.64	50.0
Training (medium)	3.33	0.47	8.3	2.83	0.69	8.3
DSI Gain 2.0						
Low	3.08	0.76	8.3	3.17	0.55	25.0
Medium	2.83	0.37	8.3	2.92	0.49	16.7
High	2.67	0.94	41.7	2.25	0.72	33.3
DSI Gain 2.3						
Low	2.75	1.16	25.0	3.33	0.85	8.3
Medium	3.17	0.69	8.3	2.75	0.72	16.7
High	2.92	0.76	8.3	2.25	0.60	41.7
DSI Gain 2.5						
Low	2.92	0.95	16.7	3.25	0.60	—
Medium	3.17	0.37	8.3	3.00	0.58	16.7
High	2.58	0.76	33.3	1.92	0.60	41.7

An analysis of variance conducted on the MOS scores reveals a significant difference between the U.S. and U.K. subject responses. The DSI differences were not significant, but local loop-loss conditions were very highly significant. The range of local loop losses was larger at the U.K. circuit end (2–15 dB) than at the U.S. end (1.5–6 dB), and the U.K. The MOS scores in general directly track the loss with lower MOS values for higher local-loop loss. Responses of the U.S. subjects are less consistent than those of the U.K. subjects, as indicated by the larger standard deviations. The U.S. MOS was generally higher for the medium-loss circuit condition. The low-loss condition had the effect of raising the receive speech level, causing the level of echo during double-talk to become more noticeable and consequently lowering the MOS. This could have a pronounced adverse effect on the U.S. subject who is protected only by an echo suppressor in the U.K., whereas the U.K. subject would be afforded better protection by the echo canceller in the U.S.

At the conclusion of the subjective evaluation, an expert assessment of the various test conditions was carried out and several observations were made. First, for the high local loop-loss conditions, the lower received speech level was perceived as a quality degradation. This was particularly apparent at the U.K. end, where double-talk caused the echo suppressor receive-side loss to be inserted, further reducing the U.K. receive signal level.

Second, modulation of the background noise was observed in both directions of transmission. This could have been the result of DSI voice gating, echo suppressor

switch action, echo suppressor insertion of receive loss during double-talk, or echo canceller nonlinear processor action. Such effects were less noticeable for the high local loop-loss condition.

Third, a very slight occurrence of DSI clipping was observed for the condition of 120 input channels with a DSI gain of 2.5.

Fourth, a crosstalk problem was observed which returned a low-level echo to the U.K. end. The crosstalk path was found to occur on the terrestrial telephone link between COMSAT Laboratories and the Etam earth station. It is not known when the crosstalk began, since it was not present during initial circuit lineup, and this may have mitigated the benefit of using an echo canceller on the U.S. end.

Conclusions

Tests were performed to demonstrate sensitivity to DSI gain and the amount of terminating line loss in terms of MOS. With respect to DSI gain, there was no statistically significant variation in terms of the MOS, indicating that there is no difference between DNI performance and DSI performance for the DSI gain values tested, namely 2.0, 2.3, and 2.5. However, with respect to the terminating line loss, there was a statistically significant variation, with the high-loss conditions generally giving the lower MOS scores, as expected. It is concluded that the TDMA system operating with the DSI interfaces is indistinguishable from continuous operation with DNI interfaces. These results pertain equally to subjects at both the U.S. and U.K. circuit ends, but the U.K. subjects on the average indicate slightly lower scores overall.

Acknowledgments

Appendix. AT&T Bell Laboratories TDMA/DSI field trial report

INTRODUCTION

AT&T, in collaboration with COMSAT, BTI, and the French PTT, recently concluded a performance study of the TDMA/DSI operation of a set of test circuits between the U.K. and the U.S., and between France and the U.S. The study included subjective interviews at the U.S. circuit end for calls originating from the U.K. and France.

Two TDMA conditions were studied: the nominal operation condition providing 2.0:1 speech compression, and the overload condition providing 2.3:1 speech compression. For each pair of countries, subjects who talked over TDMA circuits as well as frequency-division multiple-access (FDMA) circuits were interviewed, and the FDMA results provided the baseline.

TEST IMPLEMENTATION

In the study between the U.K. and the U.S., 120 channels of live traffic and 120 channels of simulated traffic were used. A Compression Telecommunications Corporation channel activity simulator (model CHAS 120-1), located at Etam, generated traffic on 120 channels at a 40-percent speech activity level. This traffic was sent over DNI speech channels to Madley, looped back, combined with 120 channels of live traffic, and sent to Etam. For 2.0 compression, 120 bearer channels were available. For the 2.3 compression, the number of bearer channels was reduced to 104.

For tests from France to the U.S., a total of 51 circuits were used in the study. To achieve a 2:1 compression condition, simulated traffic on 60 circuits was sent over DNI circuits from Etam and looped back at the earth station at Plemeur Bodou. The 60 channels of simulated traffic were combined with 42 channels of live traffic so that a total of 102 channels of traffic was sent over 51 circuits toward the U.S. For the overload condition with 2.3 compression, the number of bearer circuits was reduced to 44.

SUBJECTIVE INTERVIEWS

In the subjective interviews, a data line analyzer unit located in the Pittsburgh, Pennsylvania, international switching center was connected to the CCITT No. 6 signaling link controlling the incoming international message traffic on the FDMA/ TDMA circuits under test. This unit derives nonspeech information needed for subjective interviewing such as called numbers, seizure time, and call disposition. On a daily basis, the interviewing organization in Garwood, New Jersey, dialed up the modem located adjacent to the data link analyzer in Pittsburgh. The needed information was transmitted to a printer in the interviewing area. Clerks processed the information from the printer to ensure that the interviews were completed between 20 minutes and 1 hour after the call was made. Prior to interviewing a number, a called number was compared to a list of numbers assigned to people who did not wish to be interviewed. Interviewers using video terminals with appropriate interview questions recorded the answers.

Upon completion of the interview, the results were processed by an on-site computer. Once per day the results were transmitted or transported to Bell Laboratories for data reduction, which provided the MOS and variance on a daily updating basis.

The MOS is computed as follows. The percentage of customers who rated a call as excellent, good, fair, or poor are given values (i.e., excellent = 4, good = 3, fair = 2, poor = 1) and a mean (which becomes the MOS) and its 95-percent confidence interval are calculated for each test condition.

U.K.-U.S. SUBJECTIVE PERFORMANCE

The general opinion results contain data on the MOS with 95-percent confidence limits, and the percentage of customers who rated the call as *unacceptable* plus *acceptable with difficulty*. These results are summarized in Table A-1. The third column gives the MOS, as well as the half-width of the 95-percent confidence interval.

TABLE A-1. U.K.-U.S. GENERAL OPINION RESULTS

CONDITION	NUMBER OF INTERVIEWS	MOS	CALLS RATED UNACCEPTABLE OR DIFFICULT (%)
TDMA/DSI (2.0)	574	3.02 + 0.07	25.96
TDMA/DSI (2.3)	793	2.98 ± 0.06	26.73
FDMA	568	2.85 + 0.08	31.87

Figure A-1 shows the circuit quality distributions for the three conditions. These results indicate that the MOSs for TDMA/DSI (2.0) and TDMA/DSI (2.3) conditions were different from the MOS for the FDMA condition with a confidence level of 0.95. The TDMA/DSI (2.0) and TDMA/DSI (2.3) conditions had 0.17 and 0.13 points better MOS, respectively, when compared to the FDMA condition. The percentage of callers rating quality unacceptable or difficult was also approximately 5 percentage points worse for the FDMA case when compared to the TDMA/DSI cases. The main reasons for the improved score on the TDMA conditions appear to be lower percentages of echo and noise complaints.

The two TDMA compression conditions produced similar performances. The 2.3:1 compression overload condition does not have significantly poor performance when compared to the nominal 2.0:1 compression condition. The MOS for FDMA circuits, while somewhat low, is not untypical of international circuits with a significant amount of noise and echo control using echo suppressors. In general, the number of echo complaints was high, indicating a need for better echo control.

FRANCE-U.S. SUBJECTIVE PERFORMANCE

This section presents the subjective test data collected for U.S. customers receiving calls from France. The general opinion results are summarized in Table A-2. The circuit quality distributions are given in Figure A-2 for the three conditions. The

BAR	CONDITION	INT	MOS
1	TDMA/DSI 2.0	574	3.02
2	TDMA/DSI 2.3	793	2.98
3	FDMA	568	2.85
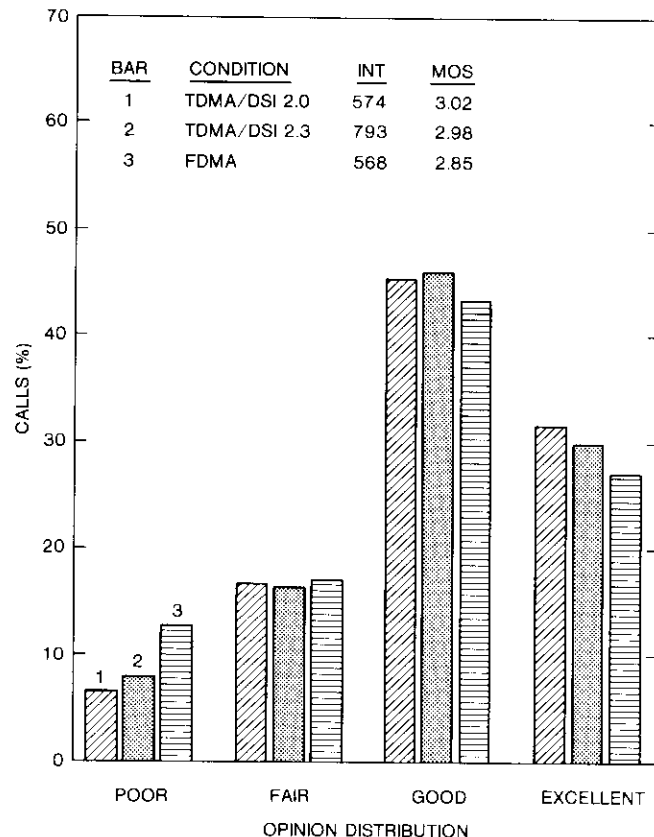
Figure A-1. *TDMA/DSI U.S.-U.K. Field Trial General Opinion Results*

TABLE A-2. FRANCE-U.S. GENERAL OPINION RESULTS

CONDITION	NUMBER OF INTERVIEWS	MOS	CALLS RATED UNACCEPTABLE OR DIFFICULT (%)
TDMA/DSI (2.0)	456	3.21 ± 0.07	19.30
TDMA/DSI (2.3)	529	3.24 + 0.07	17.96
FDMA	335	3.29 ± 0.08	18.21
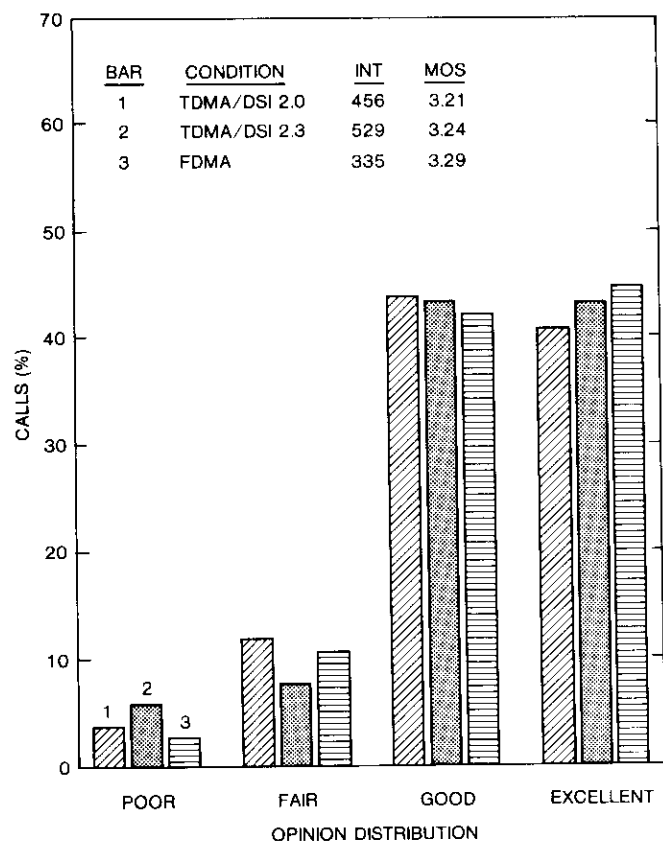
Figure A-2. *TDMA/DSI U.S.-France Field Trial General Opinion Results*

results indicate that the MOS and the percentage of subjects rating calls unacceptable or difficult for all three conditions are statistically indistinguishable. Results for noticed impairments and reasons for unfavorable response also indicate that the three conditions had similar performance.

The France-U.S. calls have higher MOS when compared to U.K.-U.S. calls. The main reason appears to be the lower level of noticed impairments such as echo, noise, and delay. The echo performance of U.K.-U.S. calls was significantly worse than for the France-U.S. calls. The noise impairments were also perceived in a higher percentage of U.K.-U.S. calls compared to the France-U.S. calls.

CONCLUSIONS

This report documents the results of the AT&T study to evaluate the TDMA operation on INTELSAT circuits between the U.K. and the U.S. and France and the U.S. Subjective measurements were conducted on two TDMA compression conditions (2.0 and 2.3) and on the baseline FDMA condition. The main conclusions are presented here.

The subjective interview results indicate that, on the U.K.-U.S. circuits, the TDMA performance for both 2.0 and 2.3 compression conditions was better than the corresponding FDMA performance, with a confidence level of 0.95. Reduced noise and echo complaints are the primary reason for the improved score on the TDMA circuits. The two TDMA conditions themselves had comparable performance. For France-U.S. circuits, the TDMA performance for both compression conditions was comparable to the FDMA condition.

The differences between the U.K.-U.S. and France-U.S. results appear to be caused by different levels of echo and noise performance for the two cases. The U.K.-U.S. FDMA calls had significant echo and noise impairments. When the circuits were cut over to TDMA operation, the noise level dropped and the echo performance also improved. For the France-U.S. circuits, the FDMA calls did not have major noise and echo problems, and the cutover to TDMA did not significantly change the level of performance.

Geostationary satellite log

C. H. SCHMITT

This note provides lists of current and planned geostationary satellites for the Fixed Satellite Service (FSS), the Maritime Mobile Satellite Service (MMSS), the Broadcasting Satellite Service (BSS), and the Space Research Service (SRS). Planned satellites are listed when information has been published by the International Frequency Registration Board (IFRB), or when satellite construction has commenced. The lists are ordered along increasing East longitude orbit position and update the previously published material [1] through December 1985.

Table 1 lists the satellites that are operating as of late December 1985, or satellites that may be capable of operating. Satellites being moved to new orbital positions are shown at their planned final positions for 1986, unless another satellite occupies the position. Refer to the Remarks column for further information.

Table 2 lists newly proposed and replacement satellites and their currently planned orbital positions. Additional technical characteristics may be found in the IFRB circulars referenced, as published weekly in the circular's special sections [2] or obtained from the country or organization listed.

Table 3 is the key to the frequency bands used in Tables 1 and 2. Sub-band allocations are designated in the Up/Down-Link Frequency column of Tables 1 and 2 by the letter suffix given that sub-band in column 1 of Table 3. Thus, 12a implies 11.7- to 12.2-GHz down-link in Region 2. Table 3 also shows the service allocations and the applicable International Telecommunications Union (ITU) region when the band is not allocated worldwide.

The author invites inquiries and comments and would appreciate receiving information on newly planned satellite networks as they become available.

References

[1] C. H. Schmitt, "Geostationary Satellite Log," *COMSAT Technical Review*, Vol. 15, No. 1, Spring 1985, pp. 149–177.

[2] *IFRB Circulars*, AR11/A/ (refers to Article 11, Section 1, which contains advanced publication requirements) or AR11/C/ (refers to Article 11, Section 2, which contains coordination requirements), and SPA/AA/ or /AJ/, The International Telecommunications Union IFRB, CH 1211, Geneva 20, Switzerland.

Carl H. Schmitt is Senior Engineer in the System Planning Department of the Space Communications Division at COMSAT.

TABLE 1. IN-ORBIT GEOSTATIONARY SATELLITES FOR FIXED, BROADCAST,
AND MARITIME-MOBILE SERVICES, LATE DECEMBER 1985

Subsatellite Longitude[a]	Launch Date	Satellite Designation	Country or Organization	Function	Up-/Down-Link Frequency (GHz)	Remarks
5.7°E	11 May 1978	OTS 2	ESA	FSS, BSS	14/11	Experimental IFRB: 5°E
7.0°E	04 Aug 1984	EUTELSAT 2 (ECS-2)	EUTELSAT-ESA	FSS	14/11	IFRB: 7°E EUTELSAT 1-3 in coordination
12.7°E	30 Jun 1983	GORIZONT 7	USSR	FSS	6/4	
12.9°E	16 Jun 1983	EUTELSAT 1 (ECS-1)	EUTELSAT-ESA	FSS	14/11	Designated ECS 1 before acceptance by EUTELSAT IFRB: 13°E EUTELSAT 1-2
19.0°E	08 Feb 1985	ARABSAT 1A	Arab League	FSS, BSS	6/4, 2.5	IFRB: 19°E
26.0°E	18 Jun 1985	ARABSAT 2A	Arab League	FSS, BSS	6/4, 2.5	IFRB: 26°E
33.6°E	26 Dec 1980	EKRAN 6	USSR	BSS	6/UHF	
34.0°E	26 Nov 1982	RADUGA 11	USSR	FSS	6/4	IFRB: 35°E STATSIONAR 2
35.0°E	15 Sep 1985	RADUGA 17	USSR	FSS	6/4	IFRB: 35°E STATSIONAR 2
40.1°E	28 Dec 1979	GORIZONT 3	USSR	FSS	6,8/4,7	IFRB: 40°E STATSIONAR 12
44.0°E	25 Aug 1983	RADUGA 13	USSR	FSS	6/4	IFRB: 40°E STATSIONAR 12
44.3°E	20 Feb 1980	RADUGA 6	USSR	FSS	6/4	IFRB: 45°E STATSIONAR 9
45.0°E	08 Aug 1985	RADUGA 16	USSR	FSS	6/4	IFRB: 45°E STATSIONAR 9
48.0°E	16 Mar 1984	EKRAN 12	USSR	BSS	6/UHF	
49.0°E	26 Jun 1981	EKRAN 7	USSR	BSS	6/UHF	
52.0°E	26 Jun 1984	GORIZONT 9	USSR	FSS	6/4	IFRB: 53°E STATSIONAR 5
53.0°E	15 Mar 1982	GORIZONT 5	USSR	FSS	6,8/4,7	IFRB: 53° (STATSIONAR 5)
57.0°E	23 May 1981	INTELSAT V (F-1)	INTELSAT	FSS	6,14/4,11	IFRB: 57°E INTELSAT V, IND 3
60.0°E	Unknown	DSCS II	U.S.-G	FSS	UHF,8/UHF,7	IFRB: 60°E
60.6°E	28 Sept 1985	INTELSAT VA (F-12)	INTELSAT	FSS	6,14/4,11	IFRB: 60°E INTELSAT VA IND 1
62.9°E	28 Sept 1982	INTELSAT V (F-5)	INTELSAT	FSS	6,14/4,11	IFRB: 63°E INTELSAT V, IND 1
			INMARSAT Lease	MMSS	1.6b,6.4b/ 1.5a,4f	IFRB: 63°E MCS IND A Comm. Sys. operational
66.0°E	19 Oct 1983	INTELSAT V (F-7)	INTELSAT	FSS	6,14/4,11	IFRB: 66°E
			INMARSAT Lease	MMSS	1.6b,6.4b/ 1.5a,4	IFRB: 66°E MCS IND D INMARSAT Spare
72.5°E	10 Jun 1976	MARISAT 2	US-COMSAT General	MMSS	UHF 1.6b,6.4c UHF 1.5a,4.1b	Operational, but unused except for UHF transponder IFRB: 72.5°E
73.4°E	30 Aug 1983	INSAT 1B	India	FSS	6/4	IFRB: 74°E (INSAT 1A)
75.0°E	May 1979	FLTSATCOM	US-G	FSS	UHF,8a/UHF,7a	IFRB: 75°E
77.0°E	13 Mar 1977	PALAPA A-2	INDONESIA	FSS	6/4	Backup for PALAPA B-1 IFRB: 77°E PALAPA-2
77.0°E	08 Apr 1983	RADUGA 12	USSR	FSS	6/4	
80.0°E	01 Aug 1984	GORIZONT 10	USSR	FSS	6,8/4,7	IFRB: 80°E STATSIONAR 13
83.0°E	08 Jul 1976	PALAPA A-1	INDONESIA	FSS	6/4	Near retirement IFRB: 83°E

TABLE 1 (continued). IN-ORBIT GEOSTATIONARY SATELLITES FOR FIXED, BROADCAST,
AND MARITIME-MOBILE SERVICES, LATE DECEMBER 1985

Subsatellite Longitude[a]	Launch Date	Satellite Designation	Country or Organization	Function	Up-/Down-Link Frequency (GHz)	Remarks
85.0°E	15 Feb 1984	RADUGA 14	USSR	FSS	6/4	IFRB: 85°E STATSIONAR 3
85.0°E	09 Oct 1981	RADUGA 10	USSR	FSS	6/4	IFRB: 85°E (STATSIONAR 3)
90.0°E	30 Nov 1983	GORIZONT 8	USSR	FSS	6,8/4,7	IFRB: 90°E (STATSIONAR 6)
90.0°E	20 Oct 1982	GORIZONT 6	USSR	FSS	6,8/4,7	IFRB: 90°E (STATSIONAR 6)
96.3°E	26 Jun 1981	EKRAN 7	USSR	BSS	6/UHF	IFRB: 99°E (STATSIONAR T2)
98.0°E	22 Mar 1985	EKRAN 14	USSR	BSS	6/UHF	
99.0°E	30 Sep 1983	EKRAN 11	USSR	BSS	6/UHF	IFRB: 99°E (STATSIONAR T2)
101.3°E	24 Aug 1984	EKRAN 13	USSR	BSS	6/UHF	
103.3°E	15 Dec 1977	SAKURA (C.S.)	Japan-NTT	FSS	6,30a/4,20a	Experimental
110.0°E	18 Jun 1983	PALAPA B-1	INDONESIA	FSS	6/4	Domestic and regional IFRB: 108°E
110.0°E	12 Feb 1986	BS-2B	Japan	FSS	2,14/12b,2	IFRB: 110°E BS-2
113.0°E	18 Jul 1978	RADUGA 4	USSR	FSS	6/4	
125.0°E	23 Jan 1984	BS-2A	Japan	BSS	2,14/12b,2	
128.0°E	22 Jun 1984	RADUGA 15	USSR	FSS	6/4	IFRB: 128° STATSIONAR 15
132.0°E	04 Feb 1983	CS2A	Japan	FSS	6,30a/4,20a	IFRB: 132°E
135.0°E	Nov 1979	DSCS II	US-G	FSS	UHF,8/UHF,7	
135.0°E	Sep 1982	DSCS III	US-G	FSS	UHF,8/UHF,7	
135.0°E	1984	CSE-A	Japan	FSS	20/10	
136.1°E	05 Aug 1983	CS 2B	Japan	FSS	6,30a/4,20a	IFRB: 136°E
140.0°E	20 Oct 1982	GORIZONT 6	USSR	FSS	6,8/4,7	IFRB: 140°E STATSIONAR 7
140.0°E	18 Jan 1985	GORIZONT 11	USSR	FSS	6,8/4,7	IFRB: 140°E STATSIONAR 7
156.0°E	Aug 1985	AUSSAT 1	Australia	FSS	14/12b,12d	IFRB: 156°E
160.0°E	Oct 1985	AUSSAT 2	Australia	FSS	14/12b,12d	IFRB: 160°E
172.0°E	31 Oct 1980	FLTSATCOM	US-G	FSS	UHF,8a/UHF,7a	IFRB: 172°E
174.0°E	31 Mar 1978	INTELSAT IVA (F-6)	INTELSAT	FSS	6/4	IFRB: 174°E INTELSAT IVA PAC 1 (To be replaced by INTELSAT V in March 1986)
175.0°E	Sep 1984	DSCS III	US-G	FSS	UHF,8/UHF,7	IFRB: 175°E
176.3°E	14 Oct 1976	MARISAT 3	US-COMSAT General	MMSS	UHF,1.6b,6.4c/ UHF,1.5a,4.1b	Spare for INMARSAT IFRB: 176.5°E
177.5°E	10 Nov 1984	MARECS B2	ESA-leased to INMARSAT	MMSS	1.6b,6,4e/ 1.5a,4	Operational 1 Jan 1985 as Pacific Ocean Maritime Satellite IFRB: 177.5°E MARECS PAC 1
178.0°E	Dec 1978	DSCS II	US-G	FSS	UHF 8/UHF 7	IFRB: 175°E
180.0°E (180.0°W)	20 Dec 1985	INTELSAT V (F-8)	INTELSAT	FSS	6,14/4,11	IFRB: 180°E INTELSAT V PAC 3
			INMARSAT Lease	MMSS	1.6b,6.4b/ 1.5a,4g	IFRB: 180°E MCS PAC A

TABLE 1 (continued). IN-ORBIT GEOSTATIONARY SATELLITES FOR FIXED, BROADCAST, AND MARITIME-MOBILE SERVICES, LATE DECEMBER 1985

Subsatellite Longitude[a]	Launch Date	Satellite Designation	Country or Organization	Function	Up-/Down-Link Frequency (GHz)	Remarks
217.1°E (142.9°W)	28 Oct 1982	SATCOM V (F-5)	US-Alascom, Inc.	FSS	6/4	IFRB: 143°W in coordination
220.9°E (139.1°W)	11 Apr 1983	SATCOM 1R	US-RCA	FSS	6/4	IFRB: 139°W in coordination
226.0°E (134.0°W)	28 Jun 1983	GALAXY 1 (USASAT 11D)	US-Hughes Comm.	FSS	6/4	IFRB: 134°W in coordination
229.0°E (131.0°W)	21 Nov 1981	SATCOM IIIR	US-RCA	FSS	6/4	IFRB: 131°W in coordination
232.0°E (128.0°W)	27 Aug 1985	ASC1	US-Amer. SAT CO.	FSS	6/4	IFRB: 128°W Adv. Publication
236.5°E (123.5°W)	09 Jun 1982	WESTAR 5	US-Western Union	FSS	6/4	IFRB: 123°W in coordination
240.0°E (120.0°W)	23 May 1984	SPACENET I	US-GTE Spacenet	FSS	6/14/4,12a	IFRB: 120°W in coordination
242.5°E (117.5°W)	12 Nov 1982	ANIK C3 (E)	Canada-TELESAT	FSS	14/12a	IFRB: 117.5°W
243.1°E (116.3°W)	27 Nov 1985	MORELOS B	Mexico	FSS	6,14/4,12a	IFRB: 116.5°W
247.0°E (113.0°W)	17 Jun 1985	MORELOS A	Mexico	FSS	6,14/4,12a	IFRB: 113.5°W
250.0°E (110.0°W)	18 Jun 1983	ANIK C2	Canada-TELESAT	FSS	14/12a	IFRB: 110°W in coordination
251.0°E (109.0°W)	16 Dec 1978	ANIK B1 (4)	Canada-TELESAT	FSS	6,14/4,12a	IFRB: 109°W
252.2°E (107.8°W)	13 Apr 1985	ANIK C1	Canada-TELESAT	FSS	14/12a	IFRB: 107.5°W in coordination
254.7°E (105.3°W)	12 Aug 1969	ATS 5	US-NASA	Experimental	UHF,6/UHF,7,4	IFRB: 105°W
255.5°E (104.5°W)	26 Aug 1982	ANIK D1	Canada-TELESAT	FSS	6/4	IFRB: 104.5°W
257.1°E (102.9°W)	08 May 1985	G-STAR 2	US-GTE	FSS	14/12a	IFRB: 103°W Adv. Publication
260.0°E (100.0°W)	09 Feb 1978	FLTSATCOM	US-G	FSS	UHF,8a/UHF,7a	IFRB: 100°W
261.0°E (99.0°W)	26 Feb 1982	WESTAR 4	US-Western Union	FSS	6/4	IFRB: 99°W in coordination
261.0°E (99.0°W)	11 Nov 1982	SBS 3 (USASAT 6B)	US-Satellite Business Systems	FSS	14/12a	IFRB: 99°W
263.0°E (97.0°W)	15 Nov 1980	SBS 1 (USASAT 6A)	US-Satellite Business Systems	FSS	14/12a	IFRB: 97°W in coordination
264.0°E (96.0°W)	28 Jul 1983	TELSTAR 301 (3A)	US-AT&T	FSS	6/4	IFRB: 95°W
265.0°E (95.0°W)	24 Sep 1981	SBS 2 (USASAT 6C)	US-Satellite Business Systems	FSS	14/12a	IFRB: 95°W in coordination
266.5°E (93.5°W)	21 Sep 1984	GALAXY III (USASAT 12B)	US-Hughes Comm.	FSS	6/4	IFRB: 93.5°W in coordination
268.8°E (91.2°W)	30 Aug 1984	SBS 4 (USASAT 9A)	US-Satellite Business Systems	FSS	14/12a	IFRB: 91°W in coordination

TABLE 1 (continued). In-Orbit Geostationary Satellites for Fixed, Broadcast, and Maritime-Mobile Services, Late December 1985

Subsatellite Longitude[a]	Launch Date	Satellite Designation	Country or Organization	Function	Up-/Down-Link Frequency (GHz)	Remarks
269.0°E (91.0°W)	10 Aug 1979	WESTAR 3	US-Western Union	FSS	6/4	IFRB: 91°W
274.0°E (86.0°W)	01 Sep 1984	TELSTAR 302 (USASAT 3C)	US-AT&T	FSS	6/4	IFRB: 86°W in coordination
277.0°E (83.0°W)	16 Jan 1982	SATCOM IV (USASAT 7B)	US-RCA	FSS	6/4	IFRB: 83°W
281.0°E (79.°W)	10 Oct 1974	WESTAR 2 (USASAT 12A)	US-Western Union	FSS	6/4	IFRB: 79°W Adv. Publication
283.2°E (76.8°W)	22 Jul 1976	COMSTAR D2 (USASAT 12C)	US-COMSAT General	FSS	6/4	IFRB: 76°W, Spare
284.0°E (76.0°W)	29 Jun 1978	COMSTAR D3 (USASAT 12C)	US-COMSAT Gen. Leased to AT&T thru 7 Apr. 1986	FSS	6/4	IFRB: 76°W Presently unused
284.9°E (75.1°W)	21 Feb 1981	COMSTAR D4 (USASAT 12C)	US-COMSAT General	FSS	6/4	
286.0°E (74.0°W)	22 Sep 1983	GALAXY 2 (USASAT 7A)	US-Hughes Comm.	FSS	6/4	IFRB: 74°W in coordination
288.0°E (72.0°W)	08 Sep 1983	SATCOM IIR (VII) (USASAT 8B)	US-RCA	FSS	6/4	IFRB: 72°W in coordination
291.0°E (69.0°W)	23 May 1984	SPACENET II	US-GTE Spacenet	FSS	6,14/4,12a	IFRB: 69°W in coordination USASAT 7C
295.0°E (65.0°W)	08 Feb 1985	SBTS-1	Brazil	FSS	6/4	IFRB: 65°W SBTS A2
307.4°E (52.6°W)	15 Dec 1981	INTELSAT V (F-3)	INTELSAT	FSS	6,14/4,11	Manuevered from 27°W during Sep 1985 IFRB: 53°W, INTELSAT V Continental 1
310.0°E (50.0°W)	19 Nov. 1978	NATO III	NATO	FSS	18,8f/2.3,7i	On 12/26/85 drifting at 0.04°E and inclination of 1.68
310.0°E (50.0°W)	22 May 1975	INTELSAT IV (F-1)	INTELSAT	FSS	6/4	IFRB: 50°W, INTELSAT IV ATL 1
317.2°E (42.8°W)	05 Apr 1983	TDRS East	US-NASA US-Systematics Gen.	SRS FSS	1,14d/2.2,13a 6/4	IFRB: 41°W
325.5°E (34.5°W)	05 Mar 1982	INTELSAT V (F-4)	INTELSAT	FSS	6,14/4,11	IFRB: 34.5°W, INTELSAT V ATL 4
329.0°E (31.0°W)	26 Sep 1975	INTELSAT IVA (F-1)	INTELSAT	FSS	6/4	Inclination of 1.7° on 12/26/85 IFRB: 31°W, INTELSAT IVA ATL 6
332.5°E (27.5°W)	29 Jun 1985	INTELSAT VA (F-11)	INTELSAT	FSS	6,14/4,11	IFRB: 27.5°W, INTELSAT VA ATL 2
334.0°E (26.0°W)	20 Dec 1981	MARECS-A	INMARSAT	MMSS	1.6b,6,4c/1.5a, 4f	INMARSAT Atlantic Ocean Region, IFRB: 26°W MARECS ATL 1
335.4°E (24.6°W)	22 Mar 1985	INTELSAT VA (F-10)	INTELSAT	FSS	6,14/4,11	IFRB: 24.5°W INTELSAT VA ATL 1
335.7°E (24.3°W)	05 Oct 1980	RADUGA 7	USSR	FSS	5,6/3	IFRB: 25.0°W, STATSIONAR 8 operates below INTELSAT VA frequencies

TABLE 1 (continued). IN-ORBIT GEOSTATIONARY SATELLITES FOR FIXED, BROADCAST,
AND MARITIME-MOBILE SERVICES, LATE DECEMBER 1985

Subsatellite Longitude[a]	Launch Date	Satellite Designation	Country or Organization	Function	Up-/Down-Link Frequency (GHz)	Remarks
337.0°E (23.0°W)	18 Jan 1980	FLTSATCOM	US-G	FSS	UHF,8a/UHF,7a	IFRB: 23°W
338.4°E (21.6°W)	25 May 1977	INTELSAT IVA (F-4)	INTELSAT	FSS	6/4	IFRB: 21.5°W, INTELSAT IVA ATL 1
341.6°E (18.4°W)	19 May 1983	INTELSAT V (F-6)	INTELSAT INMARSAT Lease	FSS MMSS	6,14/4,11 1,6b,6.4b/ 1.5a,4g	IFRB: 18.5°W, MCS ATL A is a spare for MARECS A IFRB: 18.5°W, INTELSAT V ATL 2
342.0°E (18.0°W)	Apr 1976	NATO-IA	NATO	FSS	8b,7k/7i,7L	
345.3°E (14.7°W)	19 Feb 1976	MARISAT 1	US-COMSAT General	MMSS	UHF 1,6b,6.4c/ UHF 1,5a,4.1b	Operational, but only UHF transponder used IFRB: 15°W
348.0°E (12.0°W)	Nov 1979	DSCS II	US-G	FSS	UHF,8/UHF,7	IFRB: 12°W, USGCSS 2 ATL
349.6°E (10.4°W)	14 Jun 1980	GORIZONT 4	USSR	FSS	6,8/4,7	IFRB: 11°W STATSIONAR 11 in coordination
352.0°E (8°W)	04 Aug 1984	TELECOM 1A	France	FSS	2,6,8g,14/2.2, 4,7i,12b,12d	IFRB: 8°W in coordination
355.0°E (5.0°W)	08 May 1985	TELECOM 1B	France	FSS	2,6,8g,14/2.2, 4,7i,12b,12d	IFRB: 5°W
356.2°E (3.8°W)	29 Jan 1976	INTELSAT IVA (F-2)	INTELSAT	FSS	6/4	IFRB: 4°W, INTELSAT IVA ATL 2 in coordination
357.0°E (3.0°W)	12 Mar 1983	EKRAN 10	USSR	FSS	6/UHF	
358.8°E (1.2°W)	06 Dec 1980	INTELSAT V (F-2)	INTELSAT	FSS	6,14/4,11	IFRB: 1.0°W, INTELSAT V CONT 4

[a]The list of satellite longitudes was compiled from the best information available.

TABLE 2. PLANNED GEOSTATIONARY SATELLITES FOR FIXED, BROADCAST, MARITIME-MOBILE, AND OTHER SERVICES, LATE DECEMBER 1985

Subsatellite Longitude	Launch or In-Use Date/ Period of Validity[b]	Satellite Designation	Country or Organization	Function	Up-/Down-Link Frequency (GHz)	Remarks
1.0°E	Sep 1986	GDL 5	Luxembourg	FSS/BSS	65b,12f,14/ 10.7,12d,11.2b	AR11/A/94/ADD-1/1308
3.0°E	1985	TELECOM 1C	France	FSS/BSS	2,6,8,14/2.2,4, 7,12b,12d	AR11/A/29/1339 AR11/C/116/ADD-2 AR11/C/157/1598 AR11/C/131/1594 AR11/C/116/ADD-2/1643 AR14/D/28/1669
5.0°E	1985-86	TELE-X	Norway, Sweden	FSS/BSS	2,6,30a,17a/2, 12b,20	AR11/A/27/1535 AR11/C/446/1644
6.0°E	Mar 1986/10[b]	SKYNET 4B	UK	FSS/MMSS	UHF,44/7,UHF	AR14/C/82/1677 AR11/C/183/ADD-1/1652 AR11/C/589/1652 AR11/C/183/1611
7.0°E	1984-85	EUTELSAT I-3	France	FSS/BSS	14/11,12b,12d	AR11/A/59/1578 AR11/C/446/1644 AR14C/52/1664
7.0°E	1987	F-SAT 1	France	FSS	2,14,30a/12d,20a	AR11/C/568/1649 AR11/A/79/1587 AR11/C/566-567/1649
8.0°E	Dec 1987/20	STATSIONAR-18	USSR	FSS/BSS	5d/3	AR11/A/219/1686
8.0°E	Dec 1987/20	GALS-7	USSR	FSS	7k,7l,8h,8q,8k, 8l,8p,8m,8n,8o, 7f,7q,7r,7h,7o, 7p,7c,7d,7n	AR11/A/238/1693
8.0°E	31 Dec 1987/20	VOLNA-15	USSP	AMSS	UHF,1.6g/ UHF,1.5f	AR11/A/241/1693
10.0°E	1986	APEX	France	BSS/FSS	6,30a/2,4,20a, 39a,49a	AR11/C/1583-584/1651 AR11/A/62/1578 AR14/C/79/1676
12.0°E	1982/20	PROGNOZ 2	USSR	SRS	3,2	SPA-AA/317/1471
13.0°E	31 Dec 1987	ITALSAT	Italy	FSS	30/2,20,39a,49a	AR11/A/151/1633
13.0°E	1984-85	EUTELSAT I-2	France	FSS/BSS	14/11,12b,12d	SPA-AJ/328/1492 AR11/A/61/1578, 1589 & 1582 AR11/C/445/1644 AR14/C/51/1669 AR11/D/71/1700
14.0°E	Unknown	Nigerian National System	Nigeria	FSS	6/4	SPA-AA/2091346
15.0°E	1986	AMS 1	Israel	FSS	6,14/4,11	AR11/A/39/1554 AR11/B/301593
15.0°E	1986	AMS 2	Israel	FSS	6,14/4,11	AR11/A/39/1554
16.0°E	1987	SICRAL 1A	Italy	FSS	8,14b,43a/7,12d, 20,44	AR11/A/44/1588
16.0°E	31 Dec 1986/10	EUTELSAT I-4	France	FSS	14/11e,11.7a,12g	AR11/A/218/1685
17.0°E	Unknown	SABS	Saudi Arabia	BSS	14/12b	SPA-AA/235/1387
17.0°E	1988	SABS 1-2	Saudi Arabia	BSS	14a,14/12b	AR11/A/125/1616

TABLE 2 (continued). PLANNED GEOSTATIONARY SATELLITES FOR FIXED, BROADCAST, MARITIME-MOBILE, AND OTHER SERVICES, LATE DECEMBER 1985

Subsatellite Longitude	Launch or In-Use Date/ Period of Validity[b]	Satellite Designation	Country or Organization	Function	Up-/Down-Link Frequency (GHz)	Remarks
19.0°E	Sep 1986	GDL 6	Luxembourg	FSS,BSS	6.5-7,14/11,12d	AR11/A/94/1594 ADD-1/1708
20.0°E	Unknown	Nigerian National System	Nigeria	FSS	6/4	SPA-AA/209/1346
22.0°E	1987	SICRAL 1B	Italy	MMSS/FSS	UHF,8,14,43a/7, 12d,20	AR11/A/45/1557 AR11/A/45/1588
23.0°E	Dec 1987/20	STATSIONAR-18	USSR	FSS/BSS	5d/3	AR11/A/220/1686
23.0°E	Dec 1987/20	GALS-8	USSR	FSS	7k,71,8h,8q,8k, 81,8p,8m,8n,8o/ 7f,7q,7r,7h,7o, 7p,7c,7m,7d,7n	AR11/A/239/1693
23.0°E	31 Dec 1987/20	VOLNA-17	USSR	FSS	UHF,1.6g/UHF,1.5f	AR11/A/242/1693
23.5°E	1987	DFS 1	Germany	FSS	2,14,30a/11,12d, 20,3d	AR11/A/40/1556 AR11/C/696-697/1670 AR11/C/774/1681 AR11/C/779/1681
26.0°E	Unknown	ZOHREH 2	Iran	FSS	14/11	SPA-AA/164/1278 SPA-AJ/76/1303
28.5°E	1987	DFS 2	Germany	FSS	2,14,30a/11,12d, 20a,30	AR11/A/41/1556
31.0°W	Dec 1987/12	EIRESAT	Ireland	FSS/BSS	12h/11a	AR11/A/182/1656
32.0°E	1987/10	VIDEOSAT 1	France	FSS	14/2,12d	AR11/A/80/1588 AR11/C/574/1650 AR11/C/580/1650 AR14/C/781/1676
34.0°E	Unknown	ZOHREH 1	Iran	FSS	14/11	SPA-AA/163/1278
35.0°E	Unknown	PROGNOZ 3	USSR	SRS	-/3,4	SPA-AA/318/1471
35.0°E	Jun 1988/20	STATSIONAR-D3	USSR	FSS	6a/4h	AR11/A/195/1675
35.0°E	31 Dec 1985/20	VOLNA-11	USSR	AMSS	UHF,1.6h/UHF,1.5F	AR/11/A/150/1631
38.0°E	1986	PAKSAT 1	Pakistan	FSS	14/11,12d	AR11/A/90/1592
41.0°E	Unknown	ZOHREH 4	Iran	FSS	14/11	SPA-AA/203/1330
41.0°E	1986	PAKSAT 2	Pakistan	FSS	14/12d	AR11/A/91/1592
45.0°E	Unknown	VOLNA-3	USSR	MMSS	UHF,1.6b/1.5a,UHF	SPA-AA/274/1425
45.0°E	Unknown	LOUTCH P2	USSR	FSS	14/11	SPA-AA/178/1289 SPA-AJ/122/1340
45.0°E	Jun 1988/20	STATSIONAR-D4	USSR	FSS	6a/4h	AR11/A/196/1675
45.0°E	1980	GALS-2	USSR	FSS	7k,71,8h,8q,8k,81, 8p,8m,8n,8o/7a,7m, 7d,7n,7o,7p,7f,7q, 7r,7h,	SPA-AJ/112/1335 SPA-AA/154/1262
45.0°E	31 Dec 1990/20	VOLNA-3n	USSR	FSS	1.6i/1.5a,1.5g	AR11/A/249/1697
47.0°E	Unknown	ZOHREH 3	Iran	FSS	14/11	SPA-AA/165/1278
53.0°E	Unknown	LOUTCH 2	USSR	FSS	14/11	SPA-AJ/85/1318 Leased to Intersputnik

TABLE 2 (continued). PLANNED GEOSTATIONARY SATELLITES FOR FIXED, BROADCAST, MARITIME-MOBILE, AND OTHER SERVICES, LATE DECEMBER 1985

Subsatellite Longitude	Launch or In-Use Date/ Period of Validity[b]	Satellite Designation	Country or Organization	Function	Up-/Down-Link Frequency (GHz)	Remarks
53.0°E	1 Feb 1987/10	SKYNET 4C	UK	FSS/MMSS	UHF,8,8f,8d,8e, 43b/UHF,7i,7j, 7f,7k	AR11/B/45/1626 AR11/A/84/ADD-1/1597 AR11/A/84/1588
53.0°E	1 Jun 1989/15	MORE-53	USSR	MMSS	1.6j,6c/1.51,3.7a	AR11/A/185/1662
57.0°E	1988	INTELSAT VI (IND 2)	INTELSAT	FSS	5,6 14/3,4,11	AR11/A/72/1584
57.0°E	1985	INTELSAT VA (IND 2)	INTELSAT	FSS	6,14/4,11	AR11/A/68/1580
60.0°E	1986	INTELSAT VA (IND 1)	INTELSAT	FSS	6,14/4,11	AR11/A/67/1580
60.0°E	1988	INTELSAT VI (IND 1)	INTELSAT	FSS	5,6,14/3,4,11	AR11/A/71/1584
64.5°E	Unknown	MARECS (IND 1)	INMARSAT (F)	MMSS	1.6b,6.4e/1.5a, 4f	SPA-AJ/243/1432
64.5°E	1989	INMARSAT IOR	INMARSAT (G)	MMSS	1.6b,6.4b/1.5a, 3.9b,4c,3.6a	AR11/A/178/1644
66.0°E	1986	INTELSAT V (IND 4)	INTELSAT	FSS	6,14/4,11	SPA-AA/253/1419
66.0°E	1987	INTELSAT MCS (IND D-Spare)	INTELSAT	MMSS	1.6b,6.4b,/1.5a, 4f	SPA-AA/275/1425
66.0°E	1989	INTELSAT VA 66E	INTELSAT	FSS	6,14/4,11	
70.0°E	1985/86	STW 2	China, Peoples Republic of	FSS	6/4	SPA-AA/142/1255
72.0°E	Dec 1984/10	FLTSAT A (IND)	USA	FSS/MMSS	UHF,8/UHF,7	AR11/A/100/ADD-1/ 1652, A/100/1605
72.0°W	30 Jun 1990/10	CONDOR C	Andean	FSS	6/4	AR11/A/210/1679
73.0°E	Unknown	MARECS (IND 2)	INMARSAT (F)	MMSS	1.6b,6.4e,/1.5a, 4f	AR11/D/3/1551
74.0°E	31 July 1990/20	INSAT C	India	BSS/FSS Meteoro- logical	UHF,5a-6,6.4a, 6.7/4,4.5	AR11/A/262/1702
74.0°E	July 1990/20	INSAT C	India	BSS/FSS Meteoro- logical	UHF,5a-6,6.4a, 6.7/4,4.5	AR11/A/262/1702 RES 33/A/7/1702
75.0°E	31 Dec 1986	FLTSATCOM B (IND)	USA	FSS/MMSS	43b/20	AR11/A/52/1561 AR/11/A/52/ADD-1/1587
76.0°E	31 Dec 1986/15	GOMS	USSR	WSS	8q,29b,29c/7s,7t, 1.6k,1.61,20a,20b	AR11/A/205/1678
77.0°E	Oct 1989/20	SSRD-2	USSR	FSS	14d,14e/11f,13d, 12.4a	AR11/A/188/1672
77.5°W	30 Jun 1990/10	CONDOR A	Andean	FSS	6/4	AR11/A/208/1679
80.0°E	Unknown	POTOK 2	USSR	FSS	6/4	AR11/A/179/1645 SPA-AA/345/1485
80.0°W	Jun 1989/10	NAHUEL 1	Argentina	FSS	14,6/12,4	AR11/A/203/1677
81.5°E	1 Jun 1990/10	FOTON-2	USSR	FSS	6b/4h	AR11/A/236/1692
82.5°E	Jan 1989/15	INSAT 1D	India	FSS/MMSS	5a-6,6.4a,6.7/ 4,4.5	AR11/A/126/1617 RES 33/A/3/ADD-1-10 AR14/C/91/1682

TABLE 2 (continued). PLANNED GEOSTATIONARY SATELLITES FOR FIXED, BROADCAST, MARITIME-MOBILE, AND OTHER SERVICES, LATE DECEMBER 1985

Subsatellite Longitude	Launch or In-Use Date/ Period of Validity[b]	Satellite Designation	Country or Organization	Function	Up-/Down-Link Frequency (GHz)	Remarks
83.0°E	Jan 1990/20	INSAT IIA	India	FS/MMSS	5a-6,6.4a,6.7/ 4,4.5	AR11/A/260/1702 RES 33/A/5/1702
85.0°E	Unknown	LOUTCH P3	USSR	FSS	14/11	SPA-AA/179/1289 SPA-AJ/123/1340
85.0°E	1980	GALS-3	USSR	FSS	7k,71,8h,8q,81, 8p,8m,8n,8o,/7c, 7m,7d,7n,7o,7p, 7f,7q,7r,7h	SPA-AJ/112/1335 SPA-AA/154/1262
85.0°E	Jun 1988/20	STATSIONAR-D5	USSR	FSS	6a/4h	AR11/A/197/1675
85.0°E	Unknown	VOLNA-5	USSR	MMSS	UHF,1.6b/1.5a,UHF	SPA-AJ/100/1329 SPA-AA/173/1286
85.0°E	31 Dec 1990/20	VOLNA-5M	USSR	FSS	1.6e/1.5i,1.5e	AR11/A/250/1697
85.0°W	31 Dec 1989/10	NAHUEL 2	Argentina	FSS	14,6/12,4	AR11/C/204/1677 AR11/A/204/1677
87.5°E	15 Mar 1988	CHINASAT-1	PRC	FSS	6/4	AR11/A/255/1702
89.0°W	30 Jun 1990/10	CONDOR B	Andean	FSS	6/4	AR11/A/209/1679
90.0°E	Unknown	LOUTCH 3	USSR	FSS	14/11	SPA-AJ/86/1318
90.0°E	1 Jun 1989/15	MORE-90	USSR	MMSS	1.6j,6c/1.5h,3.7a	AR11/A/154/1562
90.0°E	Unknown	VOLNA-8	USSR	MMSS	UHF,1.6b/1.5a,UHF	SPA-AA/289/1445 AR11/C/15/1589
93.5°E	Mar 1990/20	INSAT IIB	India	FSS/BSS Meteoro- logical	5a,6,6.7,6.4a/UHF	AR11/A/261/1702 RES 33/A/6/261/1702
93.5°E	1986/18	INSAT 1C	India	FSS	6/4	SPA-AJ/231/1429 AR11/C/851/1708 AR11/C/852-856/1708
95.0°E	1985	CSDRN	USSR	SRS	14d/10,11,13	SPA-AA/342/1484 (May have been launched as COSMOS 1700)
95.0°E		STATSIONAR-14	USSR			
98.0°E	15 Mar 1989/10	CHINASAT-3	PRC	FSS	6/4	AR11/A/257/1702
99.0°E	Unknown	STATSIONAR-T	USSR	FSS/BSS	6/UHF	RES-SPA2-3-AA10/1426 SPA-AJ/316/1473
99.0°E	Unknown	STATSIONAR-T2	USSR	FSS/BSS	6/UHF	SPA-AJ/316/1473
103.0°E	Dec 1988/20	STATSIONAR-21	USSR	FSS/BSS	5d/3	AR11/A/244/1692
103.0°E	31 Dec 1988/20	LOUTCH 5	USSR	FSS	14/11e,11.4b	AR11/A/243/1694
110.0°E	Unknown	BSE	Japan TCSJ	BSS	2,14/	SPA-AA/305/1459 AR11/C/10/1556
110.0°E	12 Feb 1986	BS 2	Japan	BSS	2,14/12b,2	Spare in Orbit
110.5°E	31 Dec 1988	CHINASAT II	China	FSS	6/4	AR11/A/25b/1702
113.0°E	Jun 1986[c]	PALAPA B-2	Indonesia	FSS	6/4	SPA-AA/198/1319 SPA-AJ/201/1407
118.0°E ±0.5°	Jun 1989	PALAPA B-3	Indonesia	FSS	6/4	AR11/A/157/1637

TABLE 2 (continued). PLANNED GEOSTATIONARY SATELLITES FOR FIXED, BROADCAST, MARITIME-MOBILE, AND OTHER SERVICES, LATE DECEMBER 1985

Subsatellite Longitude	Launch or In-Use Date/ Period of Validity[b]	Satellite Designation	Country or Organization	Function	Up-/Down-Link Frequency (GHz)	Remarks
128.0°E	1984	STATSIONAR-15	USSR	FSS	6/4	SPA-AA/273/1425 SPA-AJ/3071469
128.0°E	1 Jun 1980/20	GALS-10	USSR	FSS	7k,71,8h,8q,8k,81, 8p,8m,8n,8o/7f,7q, 7r,7h,7o,7p,7c,7m, 7d,7n	AR11/A/247/1695
128.0°E	Unknown	VOLNA-9	USSR	FSS/BSS MMSS	UHF,1.60/1.5a,UHF 1,2,11,34	
128.0°E	Jun 1988/20	STATSIONAR-D6	USSR	FSS	6a,4h	AR11/A/198/1675
128.0°E	31 Dec 1990/20	VOLNA-9M	USSR	FSS	1.6e/1.5i,1.5e	AR11/A/251/1697
130.0°E		ETS-2	Japan	Experimental		
130.0°E	Dec 1984/20	GALS-5	USSR	FSS	7k,71,8h,8q,8k, 81,8p,8m,8n,8o/ 7c,7m,7e,7n,7o, 7p,7f,7q,7r,7h	AR11/C/108/1578 AR11/C/28/1561 SPA-AA/339/1480
132.0°E	March 1988/10	CS-3A	Japan	FSS	5d-6,27c/17.7a,4	AR11/A/212/1680
136.0°W	30 Jun 1988/10	CS-3B	Japan	FSS	5d-6,27c/17.7a,4	AR11/A/213/1680
140.0°W	Aug 1984	GMS-3	Japan	WSS	2,4i/UHF,1.6m,1.6n	AR11/C/474/1648 AR11/A/54/1563

140.0°E	Unknown	LOUTCH 4	USSR	FSS	14/11	SPA-AJ/87/1318
140.0°E	1 Jun 1984	MORE-140	USSR	MMSS	1.6j,6c/1.5h,3.7a	AR11/A/186/1662
140.0°E	Unknown	VOLNA-6	USSR	FSS/BSS	3	
145.0°E	1987	STATSIONAR-16	USSR	FSS	6/4	AR11/A/76/1593 & 1586
150.0°E	Unknown	CSE	Japan	FSS	14/12a	AR533/6/3/1639 AR533/6/3/164 AR11/C/177/1606
150.0°E	31 Aug 1987/5	ETS-V	Japan	MMSS Experimental		AR11/A/217/1685
150.0°E	31 Dec 1987/12	JCSAT-1	Japan	FSS	14/12f	AR11/A/253/1700
154.0°E	30 Apr 1988/12	JCSAT-2	Japan	FSS	14/12f	AR11/A/254/1700
164.0°E	1986/10	AUSSAT 3	Australia (OTC)	FSS/BSS	14/12b,12d	RES 33/C/5/1643 RES 33/C/5/1647-III
164.0°E	1986/10	AUSSAT PAC III	Australia (OTC) South Pacific Region	FSS	14/12f	Adv. Publication 5/85 AR11/A/215/1684
166.0°E	31 Dec 1988/15	GOMS-2	USSR	WSS	8q,29b,29c/7s,7t, 1.6k,1.61,20a,20b	AR11/A/207/1578
167.0°E	Jun 1985/20	PACSTAR-1	Papua, New Guinea	FSS	14,6.4f/12i,3.6b	AR11/A/200/1676
167.0°E	Oct 1989/20	SSRD-2	USSR	FSS	14d,14e/11f,13d, 12.4a	AR11/A/187/1672
172.0°E	Dec 1986/10	FLTSAT B (W PAC)	USA	FSS/MMSS	43b/20	AR11/A/51/1561 AR11/A/51/ADD-1/1587
172.0°E	Dec 1984/10	FLTSATCOM A (W PAC)	USA	FSS/MMSS	UHF,8/UHF,7	AR11/A/99/1605 AR11/A/99/ADD-1/1652

TABLE 2 (continued). PLANNED GEOSTATIONARY SATELLITES FOR FIXED, BROADCAST, MARITIME-MOBILE, AND OTHER SERVICES, LATE DECEMBER 1985

Subsatellite Longitude	Launch or In-Use Date/ Period of Validity[b]	Satellite Designation	Country or Organization	Function	Up-/Down-Link Frequency (GHz)	Remarks
173.0°E	Feb 1986	INTELSAT V (PAC 1)	INTELSAT	FSS	6,14/4,11	AR11/C/170/1600 May move to 174.0°E
173.0°E	1988–89	INTELSAT VA (PAC 1)	INTELSAT	FSS	6,14/4,11	AR11/A/65/1580 May move to 174.0°E
174.0°E		INTELSAT V (PAC 1)	US-INTELSAT	FSS	6,14/4,11	AR11/A/
174.0°E	Jan 1987/10	INTELSAT VA (PAC 1)	US-INTELSAT	FSS	6,14/4,11	AR11/A/
175.0°E	Dec 1987	USGCSS 3 W (W PAC)	USA	FSS/MMSS	1.8a,1.8b,8/ 2.2a,2.2b,7	
175.0°W	Jun 1985/20	PACSTAR 2	Papua, New Guinea	FSS	14,6.4f/12i,3.6b	AR11/A/201/1676
176.0°E	1986	INTELSAT V (PAC 2)	INTELSAT	FSS	6,14/4,11	AR11/A/81/1588 SPA-AA/255/1419
176.0°E	1987	INTELSAT VA (PAC 2)	INTELSAT	FSS	6/14/4.11	AR11/A/66/1580
177.0°E	Oct 1987/10	INTELSAT VA (PAC 2)	US-INTELSAT	FSS	16,14/4,11	AR11/A/_____ formerly at 176°E AR11/A/66/1380
179.0°E	Dec 1984/10	INTELSAT V (PAC 2)	US-INTELSAT	FSS	6,14/4,11	SPA-AJ/377/1511
179.0°E	Sep 1985	INTELSAT V (PAC 2)	INTELSAT	FSS	6,14/4,11	SPA-AJ/377/1511
179.0°E	1986	INTELSAT MCS (PAC A)	INTELSAT	MMSS	1.6b, 6/1.5a,4	SPA-AJ/477/1577 SPA-AA/332/1476
180.0°E	Jan 1985/10	INTELSAT V (PAC 3)	US-INTELSAT	FSS	6,14/4,11	AR11/C/682/1668
180.0°E	1991	INTELSAT VA (PAC 3)	INTELSAT	FSS	6,14/4,11	
189.0°E (171.0°W)	1985	TDRS WEST	USA-NASA/ SPACECOM	SRS	2,14d/2.2,13	SPA-AA/232/1381 AR11/C/47/1568
190.0°E (170.0°W)	Jun 1988/20	STATSIONAR-D2	USSR	FSS	6a/4h	AR11/A/194/675
190.0°E (170.0°W)	Unknown	LOUTCH P4	USSR	FSS	14/11	SPA-AA/180/1289 SPA-AJ/124/1340
190.0°E (170.0°W)	Unknown	STATSIONAR-10	USSR	FSS	6/4	SPA-AJ/64/1280
190.0°E (170.0°W)	Unknown	VOLNA-7	USSR	MMSS	UHF,1.6b/1.5a,UHF	SPA-AA/175/1286
190.0°E (170.0°W)	1980/20	GALS-4	USSR	FSS	7k,7l,8h,8i,8j,8k, 8l,8m,8n,8o,8p/7a, 7m,7d,7n,7o,7p,7f 7q,7r,7h	SPA-AJ/114/1335 SPA-AA/156/1262
190.5°E (169.5°W)	1 Jun 1990/10	FOTON-3	USSR	FSS	6b/4h	AR11/A/237/1692
192.0°E (168.0°W)	Unknown	POTOK 3	USSR	FSS	6/4	SPA-AA/346/1485

TABLE 2 (continued). PLANNED GEOSTATIONARY SATELLITES FOR FIXED, BROADCAST, MARITIME-MOBILE, AND OTHER SERVICES, LATE DECEMBER 1985

Subsatellite Longitude	Launch or In-Use Date/ Period of Validity[b]	Satellite Designation	Country or Organization	Function	Up-/Down-Link Frequency (GHz)	Remarks
200.0°E (160.0°W)	1985	ESDRN	USSR	SRS	14d/10,11,13	SPA-AA/343/1484
214.0°E (146.0°W)	1985	AMIGO 2	Mexico	BSS	17a/12b	RES 33/A/2/1560
214.0°E (146.0°W)	Jun 1990/10	USASAT 20C (AURORA-2)	USA	FSS	6/4	AR11/A/259/1702
215.0°E (145.0°W)	Dec 1984/10	FLTSATCOM A (PAC)	USA	FSS/MMSS	UHF,8/UHF,7	AR11/A/181/1652
215.0°E (145.0°W)	Unknown	ILHUICAHUA 4	Mexico	FSS	6,14/4,12a	AR11/A/25/1533
215.0°E (145.0°W)	1 Dec 1990/20	VOLNA-21M	USSR	FSS	1.6e,1.6f/1.5a, 1.5e,1.5f	AR11/A/252/1697
216.0°E (144.0°W)	Jun 1990/10	USASAT 20B (WESTAR-7)	USA	FSS	6/4	AR11/A/258/1702
218.0°E (132.0°W)	1987	USASAT 11C (WESTAR-B)	USA	FSS	14/12a	AR11/111/1609
219.0°E (141.0°W)	Dec 1989/10	USASAT 17C (Galaxy-4)	USA	FSS	6/4	AR11/A/228/1687
219.0°E (141.0°W)	Unknown	ILHUICAHUA 3	Mexico	FSS	6,14/4,12a	AR11/A/24,1533
223.0°E (137.0°W)	Dec 1989/10	USASAT 17B (Spacenet-4)	USA	FSS	6/4	AR11/A/227/1687
224.0°E (136.0°W)	Jan 1990/10	USASAT 16D (GSTAR-3)	USA	FSS	14/12a	AR11/A/225/1687
226.0°E (134.0°W)	Jan 1990/10	USASAT 16C (ComGen-B)	USA	FSS	14/11	AR11/A/224/1687
228.0°E (132.0°W)	Unknown	US SATCOM 3	USA	FSS	6/4	SPA-AA/247/1412
230.0°E (130.0°W)	Jun 1987/10	USASAT 10D (Galaxy-B)	USA	FSS	14/11	AR11/A/108/1609
230.0°E (130.0°W)	31 Dec 1987/10	USRDSS West	USA	FSS/RDS[d]	1.6a,6.5a/2.4,5.1a	AR11/A/176/1641
234.0°E (126.0°W)	15 Sep 1987/10	USASAT 10C (Martin-B)	USA	FSS	14/12a	AR11/A/107/1609
234.0°E (126.0°)	Sep 1987/10	USASAT 10C (Martin-B)	USA	FSS	14/11	AR11/A/107/1609
236.0°E (124.0°W)	15 Sep 1986/10	USASAT 10B (Fedex-B)	USA	FSS	14/12a	AR11/A/106/1609
240.0°E (120.0°W)	Feb 1984/10	SPACENET 1	USA	FSS	14.6/4,11	AR11/C/833/1699 AR11/C/616/ADD-1/1682 AR14/C/39/1666 AR11/C/617-624/1658 AR11/C/616/1658 AR30/A/4/1567 AR11/A/10/ADD-1/1548 AR11/A/10/1525
240.0°E (120.0°W)	15 Jan 1987	USASAT 10A (SBS-5)	USA	FSS	14/12a	AR11/105/1609
246.0°E (114.0°W)	Unknown	TELESAT D2	Canada-Telesat (ANIK)	FSS	6/4	SPA-AA/358/1500
251.0°E (109.0°W)	Unknown See Remarks	TELESAT C-3	Canada-Telesat	FSS	14/12a	AR11/C/737-738/1674 AR14/C/101/1686

TABLE 2 (continued). PLANNED GEOSTATIONARY SATELLITES FOR FIXED, BROADCAST, MARITIME-MOBILE, AND OTHER SERVICES, LATE DECEMBER 1985

Subsatellite Longitude	Launch or In-Use Date/ Period of Validity[b]	Satellite Designation	Country or Organization	Function	Up-/Down-Link Frequency (GHz)	Remarks
252.0°E (110.0°W)	1986	ANIK C2	Canda-Telesat	FSS	14/12a	AR11/C/3/1154 AR14/C/86/1679 AR11/C/830-831/1698
252.5°E (107.5°W)	1985/10	ANIK C-1	Canada TELESAT	FSS	14/12a	AR11/C/832/1698
253.5°E (106.5°W)	31 Dec 1987/10	MSAT	Canada	FSS/MMSS	UHF-EHF/UHF-EHF	AR11/A/55/1563 AR14/C/32/1663 AR11/C/797-811/1689 AR11/A/56/1563 AR14/C/33/1663 AR11/A/56/ADD-1/1678 AR14/C/37/1664 AR11/C/797-811/1689
254.0°E (106.0°W)	1985	GSTAR-I	US-GTE Satellite	FSS	14/12a	AR11/A/14/1525 AR11/A/14/ADD-1/1548
255.0°E (105.0°W)	Nov 1984/10	FLTSATCOM A (E PAC)	USA	FSS/MMSS	UHF,8/UHF,7	AR11/A/98/ADD-1/1652 AR11/A/98/1605 @ 100°W
257.0°E (103.0°W)	1986	GSTAR-II	US-GTE Satellite	FSS	14/12a	AR11/A/15/1525 AR11/A/15/ADD-1/1548
259.0°E (101.0°W)	Dec 1989/10	USASAT 17A	USA	FSS	6/4	AR11/A/226/1687
259.0°E (101.0°W)	Jan 1990/10	USASAT 16B (Ford-1)	USA	FSS	16/11	AR11/A/223/1687
260.0°E (100.0°W)	30 Sep 1987/10	USRDSS Central	USA	FSS/RDS	1.6a,6.5a/2.4, 5.1a	AR11/A/175/1641
267.0°E (93.0°W)	Jan 1990/10	USASAT 16A (Ford-2)	USA	FSS	14/11	AR11/A/222/1687
269.0°E (91.0°W)	20 Dec 1985	WESTAR VI-S	US-Western Union	FSS	6/4	Will replace WESTAR-III which will move to 79.0°W. WESTAR II will be retired in early 1986.
271.5°E (88.5°W)	Sep 1985/10	USASAT 12D	USA	FSS	6/4	AR11/A/124/1615
271.5°E (88.5°W)	Feb 1984/10	SPACENET 111	USA	FSS	14,6/4,11	AR11/C/834/1699
273.0°E (87.0°W)	14 Oct 1985 15 Jun 1985/10	SATCOM K-1 (USASAT 9B)	US-RCA USA	FSS	14/12a	Under Construction AR11/A/102
274.0°E (86.0°W)	1985	USASAT 3C (-)	USA	FSS	6/4	AR11/C/246
275.0°E (85.0°W)	15 Mar 87/10	USASAT 9C (RCA-A)	USA	FSS	14/12a	AR11/A/103/1609
277.0°E (83.0°W)	1988	STSC 1	Cuba	FSS	6/4	AR11/A/58/1578, Note 83.0°W occupied by USASAT 7B or SATCOM IV
277.0°E (83.0°W)	Jan 1987/10	USASAT 9D (RCA-B)	USA	FSS	14/11	AR11/A/104/1609
279.0°E (81.0°W)	Dec 1986	USASAT 7D (ASC-2)	USA	FSS	6,14/4,12a	AR11/C/50/1568: Was 79.0°W AR11/A/12/1525 AR11/C/257/1623

Subsatellite Longitude	Launch or In-Use Date/ Period of Validity[b]	Satellite Designation	Country or Organization	Function	Up-/Down-Link Frequency (GHz)	Remarks
281.0°E (79.0°W)	1985	TDRS Central	USA-NASA/ SPACECOM USA-SYSTEMAT. GEN	SRS FSS	2,14d/2.2,13a 6/4	SPA-AA/233/1381
281.0°E (79.0°W)	15 Mar 1987	USASAT 11A (Martin-A)	USA	FSS	14/12a	AR11/A/109/1609
283.0°E (77.0°W)	15 Jun 1987/10 27 Nov 1985	USASAT 11B (Fedex-A)	USA RCA	FSS	14/12a	AR11/A/110/1609 Under Construction
284.6°E (75.4°W)	1986 1986	SATCOL 1A SATCOL 1B	Colombia Colombia	FSS FSS	6/4 6/4	SPA-AA/322,323/1474 AR11/C/79/1573
285.0°E (75.0°W)	1986	SATCOL 2	Colombia	FSS	6/4	SPA-AJ/127/1343 SPA-AA/324/1474 AR11/C/811/1573
285.0°E (75.0°W)	Jan 1990/10	USASAT 18A (ComGen-A)	USA	FSS	14/11	AR11/A/230/1687
287.0°E (73.0°W)	Jan 1990/10	USASAT 18B (WESTAR-A)	USA	FSS	14/11	AR11/A/231/1687
290.0°E (70.0°W)	1985	USASAT 7C (Spacenet-2)	USA	FSS	6/4	AR11/A/1525 FCC: 69.0°W
290.0°E (70.0°W)	30 Jun 1987/10	USRDSS East	USA	FSS/RDS	1.6a,6.5a/2.4, 5.1a	AR11/A/174/1641
293.0°E (67.0°W)	Late 1987	USASAT 8A (SATCOM-6)	USA (RCA)	FSS	6/4	AR11/C/394/1629 A/36/1553
294.0°E (66.0°W)	30 Jun 1989	USASAT 15D (RCA-C)	USA	FSS	14/12a	AR11/A/165 FCC: 67.0°W
295.0°E (65.0°W)	1985	SBTS A-2	Brazil	FSS	6/4	AR11/A/17/1526
296.0°E (64.0°W)	1988	USASAT 15C (ASC-4)	USA	FSS	14/12a	AR11/A/
297.0°E (63.0°W)	1986	USASAT 14D (-)	USA	FSS	6/4	AR11/C/99/1576 confirm AR11/A/37/1553
298.0°E (62.0°W)	1988/10	USASAT 15B (SBS-6)	USA	FSS	14/11,12a	AR11/A/163/1637
299.0°E (61.0°W)	1989/10	USASAT 14C (SATCOM-7)	USA	FSS	6/4	AR11/A/160/1637
300.0°E (60.0°W)	01 Jan 1986/10	INTELSAT IBS 300.0°E	INTELSAT	FSS	5c-6,14/4a,11d, 11f,12d,	AR11/A/167/1638
300.0°E (60.0°W)	31 Dec 1988/10	USASAT 15A (-)	USA	FSS	14/12a	AR11/A/162/1637
300.0°E (60.0°W)	Dec 1989/10	USASAT 17D (-)	USA	FSS	6/4	AR11/A/229/1687
300.0°E (60.0°W)	Jan 1986/10	INTELSAT VA	US-INTELSAT	FSS	6,14/4,11	AR11/A/166/1638
302.0°E (58.0°W)	1987	USASAT 8C (-)	USA	FSS	6/4 10.7-12.744 11.7-12.2	AR11/A/38/1553
302.0°E (58.0°W)	30 Jul 1988/10	USASAT 13E (ISI)	USA	FSS-Intern	14/11,12a,12b,12c	AR11/A/136/1620
303.0°E (57.0°W)	30 Sep 1987/10	USASAT 13H (PANAMSAT I)	USA	FSS	5c-6/4,11b	AR11/A/177/1643

TABLE 2 (continued). PLANNED GEOSTATIONARY SATELLITES FOR FIXED, BROADCAST, MARITIME-MOBILE, AND OTHER SERVICES, LATE DECEMBER 1985

Subsatellite Longitude	Launch or In-Use Date/ Period of Validity[b]	Satellite Designation	Country or Organization	Function	Up-/Down-Link Frequency (GHz)	Remarks
304.0°E (56.0°W)	01 Apr 1986/10	INTELSAT VA 304.0°E	INTELSAT	FSS	6,14/4,11	AR11/A/168/1638
304.0°E (56.0°W)	01 Apr 1986/10	INTELSAT IBS 304.0°E	INTELSAT	FSS	5c-6,14/4a,11d, 11f,12d	AR11/A/169/1638
304.0°E (56.0°W)	30 Jul 1988/10	USASAT 13D (ISI)	USA	FSS	6/4	AR11/C/246/1620
305.0°E (55.0°W)	31 Dec 1988/10	USASAT 14B (-)	USA	FSS	6/4	AR11/A/159/1637
307.0°E (53.0°W)	1986[e]	INTELSAT V CONTINENTAL 1	INTELSAT	FSS	6,14/4,11	AR11/A/82/1588
307.0°E (53.0°W)	1986[e]	INTELSAT IBS 307.0°E	INTELSAT	FSS	6,14,14b/4,11,12a	Under construction
307.0°E (53.0°W)	April 1988/10	INTELSAT VA CONTINENTAL 1	US-INTELSAT	FSS	6,14/4,11	AR11C/674/1667 AR11/A/115/1609
310.0°E (50.0°W)	Unknown	INTELSAT IVA ATL 2	INTELSAT	FSS	6/4	SPA-AJ/371/1509: 1°W SPA-AJ/213/1418: 181.5°W SPA-AA/66/1170 SPA-AA/49/1161
310.0E (50.0°W)	1985	INTELSAT IVA ATL 2	INTELSAT	FSS	6/4	AR11/C/140/1596
310.0°E (50.0°W)	1986	INTELSAT VA CONTINENTAL 2	INTELSAT	FSS	6,14,4,11	AR11/A/74/1586
310.0°E (50.0°W)	1986	INTELSAT IBS 310.0°E	INTELSAT	FSS	6,14/4,11,12	AR11/A/129/1617
310.0°E (50.0°W)	Jun 1986/10	INTELSAT V CONTINENTAL 2	US-INTELSAT	FSS	6,14/4,11	AR11/A/74/1586 AR11/C/594/1660
310.0°E (50.0°W)	30 Dec 1987/10	USASAT 13C (ORION)	USA	FSS-Intern	14/11a,11.4a	AR11/A/134/1618
313.0°E (47.0°W)	30 Sep 1987/10	USASAT 13B (ORION)	USA	FSS	14/11e,11.4a	AR11A/133/1618
315.0°E (45.0°W)	1 Jan 1988/10	USASAT 13F (CYGNUS)	USA	FSS-Intern	14,12a/11a,12d,	AR11/A/154/1635
315.0°E (45.0°W)	Jan 1989/10	USASAT 13I (PANAMSAT II)	USA	FSS	6/4,11	AR11/A/199/1675
316.5°E (43.5°W)	31 Dec 1988/10	VIDEOSAT-3	France	FSS	14,2.0/11f,12d,	AR11/A/148/1631 AR11/C/766/1678 AR14/C/110/1698
317.0°E (43.0°W)	01 Jun 1988/10	USASAT 13G (CYGNUS)	USA	FSS-Intern	14/12a,11a,12d	AR11/A/155/1635
319.0°E (41.0°W)	31 Dec 1988/10	USASAT 14A (TDRS-1)	USA	FSS	6/4	AR11/A/158/1637
319.5°E (40.5°W)	1 Apr 1986/10	INTELSAT VA	INTELSAT	FSS	6,14/4,11	AR11/A/127/1617
319.5°E (40.5°W)	1 Apr 1986/10	INTELSAT IBS	INTELSAT	FSS	6a,14/4a,11d,11b, 12d ADD-1/1628)	AR11/A/130/1617 (AR11/A/130/
322.5°E (37.5°W)	1987/10	VIDEOSAT-2	France	FSS	14/2,12d	AR11/A/86/1589 AR11/C/727/1673 AR14/C/76/1676

TABLE 2 (continued). PLANNED GEOSTATIONARY SATELLITES FOR FIXED, BROADCAST, MARITIME-MOBILE, AND OTHER SERVICES, LATE DECEMBER 1985

Subsatellite Longitude	Launch or In–Use Date/ Period of Validity[b]	Satellite Designation	Country or Organization	Function	Up-/Down-Link Frequency (GHz)	Remarks
322.5°E (37.5°W)	1987	USASAT 13A (ORION)	USA	FSS	14/11,11a,4a	AR11/132/1618
325.5°E (34.5°W)	1985	INTELSAT MCS, ATL E	INTELSAT	FSS/MMSS	1.6a,6.4a/1.5a, 4.1a,4.2	SPA-AJ/350/1500 SPA-AA/284/1432
325.5°E (34.5°W)	1987	INTELSAT VA ATL 3	INTELSAT	FSS	6,14/4,11	AR11/A/63/1580
329.0°E (31.0°W)	1986	UNISAT 1 ATL TELECOM	U.K.-BRITISH	FSS	14/11,12b,12d	AR11/A/26/1534 See entry below
329.0°E (31.0°W)	30 Jun 1986/10	UNISAT 1	U.K.	FSS/BSS	17c,17b,14a/12d, 2.2,4,11.7a,12e,	AR11/C/576/1650 AR11/A/23/1532
329.0°E (31.0°W)	01 Jan 1987/10	INTELSAT VA ATL 6	INTELSAT	FSS	6,14/4,11	AR11/A/119/1611 (AR11/A/119/ ADD-1/1628) (AR11/A/119/ ADD-2/1638)
329.0°E (31.0°W)	01 Jan 1987/10	INTELSAT V ATL 6	INTELSAT	FSS	6,14/4,11	AR11/A/118/1611
332.5°E (27.5°W)	01 Jan 1987/13	INTELSAT VI ATL 2	INTELSAT	FSS	5,6,14/3,4,11	AR11/A/70/1584
333.5°E (26.5°W)	Dec 1982/20	GALS-1	USSR	FSS	7k,7l,8h,8q,8k,8i, 8p,8m,8n,8o/7c,7m, 7d,7n,7o,7p,7f,7q, 7r,7h	SPA-AJ/365/1508 SPA-AJ/111/1335 SPA-AA/153/1262
333.5°E (26.5°W)	31 Dec 1987/20	VOLNA-13	USSR	AMSS[f]	UHF,1.6g/UHF,1.5f	AR11/A/240/1693
333.5°E (26.5°W)	Dec 1987/20	STATSIONAR-17	USSR	FSS/BSS	5d/3	AR11/A/219/1686
333.5°E (26.5°W)	Jun 1988/20	STATSIONAR-D1	USSR	FSS	6a/4h	AR11/A/193/1675
334.0°E (26.0°W)	31 Aug 1988/10	INMARSAT AOR-CENTRAL	UK	MMSS	1.6b,6.4b/1.5a, 3.9b,4c,3.6a	AR11/A/152/1634
335.0°E (25.0°W)	Unknown	LOUTCH-P1	USSR	FSS	14/11	SP-AA/177/1289
335.0°E (25.0°W)	Unknown	STATSIONAR 8	USSR	FSS	6/4	SPA-AJ/62/1280
335.0°E (25.0°W)	Unknown	VOLNA-1	USSR	MMSS	UHF,1.6b/1.5a, UHF	SPA-AA/169/1286
335.0°E (26.5°W)	1 Jun 1990/20	GALS-9	USSR	FSS	7k,7l,8h,8q,8k, 8l,8p,8m,8n,8o/ 7f,7q,7r,7h,7o, 7p,7c,7m,7d,7n	AR11/A/246/1695
335.5°E (24.5°W)	1987	INTELSAT VI (ATL 1)	INTELSAT	FSS	6,14/4,11	AR11/A/69/1584
335.5°E (24.5°W)	Unknown	INTELSAT MCS (ATL D)	INTELSAT	MMSS	1.6b,6.4b/1.5a,4g	SPA-AJ/349/1500
336.0°E (24.0°W)	Unknown	PROGNOZ 1	USSR	SRS	-/3,4	SPA-AA/316/1471
337.0°E (23.0°W)	Dec 1986/10	FLTSAT B (E ATL)	USA-G	FSS/MMSS	UHF,8/UHF,7	AR11/A/48/1561 AR11/A/48/ADD-1/1587
337.0°E (23.0°W)	Unknown	MARECS, ATL 2	France	FSS/MMSS	1.6b,6.4b, UHF/1.5a,4d,UHF	SPA-AJ/241/1432 SPA-AA/219/1351 AR11/D/3/1551

TABLE 2 (continued). PLANNED GEOSTATIONARY SATELLITES FOR FIXED, BROADCAST, MARITIME-MOBILE, AND OTHER SERVICES, LATE DECEMBER 1985

Subsatellite Longitude	Launch or In-Use Date/ Period of Validity[b]	Satellite Designation	Country or Organization	Function	Up-/Down-Link Frequency (GHz)	Remarks
338.5°E (21.5°W)	1986	INTELSAT V (ATL 5)	INTELSAT	FSS	6,14/4,11	SPA-AA/252/1419
338.5°E (21.5°W)	01 Jan 1989/10	INTELSAT VA (338.5°E)	INTELSAT	FSS	6,14/4,11	AR11/A/180/1645 SPA-AA/48/1161 SPA-AA/65/1170
340.0°E (20.0°W)	1985	GDL 4	Luxembourg	FSS/BSS	6.5-7,14/11,12d, 6.5b,12f,14/10.7, 11.2b,12d	AR11/A/92/1594/ ADD-1/1708
341.0°E (19.0°W)	1985	TDF 1	France	BSS	17a,12b	AR11/A/57/1570 AR11/C/107/1578
341.0°E (19.0°W)	01 Jun 1985	TDF 1	France (17 GHz)	BSS	17b	AR11/C/142/1547 RR1042/2/1521
341.0°E (19.0°W)	01 Jun 1985/10	TDF 1	France (11 GHz)	FSS/BSS	11.2a	AR11/C/124/1592 RR1042/2/1521
341.0°E (19.0°W)	01 Jun 1985/10	TDF 1	France (2 GHz)	FSS/BSS	2.2/2.2	AR11/C/107/1578 RR1042/2/1521 AR11/C/703/1670 AR11/C/741/1674 AR14/C/88/1680 AR14/C/106/1695
341.0°E (19.0°W)	1985	L-SAT	ESA (France)	BSS/FSS	13a,14a,30a/12b, 20a	SPA-AA/308/1463 AR11/A/33/1544 AR11/A/88/1590 AR11/A/57/1570 AR11/C/124/1592
341.0°E (19.0°W)	1985-87	TV-SAT	Federal Republic of Germany	BSS	17a,17.3a,18.0a, 2.0,11.7a,12e,2.0	SPA-AA/311/1464 SPA-AA/325/1474 SPA-AA/366/1526 AR14/C/4/1550 AR11/C/608/1656 AR11/C/609/1656
341.0°E (19.0°W)		L-SAT (17 GHz)	France	BSS	17a	AR11/C/6/1554 AR11/A/308/1463 AR11/C/782/1682 AR14/D/23/1707
	01 Jul 1986	L-SAT	France (30/20 GHz)	FSS/FSS	27b/18a,29.6a	AR11/C/232/1619 AR11/A/32/1544
	01 Jul 1986	L-SAT (14,13⅝/12 GHz)	France	BSS/FSS	14c,13c,12d ADD-1/1643	AR11/C/174/1605 AR11/C/174/ SPA-AA/337/1479 AR11/A/88/1590
341.0°E (19.0°W)	01 Jul 1986/10	L-SAT	France (2/2 GHz)	BSS/FSS	2.0/2.2	AR11/C/176/1605 AR11/S/33/1544
341.0°E (19.0°W)	1986	HELVESAT 1	Switzerland	BSS	17a,18/12b,2	SPA-AA/365/1512
341.0°E (19.0°W)	1986	SARIT	Italy	BSS	17a,18/2b	SPA-AA/360/1505 SPA-AA/371/1547
341.0°E (19.0°W)	1986	LUX-SAT	Luxembourg	BSS	17a/12b,17.3a, 11.7a,12.4,18.0a	AR11/A/20/1529
341.5°E (18.5°W)	1986-87	INTELSAT VA	INTELSAT (ATL 4)	FSS	6,14/4,11	AR11/A/64/1580

TABLE 2 (continued). PLANNED GEOSTATIONARY SATELLITES FOR FIXED, BROADCAST, MARITIME-MOBILE, AND OTHER SERVICES, LATE DECEMBER 1985

Subsatellite Longitude	Launch or In-Use Date/ Period of Validity[b]	Satellite Designation	Country or Organization	Function	Up-/Down-Link Frequency (GHz)	Remarks
341.5°E (18.5°W)	1986	INTELSAT IBS (341.5°E)	INTELSAT	FSS	6,14/4,11,12a,12d	Under construction by Ford Aerospace; replaces INTELSAT VA above
342.0°E (18.0°W)	15 Oct 1989	SATCOM II	BELGIUM	FSS	8/7	SPA-AJ/137/1355 SPA-AA/144/1257
343.5°E (16.5°W)	01 Jan 1986/10	INTELSAT V (343.5°E)	INTELSAT	FSS	6,14/4,11	AR11/A/172/1639
343.5°E (16.5°W)	01 Jul 1986/10	INTELSAT VA (343.5°E)	INTELSAT	FSS	6,14/4,11	AR11/A/170/1638
343.5°E (16.5°W)	01 Jul 1986/10	INTELSAT IBS (343.5°E)	INTELSAT	FSS	6a,14/4a,11d,11b, 12d	AR11/A/171/1638
344.0°E (16.0°W)	01 Jun 1986/20	WSDRN	USSR	FSS/SR	14d,11b,13	AR11/C/67/1570 SPA-AA/341/1484
344.0°E (16.0°W)	17 Oct 1989/20	SSRD-2	USSR	FSS	4j,14e/11f,13d, 12.4a	AR11/A/189/1672
345.0°E (15.0°W)	Nov 1984/10	FLTSATCOM A (ATL)	USA-G	FSS/MMSS	UHF,8/UHF,7	AR11/A/97/ADD-1/1652 AR11/97/1605 @ 23°W
345.0°E (15.0°W)	31 Aug 1985	INMARSAT AOR-EAST	UK	MMSS	16b,6.1a,6.4a, 6.4d/1.5a,3.9b,4c, 3.6a	AR11/A/153/1634
345.0°E (15.0°W)	01 Jun 1990/10	FOTON-1	USSR	FSS	6b/4h	AR11/A/235/1692
345.0°E (14.0°W)	31 Dec 1987/15	GOMS-1	USSR	WSS	8q,29b,29c/7s,7t, 1.6k,1.61,20a,20b	AR11/A/206/1578
345.0°E (14.0°W)	01 Jun 1989/15	MORE-14	USSR	MMSS	1.6j,6c/1.5h,3.7a	AR11/A/183/1662
346.0°E (14.5°W)	Unknown	LOUTCH 1	USSR	FSS	14/11	SPA-AA/157/1262 SPA-AJ/84/1318
346.0°E (14.0°W)	1980/10	VOLNA-2	USSR	MMSS	1.6c/1.5c	SPA-AJ/97/1329 SPA-AA/170/1286: 14°W
346.0°E (14.0°W)	31 Dec 1982	STATSIONAR-4	USSR	FSS	6.1b/3.8a	SPA-AJ/336/1494 SPA-AA/92/1197
346.5°E (13.5°W)	Unknown	POTOK 1	USSR	FSS	-/4	SPA-AA/344/1485
347.5°E (12.5°W)	Unknown	MAROTS-B	France	MMSS	1.6b,UHF/1.5a,UHF	SPA-AA/204/133
348.0°E (12.0°W)	Early 1988/10	HIPPARCOS	France	FSS/SR	2.0/2.2	AR11/A/138/1621 AR11/A/138/ADD-1/1636 AR14/C/64/1673
349.0°E (11.0°W)	1986	F-SAT 2	France	FSS	2,14,30a/12d,20a	AR11/C/466/1647 AR11/A/73/1586 AR11/C/467-468/1647 AR14/C/71/1675
356.0°E (4.0°W)	01 Jul 1987/10	INTELSAT V CONT 3	INTELSAT	FSS	6,14/4,11	AR11/A/112/1609
356.0°E (4.0°W)	01 Jul 1986/10	INTELSAT VA CONT 3	INTELSAT	FSS	6,14/4,11	AR11/A/116/1609 AR11/A/116/ ADD-1/1628) (AR11/A/116/ ADD-2/1638)

TABLE 2 (continued). PLANNED GEOSTATIONARY SATELLITES FOR FIXED, BROADCAST, MARITIME-MOBILE, AND OTHER SERVICES, LATE DECEMBER 1985

Subsatellite Longitude	Launch or In-Use Date/ Period of Validity[b]	Satellite Designation	Country or Organization	Function	Up-/Down-Link Frequency (GHz)	Remarks
359.0°E (1.0°W)	1986	INTELSAT V CONT 4	INTELSAT	FSS	6,14,4,11	SPA-AJ/371/1509
359.0°E (1.0°W)	01 Jan 1987/10	INTELSAT VA CONT 4	INTELSAT	FSS	6,14,4,11 ADD-2/1638)	AR11/A/117/1609 (AR11/117/ ADD-1/1628) (AR11/117/ AR11/A/117/ ADD-2/1638)
359.0°E (1.0°W)		SKYNET 4A	UK	FSS/MMSS	UHF,44/7,UHF	AR11/C

[a]The list of satellite longitudes was compiled from the best information available.
[b]The period of validity is the number of years over which the frequency assignments of the space stations are to be used. Typical periods range from 10 to 20 years.
[c]A 2- to 3-year delay possible due to shuttle launch delays.
[d]Radiolocation Service.
[e]Either CONT 1 or 307°E will be operated at this location.
[f]Aeronautical Mobile-Satellite Service.
[g]This frequency band is not on the coordination request.

TABLE 3. FREQUENCY BAND KEY WITH SERVICE ALLOCATIONS[a]

Frequency Abbreviation	ITU Frequency Band (GHz) and Service	Link Direction
UHF	0.13 to 1.5	Up or Down (See Tables 1 and 2)
1.5a	1.530 to 1.535, MMSS 1.535 to 1.544, MMSS	Up
1.5b	1.535 to 1.5425, MMSS	Down
1.5c	1.536275 to 1.536525, MMSS 1.543575 to 1.543825, MMSS	Down
1.5d	1.537 to 1.541, MMSS 1.5148 to 1.541515	Down
1.5e	1.5425 to 1.544	Down
1.5f	1.545 to 1.559	Down
1.5g	1.5425 to 1.5440	Down
1.5h	1.5345 to 1.5370	Down
1.5i	1.530 to 1.5345	Down
1.6a	1.610 to 1.6265, MMSS	Up
1.6b	1.6265 to 1.6455, MMSS	Up
1.6c	1.63775 to 1.638025, MMSS 1.652245 to 1.652495, MMSS	Up
1.6d	1.6385 to 1.6425, MMSS	Up
1.6e	1.6265 to 1.636	Up
1.6f	1.6465 to 1.6605	Up
1.6g	1.6665 to 1.6605	Up
1.6h	1.646 to 1.660	Up
1.6i	1.627 to 1.636	Up
1.6j	1.6360 to 1.63857	Up
1.6k	1.6825 to 1.6875	Down

TABLE 3 (continued). FREQUENCY BAND KEY WITH SERVICE ALLOCATIONS[a]

Frequency Abbreviation	ITU Frequency Band (GHz) and Service	Link Direction
1.61	1.696 to 1.697	Down
1.6m	1.6716 to 1.6947	Down
1.6n	1.6938 to 2.290	Down
2	Various 2-GHz frequencies	Up or Down (See Tables 1 and 2)
2a	2.09638 to 2.118875	Up
2.5	2.5 to 2.69, BSS	Down
3	3.400 to 3.950, BSS	
3.6a	3.6 to 3.621, FSS/MMSS feeder	Down
3.6b	3.615 to 4.200	Down
3.7a	3.75705 to 3.75955	Down
3.8a	3.800 to 3.850, FSS	Down
3.9a	3.945 to 3.946, FSS 3.954 to 3.955, FSS	Down
3.9b	3.945 to 3.955, MMSS/FSS	Down
4	3.700 to 4.200, FSS	Down
4a	3.700 to 4.100, FSS	Down
4b	4.175 to 4.200, FSS/MMSS feeder	Down
4c	4.179 to 4.200, FSS/MMSS feeder	Down
4d	4.188 to 4.2005, FSS/MMSS feeder	Down
4e	4.1925 to 4.200, FSS/MMSS feeder	Down
4f	4.195 to 4.200, FSS/MMSS feeder	Down
4g	4.195 to 4.2005, FSS/MMSS feeder	Down
4h	4.500 to 4.800 4.6 to 4.7	Down Down

TABLE 3 (continued). FREQUENCY BAND KEY WITH SERVICE ALLOCATIONS[a]

Frequency Abbreviation	ITU Frequency Band (GHz) and Service	Link Direction
4i	4.020 to 4.024	Up
4.1a	4.195 to 4.199, FSS/MMSS feeder	Down
4.1b	4.195 to 4.199, FSS/MMSS feeder	Down
4.2a	4.200 to 4.250, FSS/MMSS feeder	Down
4.5	4.500 to 4.510 FSS/MMSS feeder	Down
5	5.725 to 5.925, FSS	Up
5a-6	5.725 to 6.225 FSS	Up
5b-6	5.925 to 6.300, FSS	Up
5c-6	5.925 to 6.925, FSS	Up
5d	5.725 to 6.275	Up
5d-6	5.955 to 6.395	Up
5.1a	5.116875 to 5.133125, FSS	Down
6	5.925 to 6.425, FSS	Up
6a	6.425 to 6.725	Up
6b	6.525 to 6.625	Up
6c	6.08275 to 6.08525	Up
6.1a	6.170 to 6.180, MMSS/FSS	Up
6.1b	6.125 to 6.175, FSS	Up
6.1c	6.1725 to 6.1765, FSS/MMSS feeder	Up
6.2b	6.258 to 6.262, FSS/MMSS	Up
6.4a	6.409 to 6.425, FSS/MMSS feeder	Up
6.4b	6.417 to 6.425, FSS/MMSS feeder	Up
6.4c	6.420 to 6.424, FSS/MMSS feeder	Up
6.4d	6.425 to 6.441, MMSS/FSS feeder	Up

TABLE 3 (continued). FREQUENCY BAND KEY WITH SERVICE ALLOCATIONS[a]

Frequency Abbreviation	ITU Frequency Band (GHz) and Service	Link Direction
6.4e	6.420 to 6.425 FSS/MMSS feeder	Up
6.4f	6.485 to 7.075	Up
6.5a	6.524875 to 6.541125, FSS, RD (Radiolocation applications)	Up
6.5b	6.500 to 7.000, FSS, Region 1	Up
6.6a	6.425 to 6.725	Up
6.6b	6.525 to 6.625	Up
6.7	6.735 to 6.975 FSS, Region 1	Up
7	7.25 to 7.75, FSS	Down
7a	7.25 to 7.30, FSS	Down
7b	7.90 to 7.95, FSS	Up
7c	7.25 to 7.31, FSS	Down
7d	7.34 to 7.40, FSS	Down
7e	7.42 to 7.51, FSS	Down
7f	7.53 to 7.60, FSS	Down
7g	7.62 to 7.68, FSS	Down
7h	7.70 to 7.75, FSS	Down
7i	7.250 to 7.385	Down
7j	7.25 to 7.49 / 7.42 to 7.505	Down / Down
7k	7.615 to 7.675 / 7.900 to 7.950	Down / Up
7l	Various 7.4 frequencies / 7.950 to 8.000	Down / Up
7m	7.3 to 7.35	Down
7n	7.4 to 7.45	Down

TABLE 3 (continued). FREQUENCY BAND KEY WITH SERVICE ALLOCATIONS[a]

Frequency Abbreviation	ITU Frequency Band (GHz) and Service	Link Direction
7o	7.45 to 7.5	Down
7p	7.5 to 7.55	Down
7q	7.6 to 7.65	Down
7r	7.65 to 7.7	Down
7s	7.4625 to 7.4675 / 7.28 to 7.48, FSS	Down / Down
7t	7.456 to 7.494 / 7.27 to 7.29, FSS	Down / Up
7u	7.98 to 7.99, FSS	Down
7v	7.257 to 7.259, FSS	Up
8	7.9 to 8.4	Up
8a	7.96 to 8.03, FSS	Down
8b	7.98 to 8.03, FSS	Up
8c	8.16 to 8.23, FSS	Up
8d	8.25 to 8.32, FSS	Up
8e	8.34 to 8.40, FSS	Up
8f	8.145 to 8.230 FSS/MMSS	Up
8g	7.975 to 8.165, FSS	Up
8h	7.975 to 8.035 / 8.000 to 8.050	Up / Up
8i	8.15 to 8.2 / 8.060 to 8.120	Up / Up
8j	7.980 to 8.105 / 8.025 to 9	Up / Up
8k	8.1 to 8.15	Up
8l	8.15 to 8.2	Up

TABLE 3 (continued). FREQUENCY BAND KEY WITH SERVICE ALLOCATIONS[a]

Frequency Abbreviation	ITU Frequency Band (GHz) and Service	Link Direction
8m	8.25 to 8.3	Up
8n	8.3 to 8.35	Up
8o	8.35 to 8.4	Up
8p	8.2 to 8.25	Up
8q	8.05 to 8.1 8.17638 to 8.198875	Up Up
8r	7.98 to 8.16, FSS	Up
10	10.700 to 10.950, FSS, Region 1	Down
11	10.700 to 11.700, FSS	Down
11a	10.7 to 11.2, FSS	Down
11b	10.7 to 11.5, FSS/SRS secondary	Down
11c	10.905 to 11.200, FSS	Down
11d	10.950 to 11.65, FSS	Down
11e	10.950 to 11.200, FSS	Down
11f	11.0 to 11.4, FSS	Down
11g-12	11.700 to 11.950, FSS	Down
11.2a	11.2 ±500 Hz, FSS	Up
11.2b	11.2 to 11.7, FSS, Region 1	Down
11.4a	11.45 to 11.47, FSS	Down
11.4b	11.45 to 11.70, FSS	Down
11.7a	11.7 to 11.714, FSS, Region 1	Down
12a	11.7 to 12.2, FSS, Region 2	Down
12b	11.7 to 12.5, BSS, Regions 1 and 3	Down
12c	12.2 to 12.7, BSS, Region 2	Down

TABLE 3 (continued). FREQUENCY BAND KEY WITH SERVICE ALLOCATIONS[a]

Frequency Abbreviation	ITU Frequency Band (GHz) and Service	Link Direction
12d	12.5 to 12.75, FSS, Regions 1 and 3	Down
12e	12.487 to 12.500, FSS/BSS	Down
12f	12.25 to 12.75, FSS, Region 3	Down
12g	12.50 to 12.58, FSS	Down
12h	12.75 to 13.25, FSS	Up
12i	11.7 to 12.7	Down
12.4	12.489 to 12.500, FSS, Region 1	Down
12.4a	12.40 to 12.85	Down
13a	13.0–13.25 FSS/SRS	Down
13b	13.25 to 14.0, SRS secondary	Up
13c	13.16 to 13.31 FSS/BSS	Up
13d	13.40 to 13.64	Down
14	14.0 to 14.5, FSS	Up
14a	14.0 to 14.9, FSS	Up
14b	14.0 to 14.25, FSS	Up
14c	14.09 to 14.32, FSS	Up
14d	14.5 to 15.5, SRS Secondary	Up
14e	14.5 to 14.8, FSS	Up
17a	17.3 to 18.1, FSS/BSS feeder	Up
17b	17.3 to 17.65, FSS	Up
17c	17.37 to 18.0, RSS	Up
17d	17.7 to 20.0, FSS	Down
17.3a	17.3 to 17.314, FSS	Up
17.3b	17.30 to 17.303, FSS	Up

TABLE 3 (continued). FREQUENCY BAND KEY WITH SERVICE
ALLOCATIONS[a]

Frequency Abbreviation	ITU Frequency Band (GHz) and Service	Link Direction
17.7a	17.725 to 19.245	Down
18a-1a	18.9 to 19.8, FSS/BSS	Down
18.0a	18.089 to 18.1, FSS	Up
20	20.2 to 21.2, FSS	Down
20a	20.300 to 20.374	Down
20b	20.030 to 20.190	Down
27a	27.5 to 30.0, FSS	Up
27b	27.99 to 28.69, FSS	Up
27c	27.525 to 29.045	Up
29b	29.150 to 29.310	Up
29c	29.456 to 29.494	Up
29.6a	29.655 to 29.656, FSS/BSS	Down
30	30.0 to 31.0, FSS	Down
39a	39.5 to 40.0, FSS	Up
43a	43.5 to 47, MSS	Not specified
43b	43.5 to 45.5, FSS/MMSS	Up
49	49.0 to 50.0 FSS	Up

[a]If regions (ITU) are not shown, the allocation is worldwide.

Translations of Abstracts

Equipement de gestion du réseau AMRT

G. D. HODGE, R. J. COLBY, C. KULLMAN, ET B. H. MILLER

Sommaire

Le rôle critique que joue l'installation AMRT du Centre d'exploitation INTELSAT (IOCTF), dans le bon fonctionnement du réseau d'accès multiple par répartition dans le temps (AMRT), nécessite l'utilisation d'un équipement de télécommunications en temps réel à réponse très rapide. L'article décrit les conditions générales requises en matière de surveillance et de gestion d'un système centralisé, l'accent étant mis sur la fourniture d'un équipement de formation de réseau décentralisé permettant aux stations de référence et de surveillance AMRT de communiquer avec l'installation AMRT de l'IOCTF. Celle-ci doit assurer un débit d'information jusqu'à concurrence de quatre messages par seconde. La capacité du Centre à assurer ce débit a été démontrée au cours de la mise au point du système IOCTF et les résultats de ces essais sont résumés dans l'article.

Appareil de surveillance du système INTELSAT d'acces multiple par répartition dans le temps

J. S. BARNETT, C. R. THORNE, H. L. PARKER, ET A. BERNTZEN

Sommaire

L'article décrit les caractéristiques opérationnelles des mesures effectuées au moyen de l'appareil de surveillance du système INTELSAT d'accès multiple par répartition dans le temps utilisé pour faciliter l'exploitation du réseau de concentration numérique des conversations AMRT. Les quatre paramètres courants mesurés décrits dans l'article sont la puissance relative des paquets, la fréquence centrale, l'erreur de position de paquet, et le pseudo-taux d'erreur sur les bits. Trois autres paramètres peuvent également être mesurés: le point de fonctionnement des répéteurs, la p.i.r.e. d'émission, et le rapport porteuse-à-bruit. Généralement, l'appareil de surveillance AMRT vérifie de façon cyclique chaque paquet de trafic et de référence dans quatre répéteurs au maximum pour extraire des données sur le fonctionnement du système et indiquer l'existence, à la station de référence et au Centre d'exploitation d'INTELSAT, de conditions échappant aux limites de tolérance. Le cas échéant, l'appareil de surveillance peut passer au mode de commande directe pour la mesure de paquets choisis lors du dépistage de défaillance. Outre une description de la conception du système, de l'architecture du logiciel et des mesures afférentes à la mise en oeuvre des équipements, l'article contient une évaluation de la performance du système.

la asignación de ráfagas de referencia y la programación de ráfagas. La información contenida en el BTP es transferida a todas las estaciones de referencia y de tráfico en forma de un Plan maestro de asignación de ráfagas (MTP) y de un Plan condensado de adquisición de ráfagas (CTP). En el presente se describen los algoritmos preparados de cada uno de los procesos de elaboración del BTP, así como los algoritmos y procedimientos utilizados para formular los MTP y CTP. También se analiza un sistema de programación para utilizar estos algoritmos.

Ventajas del TDMA y el TDMA con conmutación a bordo de los satélites INTELSAT V y VI

S. J. CAMPANELLA, B. A. PONTANO, Y J. L. DICKS

Abstracto

Dado que las terminales del sistema de acceso múltiple por distribución en el tiempo (TDMA) comparten una portadora común en el dominio temporal, el número de cadenas de conversión ascendentes y descendentes necesarias para poner en práctica una red TDMA se reduce considerablemente en comparación con las que se requieren cuando se emplea la técnica de acceso múltiple por distribución de frecuencia (FDMA). Se presenta un modelo de costos basado en el número de cadenas de conversión ascendentes y descendentes para el TDMA y el FDMA, mediante el cual se determina cuántas estaciones se requieren para que el costo de implantación del TDMA sea inferior al del FDMA. El modelo se aplica a un sistema dotado de un solo haz de cobertura terrestre, al sistema de haces múltiples del INTELSAT V con conexiones estáticas y al sistema de haces múltiples del INTELSAT VI con conexiones de conmutación estática o dinámica.

Se sabe que con el TDMA con conmutación dinámica habrá mejor conectividad entre los haces, se podrá ajustar la capacidad del tráfico de un haz a otro en incrementos de un solo canal telefónico y la red TDMA podrá trabajar con dos estaciones de referencia, en vez de cuatro, en cada región oceánica. Entre las demás ventajas del TDMA aquí examinadas figuran la operación de una sola portadora por transpondedor, que duplica la potencia disponible en el transpondedor en comparación con la del FDMA; la aptitud para atender variaciones en el volumen de tráfico cambiando la ubicación y la duración de las ráfagas, y la capacidad para efectuar la conmutación dinámica entre haces múltiples, que en el futuro puede evolucionar en sistemas TDMA con salto entre haces.

Author Index, CTR 1985

Index of 1985 Publications
by COMSAT Authors

The following is a cross-referenced index of publications by COMSAT authors in 1985, not including papers published in the *COMSAT Technical Review*. Copies of these publications may be obtained by contacting the COMSAT authors at COMSAT Corporation, 22300 Comsat Drive, Clarksburg, Maryland 20871.

ABDELAZIZ, M. H., and Pickholtz, R. L.,* "Delay Behavior of Reserved Priority Channels Operating on a CSMA/CD Protocol," IEEE International Conference on Communications, Chicago, IL, June 23–26, 1985, *Conference Record,* Vol. 3, pp. 1099–1104.

ABITA, J. L., "Technology: Development to Production," *IEEE Transactions on Engineering Management,* Vol. EM-32, No. 3, August 1985, pp. 129–131.

ABITA, J. L., see Geller, B. D.; Holdeman, L. B.; Hung, H.-L.

BARBER, R. C., see Holdeman, L. B.

BARGELLINI, P. L., "Satellite and Space Communications," *Reference Data for Engineers: Radio, Electronics, Computer, and Communications,* Chapter 27, 7th ed., E. C. Jordan, Editor, Indianapolis, IN: Howard W. Sams and Company, Inc., 1985.

BARNETT, J., and Phiel, J. F.,* "INTELSAT TDMA System Monitor," *International Journal of Satellite Communications,* Vol. 3, Nos. 1 and 2, January–June 1985, pp. 57–69.

BENJAMIN, M. C., and Bogaert, W. M., "COMSAT's TDMA Traffic Terminal," *International Journal of Satellite Communications,* Vol. 3, Nos. 1 and 2, January–June 1985, pp. 15–25.

BOGAERT, W. M., see Benjamin, M. C.

BONETTI, R. R., and Williams, A. E., "High Power Multiplexer for DBS Earth Stations," European Microwave Conference, Paris, France, September 1985, *Proc.,* pp. 364–369.

BONETTI, R. R., see Williams, A. E.

BUSH, W. G., see Williams, A. E.

CHANG, A. T. C.,* and Fang, D. J., "The Effect of Scintillation on the Active Microwave Remote-Sensing Sensors," *International Journal of Remote Sensing,* Vol. 6, No. 7, 1985, pp. 1231–1240.

---

* *Non-COMSAT author.*

COOK, W., see Hodge, G.

DIFONZO, D. F., see Krichevsky, V.

EFFLAND, J., "An Automated Antenna Measurement System," International Symposium on Antennas and Propagation, Kyoto, Japan, August 20–22, 1985, Paper 034-1, *Proc.*, pp. 181–184.

EFFLAND, J., see Price, R.

EKELMAN, E. P., and Gilmore, S. W., "Retrofitting an Earth Station Antenna for Dual Polarization: Design Considerations," IEEE AP-S International Symposium on Antennas and Propagation, Vancouver, Canada, June 17–21, 1985, *Digest*, Vol. 1, pp. 323–326.

ENOBAKHARE, E., see Hung, H.-L.

EZZEDDINE, A., Hung, H.-L. A., and Huang, H. C., "High-Voltage FET Amplifiers for Satellite and Phased-Array Applications," IEEE MTT-S International Microwave Symposium, St. Louis, MO, June 4–6, 1985, *Digest*, pp. 336–339.

FANG, D. J., and Sandrin, W. A., "Study of Propagation Effects Applicable to L-Band Ship-Earth Stations," International Symposium on Antennas and Propagation, Kyoto, Japan, August 20–22, 1985, *Proc.*, Vol. 1, pp. 333–336.

FANG, D. J., see Chang, A.T.C.

GELLER, B. D., and Abita, J. L., "A 3.7- to 4.2-GHz Monolithic Medium Power Amplifier," *Microwave Journal*, Vol. 28, No. 9, September 1985, pp. 187–190, 193–195.

GELLER, B. D., see Potukuchi, J. R.

GILMORE, S. W., see Ekelman, E. P.

GRUNER, R. W., "Design Procedure for a Distributed Reactance Waveguide Polarizer," IEEE AP-S International Symposium on Antennas and Propagation, Vancouver, Canada, June 17–21, 1985, *Digest*, Vol. 2, pp. 635–638.

GUPTA, R. K., see Potukuchi, J. R.

HODGE, G., Johnson, R., Cook, W., and Saralkar, K., "INTELSAT Operations Center TDMA Facility," *International Journal of Satellite Communications*, Vol. 3, Nos. 1 and 2, January–June 1985, pp. 71–76.

HOLDEMAN, L. B., Barber, R. C., and Abita, J. L., "An Approach to Fabricating Sub-Half-Micrometer-Length Gates for GaAs Metal-Semiconductor Field-Effect Transistors," *Journal of Vacuum Science and Technology: B*, Vol. 3, No. 4, July/August 1985, pp. 956–958.

HOLDEMAN, L. B., and Holdeman, J. T., Jr.,* "Torque on a Spinning Superconducting Sphere Inside a Superconducting Cylinder or Spherical Cap," *Journal of Applied Physics*, Vol. 57, No. 3, February 1, 1985, pp. 684–697.

HUANG, H. C., see Ezzedine, A.; Hung, H.-L.; Mahle, C.

HUNG, H.-L., Enobakhare, E., Abita, J., McNally, P., Mahle, C., and Huang, H., "GaAs FET MMIC Low-Noise Amplifiers for Satellite Communications," *RCA Review*, Vol. 46, December 1985, pp. 431–440.

HUNG, H.-L., see Ezzedine, A.; Van Der Merwe, D. G.

JOHNSON, R., see Hodge, G.

KARIMULLAH, K., see Williams, A. E.

KING, C., Trusty, P., Jankowski, J.,* Duesing, R.,* and Roach, P.,* "INTELSAT TDMA/DSI Burst Time Plan Development," *International Journal of Satellite Communications*, Vol. 3, Nos. 1 and 2, January–June 1985, pp. 35–43.

KRICHEVSKY, V., and DiFonzo, D. F., "Optimum Beam Scanning in Offset Single and Dual Reflector Antennas," *IEEE Transactions on Antennas and Propagation*, Vol. AP-33, No. 2, February 1985, pp. 179–188.

LEE, B. S., see Sorbello, R. M.

LEE, S. H., and Rudduck, R. C., "Aperture Integration and GTD Techniques Used in the NEC Reflector Antenna Code," *IEEE Transactions on Antennas and Propagation*, Vol. AP-33, No. 2, February 1985, pp. 189–194.

LYONS, J. W., III, "In-Orbit Performance of INTELSAT Spacecraft Solar Arrays," 20th Intersociety Energy Conversion Engineering Conference, Miami Beach, FL, August 18–23, 1985, *Proc.*, Vol. 1, pp. 1.43–1.47.

MAHLE, C., and Huang, H. C., "MMIC's in Communications," *IEEE Communications Magazine*, Vol. 23, No. 9, September 1985, pp. 8–16.

MAHLE, C., see Hung, H.-L.

McNALLY, P., see Hung, H.-L.

MOTT, R. C., see Potukuchi, J. R.

OISHI, T., and Kahn, W. K.,* "Stokes Vector Representation of the Six-Port Network Analyzer: Calibration and Measurement," IEEE MTT-S International Microwave Symposium, St. Louis, MO, June 4–6, 1985, *Digest*, pp. 503–506.

PAUL, D. K., "Communications via Undersea Cables: Present and Future," 29th Annual Society for Photo-Optical Instrumentation Engineers Meeting, San Diego, CA, August 18–23, 1985, *Proc.*, Vol. 559, pp. 36–50.

PONTANO, B., "The INTELSAT TDMA/DSI System: An Overview of the Special Issue," *International Journal of Satellite Communications,* Vol. 3, Nos. 1 and 2, January–June 1985, pp. 5–9.

POTUKUCHI, J. R., Geller, B. D., Mott, R. C., and Gupta, R. K., "Design and Development of Monolithic 6/4-GHz Transponder Subsystems," Government Microcircuit Applications Conference, Orlando, FL, November 5–7, 1985, *Digest,* pp. 353–354.

PRICE, R., Stuart, T., Effland, J., Sato, I.,* Tamagawa, I.,* Mori, I.,* and Iwata, R.,* "Dual Frequency Band Antenna for INTELSAT Earth Stations," International Symposium on Antennas and Propagation, Kyoto, Japan, August 20–22, 1985, Paper 232-2, *Proc.,* pp. 923–926.

RAPPAPORT, C. M.,* and Zaghloul, A. I., "Optimized Three-Dimensional Lenses for Wide-Angle Scanning," *IEEE Transactions on Antennas and Propagation,* Vol. AP-33, No. 11, November 1985, pp. 1227–1236.

REINHART, E. E., "An Introduction to the RARC '83 Plan for DBS Systems in the Western Hemisphere," *IEEE Journal on Selected Areas in Communications,* Vol. SAC-3, No. 1, January 1985, pp. 13–19.

REINHART, E. E., "Direct Satellite Broadcasting at Millimeter Wavelengths," IEEE International Conference on Communications, Chicago, IL, June 23–26, 1985, *Conference Record,* Vol. 3, pp. 1270–1276.

ROGERS, D. V., "Propagation Considerations for Satellite Broadcasting at Frequencies Above 10 GHz," *IEEE Journal on Selected Areas in Communications,* Vol. SAC-3, No. 1, January 1985, pp. 100–110.

ROGERS, D. V., and Allnutt, J. E.,* "Some Practical Considerations for Depolarization Compensation in 14/11- and 14/12-GHz Communications Satellite Systems," *Electronics Letters,* Vol. 21, No. 23, November 1985, pp. 1093–1094.

RUDDUCK, R. C., see Lee, S. H.

SANDRIN, W. A., see Fang, D. J.

SARALKAR, K., see Hodge, G.

SORBELLO, R. M., and Lee, B. S., "A 12/17-GHz Transmit/Receive Feed Module for DBS Antenna Applications," IEEE AP-S International Symposium on Antennas and Propagation, Vancouver, Canada, June 17–21, 1985, *Digest,* Vol. 2, pp. 489–492.

STUART, T., see Price, R.

STOCKEL, J., "Self-Discharge Performance and Effects of Electrolyte Concentration on Capacity of Nickel-Hydrogen Cells," 20th Intersociety Energy Conversion Engineering Conference, Miami Beach, FL, August 18–23, 1985, *Proc.,* Vol. 1, pp. 1.171–1.174.

SUYDERHOUD, H. G., "User Quality Assurance in Telephone Network System Parameters," IEEE International Conference on Communications, Chicago, IL, June 23–26, 1985, *Conference Record,* Vol. 1, pp. 336–343.

TRUSTY, P., see King, C.

VAN DER MERWE, D. G.,* Hung, H-L. A., Cannitz, L.,* and Eastman, L. F.,* "GaAs MBE Monolithic Low-Noise Amplifiers at X-Band," 15th European Microwave Conference, Paris, France, September 9–13, 1985, *Proc.,* pp. 919–924.

WICKHAM, M. E., "Design and Development of an Advanced Microwave Power Leveling Loop," International Telemetering Conference, Las Vegas, NV, October 28–31, 1985, *Proc.,* Vol. 21, pp. 63–84.

WILLIAMS, A. E., and Bonetti, R. R., "Design of Very Narrow Bandwidth Dielectric Resonator Microwave Filters," Government Microcircuit Applications Conference, Orlando, FL, November 5–7, 1985, *Digest,* pp. 341–342.

WILLIAMS, A. E., Bonetti, R. R., Karimullah, K., and Piccinni, M.,* "Microwave Receive Filter for a Regenerative Repeater," 15th European Microwave Conference, Paris, France, September 9–13, 1985, *Proc.,* pp. 349–354.

WILLIAMS, A. E., Bush, W. G., and Bonetti, R. R., "Predistorted Techniques for Multiple-Coupled Resonator Filters," *IEEE Transactions on Microwave Theory and Techniques,* Vol. MTT-32, No. 5, May 1985, pp. 402–406.

WILLIAMS, A. E., Tang, W. C.,* and Inher, C.,* "High Power Output Multiplexer for First DBS Application," 15th European Microwave Conference, Paris, France, September 9–13, 1985, *Proc.,* pp. 355–363.

WILLIAMS, A. E., see Bonetti, R. R.

ZAGHLOUL, A. I., "Statistical Analysis of e.i.r.p. Degradation in Antenna Arrays," *IEEE Transactions on Antennas and Propagation,* Vol. AP-33, No. 2, February 1985, pp. 217–221.

ZAGHLOUL, A. I., see Rappaport, C. M.

* *Non-COMSAT author.*

* *Non-COMSAT author.*

Glossary

ACI	adjacent channel interference
ACSSI	adjacent channel spectrum spreading interference
ACTP	abridged condensed time plan
AIS	antenna interface subsystem
AM	amplitude modulation
ASR	adjacent secondary response
ASSR	acquisition and steady-state reception
AWGN	additive white Gaussian noise
B/B	back-to-back
BCH	Bose-Chaudhuri-Hocquenghem
BER	bit error rate
BG	Board of Governors (INTELSAT)
BGP	background processor
BMLA	burst mode link analyzer
BPF	bandpass filter
BQ	burst qualified
BSS	Broadcasting Satellite Service
BT	bandwidth-time product
BTP	burst time plan
BTS	burst timing synchronization
BW	bandwidth
CADC	control and display console
CAW	common acquisition window
CCI	co-channel interference
CCIR	International Radio Consultative Committee
CCS	communications control software
CDC	control and delay channel
CEPT	Conference of European PTTs
C/I	carrier-to-interference ratio
C/N	carrier-to-noise ratio
COMSAT	Communications Satellite Corporation
CPU	central processing unit
CSM	communications system monitor
CTP	condensed time plan
CTTE	common TDMA terminal equipment
DCE	data communications equipment
DEMUX	demultiplexer
D/L	down-link

315

DNI	digital noninterpolation
DNTX	do not transmit
DPI	dual-path interference
DS	driver software
DSE	data switching exchange
DSI	digital speech interpolation
DTE	data terminal equipment
E_b/N_o	energy-per-bit to noise power density ratio
EFDS	error-free decisecond
EFS	error-free second
e.i.r.p.	equivalent isotropic radiated power
ESC	engineering service circuit
ESOC	Earth Station Ownership Consortium
FDM	frequency division multiplex
FDMA	frequency division multiple access
FEC	forward error correction
FM	frequency modulation
FSS	Fixed Satellite Service
GCE	ground control equipment
GDU	graphics display unit
GMA	gated mode acquisition
G/T	gain-to-noise temperature ratio
HDLC	high-level data link control
HPA	high-power amplifier
IC	international channel
IF	intermediate frequency
IFL	interfacility link
IFMU	IF measurement unit
IFRB	International Frequency Registration Board
INS	INTELSAT network simulator
INTELSAT	International Telecommunications Satellite Organization
IOC	INTELSAT Operations Center
IOCTF	INTELSAT Operations Center TDMA Facility
IOR	Indian Ocean Region
ISDN	Integrated Services Data Network
ISI	intersymbol interference
ISL	intersatellite link
ITA	International Telegraph Alphabet
ITDB	INTELSAT traffic data base
ITU	International Telecommunications Union

LHCP	left-hand circular polarization
LNA	low-noise amplifier
LPF	low-pass filter
MCU	measurement control unit
MLA	microwave link analyzer
MMSS	Maritime Mobile Satellite Service
MOS	mean opinion score
MP	major path
MPRT	master primary reference terminal
MTP	master time plan
MTTR	mean time to restore
MUX	multiplexer
NPRC	network packet recirculator/concentrator
OBE	out-of-band emission
OMC	operations and maintenance center
OMT	orthomode transducer
OMUX	output multiplexer
OSC	opposite secondary command
OSR	opposite secondary response
PB	phonetically balanced
PBER	pseudo bit error rate
PCM	pulse-code modulation
PM	phase modulation
PN	pseudo noise
PRB	primary reference burst (can be either RB1 or RB2)
PSF	packet store and formatter
PSI	packet-switched interface
PSK	phase-shift keying
PVC	permanent virtual circuit
QPSK	quadrature phase-shift keying
RB	reference burst
RBID	reference burst identification
RF	radio frequency
RFS	receive frame synchronization
RHCP	right-hand circular polarization
RSE	reference station emulator
RSSD	reference station status display
RTE	reference terminal equipment
Rx	receive

SAC	status, alarm, and control
SC	satellite channel
SCPC	single channel per carrier
SDNTX	selective do not transmit
SG	supergroup
SIU	status interface unit
SMA	search mode acquisition
S/N	signal-to-noise ratio
SOF	start of frame
SORF	start of receive frame
SPE	signal processing equipment
SRS	Space Research Service
SSOG	Satellite Systems Operations Guide (INTELSAT)
SSR	steady-state reception
SS/TDMA	satellite-switched TDMA
TACTP	test abridged CTP
TC	terrestrial channel
TDMA	time division multiple access
TFA	transmit frame acquisition
TFS	transmit frame synchronization
TIM	terrestrial interface module
TRMS	TDMA reference and monitoring station
TRT	timing and reference transponder
TSM	TDMA system monitor
TSSD	TDMA system status display
TTY	teletype (orderwire)
TWTA	traveling wave tube amplifier
Tx	transmit
U/L	up-link
UW	unique word
VOW	voice orderwire
VT	video terminal
WT	bandwidth symbol period product